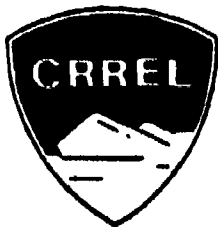


TL 637



Draft Translation 637
July 1977

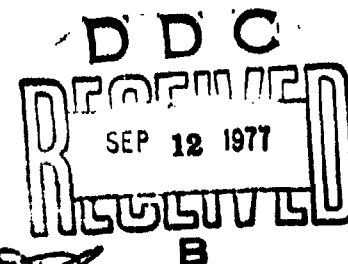


AD A 044002

THERMAL CONDUCTIVITY OF SOILS

O. Johansen

Graphics not reproducible



CORPS OF ENGINEERS, U.S. ARMY
COLD REGIONS RESEARCH AND ENGINEERING LABORATORY
HANOVER, NEW HAMPSHIRE

Unclassified

SECURITY CLASSIFICATION OF THIS PAGE (When Data Entered)

REPORT DOCUMENTATION PAGE		READ INSTRUCTIONS BEFORE COMPLETING FORM
1. REPORT NUMBER Draft Translation 637	2. GOVT ACCESSION NO. <i>141-1000-71-657</i>	3. RECIPIENT'S CATALOG NUMBER
4. TITLE (and Subtitle) THERMAL CONDUCTIVITY OF SOILS		5. TYPE OF REPORT & PERIOD COVERED
7. AUTHOR(s) <i>Johansen</i>		6. PERFORMING ORG. REPORT NUMBER
9. PERFORMING ORGANIZATION NAME AND ADDRESS U.S. Army Cold Regions Research and Engineering Laboratory Hanover, New Hampshire		8. CONTRACT OR GRANT NUMBER(s)
11. CONTROLLING OFFICE NAME AND ADDRESS	10. PROGRAM ELEMENT, PROJECT, TASK AREA & WORK UNIT NUMBERS	
14. MONITORING AGENCY NAME & ADDRESS (if different from Controlling Office)	12. REPORT DATE July 1977	13. NUMBER OF PAGES 291
	15. SECURITY CLASS. (of this report)	16. DECLASSIFICATION/DOWNGRADING SCHEDULE
18. DISTRIBUTION STATEMENT (of this Report) Approved for public release; distribution unlimited.		
17. DISTRIBUTION STATEMENT (of the abstract entered in Block 20, if different from Report)		
19. SUPPLEMENTARY NOTES <i>027 100</i>		
19. KEY WORDS (Continue on reverse side if necessary and identify by block number) THERMAL CONDUCTIVITY HEAT TRANSFER SOILS--MOISTURE CONTENT		
20. ABSTRACT (Continue on reverse side if necessary and identify by block number) The aim of this investigation has been to create a mathematical model for calculating thermal conductivity of soils with ordinary soil parameters as input data. One part of this work has been devoted to literature studies on heat-transfer mechanisms in moist materials. These studies have made it possible to give bounds for the different domains where the various mechanisms have an appreciable influence on the total heat transfer.		

DRAFT TRANSLATION 637

ENGLISH TITLE: THERMAL CONDUCTIVITY OF SOILS

FOREIGN TITLE: VARMELEDNINGSEVNE AV JORDARTER

AUTHOR: O. Johansen

SOURCE: Trondheim, Group for Thermal Analysis of Frost in the
Ground, Institute for Kjoleteknikk, 1975, 231p.

Translated by Rosetta Stone, Nashua, N.H. for U.S. Army Cold Regions
Research and Engineering Laboratory, 1977, 291p.

NOTICE

The contents of this publication have been translated as presented in the original text. No attempt has been made to verify the accuracy of any statement contained herein. This translation is published with a minimum of copy editing and graphics preparation in order to expedite the dissemination of information. Requests for additional copies of this document should be addressed to the Defense Documentation Center, Cameron Station, Alexandria, Virginia 22314.

ACCESSION for	
NTIS	White Section <input checked="" type="checkbox"/>
DDC	Buff Section <input type="checkbox"/>
UNANNOUNCED	<input type="checkbox"/>
JUSTIFICATION	
BY	
DISTRIBUTION/AVAILABILITY CODES	
Dist	Avail and/or SPECIAL
<i>A</i>	

TRANSLATOR'S

NOTES: To the translation of "THERMAL CONDUCTIVITY OF SOILS",
by Oistein Johansen.

The following general remarks apply.

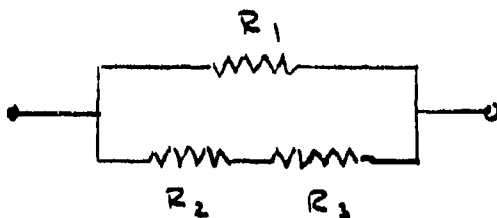
1. The author makes no distinction between sections (arabic or "normal" numerals) and sub-sections (A, B, C, etc.). Thus, references of the type "discussed in the previous section" may refer to either section or subsection.
2. Certain words or expressions used by the author may not have a direct, one-to-one correspondence in English. In such cases, alternate translations are given in parenthesis.
3. Expressions of the type "Hazens formel" can mean either "Hazen's formula" or "Hazens' formula". The translation may contain some errors in this respect.
4. The original is notoriously inconsistent in the use of subscripts, both in formulas and in the text. A major effort would be required to correct for this and the translation follows the original in this respect.
5. The author was at one point associated with "Institutt for Kjøleteknikk" at NTH (Norwegian Technical University). In at least one figure caption, the original presents the translation: "Institute for Refrigeration Engineering", which seems to be a misnomer. This group is clearly active in the study of thermal phenomena associated with frost penetration in and prevention of frost damage to various kinds of structures in a cold (artic) climate. The least of their worries would appear to be engineering or design of refrigeration systems, since nature already has taken care of that aspect. "Institute for Cold Technology" is proposed as a more descriptive translation.

6. About 20 percent of the sentences in the original contain a word or phrase equivalent to "however". A concentrated effort has been made to eliminate as many of these as possible, particularly when they occur in two or more consecutive sentences.

A number of foot-notes have been included in the translation to clarify certain items. The following comments were deemed too long for inclusion as foot-notes:

1. In chapter I, Eq 31, the meaning of d_{10} is not entirely clear. From the comments following Eq 30 it appears that d_{10} means "the diameter that 10 percent of the particles are less than". The line below Eq 31 ends with "gjennomgang", which means "passing through" or "penetration". That would indicate that the subscript 10 for d some-how relates to the percentage of water "passing through" or "penetrating" the material. Another possible interpretation of "gjennomgang" is "intersection", i.e. the point where the diameter distribution intersects the 10 percent level.
2. Water content is denoted by upper and lower case w in different parts of the report. The translation may retain some of these inconsistencies.
3. Eqs 27 and 28 of chapter II are based on the following two resistor networks

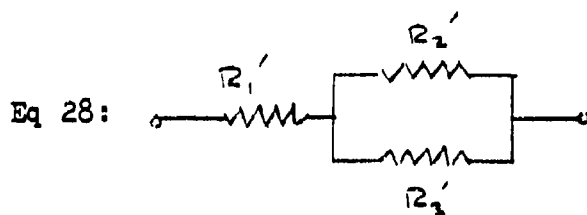
Eq 27:



$$R_1 = 1 / \lambda_1 \beta$$

$$R_2 = \frac{\phi}{(1-\beta) \lambda_1}$$

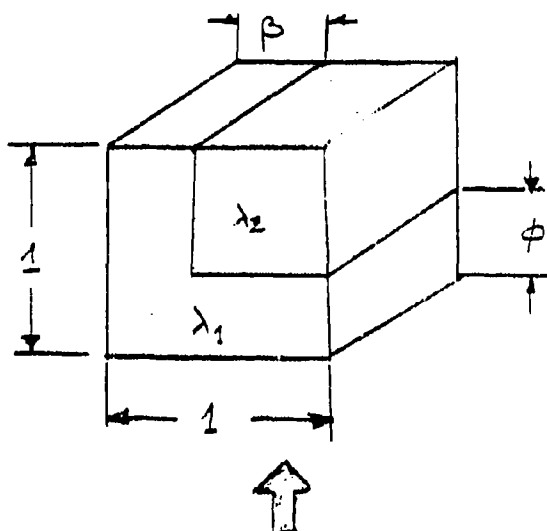
$$R_3 = \frac{1-\phi}{(1-\beta) \lambda_2}$$



$$R_1' = \phi / \lambda_1$$

$$R_2' = \frac{1 - \phi}{\lambda_1 \beta}$$

$$R_3' = \frac{1 - \phi}{(1 - \beta) \lambda_2}$$



Heat flow

5. The appendix treating heat flow in cylindrical bodies contains certain ambiguous notations. In the translation, lower case x without subscript is used only in Eq 6, while capital X has been used for the parameter defined by Eq 8. Also, expressions of the type beix_1^2 have been changed to the better defined form $(\text{beix}_1)^2$ (see Eq 14).

THERMAL CONDUCTIVITY OF SOILS *

OF

Siviling. Øistein Johansen
Institutt for kjøleteknikk
7034-Trondheim-NTH
1975

* With summary and figure captions in English.

THERMAL CONDUCTIVITY OF SOILS

Øistein Johansen

FOREWORD

This report will be submitted as a Ph.D. thesis. The work on which it is based was begun in the fall of 1968 in the form of a M.Sc. thesis at the Institute for Cold Technology, Norwegian Institute of Technology (NTH), where I performed theoretical and experimental studies of heat convection in coarse fill materials. The National Road Laboratory took an interest in this work and funded an extension of the study.

At that time, a more extensive research program was initiated under the direction of the "Committee for Frost in the Ground", with economic support from the Norwegian Scientific Research Council and the Highway Authority. Some of the work was performed by a group at NTH, with participation by the Institute for Cold Technology. This group concentrated on generating theoretical methods for analysis of thermal conditions in structures subjected to frost. The work included a study of thermal parameters for soil materials, which since that time has been my field of activity. This program has thus provided the funds for performing the investigations on which this report is based.

Cooperation within the research team at NTH has been of great value to the investigation and has contributed toward a goal-oriented study. I also wish to stress the importance of taking part in meetings and conferences arranged by the Committee for Frost on

the Ground for the final form of the report. Work on presentations and papers has taken considerable time but also provided valuable experience in arranging the material.

The professional support given by my co-workers at the Institute has also been of great importance for the results presented here. In particular, I wish to thank Mr. Per Erling Frivik, M. Sc., who has directed the work of the group, as well as other co-workers who have performed much of the practical work in connection with the development of test equipment and who have given valuable help in performing the experiments.

Special thanks are extended to my thesis supervisor, Professor Gustav Lorentzen, Sc.D., for advice and encouragement during my work on the thesis.

The report was written while I was employed at the National Road Laboratory. I wish to thank the management and colleagues here for the consideration they have shown despite the fact that this work has taken more time than originally estimated.

Oslo in June, 1975

Øistein Johansen

INDEX

	<u>Page</u>
Foreword	iii
Index	v
Symbols	viii
1. Latin letters	viii
2. Numbers independent of units	x
3. Greek letters	xi
4. Mathematical symbols	xiii
5. Often used indexes (subscripts)	xiii
6. Conversion factors	xiv
Bibliography	xv
INTRODUCTION	1
CHAPTER I: HEAT TRANSPORT IN MOIST SOIL	3
1. Thermal Radiation	4
2. Combined Moisture and Heat Transport	11
A. Water vapor diffusion	11
B. Capillary water transport	14
C. Contribution of vapor diffusion to thermal conductivity	17
3. Convection	20
A. Heat Transport	20
B. Liquid transport in porous materials	23
C. Forced convection	26
D. Free convection	31
4. Heat Transport in Freezing Soils	38
5. The Effects of Various Heat Transport Mechanisms	42
REFERENCES	47
CHAPTER II: THEORIES FOR HEAT CONDUCTION IN COMPOSITE MATERIALS	50
1. Exact Theory	50
2. Evaluation of Limits	54
A. Limits according to Hashin-Shtrikman	54
B. Limits based on point correlations	57
C. Other evaluations of limits	62
D. Conclusion	65
3. Mathematical Models	67
A. Introduction	67
B. "Exact" calculations	68
C. Approximate methods based on electrical field theory	70
D. Approximate calculations based on elements connected in series or shunt	76
E. The geometric mean model	80
F. Conclusion	83
REFERENCES	85

	Page
CHAPTER III: SOIL PARAMETERS	88
1. Thermal Conductivity of Soil Generating Materials	88
A. Soil generating minerals	88
B. Quartz content in loose deposits	91
C. Thermal conductivity for the components	95
2. Volumetric Composition and Texture	104
A. Volume ratios in soil materials	104
B. The importance of texture	107
C. Unfrozen water	113
3. Soil Material Classification	118
A. Geotechnical analysis	118
B. Supplemental analysis	123
REFERENCES	125
CHAPTER IV: EXPERIMENTAL METHODS FOR DETERMINING CONDUCTIVITY IN SOIL MATERIALS	127
1. Thermal Conductivity Measurements in Materials Containing Moisture	127
2. Stationary Methods	131
A. Kersten's cylindrical test unit	131
B. Planar test unit	136
3. Thermal Conduction Probes	143
A. Influence of finite size and varying thermal properties	143
B. The effects of moisture transport	149
C. Experimental arrangement	152
4. Other Transient Methods	157
A. Linear temperature rise	157
B. Constant thermal flux	161
C. Periodic variation of temperature	165
D. Conclusion	173
REFERENCES	174
CHAPTER V: EXPERIMENTAL INVESTIGATIONS OF THERMAL CONDUCTIVITY IN SOIL MATERIALS	177
1. Dry Soil Materials	178
A. Introduction	178
B. Measurements performed by Smith	180
C. Investigation performed by the author	181
D. Empirical relations	189
E. Stabilized materials	193
F. Conclusion	197
2. Saturated Mineral Soil Materials	199
A. Introduction	199
B. Measurements performed by Kersten	200
C. Ocean Sediments	202
D. Conclusion	204

	Page
3. Moist Mineral Oils	205
A. Introduction	205
B. Study by Kersten	207
C. Investigation of Norwegian soil materials	214
D. Conclusion	217
4. Soil Materials Containing Humus	218
A. Introduction	218
B. Measurements on peat and bog	219
REFERENCES	222
CHAPTER VI: METHODS FOR COMPUTING THERMAL CONDUCTIVITY OF SOIL MATERIALS	224
1. Existing Methods	224
A. Analytical methods	224
B. Empirical methods	230
C. Conclusion	246
2. New Methods for Determining Thermal Conductivity in Soil Materials	248
A. Introduction	248
B. Mathematical model for mineral soils	248
3. Effects of Variations in Soil Parameters	254
A. Effects on conductivity calculations	254
B. Conclusions	266
4. Effects of Conductivity Variations ...	270
A. Introduction	270
B. Effects of conductivity, variations	271
C. Conclusion	275
REFERENCES	276
SUMMARY	278
POST-SCRIPT	284
APPENDIX	286
REFERENCES	291

SYMBOLS

1. Latin letters

A	attenuation ratio	-
$a = \lambda/cp$	thermal diffusivity	m^2/s
$A_m = \lambda e/(cp)_f$	thermal diffusivity, included in Rayleigh's number	m^2/s
a,b,c,d	constants in Kersten's equations	-
$c = \rho cp$	thermal capacity, by volume	J/m^3K
c	specific heat	J/kgK
c	clay content	-
Da	diffusion coefficient for water vapor in air	m^2/s
$D_{\theta v}$	isothermal water vapor diffusivity	m^2/s
$D_{\theta l}$	isothermal water diffusivity	m^2/s
D_{Tv}	thermal water vapor diffusivity	m^2/sK
d	diameter (of particles)	m, m
d_{ekv}	equivalent diameter	m
E	electrical field strength	V/m
F	frost quantity	$h^{\circ}C$
$F_i, i = 1, 2, \dots$	factor in Fricke's equation	-
f	form factor, in expressions for specific surface area	-
G_1, G_2	factors depending on average cell geometry for components "1" and "2". Used in Fricke's equations.	-
g	gravity acceleration	m^2/s

$g_i, i = a, b, c$	form factor. Used in Fricke's equations.	-
h	thickness	
i	potential gradient	m/m
K	hydraulic conductivity	m/s
$K = k/u$	permeability	m/s (cm/s)
k	permeability	m^2
L	latent heat of water	J/kg, Wh/kg
l	length	m
n	porosity	-
$n_i, i = 1, 2, \dots$	relative volume for component "i"	-
o_v	relative volume of organic materials	-
P_o	total pressure	N/m^2
p	partial pressure	N/m^2
p''	saturation pressure	N/m^2
q	quartz content	-
q	heat flux	W/m^2
q_l	water flux	kg/m^2s
q_v	water vapor flux	kg/m^2s
R	gas constant	$m^2/s-k$
r	vaporization heat	J/kg
r	radius	m
S	specific surface area	m^2/m^3
S_r	degree of saturation	-
T	temperature	K, $^{\circ}C$
t	time	s
v	specific volume	m^3/kg

v	flow velocity	m/s
V_5, V_{10}	water content which gives 5 (10) mm penetration (sinking) of cone in consistency measurements (relative to dry weight)	-
w	relative water content by dry weight	-
w_v	relative water volume	-
w_w	relative water content by wet (total) weight	-
w_{25}, w_{100}	water content which causes flowing for 25 (100) blows in Lassagrande's flow limit test-set (ratio by weight)	-
$w_L (= w_{25})$	flow limit	-
w_u	unfrozen water ratio by weight (water/dry material)	-
$x = r \sqrt{w/a}$	angular velocity	-
x, y, z	space coordinates	m

2. Numbers independent of units

$ Fo = at/r^2 $	Fourier's number
$ Ke = \frac{(\lambda - \lambda^0)}{(\lambda^1 - \lambda^0)} $	Kersten's number. Normalized conductivity.
$ Nu = \lambda e / \lambda^0_e $	Nusselt's number; free convection.
$ Nu_r = \alpha_r d / \lambda_2 $	Nusselt's number; radiation
$ Pe_m = d \cdot v \cdot (cp) f / \lambda_f $	Peclet's number, modified
$ Ra = \frac{aghk\Delta T}{a_m v} $	Rayleigh's number, free convection in porous materials
$ Ra_k $	critical Rayleigh's number

3. Greek letters

α	expansion coefficient, by volume	$^{\circ}\text{C}^{-1}$
$\alpha = \lambda_2/\lambda_1$	conductivity ratio	-
α, β	constants (coefficients) in Kersten's equations	-
α, β	factors (coefficients) in equation for unfrozen water content	-
α, β	factors (coefficients) in empirical equation	-
α_r	heat transfer coefficient for radiation	W/m^2
$\beta = \frac{\lambda - \lambda_1}{\lambda + 2\lambda_1}$	normalized conductivity	-
β	rate of temperature rise	$^{\circ}\text{C}/\text{s}$
β	dimension in cubical unit cell	-
γ_d	dry density	kg/m^3
γ_s	specific weight	-
γ_m	specific weight of mineral component	kg/m^3
γ_o	specific weight of organic component	kg/m^3
Δ	denotes differences or small variations	-
δ	gap opening (width)	-
ϵ	emission factor (coefficient)	-
ϵ	dielectric constant	As/Vm^1
η	dynamic viscosity	Ns/m^2
θ	moisture content by volume (in Chapter I)	-
$\Lambda_i, i = 1, 2, \dots$	integrals containing point correlations (Brown's equation).	-
λ	thermal conductivity	W/mK
$\lambda_i, i = 1, 2, \dots$	thermal conductivity of component " i "	"

1) This is the unit for absolute dielectric constant. The parameters ϵ_1 and ϵ_2 used in Eq. 20 of Chapter II are relative

constants, i.e. pure numbers (Translator's note).

λ^1	thermal conductivity of saturated material	W/mK
λ^0	thermal conductivity of dry material	
λ_e	effective thermal conductivity, e.g. including contributions from convection	
λ^0_e	steady state conductivity	
λ^*, λ_*	upper and lower Hashin-Shtrikman-limits	W/mK
λ subscr.	other subscripts (indexes) are explained in the text where they occur.	"
ν	kinematic viscosity	m ² /s
ξ	frost depth	m
Π	mathematical symbol for product, e.g.:	
	$\prod_{i=1}^p a_i = a_1 \cdot a_2 \cdot \dots \cdot a_p$	
ρ	density	
Σ	mathematical symbol for sum, e.g.	
	$\sum_{i=1}^p a_i = a_1 + a_2 + \dots + a_p$	
σ	radiation constant for black bodies	W/m ² K ⁴
ϕ	potential	N/m ² , m
ϕ	relative humidity	-
ϕ	dimension of cubical unit cell	-
$\phi_1(\vec{r})$	function which assumes values 0 or 1 if the (position) vector \vec{r} falls outside or inside component "i", respectively	

moisture potential (suction)	N/m ² , m
angular velocity	rad/s

4. Mathematical symbols

∇	gradient operator, e.g.: $\nabla T = (\partial T / \partial x)\vec{i} + (\partial T / \partial y)\vec{j} + (\partial T / \partial z)\vec{k}$. ¹⁾
∇^2	Laplace's operator, e.g.: $\nabla^2 T = \partial^2 T / \partial x^2 + \partial^2 T / \partial y^2 + \partial^2 T / \partial z^2$
\rightarrow	denotes vector quantity
$\langle \rangle$	average by volume, e.g.: $\langle \phi_i(\vec{r}) \rangle = \frac{1}{V} \int_V \phi_i(\vec{r}) dv$

5. Often used indexes (subscripts)

e	effective, e.g. effective conductivity λ_e , which includes contributions from convection, etc.
f	liquid, e.g. thermal capacitance by volume for a liquid (cp) f.
i = 1, 2, ...	denotes component. In composite materials, the components are numbered according to increasing conductivity: $\lambda_1 < \lambda_2 < \dots < \lambda_i < \dots < \lambda_p$
i = a, b, c	subscripts for form factors in Fricke's equation.
v	volume, e.g. water content by volume W_v .
0	when occurring as a superscript for conductivity λ , dry material is indicated.
1	when occurring as a superscript for conductivity λ , saturated material is indicated.

1) \vec{i} , \vec{j} and \vec{k} denote unit vectors along x, y and z-axes, respectively (Translator's note).

6. Conversion factors

$$1 \text{ kcal} = 4187 \text{ Ws (J)} = 1,163 \text{ Wh}$$

$$1 \text{ kcal/mh}^{\circ}\text{C} = 1,163 \text{ W/mK}$$

BIBLIOGRAPHY

A

- P. Adivarahan et al: Heat Transfer in Porous Rocks. Society of Petroleum Engineers Journal, 1962, pp. 290-296.
- L. Alberts et al: The Influence of Low Moisture Content on the Conductivities of a Granular Substance. Brit. J. Appl. Phys. 17 1966, pp. 951-955.
- M. Abramowitz and I. Stegun. Ed.: Handbook of Mathematical Functions. Nat. Bur. of Standards, Appl. Math. Ser., New York, 1969, p. 374.
- Analyseforskrifter. Statens vegvesen, 1966.
 1. Jordarter. 111. Spesifikk vekt - vanninnhold - romvekt.
- Analyseforskrifter. Statens vegvesen, 1966, 1 Jordarter, 141. Mekaniske egenskaper.
- Analyseforskrifter. Statens vegvesen, 1966, 1 Jordarter, 161. Komprimering, p. 5.
- D.M. Anderson and A.R. Tice: Predicting unfrozen water contents in frozen soils from surface area measurements. Highway Res. Rec. No. 393, 1972, pp. 12-18.
- E. Angen: Analyse av vanninnhold i vegkonstruksjoner. Intern rapport. SINTEP, NTH, Trondheim, 1973.
- W.B. Argo and J.M. Smith: Heat Transfer in Packed Beds. Chemical Engineering Progress, 49 (8), 1953, pp. 443-451.
- B
- L. Barden et al: The Collapse Mechanism in Partly Saturated Soil. Engineering Geology, 7 (1), 1973, pp. 49-60.
- Beck: Transient Determination of Thermal Properties. Nuclear Engineering and Design, 3, 1966, pp. 373-381.
- M. Beran: Use of the Vibrational Approach to Determine Bounds for the Effective Permittivity in Random Media. Nuovo Cimento. 38, (2), 1965, pp. 771-782.
- M.J. Beran: Application of Statistical Theories to Heterogeneous Materials. Phys. Stat. Sol. (a), 6, 1971, p. 365.
- E. Berge and Ø. Aarvold: Some physical properties of grass silage. Meldinger fra Norges Landbrukshøgskole. 52, (1), 1974.
- G.S.G. Beveridge and D.P. Haughey: Axial Heat Transfer in Packed Beds. Stagnant Beds Between 20 and 750°C. Int. J. Heat Mass, 14, 1971, pp. 1093-1113.
- F. Birch and H. Clark: The Thermal Conductivity of Rocks. American Journal of Science, 238, (5), 1940, pp. 529-558.

- J.H. Blackwell: A. Transient Heat Flow Method for Determining the Thermal Constants. J. Appl. Phys. 25, (2), 1954, pp. 137-144.
- J.H. Blackwell: The Axial-Flow Error in the Thermal Conductivity Probe, Can. J. Phys. 34, 1956, pp. 412-417.
- C.A. Bower and J.O. Goertzen: Surface area of soils and clays by an Equilibrium Ethylene Glycol Method. Soil Science, 87, 1959, pp. 289-292.
- E. Brendeng and P.E. Frivik: New Development in Design of Equipment for Measuring Thermal Conductivity and Heat Flow. Institutt for kjøleteknikk, Trondheim, NTH, 1973.
- W.F. Brown: Solid Mixture Permittivities. The Journal of Chemical Physics, 23, (8), 1955, pp. 1514-1517.
- W.F. Brown, Jr.: Dielectric Constants, Permeabilities, and Conductivities of Random Media. Trans. of the Soc. of Rheology 9, (1), 1965, pp. 357-380.
- D.A.G. Bruggeman: Dielektrizitätskonstanten und Leitfähigkeiten von Vielkristallen der nichtregularen Systeme. Ann. Physik 5, (25), 1936, pp. 645-664.
- Burke and Plummer: Referert i Chemie Ing.-Techn., 25, 1953, p. 262.
- Bygg. Huvuddel 1B. Almanns Grunder: Avd. 17:4, pp. 306-308. AB Byggmastarens Forlag Stockholm 1972.
- C.J.F. Hottcher (1938): Referert av D. Polder (1946). See ref. (36).

C

- J.W. Cary: Water Flux in Moist Soil: Thermal Versus Suction Gradients. Soil Science, 100, (3), 1965, pp. 168-175.
- H.S. Carslaw and J.C. Jaeger: Conduction of Heat in Solids. Sec. ed. Oxford Press, 1959, p. 345.
- J.C. Champoussin: Determination Simultane des caracteristiques termocinetiques des solides. Int. J. Heat. Mass. 15, 1972, pp. 1407-1418.
- S.C. Cheng and R.I. Vachon: The Prediction of the Thermal Conductivity of Two and Three Phase Solid Heterogeneous Mixtures. Int. J. Heat Mass. Transfer. 12, 1969, pp. 249-264.
- S.C. Cheng and R.I. Vachon: A Technique for Predicting the Thermal Conductivity of Suspensions, Emulsions and Porous Materials. Int. J. Heat Mass. Transfer, 13, 1970, pp. 537-546.

- C. Codegone et al: Resonant Thermal Waves in Insulating Slabs.
IIR. Commission 2. (Trondheim) 1966. (Saertrykk)
- S.R. Coriell and J.L. Jackson: Bounds on Transport Coefficients of Two-Phase Materials. J. Appl. Phys. 39, (10), 1968, pp. 4733-4736.
- P.B. Corson: Correlation functions for predicting properties of heterogeneous materials. I. Experimental measurements of spatial correlation functions in multiphase solids. J. Appl. Phys. 45, (7), 1974, pp. 3159-3164.
- P.B. Corson: Correlation functions ...II. Empirical construction of spatial correlation functions for two-phase solids. J. Appl. Phys. 45, (7), 1974, pp. 3165-3170.
- P.B. Corson: Correlation functions ...IV. Effective thermal conductivity of two-phase solids. J. Appl. Phys. 45, (7), 1974, pp. 3180-3182.
- D. Croney and J.D. Coleman: Pore Pressure and Suction in Soil. Fra "Pore Pressure and Suction in Soils". Butterworths. London 1961, pp. 31-37.
- J.A. Currie: Gaseous Diffusion in Porous Media. Part 2 - Dry Granular Materials, British Journal of Applied Physics, 11, 1960, pp. 318-324.
- J.A. Currie: Gaseous Diffusion in Porous Media. Part 3 - Wet Granular Materials. British Journal of Applied Physics, 12, 1961, pp. 275-281.

D

- W.E.A. Davies: The theory of composite dielectrics. J. Phys. D: Appl. Phys. 4, 1971, pp. 318-327.
- F. De Ponte and P.E. Frivik: Automatic Control of Guarded Hot Plate Apparatuses. Institutt for kjøleteknikk, Trondheim, NTH, 1972.
- D.A. de Vries: Het warmtgeleidingsvermogen van grond. Med. Landbouwhogeschool. Wageningen, 52, 1952.
- D.A. de Vries: Simultaneous Transfer of Heat and Moisture in Porous Media. Transactions, American Geophysical Union, 39, (5), 1958.
- D.A. de Vries and A.J. Peck: On the Cylindrical Probe Method of Measuring Thermal Conductivity. Aust. J. Physics, 11, 1958, pp. 255-271.

- R.G. Deissler and J.S. Boegli: An Investigation of Effective Thermal Conductivities of Powders in Various Gases. Transactions of the ASME, October 1958, pp. 1417-1425.
- P.B. Desphande and J.R. Cooper: Thermal Conductivity of Two-Phase Systems. J. Heat Transfer. Trans. of the ASME, May 1972, pp. 249-264.

E

- J.W. Elder: Steady Free Convection in a Porous Medium Heated from Below. J. Fluid Mech. 1967, 27, pp. 29-48.
- M.A. Elsayed: Bounds for effective thermal, electrical, and magnetic properties of heterogeneous materials using higher order statistical information. J. Math. Physics, 15, (11), 1974, pp. 2001-2015.
- I.M. Eltantawy and P.W. Arnold: Reappraisal of Ethylene Glycol Mono-Ethyl Ether (EGME) Method for Surface area Estimation of Clays. Journal-Soil Science, 24, 1973, pp. 232-238.
- S. ERgun: Flüssigkeitsströmung durch Füllkörpersäulen (Festbetten). Referat i Chemie Ing.-Techn., 25, 1953, p. 262.

F

- O.T. Farouki: Physical Properties of Granular Materials with Reference to Thermal Resistivity. Highway Res. Rec. 128, 1966., pp. 25-43.
- T.P. Fidelle and R.S. Kirk: A study of Unidirectional Versus Tridirectional Heat Flux Models. AIChE Journal, 17, (6), 1971, pp. 1427-1434.
- A.K. Fleming: Applications of a Computer Program to Freezing Processes. Proceedings of the XII International Congress of Refrigeration. Washington, D.C. 1971.
- P.E. Frivik, Institutt for kjøleteknikk, NTH, 1974. Upubliserte resultater.
- P.E. Frivik et al: Sondeapparat. Rapport fra Grupper for termisk analyse av frost i jord. Institutt for kjøleteknikk, Trondheim, NTH, 1975.

G

- A. Gemant: The Thermal Conductivity of Soils. Journal of Applied Physics, 21, 1950, pp. 750-752.
- K. Gotoh: Thermal Conductivity of Two-Phase Heterogeneous Substances, Int. J. Heat Mass Transfer, 14, 1971, pp. 645-646.
- C.G. Gurr et al: Movement of Water in Soil Due to a Temperature Gradient. Soil Science 74 (5) 1952, pp. 335-345.

H

- Z. Hashin and S. Shtrikman: A Variational Approach to the Theory of the Effective Magnetic Permeability of Multi-phase Materials. J. Appl. Phys. 33, (10), 1962, pp. 3125-3131.
- P. Hoekstra et al: Measuring the Thermal Properties of Cylindrical Specimens by use of Sinusoidal Temperature Waves. Cold Regions Research and Engineering Laboratory, Technical Report 244, Oct. 1973.
- A. Holmes: Principles of Physical Geology. Nelson, London 1965, p. 84.
- P.C. Hooper and F.R. Lepper: Transient Heat Flow Apparatus for the Determination of Thermal Conductivities. Heating, Piping & Air Conditioning. Aug. 1950, pp. 129-134.
- K. Horai: Thermal Conductivity of Rock-Forming Minerals. J. Geophys. Res. 76, (5), 1971, pp. 1278-1308.
- E. Hogberg: Vattenhaltens innverkan på densitet og kompressibilitet hos packade jordarter. Byggforskningen. Rapport R8, 1972, p. 87.

I, J

- J.L. Jackson and S.R. Coriell: Transport Coefficients of Composite Materials, J. Appl. Phys., 39, (5), 1968, pp. 2349-2354.
- Y. Jame and D.I. Norum: Phase Composition of a Partially Frozen Soil. Department of Agricultural Engineering, Univ. of Saskatchewan, Saskatoon.

- Ø. Johansen: Undersøkelse av varmetransporten i kult og pukklag. Det store ekuamensarbeid. Institutt for kjøleteknikk, NTH, Trondheim, Høst 1968.
- Ø. JOhansen: Innflytelse av fri konveksjon i grovkornede vegbyggings-materialer. Institutt for kjøleteknikk, NTH, Trondheim, 1970.
- W.D. Joshua and E. De Jong: Soil Moisture Movement under Temperature Gradients. Can. J. Soil. Scie. 53, 1973, pp. 49-57.

K

- P.W. Kasameyer et al: Layers of High Thermal Conductivity in the North Atlantic. J. Geophys. Res. 77 (17), 1972, pp. 3162-3167.
- K. Katayama et al: Thermal Properties of Wet Porous Material Near Freezing Point. ASHRAE Journal April 1973, pp. 56-61.
- M.S. Kersten: Thermal Properties of Soils, Univ. of Minnesota, Eng. Experiment Station, bull. 28, June 1949.
- W.T. Kierkus et al: Radial-Axial Transient Heat Conduction in a Region Bounded Internally by a Circular Cylinder of Finite Length. Dept. of Mechanical Engineering, The University of Calgary, Calgary, Alberta. (Preprint)
- A. Knutson and R.-Saetersdal: Teleregistering 1967/68. Veglaboratoriet. Intern rapport. Oslo 1969, p. 8.
- A. Knutson: Theory and Experience Regarding Frost Penetration and Frost Heaving, Symp. on Frost Action on Roads. I. Paris 1973, pp. 223-233.
- A.F. Knutson: Upubliserte resultater, 1973.
- O. Krischer: Die Leitfähigkeit des Erdbodens. Beiheft zum Gesundheits-Ingenieur. Reihe I, Heft 33, München 1934.
- O. Krischer and H. Esdorn: Wärmeleitung und Dampfdiffusion in feuchten Gütern. VDI-Forsch.-Heft 402, Berlin 1940.
- O. Krischer and H. Esdorn. Einfaches Kurzzeitsverfahren zur gleichzeitigen Bestimmung der Wärmeleitnahl, der Wärmekapazität und der Wärmeeindringzahl fester Stoffe. VDI-Forschungsheft, 450, 1955, pp. 28-39.
- D. Kunii and J.M. Smith: Heat Transfer Characteristics of Porous Rocks. A.I. Ch. E. Journal, 6 (1), 1969, pp. 71-78.

R.J. Kunze et al: Factors Important in the Calculation of Hydraulic Conductivity. Soil Sci. Soc. Amer. Proc., 32, 1968, pp. 760-765.

L

E.R. Lapwood: Convection of A Fluid in a Porous Medium. Proc. Cambr. Soc. 44, 1948, pp. 508-521.

P.F. Low et al: Some Thermodynamic Relationship for Soils at or Below the Freezing Point: Freezing Point Depression and Heat Capacity. Water Resources Research, 4, 1968, pp. 379-394.

A.V. Luikov: Analytical Heat Diffusion Theory. Academic Press, New York, 1968, p. 312.

M

M.W. Makowski and K. Mochlinski: An Evaluation of Two Rapid Methods of Assessing the Thermal Relativity of Soil. Proceedings. Institution of Electrical Engineers, 103, A (11), 1956, pp. 443-470.

S. Masamune and J.M. Smith: Thermal Conductivity of Beds of Spherical Particles, Ind. and Eng. Chem. Fundamentals, 2, (2).

Mc Gaw: Thermal Conductivity of Compacted Sand/Ice Mixtures. Highway Res. Rec. 215, 1968, pp. 35-47.

R. McGaw: Heat Conduction in Saturated Granular Materials, Highway Res. Board. Spec. Rep. No. 103, 1969, Pp. 114-131.

R.E. Meredith and C.W. Tobias: Resistance to Potential Flow through a Cubical Array of Spheres. J. Appl. Phys. 31, (7), pp. 1270-1273.

M.N. Miller: Bounds for Effective Electrical, Thermal and Magnetic Properties of Heterogeneous Materials, J. Math. Physics, 10, (11), 1969, pp. 1988-2004.

A. Missenard: Conductivité Thermique. Editions Eyrolles, Paris 1965, p. 356.

N

Y. Nakano and J. Brown: Mathematical Modeling and Validation of the Thermal Regimes in Tundra Soils. Arctic and Alpine Research 4, (1), 1972, p. 19-38.

O

K. Ofuchi and D. Kunii: Heat-Transfer Characteristics of Packed Beds with Stagnant Fluids, Int. J. Heat Mass Transfer, 8, 1965, pp. 749-757.

P,Q

E. Palm et al: On steady convection in a porous medium. Preprint series. Matematisk Institutt. Universitetet i Oslo, 1971.

F.J. Pettijohn: Sedimentary rocks. Second edition. Harper & Brothers, New York 1957, p. 115.

J.R. Philip and D.A. de Vries: Moisture Movement in Porous Materials under Temperature Gradients. Transactions American Geophysical Union, 38, (2), 1957, pp. 222-232.

D. Polder and J.H. van Santer: The Effective Permeability of Mixture of Solids. Physica, 12, (5), 1948, pp. 257-271.

S. Prager; Improved Variational Bounds on Some Bulk Properties of a Two-Phase Random Medium, J. Chem. Phys. 50, (10), 1969, pp. 4305-4312.

R

E.H. Ratcliffe: The Thermal Conductivities of Ocean Sediments. J. Geophys. Res. 65 (5), 1960, pp. 1535-1541.

Lord Rayleigh (1892). Referert av Meredith (1969) (18).

J.A. Reynolds and J.M. Hough: Formulae for Dielectric Constant of Mixtures. Proc. Phys. Soc. (London) B70, 1957, pp. 769-775. (Referert H. Fricke (1924)).

R.L. Rollins et al: Movement of Water in Soil due to a Temperature Gradient. Highway Research Board Proc. 33, 1954, pp. 492-508.

C.W. Rose: Water Transport in Soil with a Daily Temperature Wave. I. Theory and Experiment. Aust. J. Soil Res., G. 1968, pp. 31-44.

S

E. Saare and C.G. Wenner: Värmeledningstal hos olika jordarter. Statens nämnd för byggnadsforskning. Handlingar no. 31, 1957.

- J.H. Sass et al: Thermal Conductivity of Rocks from Measurements on Fragments. J. Geophys. Res. 76. (4), pp. 3391-3401.
- A.E. Scheidegger: The Physics of Flow through Porous Media. Univ. of Toronto Press, 1957.
- E. Schmidt: Einführung in die Technische Thermodynamik. Springer Verlag, Berlin 1963, p. 394.
- R. Selmer-Olsen: Om norske jordarters variasjon i korngradering og plastisitet. Norges Geologiske Undersøkelse no. 186, 1954, p. 40 and fig. 30.
- R. Selmer-Olsen: En regional undersøkelse av norske kvartaere leirers finfraksjon basert på DTA. Rapport sendt til NTNf. Geologisk Institutt, NTH, Trondheim 1961, p. 29 f.f..
- R. Selmer-Olsen: Ingeniørgeologi. Del 1. Generell geologi. Tapir forlag. Trondheim 1971, pp. 8, 12 and 175.
- R. Selmer-Olsen: Ingeniørgeologi. Del II. Løsmasser. Kompendium. Geologisk Institutt. NTH, 1973.
- W.A. Sinclair et al: Soil Thermal Resistivity. Typical Field Values and Calculating Formulas, part IV. In: Soil Thermal Characteristics in Relation to Underground Power Cables. AIEE Transaction paper No. 60-785, pp. 71-94.
- A.G. Shashov et al: Thermophysical Properties of Thermally Insulating Materials in the Cryogenic Temperature Region. Int. J. Heat Mass. 15, 1972, pp. 2385-2390.
- I. Szanto and J. Aquirre Puente: Etudes des caracteristiques thermiques des milieux poreux fins humides. Proc. XIIIth Intern Congr. of Refrigeration. Washington, D.C. 1971, Vol. I, pp. 751-757.
- Sv. Skaven-Haug: Frostfundamenters dimensjonering. Frysevarme og jordvarme. Frost i jord, (3) 1971, pp. 9-27.
- Sv. Skaven-Haug: The Design of Frost Foundations. Norwegian Geotechnical Institute. Publ. 90, Oslo 1971.
- Sv. Skaven-Haug: Romforhold i jordmaterialer. Meddelelser fra det norske myrselskap. 70, (4) 1972, pp. 89-102.
- W.O. Smith and H.G. Byers: The Thermal Conductivity of Dry Soils of Certain of the Great Soil Group. Am. Soc. Soil Sci. Proc. 3, 1938, pp. 13-19.
- W.O. Smith: Thermal Conductivities in Moist Soils. Soil Sci. Soc. Am. Proc. 4, 1939, pp. 32-40.

- W.O. Smith: The Thermal Conductivity of Dry Soil. Soil Science, 53, 1942, pp. 435-459.
- H. Sveian: Norske jordarters kvartsinnhold. Hovedoppgave i Ingeniørgeologi, Geologisk Institutt, NTH. Høst 1972.
- H. Sveian: Undersøkelse av kvartsinnhold i løsmasser ved hjelp av DTA. Utført for Institutt for kjøleteknikk, Trondheim, 1973.
- I. Szanto and J. Aguirre Puente: Etude des caractéristiques des milieux poreux fins humides.

T

- K. Terzaghi and R.B. Peck: Soil Mechanics. John Wiley & Sons, New York, 1948, p. 32.
- J. V. Thue: Redusert fundamentdybde, - termiske problemer. Del I. Institutt for husbyggingsteknikk. Trondheim, NTH, p. 82.
- A.R. Tice et al: The prediction of Unfrozen Water Contents in Frozen Soils from Liquid Limit Determinations. Symposium on Frost Action on Roads. I. OECD. Paris 1973, pp. 329-344.
- G.T. Tsao: Thermal Conductivity of Two-Phase Materials. Ind. Eng. Chem. 53, (5), 1961, pp. 395-397.

U,V,W

- E.M.F. van der Held and F.G. van Drunen: A Method of Measuring the Thermal Conductivity. Physica 15, (10), 1949, pp. 865-881.
- M. van Rooyen and H.F. Winterkorn: Structural and Textural Influences on Thermal Conductivity of Soils. Highway Research Board. Proceedings. Washington, D.C. 1959, pp. 576-621.
- L. van Zee and C.L. Babcock: A Method for the Measurement of Thermal Diffusivity of Molten Glass. J. Am. Ceram. Soc., 34 (8) 1951.
- Vegnormaler. Statens vegvesen. Vegbygging. Overbygning med bituminest dekke. 1970. Kapittel VI. Avan...3.

- K. Wakao and K. Kato: Effective Thermal Conductivity of Packed Beds. Journal of Chemical Engineering of Japan. 2, (1), 1969, pp. 24-33.
- N. Wakao et al: View Factor between two Hemispheres in Contact and Radiation Heat-Transfer Coefficient in Packed Beds. Int. J. Heat Mass Transfer, 12, 1969, pp. 118-120.
- N. Wakao: Effect of Radiating Gas on Effective Thermal Conductivity of Packed Beds. Chemical Engineering Science, 28, 1973, pp. 1117-1118.
- G.K.H. Walther: Zur mathematischen Behandlung der Stationären Wärmeleitung in stückweise homogen Medien. Kernforschungsanlage Jülich. 657-MA, 1970.
- J.E. Warren and H.S. Price: Flow in Heterogeneous Porous Media. Society of Petroleum Engineers Journal, Sept. 1961, pp. 153-169.
- A. Watzinger et al: Undersøkelse av masseutskiftningsmaterialer for veg og jernbanebygging. Medd. fra Vegdirektøren 1938, no. 6.
- A. Watzinger et al: Undersøkelse av masseutskiftningsmaterialer for veg og jernbanebygging. Medd. fra Vegdirektøren 1941, no. 6, 7 and 8.
- A. Watzinger et al: Masseutskiftningsmaterialer for teleforbygning på veg og jernbane. Norges Geotekniske Institutt. Oslo 1965, p. 106.
O. Wiener (1912): Referert av W.F. Brown (1965).
- P.J. Williams: Unfrozen Water Content of Frozen Soils and Soil Moisture Suction. Geotechnique, 14 (3) 1964, pp. 231-246.
- W. Woodside: Probe for Thermal Conductivity Measurement of Dry and Moist Materials. Heating, Piping & Air Conditioning, Sept. 1958, pp. 163-170.
- W. Woodside and J.B. Cliffe: Heat and Moisture Transfer in Closed Systems of Two Granular Materials. Soils Science, 87, 1959, pp. 166-173.
- W. Woodside and C.M. A de Bruyn: Heat Transfer in a Moist Clay. Soil Science, 87, 1959, pp. 166-173.
- W. Woodside and J.H. Messmer: Thermal Conductivity of Porous Media. I. Unconsolidated Sand. J. Appl. Phys., 32, (9) 1961, pp. 1688-1699.

X,Y,Z

S. Yagi and D. Kunii: Studies on Effective Thermal Conductivities in Packed Beds. A.I. Ch. E. Journal, 3, (3), 1957, pp. 373-381.

P. Zehner and E.U. Schlunder: Einfluss der Wärmestrahlung und des Druckes auf den Wärmetransport in nicht durchgeströmten Schüttungen. Chemie-Ing.-Techn. 44 (23), 1972, pp. 1303-1308.

INTRODUCTION

Knowledge of heat related parameters for minerals is necessary in connection with any analysis of temperature distributions in the ground. This is particularly important when analysing structures which are subject to frost or have to be protected against thawing (structures in permafrost). Artificial freezing of soil or crushed rock in connection with tunneling and control of temperature distribution around buried LNG storage tanks are other areas where thermal analysis is applied and for which knowledge of thermal properties of minerals is crucial.

When such analysis is to be performed, there is often information available about the kinds of minerals involved but only seldom are thermal parameters known for the entire structure. Thus, in most cases one has to determine these parameters from the more or less complete information available about the minerals. In short, this is the starting point for this study and the emphasis is placed on finding methods for determining thermal properties of the minerals.

Methods which have been mostly used previously to treat this problem have been based on empirical correlation between a limited set of mineral parameters and results from systematic heat transfer measurements with selected minerals. This has given results with relatively wide tolerance limits. These methods may have been satisfactory for approximate determination of frost penetration. However, while using modern computer programs for finding temperature distribution in the ground, researchers have felt a need for improved accuracy of thermal parameters.

A possible approach for narrowing the tolerance limits would be to utilize more mineral parameters when correlating with experimental results. This would certainly require a very comprehensive experimental data base with wide variation span in types of minerals and choice of parameters. Before such an experimental program is

undertaken, one has to clarify the most fundamental relations between mineral parameters and thermal properties, in order to arrive at the most conclusive test program possible.

In the study at hand it has been found that it is more useful to emphasize clarification of basic relations through theoretical studies of, among other things, heat transport processes in moist materials and heat conductivity of composite minerals. This analysis has resulted in a method for reduction of experimental data which has made it possible to utilize already existing test data for developing a complete method for determining thermal properties of soil materials. At the same time, these methods will allow more efficient planning of future test programs.

Still, the extensive measurements which are required to supplement existing results and verify their validity for Norwegian conditions will place great demands on our capacity for testing. To meet these requirements, it has been necessary to develop new and more efficient methods of measuring thermal properties of soils. However, heat conduction measurements in moist materials pose very special requirements on test methods, due to moisture transport in the presence of temperature gradients. Thus, one must try to find methods which combine the requirements on short test periods and small temperature gradients. As part of this effort, several types of test gear for measuring conduction have been developed and built. These may be a valuable supplement to more conventional, stationary test equipment.

To arrive at a method for determining thermal conduction properties in minerals, which can be used at several levels, it was necessary to clarify basic relations between conventional data for soil materials and the more fundamental parameters which determine thermal conduction properties. Through these studies, an effort has been made to arrive at relations which can be utilized for indirect determination of parameters which in many cases are left out during

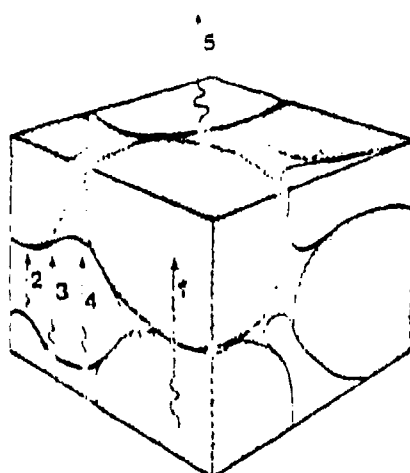
geotechnical analysis. A mathematical model developed along these lines will consequently give increased accuracy in proportion to the information available on the minerals involved. When using mathematical models it is important to know the relation between accuracy and level of information. Part of this report is therefore devoted to a study of this topic. The effects of uncertainties in thermal conductivity values on thermal computations is also discussed.

These introductory remarks are intended to give an overview of the approach taken for the study at hand. It will be evident that this study has an interdisciplinary character, in that areas which traditionally fall outside the field of thermal technology have been treated. For experts in those areas, the material may appear elementary and in part superficial. However, the main intent is to include all major aspects in developing the mathematical model.

CHAPTER I

HEAT TRANSPORT IN MOIST SOIL.

For computing temperature distribution in and around structures placed on the ground one normally uses ordinary differential equations for heat conduction, together with boundary conditions (39). Heat transport in moist and porous materials can, however, be influenced by a number of different mechanisms, in addition to heat conduction. If these phenomena can be incorporated in an equivalent heat conductivity for the porous material, one can without significant difficulty use numerical methods designed to handle nonlinear problems involving temperature dependent thermal parameters. Problems arise only when the heat transport is controlled by potentials other than the temperature gradient, so that the mass distribution becomes a function of time.



1. Leading & partikler og
væske. Conduction in solid
and liquid.
2. Leading & luft. Conduction
in air.
3. Stråling mellem partikler.
Radiation particle to
particle.
4. Diffusion.
Vapour diffusion.
5. Konvektion i poreluft.
Convection in pore air.

FIG. 1. Varmetransportmekanismer i fuktig jord. Heat
transfer mechanisms in moist soil.

The different mechanisms which can contribute to heat transport in a moist soil material are illustrated in Figure 1. These mechanisms will be discussed in the following, in order to clarify some of the limitations inherent in a mathematical model on heat conduction only.

1. THERMAL RADIATION

The share of thermal radiation in the effective heat conductivity increases with increased pore area and increasing temperature. This can be illustrated by the simple case of radiation across a gap between two parallel surfaces at temperatures T_1 and T_2 . If the emissivity of both surfaces is ϵ , the transferred heat flux can be expressed as

$$q_{12} = \frac{\sigma}{2/\epsilon - 1} (T_1^4 - T_2^4) \text{ (W/m}^2\text{)} \quad 1$$

where σ is the radiation constant for a black surface.

($\sigma = 5.77 \cdot 10^{-8} \text{ W/m}^2 \text{ K}^4$)¹⁾. The resulting contribution λ_r to the effective heat conductivity across the slot is given by

$$\lambda_r = q_{12} \delta / (T_1 - T_2) \text{ (W/mK)} \quad 2$$

where δ is the width of the gap.

1) K here stands for degrees Kelvin (Translator's Note).

If $T_1 - T_2$ is small (which is often the case for narrow gaps),
Eqs 1 and 2 give

$$\lambda_r = \frac{4\sigma}{2/\epsilon - 1} T^3 \delta \quad (\text{W/mK}) \quad 3$$

One can also define a heat conduction coefficient for radiation
across a gap

$$\alpha_r = \frac{4\sigma}{2/\epsilon - 1} T^3 \quad (\text{W/m}^2\text{K}) \quad 4$$

Expressions 3 and 4 cannot readily be applied to the complicated
geometry of e.g. a particle fill. Still, similar expressions have
been used as a basis for several studies of radiation effects in
particle fills. (1,2,3). Wakao and Kato (4,5) have instead used
the radiation transfer between two half spheres touching each
other, where each sphere is assumed to have a constant surface
temperature. This led to a heat transfer coefficient based on the
areas of the spheres

$$\alpha_r = \frac{4\sigma}{2/\epsilon - 0.264} T^3 \quad (\text{W/m}^2\text{K}) \quad 5$$

Wakao and Kato used this heat transfer coefficient for numerical
analysis of regular lattices of identical spheres (4,5,6). Two
packing configurations were studied, cubic lattice with an equi-
valent porosity $n = 0.476$ and orthorhombic lattice with an equivalent
porosity $n = 0.395$. Figure 2 shows the two packing configurations
and the assumed heat flow is indicated by arrows.¹⁾

1) There seem to be no "arrows" in Figure 2, but that is what
the text says. (Translator's note)

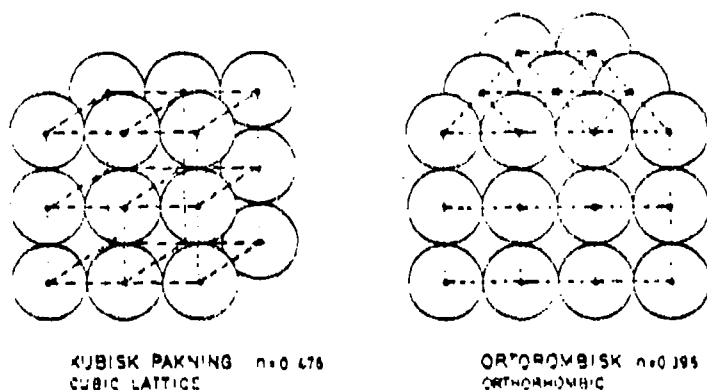


FIG. 2. Regular kulepakninger for numerisk analyse.
Regular sphere packings for numerical calculations.

The results of their computations were presented in the form of curves with a dimensionless Nusselt number for radiation Nu_r as a parameter.

$$Nu_r = \alpha_r d_p / \lambda_s$$

6

where α_r is defined by Eq 5, d_p is the particle diameter and λ_s is the thermal conductivity of each particle. Figure 3 shows the result obtained for orthorhombic configuration ($n = 0.395$).

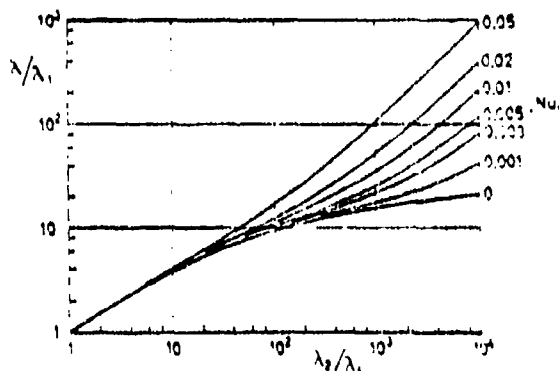


FIG. 3. Innflytelsen av stråling på ledningsevnen av
regulære kulepakninger (basert på data 1971).
Influence of radiation on the conductivity of
regular sphere packings.

Comparable results have been presented by Zehner and Schlunder (3). Although their calculations were based on a different model, the results do not differ significantly from those quoted here.

Even if soil conditions differ significantly from the comparatively simple geometrical models on which Wakao's results are based, in terms of granule shape and size as well as packing configuration, these results can give a hint as to the magnitude of the effects of radiation. In addition, one may assume that the effect of radiation is less when the particle sizes vary widely, as compared to spheres of the same diameter, even if the average size is the same in both cases. The following calculations can thus be assumed to yield an upper bound for the effects of thermal radiation.

Wakao and Kato (5) have used the results shown in Figure 3 to derive an empirical equation of the form

$$\lambda_e = \lambda_e^0 + 1.3 \cdot \alpha_r \cdot d_p \quad (\text{W/mK}) \quad 7$$

where λ_e^0 is the effective thermal conductivity of the material when no radiation takes place. This equation was derived on the basis of both packing configurations and is said to be approximately valid also outside the considered range of porosity ($n = 0.395$ to 0.476).

Eq 7 and the results shown for $Nu_r = 0$ in Figure 3 were used for calculating the following examples. Since the study of dry soil is of interest, thermal properties for gas and solid material are assumed to be those of air and granite, respectively. See Table 1.

Table 1. Conductivity for air and granite at different temperatures W/mK.

Temperature, °C	-50	0	50	100	150	200
Air (7)	0.0164	0.0241	0.0277	0.0310	0.0338	0.0367
Granite (8)	3.91	3.65	3.37	3.11	2.94	2.79

It should be noted that the conductivity for air increases with temperature, while the opposite occurs for granite. The same is true for most minerals, except for some alkaline materials such as gabbro, for which the conductivity is nearly constant or decreases slightly with temperature in this range (8).

Figure 4 shows the results for different particle size, as function of temperature. One finds that even for a particle diameter of 20 mm, the effect of radiation amounts to no more than 10 percent at normal atmospheric temperatures, while in sand (particle diameters below 2 mm) the effect is less than 1 percent under the same conditions. In these calculations, the porosity was assumed to be $n = 0.395$ (orthorhombic configuration), which corresponds to a dry density for sand of about 1600 kg/m^3 . For higher densities, the effect of radiation will of course be even less and in moist materials it will be completely insignificant. In short, this indicates that radiation will be responsible for a negligible portion of the heat transport on moist soils, while it can play some part in coarse, crushed stone materials.

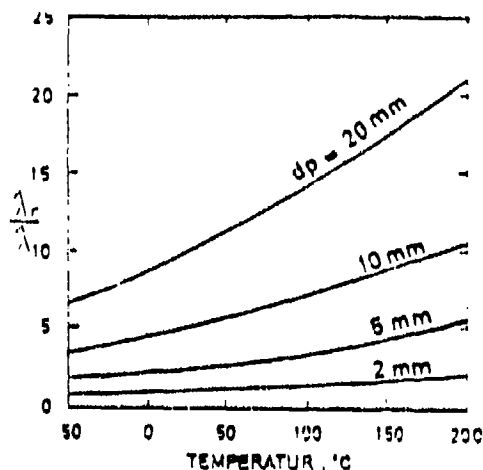


FIG. 4. Indflytelse af stråling på ledningsevnen i tørre jordmaterialer. Beregninger baseret på ligning 7 og fig. 3. Influence of radiation on the conductivity of soils. Calculations based on equation 7 and fig. 3.

$$q_v = \frac{D_a}{RT} \nabla p \quad (\text{kg/m}^2\text{s}) \quad 3^1)$$

R is the water vapor gas constant (461 J/kgK)

T is absolute temperature (K)

p is water vapor partial pressure (bar, 10^5N/m^2)

D_a is water vapor diffusion coefficient in air (m^2/s)

Krishner and Rohmaltor (9) have determined this diffusion coefficient to be

$$D_a = \frac{0.244}{P_0} \cdot \frac{T}{273}^{2.3} \quad (\text{m}^2/\text{s})$$

where P_0 is the total pressure (bar).

The water vapor pressure in a soil material will depend on both temperature and relative humidity of the air in the pores. The relative humidity also depends on how firmly bound the water is. The binding energy can be described by a moisture potential and the relative humidity ϕ is given by

$$\psi = \rho_w RT \ln \phi \quad (\text{N/m}^2) \quad 9$$

ρ_w is the density of water (kg/m^3)

R, gas constant of water vapor (461 J/kgK)

T, absolute temperature (K)

The dependence of ψ on water content depends on the soil material. Figure 5 shows moisture potential curves for a number of selected soil materials. The scale for relative humidity is derived from Eq. 9 and superimposed on the scale for moisture potential.²⁾

1) In the original, p is shown as a subscript to the gradient symbol ∇ . The same occurs in Eq 10, but the more conventional notation has been chosen for the translation.

2) "Moisture potential" could also be termed "suction".

(Translator's notes)

It is evident that the relative humidity falls off significantly only for comparatively low water content, even for finer grain soils.

If one assumes a certain relative humidity ϕ in the pore air, the vapor pressure gradient can be expressed as a total differential which is a function of the gradients for both humidity and temperature

$$\nabla p = p'' \frac{\partial \theta}{\partial \phi} \nabla \theta + \phi \frac{\partial p}{\partial T} \nabla T \quad 10$$

where θ is the water content in volume ratio.

The first term¹⁾ in the right hand member of Eq 10 represents the pressure gradient due to moisture gradients, while the second term expresses the vapor pressure gradient due to temperature variations.

As previously mentioned, Eq 8 (Fick's law) is valid for diffusion of water in air. In soil materials, the diffusion rate will be reduced due to presence of water and particles. Experiments with porous materials show that the diffusion rates are strongly reduced as the porosity decreases in dry materials. Figure 6 shows results from measurements by Currie on diffusion of hydrogen in dry and moist soils (13, 14).

However, Philip and de Vries (15) have pointed out that water vapor and gas diffusion in moist materials are different, since water and water vapor interact.

1) Double prime on p stands for saturation pressure. See notations. (Translator's note).

2. COMBINED MOISTURE AND HEAT TRANSPORT

A. Water vapor diffusion

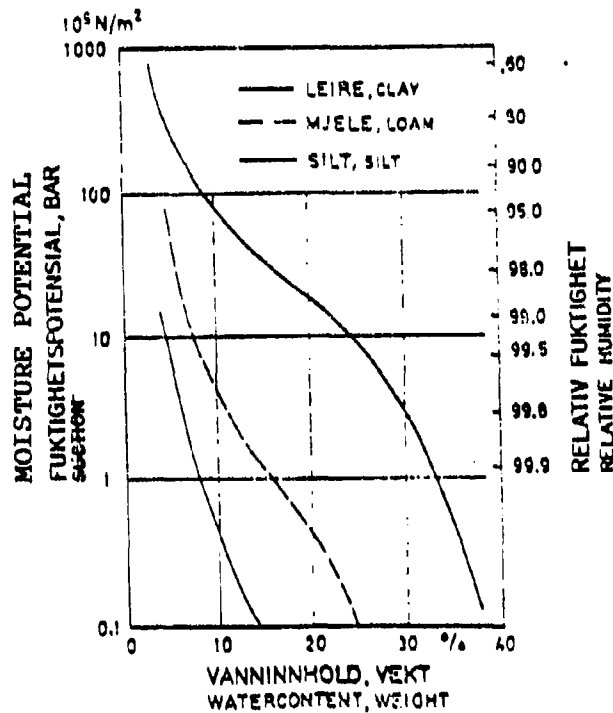
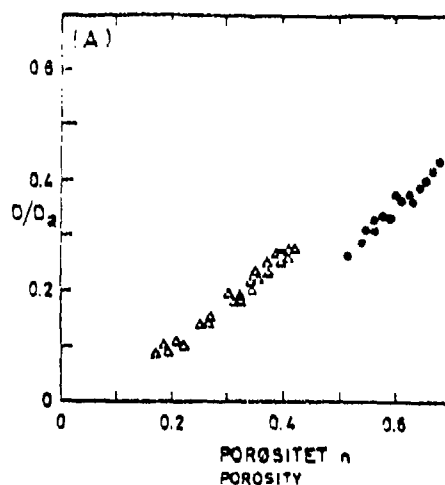
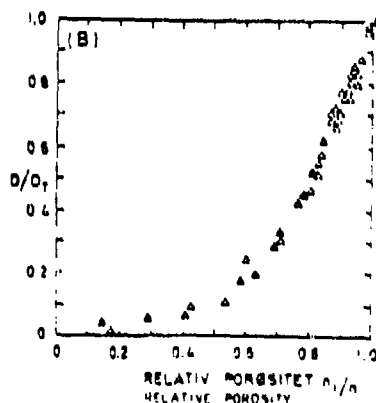


FIG. 5. Fuktighetspotensial og relativ fuktighet i forskjellige jordarter. Suction and relative humidity of different soils.

Partial pressure variations for water vapor in the pores of a soil material will cause diffusion in the direction of falling pressure. Water vapor diffusion in air is determined by Fick's law



A. Diffusjon i tørre materialer. D_a er diffusjonstall for hydrogen i luft. Diffusion in dry materials. D_a is coefficient of diffusion of hydrogen in air.



B. Diffusjon i fuktig jord. D_r er diffusjonstall for hydrogen i tilsvarende tørre materialer. n_r er volumandel i luft. Diffusion in moist soils. D_r is coefficient of diffusion in corresponding dry materials. n_r is volumefraction of air.

FIG. 6. Målinger av diffusjon av hydrogen i jord og fyllinger av glasskuler (Currie 1960, 1961). Diffusion of hydrogen in soils and beds of glass spheres.

BEST AVAILABLE COPY

They claim that this permits water transport via water lenses in the moist soil material, of the same magnitude as that due to vapor diffusion. The temperature dependent diffusion is also governed by the temperature gradients in the air within the pores, which is always greater than the average gradient. Together, these effects result in a larger diffusion in moist soils than that obtained by considering diffusion rates for gases only.

Based on the previous discussion one can define two diffusion coefficients for vapor diffusion due to moisture and temperature variations, D_{θ_v} and D_{T_v} , respectively

$$q_v/\rho_w = - D_{\theta_v} \nabla \theta - D_{T_v} \nabla T \quad (\text{m}^3/\text{m}^2\text{s}) \quad 11$$

where both D_{θ_v} (m^2/s) and D_{T_v} (m^2/sK) contain correction factors which account for the previously mentioned increase in diffusion rate, relative to the case of gas diffusion in comparable materials.

The moisture dependent diffusion rate for different water content is very dependent on the shape of the water potential curve for the soil material (Figure 5), i.e. of (ψ/ψ_0) , c.f. Eq 10. This means that the contribution due to moisture dependent diffusion will be quite small except for the lowest values of water content where the relative humidity falls significantly below $\phi = 1.0$.

On the other hand, the temperature dependent diffusion coefficient D_{T_v} will decrease when the relative humidity in the soil starts to fall off due to low water content. It will also decrease when the water content increases, since the pores are then to a large extent filled with water. The maximum for D_{θ_v} ¹⁾ will occur for relatively low water content, when there is still a low degree of continuity in the pore water. (c.f. ref. 13)

1) From the context it appears that this is a misprint in the original. It should probably read D_{T_v} . (Translator's note)

B. Capillary water transport.

If a soil material, where the humidity is equally distributed at the outset, is subjected to a temperature gradient, the previously mentioned vapor diffusion will give rise to a transport of moisture in the direction of falling temperature. In a closed system, this will result in a drying out of the warm side and an increase in humidity on the cold side, as has been demonstrated by numerous experiments (16, 17, 18, 19, 20, 21). This will result in moisture gradients, which form a potential for capillary water transport in a direction opposite to that of the vapor diffusion caused by temperature. This water transport depends both on the moisture potential of the soil and on its permeability, i.e. its hydraulic conductivity K (m)¹⁾, for different moisture content. Darcy's law for water transport in moist materials can be expressed as

$$q_1/\rho_w = -KV\phi \quad (m/s) \quad 12$$

K is hydraulic conductivity (m/s)¹⁾

ϕ is the total potential, expressed in metres, which is common in this context.

If the effect of gravity is neglected, the potential gradient is given by the moisture potential ψ (here in metres) and the moisture gradient $\nabla\theta$:

$$\nabla\phi = \frac{\partial\psi}{\partial\theta} \nabla\theta \quad (m/m) \quad 13$$

Eqs 12 and 13 can be used to define a moisture diffusivity

$$D_{\theta_1} = K \frac{\partial\psi}{\partial\theta} \quad (m^2/s) \quad 14$$

Darcy's law (Eq 12) then takes the form

$$q_1/\rho_w = -D_{\theta_1} \nabla\theta \quad 15$$

1) The original gives two units for K , m (length) and m/s (velocity). (Translator's note)

The change in this moisture diffusivity due to varying water content is highly dependent on the hydraulic conductivity K . Figure 7 shows its variation for some fine grain soils. It can be seen that the diffusivity decreases sharply for low water contents, where the continuity of the pore water is broken. It is also evident that this decrease occurs for higher water content in the finer grain materials.

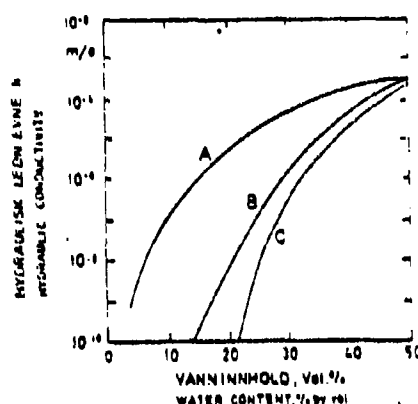


FIG. 7. Hydraulisk lednings-
evne av noen jordarter
(Kunze 1961). Hydraul-
ic conductivity of
some soils.

- A. Medium sand
- B. Leirig allt
silt loam
- C. Siltig leire
silty clay loam

Figure 8 shows a partially qualitative¹⁾ summary of how the previously defined diffusivities change as function of water content. The broken (dotted) lines indicate how the three diffusivities tend to fall for a finer grain material. This partially qualitative presentation shows a region for relatively low water contents where the thermal vapor diffusivity dominates over the two moisture dependent diffusivities. As indicated, this region will move

1) The original uses the word "skjematisk", translated by "schematically" in Fig 8, which indicates an intention to show a qualitative trend rather than to present quantitative numbers. (Translator's note)

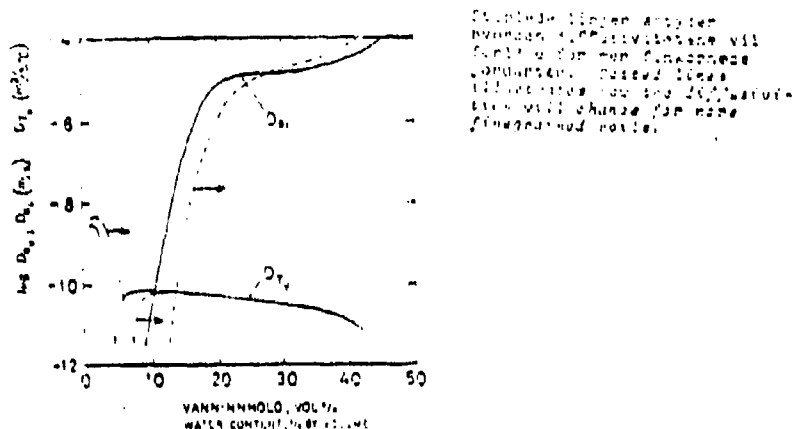


FIG. 8. Forløpet av de forskjellige fuktdiffusiviteter vist skjematisk. Moisture diffusivities drawn schematically.

In experiments where moist soil materials are subjected to temperature gradients, it has also been demonstrated that remarkably large moisture gradients occur for comparatively low water content. As an example, Figure 9 shows the results obtained in Smith's classic experiments in 1939 (22). Somewhat simplified, Smith calculated the moisture gradient as the difference in water content between the cold and warm sides of the test container (which was 3/4" thick). The temperature gradients are in the order of 4°C/cm, but vary somewhat from experiment to experiment. The settling¹⁾ time is not given

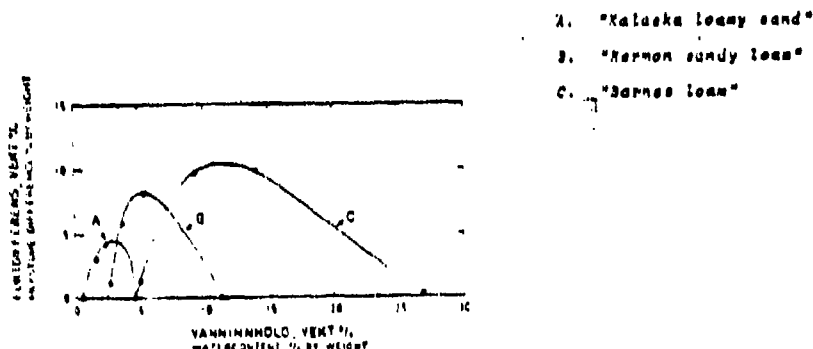


FIG. 9. Fuktgradienter over jordersver utsatt for temperaturgradienter på ca. 4°C/cm (Smith 1939). Moisture gradients in soil samples from temperature gradients of 4°C/cm.

1) "Oppholdstid" means "duration", i.e. the time during which the moisture gradient were allowed to build up. (Translator's note)

Evidently, also in this case the previously mentioned tendency is present for translation of the critical region towards higher water content for finer grain soil materials.

This effect is obviously very important in connection with experiments designed to determine thermal conductivity of soils. This will be discussed in more detail in the chapter on heat conduction measurements (chapter IV).

C. Contribution of vapor diffusion to thermal conductivity.

The mentioned vapor diffusion will contribute to the heat transport in the form of latent heat exchanged during vaporization and condensation. The temperature dependent vapor diffusion will be controlled by the same temperature field as the thermal conduction in the pore air. It is thus possible to include this contribution to the heat transport in the apparent thermal conductivity. The vapor pressure gradient due to a temperature gradient was given by Eq 10:

$$\nabla p_t = \phi \frac{\partial p''}{\partial T} \nabla T \quad 16$$

According to Fick's law, the amount of diffused vapor is given by

$$q_v = \frac{D_a}{RT} \phi \frac{\partial p''}{\partial T} \quad (\text{kg/m}^2\text{s}) \quad 17$$

while the amount of transported heat is

$$q = r q_v \quad (\text{W/m}^2) \quad 18$$

where r is the latent heat due to vaporization of water, equivalent to 2450 KJ/kg at 20°C/

The contribution to the air conductivity is

$$\lambda_v = \phi \frac{rD_a}{RT} \frac{\partial p''}{\partial T}$$

19

while the apparent air conductivity λ' is given by

$$\lambda' = \lambda_a + \lambda_v$$

20

where λ_a is the conductivity of air.

Figure 10 shows how λ_v varies as a function of temperature ($\phi = 1.0$), as compared to the conductivities for air and water at the same temperatures (23).

The rapid rise with increasing temperature is clearly due to the fact that the water vapor pressure increases almost exponentially with temperature.

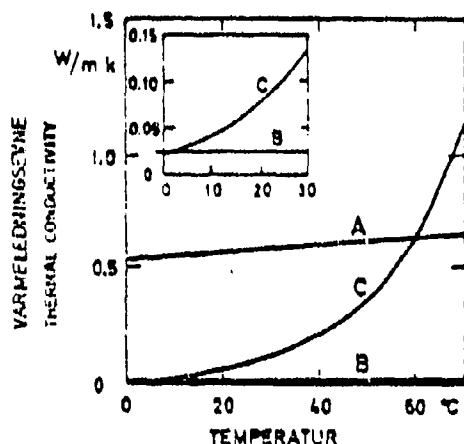


FIG. 10.
Dampdiffusionsbidrag till
värmeledningsvärdet i fuktig luft
(kurva C) summerat med
värmeledningsvärdet av luft (B)
och vatten (A). Apparent
conductivity of moist air
due to vapour diffusion (C),
compared to conductivities
of air (B) and water (A).

This phenomenon is a major contribution to the increase in conductivity with increasing temperature for moist soil materials. This is evident from measurements of thermal conductivity performed by de Vries on sand at various temperatures. His results are reproduced in Figure 11. For both extremely high and low saturation levels, where the thermal vapor diffusion is li-

mitted, the dependence on temperature is weak, while this dependence is strong for low to moderate degrees of saturation, where the thermal diffusion is significant.

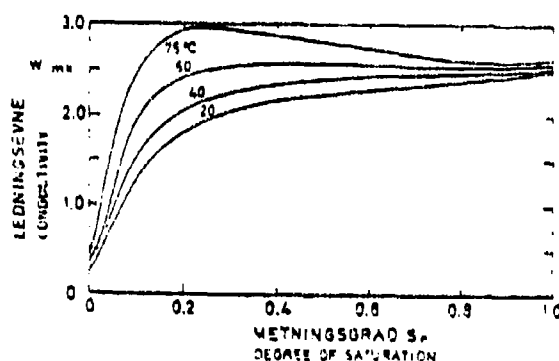


FIG. 11. Varmerledningssevne av fuktig sand ved forskjellige temperaturnivåer (de Vries 1952). Thermal conductivity of moist sand at different temperature levels.

The moisture dependent vapor diffusion will also contribute to the heat transport when latent heat is transferred. Phillip and de Vries (15) have combined the contributions of vapor diffusion to heat transport in a differential equation for thermal conductivity in soil

$$C \frac{\partial T}{\partial t} = \nabla(\lambda_e \nabla T) + r \nabla(D_{e_v} \nabla \theta) \quad 21$$

C is the specific heat, by volume, of the soil material (J/m^3K).

λ_e is the thermal conductivity of the soil material, including the contribution from vapor diffusion (W/mK).

This equation differs from the conventional differential equation for thermal conduction, the Fourier equation

$$-\frac{\partial T}{\partial t} = a \nabla^2 T \quad 22$$

$a = \frac{\lambda}{c_p}$, thermal diffusivity (m^2/s)

c is specific heat (J/kgK)

ρ is density (kg/m³)

First of all, Eq 21 assumes a temperature dependent thermal conductivity, while the Fourier equation usually presumes constant thermal properties. In addition, Eq 21 contains a term which is related to humidity. This creates obvious problems in connection with thermal conductivity measurements in moist soil materials, when transient methods are used and the result interpretation is based on the simple Fourier equation. These problems will be discussed in the chapter on heat conductivity measurements (Chapter IV). In this context it should be pointed out that the problem is simplified somewhat by the fact that the last term in Eq 21 usually is negligible, except for extremely low water content when the relative humidity in the soil starts to decrease. As mentioned previously the water content will also increase for more fine grain materials.

3. CONVECTION

A. Heat transport

Heat transport due to convection in porous materials can be of two types, forced convection and free convection. The first type is due to forced currents in the liquid which fills the pores, while the second type is caused by temperature gradients and upward migration of the liquid. Forced convection in soils and fill materials can, for example, be associated with ground water flow or wind forces on exposed fill such as railroad banks. Free convection can occur due to upward heat flow in rock fill.

The total heat transport due to thermal flux in porous materials can be ascribed to several phenomena (mechanisms). Except for heat transport via currents in the liquid, heat conduction in solid particles and in the liquid are the most significant. In

addition, convection between particles and liquid may contribute, as well as heat transport due to "turbulent" mixing of liquids with different temperatures within the "pore strata". The latter effect is often termed "turbulent diffusion" or dispersion and can be included as a velocity dependent contribution to the thermal conductivity of the liquid (25).

For low velocities of flow, the temperature differences between liquid and particles will be small and the convection between these media can be neglected. The total heat transport can then be described by the equation

$$\lambda'_e v^2 T + (c_p)_f \bar{v} \nabla T = (c_p)_m \frac{\partial T}{\partial t} \quad 23$$

λ'_e is the effective conductivity for the porous material, including the contribution from dispersion (W/mK)

$(c_p)_f$, (is) thermal capacity of the liquid (J/m³K)

$(c_p)_m$, (is) thermal capacity of the liquid-filled porous material

Eq 23 is used for determining the equivalent (effective) thermal conductivity in experiments with flowing liquids or gases, e.g. in columns filled with spherical particles (25, 26, 27). Such experiments have been made with the axial thermal flow both in the same and the opposite direction of that of the liquid. In both cases one has found a significant increase in the equivalent conductivity λ_e when the flow rate increases. This increase is comparable to the previously mentioned contribution from turbulent diffusion, see Fig 12¹⁾.

It appears as if no experiments have been performed with vertical

1) This sentence was almost unreadable in the original (page 17, bottom), so this is a "guesstimate". (Translator's note)

heat flow and planar horizontal liquid flow in porous materials, similar to horizontal ground water flow in a soil layer. There is still reason to assume that the previously mentioned increase in the effective vertical conductivity also should occur in such cases, provided that the flow rate is sufficiently high.

Yagi and Kunii have formulated a partially empirical expression for the effect of axial liquid flow on the radial thermal conductivity in particle filled columns. They define the effective conductivity as a sum

$$\lambda_e^1 = \lambda_e^0 + \lambda_t$$

24

where λ_e^0 is the conductivity for no liquid flow

λ_t is the contribution due to "lateral mixing"

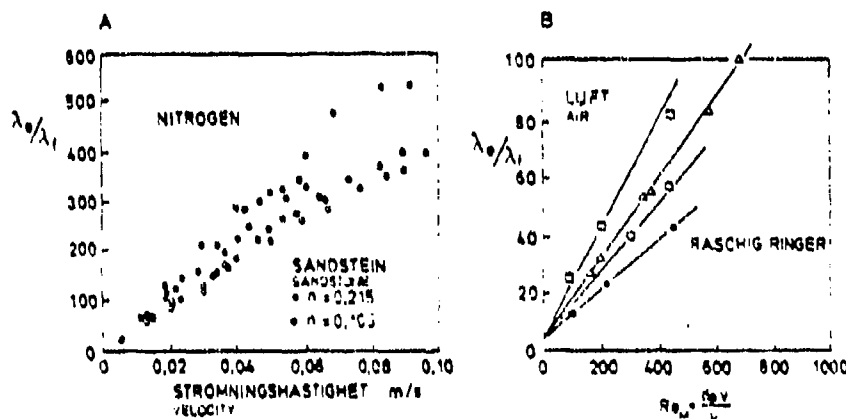


FIG. 12. Innflytelse av strømmende væske på effektiv leuingssevne av porøse materialer. A. Varmestrom i rødstrom med væske (24). B. Påvirkning av flytende væske på den effektive konduktiviteten av porøse materialer. A. Varmestrom og væske (24). B. Varmestrom og væske (24).

BEST AVAILABLE COPY

The contribution λ_c is given by

$$\frac{\lambda_t}{\lambda_f} = (\alpha\beta) P_{e_m} \quad 25$$

α and β are dimension-less factors

P_{e_m} , modified Peckel's number

$$P_{e_m} = d_p (c\phi)_f v / \lambda_f$$

d_p is the average particle diameter (m)

$(c\phi)_f$ is the specific heat, by volume, of the liquid (J/m³K)

v is liquid flow rate in open cross-section (m/s)

λ_f is thermal conductivity of the liquid (W/mK)

Values for $(\alpha\beta)$ are determined empirically for various particle configurations. For spheres and cylinders, $(\alpha\beta)$ has been found to be in the range 0.08 to 0.14 (26).

As shown by Eq 24, the contribution due to liquid flow will increase in proportion to average particle size and liquid flow rate.

B. Liquid transport in porous materials

For low flow rates, the liquid transport in porous materials is determined by Darcy's law (27)

$$\vec{v} = - \frac{k}{\eta} (\nabla p - \rho \vec{g}) \quad 26$$

v is velocity (flow rate)¹ in "open cross-section"

k is the permeability

η is the dynamic viscosity of the liquid

1) The original does sometimes not clearly define whether "liquid transport" refers to flow rate (m³/s or kg/s) or velocity (m/s). I sincerely hope the distinction is evident to the reader (Translator's note)

ρ is the density of the liquid
 P is the pressure in the liquid
 g is the gravitation (acceleration) constant

The permeability k depends on the particle size, distribution and shape, in addition to the porosity of the material. The frequently used Kozeny-Carman equation for permeability contains porosity n , as well as specific surface area per unit volume, S :

$$k = \frac{n^3}{5S^2(1-n)^2} \text{ (m}^2\text{)} \quad 27$$

The specific surface area for particles with diameter d_p is given by

$$S = 6/d_p \text{ (m}^2\text{/m}^3\text{)} \quad 28$$

This results in the following expression for the permeability of fills consisting of identical spheres:

$$k = \frac{n^3}{180(1-n)^2} d^2 \text{ (m}^2\text{)} \quad 29$$

For a mixture of spheres of different diameters one can use an equivalent diameter d_p . From calculations of specific surface area one finds that this average or equivalent diameter should be the harmonic mean of the different diameters

$$\frac{1}{d_p} = \frac{\sum_{i=1}^n \frac{P_i}{d_i}}{\sum_{i=1}^n P_i} \quad 30$$

This means that the equivalent diameter will be close to the smallest diameter in the particle distribution. In empirical formulas for the permeability of sand one can thus use d_{10} or d_{30} (i.e. the diameter which 90 or 70 percent of the particles exceed)¹⁾ as the equivalent diameter.

1) Literal translation: "the diameter that 10 or 30 percent of the particles are less than". (Translator's note)

As an example, Hazen's formula for water permeability of loosely packed sand consisting of particles of equal size¹⁾ reads (28)

$$K = 116 d_{10}^2 (0.7 + 0.03t) \text{ (cm/s)} \quad 31$$

d_{10} is the particle size in cm for 10 percent penetration¹⁾

t is the temperature ($^{\circ}\text{C}$)

K is defined from Darcy's law, with potentials defined in terms of pressure height and static height:

$$v = Ki \quad 32$$

where i is the potential gradient in m/m (or cm/cm). Calculations show that K , given by Hazen's formula, corresponds to the earlier defined parameter k , according to the Kozeny-Carman equation, for a porosity near $n = 0.45$. This corresponds to a dry density for sand of about $1,500 \text{ kg/m}^3$ ($\gamma_s = 2,700 \text{ kg/m}^3$).

Figure 13 shows the permeability k for different porosities, calculated from the Kozeny-Carman equation, along with corresponding values of k from Hazen's formula. The range of d_{10} for common soil materials is also shown.

For higher velocities of flow, the velocity is no longer proportional to the pressure gradient in the manner expressed by Darcy's law. As an example, Ergun (29) gives the following empirical relation between pressure gradient and flow velocity in particle fills

$$\Delta p/l = 150 \frac{(1-n)^2}{n^3} \cdot \frac{v}{d^2} + 1.75 \frac{1-n}{n^3} \cdot \frac{v^2}{d} \quad 33$$

For low flow velocities, the second term in the right hand member of Eq 33 will be much smaller than the first. The expression will then correspond to the Kozeny-Carman equation. For high

1) See appendix to translation (Translator's note)

velocities, the first term will be negligible in comparison to the second. The equation will then approach the form suggested by Burke and Plummer (30), where the flow velocity is proportional to the square root of both the pressure gradient and the particle size.

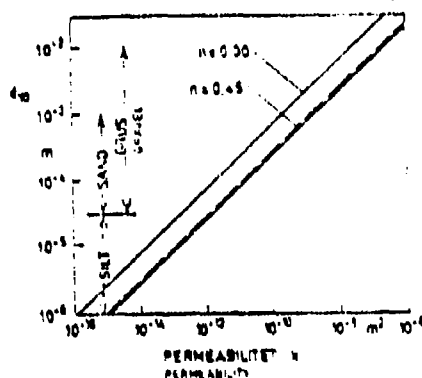


FIG. 13. Permeabilitet av jordarter beregnet etter Hazens formel ---, sammenliknet med beregninger etter Kozeny-Carman likningen -. Permeability of soils calculated from Hazen's equation --- compared to calculations based on Kozeny-Carman's equation.

C. Forced Convection

Based on the expression for permeability or Eq 33 one can estimate the magnitude of the velocity in ground water currents in soil materials. The potential gradient can for these cases be expressed as a "terrain slope" h/l (m/m). In Figure 14, flow velocities have been calculated for varying diameter (d_{10}) and three different potential gradients h/l . These calculations were based on Darcy's law and Hazen's formula, with corrections due to the second order term in Eq 33 for large flow velocities. These corrections give rise to the typical "knees" in the curves for high velocities.

In the case of flowing ground water, the liquid flow will usually be nearly perpendicular to the direction of the heat flow. The

contribution to heat flow by the liquid can then be ascribed principally to the previously mentioned dispersion. If one assumes that the case of vertical heat flow in the presence of (horizontal) planar liquid flow is analogous to the case of radial heat flow in a column with axial flow of liquid, the contribution due to dispersion can be derived from the empirical relations of Yagi and Kuni ¹, established for the latter case, see Eqs 24 and 25.

Figure 15 shows results from calculations based on this assumption and (liquid) flow velocities corresponding to a terrain slope $h/l = 1/10$ (see figure 13).

For sandy materials one finds that the effect of ground water flow is slight except in the case of very coarse sands, where the dispersion effects may increase the conductivity by up to 20 percent. For still coarser materials, such as gravel or rock, this effect may be of an entirely different magnitude. However, ground water flow seldom occurs in coarse gravel, due to its excellent drainage properties.

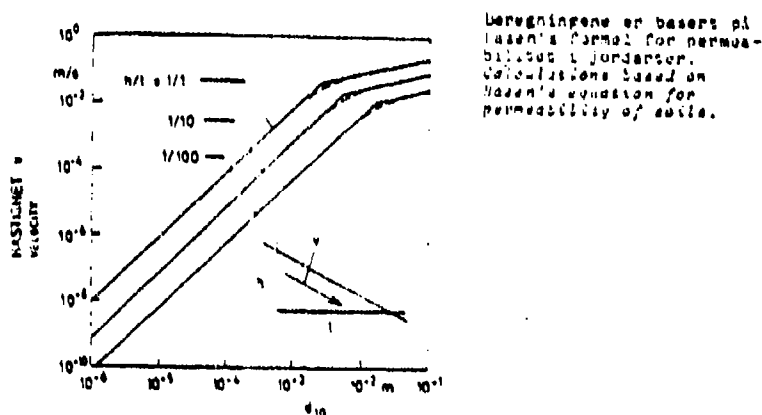


FIG. 15. Hastigheter i grunnvannstrømmer i forskjellige jordarter ved varierende terrenghellingene.
Flow velocities in ground water in different soils at a variety of gradients.

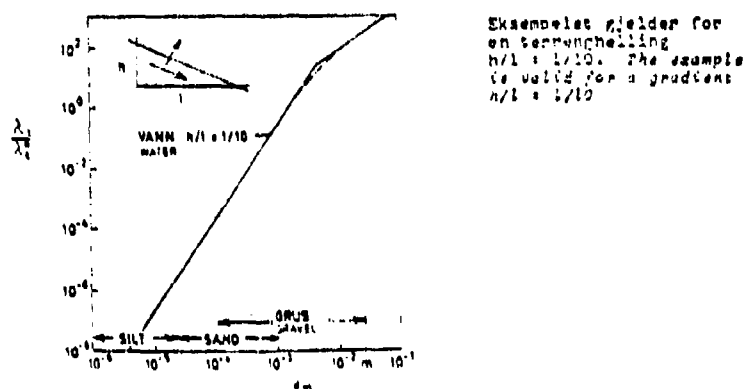


FIG. 15. Relativ andel av dispersjonen til den vertikale ledningsevnen i jordlag gjennomstrømt av vann. Influence of supulant diffusion on the vertical conductivity of soils with flowing water.

The effect of wind on open fill was treated in an experimental study of heat transport in rock fill, performed at the Institute for Cold Technology from 1968 to 1969. (31) For these experiments, a crushed rock material was laid to about 50 cm thickness in a refrigerated room at the laboratory, see Figure 16. A total of 150 thermoelements were placed within the rock layer, at 7 different depths (planes) and with 22 elements at each depth (plane), in order to monitor the temperature distribution. Below the rock layer, 9 heat flux guages (meters) were installed for measuring heat transport. The temperatures at top and bottom were controlled by means of heat exchanger plates, in which alcohol could circulate, as well as by the air temperature in the room, by means of cooling devices. The primary objective was to study the effects of free convection in the presence of vertical heat flow. Those results will be treated in the following section. Here, experiments relating to "wind loads" will be discussed.

The two fans located at one end of the rock bed gave an air velocity of about 2 m/s across the fill. The air temperature was

10°C, while the temperature at the bottom of the fill ranged from 2 to 4°C. Figure 17 shows the isotherm surface for 9°C, obtained through temperature measurements in the fill after stabilization. Temperature profiles along the center line cut of the rock fill are shown in Figure 18. Both these representations show that there may occurred a strong influx of room

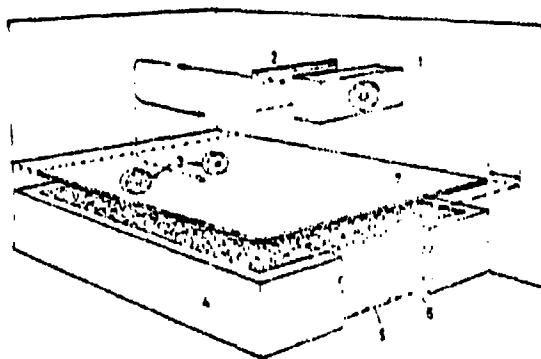


FIG. 16. Skisse av forsøksoppstilling for undersøkelse av konveksjon i steinfyllingen (Jonassen 1970). Sketch of experimental stand for investigation of convective heat transfer in beds of crushed rock.

- | | |
|--------------------------|--|
| 1. Luftkøler. Air cooler | 5. Varmefluksmåler. Heat flux meter. |
| 2. Varmegavn. Heater | 6. Varme/kjølerør. Heating/cooling coils. |
| 3. Vifter. Fans | 7. Flyttbar perforert plate. Movable perforated plate. |
| 4. Isolasjon. Insulation | |

air in the upper layers of the fill and that this influx helps to maintain a temperature close to that of the air in the room deep down in the rock fill. The average effective conductivity of the fill was determined to be 1.46 W/mK, as compared to 0.45 W/mK for the same conditions but with no forced air current. This illustrates that even small wind velocities result in large changes in temperature distribution and heat transport in coarse rock fill. For high wind velocities, the demonstrated air influx can practically eliminate the thermal resistance, particularly if the air can penetrate completely into the fill. In the wintertime, the outer surfaces of such fill may be

covered¹⁾ by ice or snow, but during the autumn months and in cold periods with no snow cover this mechanism can result in extremely heavy loss of heat from the ground. The importance of covering¹⁾ top and side surfaces of coarse fills with some-what finer gravel or crushed rock is obvious.

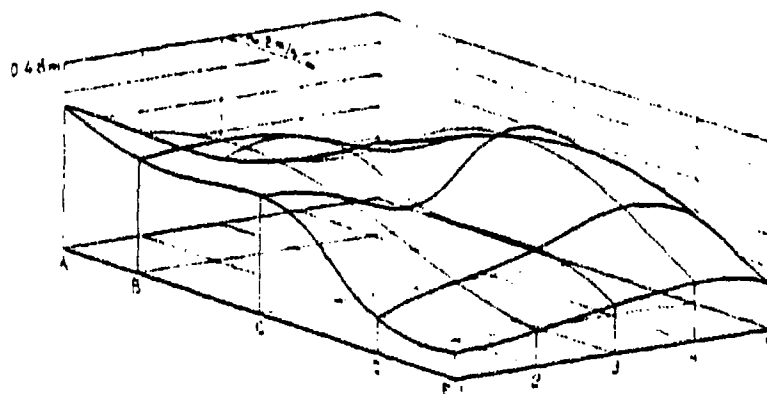


FIG. 17. Isothermplan for 0°C ved forsøk med vindskjænnning på overflaten av en steinfylling (Johansen 1970). Isothermial plane of 0°C from experiments with wind velocities at the surface of a bed of crushed rock.

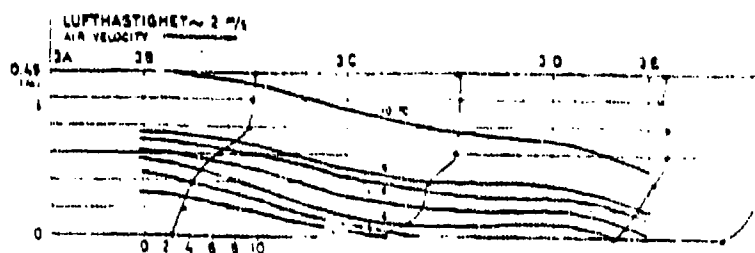


FIG. 18. Temperaturprofiler i snitt 3-3 ved samme forsøk. Temperature profiles in section 3-3 from same experiment.

1) The original uses the word "tette(t)", meaning "tighten(ed)" or "caulk(ed)" i.e. ice, snow or finer grain materials can prevent influx of cold air (Translator's note)

D. Free Convection

Free convection in a porous material is often associated with vertical heat flow in a horizontal layer of a certain thickness. The temperature gradient causes density variations in the liquid in the pores, which in turn results in liquid flow (transport). The flow pattern is often characterized by polygon cells. However, experiments with both liquid layers and liquid-filled porous materials show that the liquid does not start to flow until a certain critical temperature has been reached. To be more exact, this means that the liquid is at rest (i.e. stable) in the steady state for temperature gradients below a critical value. For gradients above that limit, the heat transport through the layer will increase in proportion to the square of the temperature gradient. The critical temperature difference across a layer of a certain thickness is inversely proportional to the thickness of the layer and the permeability of the material. This means that convection sets in for a lower temperature difference if the thickness of the layer increases.

Analytical studies of these relations lead to definition of a specific, dimension-less (scalar) parameter Ra , Rayleigh's number for porous layers containing liquids

$$Ra = \frac{\Delta T g h k}{a_m}$$

37

T is the temperature difference

h is the thickness of the layer

g is the gravity (acceleration) constant

α is the temperature expansion coefficient of the liquid

ν is the kinetic viscosity of the liquid

a_m is the temperature diffusivity for the porous material

$$a_m = \lambda_o / (c\rho)_f$$

k is the permeability of the porous material

Lapwood (33) has calculated critical Rayleigh's numbers for layers of liquid-filled porous materials for various boundary conditions:

(1) Two impregnable and conductive boundary surfaces : $Ra_k = 40$

(2) Conductive boundary surfaces, the lower impregnable, the upper free liquid: $Ra_k = 27$

Experimental studies for heat transport for Rayleigh numbers above the critical value show that the effective conductivity λ_e , averaged over an area, increases in direct proportion to the Rayleigh number. For such numbers below a certain limit $Ra = Ra_1$, Edder (34) found, for conditions corresponding to (1) above:

$$Nu = Ra/40, \quad 40 < Ra < Ra_1 \quad 38$$

Nu corresponds to Nussels number and gives the ratio between effective conductivity and conductivity without convection.

For other boundary values the equation has the form

$$Nu = Ra/Ra_c^{1)}, \quad Ra_c < Ra < Ra_1 \quad 39$$

When Rayleigh's number exceeds Ra_1 , Nu will be smaller than the value given by the linear relation, see e.g. the discussion by ● Palm, Weber and Kvernvoll in (35).

As mentioned before, the experimental arrangement described in the previous section was used to study the effect of free convection in rock fill in the presence of vertical heat flow. These experiments are described in an internal report at the Institute for Cold Technology in 1970 (32). The experiments were conducted with dry crushed rock having particle sizes in the range from

1) Subscript c is used to denote "critical", while k was used previously. (Translator's note)

20 to 80 mm. The rock was rather loosely packed and had a dry density of about $1,500 \text{ kg/m}^3$. The layer was 0.48 m thick and covered an area of $1.8 \times 2.2 \text{ m}$. The arrangement in the refrigerated room is shown in Figure 16, see the previous section. During the free convection experiments, a cover plate was installed at a certain height above the layer to protect it from air movements caused by the air cooler. As stated before, heat transport through the layer was measured with 9 heat flow gauges evenly distributed across the area, while temperature distributions were recorded in 7 horizontal cuts, spaced 8 cm apart and with 22 sensors in each. The latter allowed generation of temperature profiles and isotherms within the rock layer.

A total of 9 experiments were made with the heat flow directed upwards. These were separated in two groups, corresponding to different boundary conditions. In the first group (5 experiments), the rock layer was exposed to the air in the room, while in the second group the upper surface was covered (i.e. impregnable upper boundary). The cover consisted of a plastic sheet with a layer of sand on top. In both cases, the boundaries are partially conductive (i.e. not ideal heat conductors). Among other things, this causes large variations in temperature near the upper and lower boundaries when convection occurs.

In addition to these experiments, one was performed with downward heat flow, to determine the conductivity of the layer when no convection occurs. The average temperature during this test was about 3°C , which was assumed to be representative for the temperature range used. The most important results from these 10 experiments are summarized in Table II.

Table II: Experiments with free convection in crushed rock (32).

Permeability $K = 0.97 \cdot 10^{-6} \text{ m}^2$

Experiment ^{x)}	$\Delta T(^{\circ}\text{C})$	$t_m(^{\circ}\text{C})$	Ra	$\lambda_e(\text{W/mK})$	N_u	Ra/Ra_k
1 a	10.8	-	-	0.45	1.0	-
2 c	2.6	5.8	8.26	0.50	1.10	0.32
2 d	4.7	3.3	15.82	0.46	1.02	0.61
2 a	9.0	- 5.5	31.99	0.55	1.20	1.25
2 c	11.5	-13.4	44.72	0.79	1.75	1.74
2 f	19.0	-28.5	87.40	1.13	2.50	3.32
3 a	7.3	- 1.5	25.10	0.43	0.98	0.63
3 b	12.8	- 3.2	45.06	0.52	1.16	1.13
3 c	17.4	- 8.5	65.02	0.70	1.54	1.63
3 d	19.6	-16.9	77.40	0.80	1.77	1.95

x) Experiment 1: Down-ward heat flow

Experiment 2: Up-ward heat flow, upper surface exposed

Experiment 3: Up-ward heat flow, upper surface covered

The relation $Nu = Nu(Ra)$ given by these experiments is shown in Figure 19a. By interpolation, one finds that the critical Rayleigh numbers for exposed and covered upper boundary are approximately $Ra = 26$ and $Ra = 41$, respectively. This comes rather close to the theoretical values obtained for corresponding boundary conditions. However, the theory assumes the boundary surfaces to be ideal heat conductors. Figure 19 also clearly shows $Nu(Ra)$ to be a linear relation when the Rayleigh number exceeds a certain value.

Figure 19b, where Nussels' number is plotted as a function of Ra/Ra_k (the ratio between the Rayleigh number and its critical value) clearly shows that Eq 39 holds for $Ra > Ra_k$, up to a certain value for Ra .

For the material used, with a thickness of 0.48 m, the theoretical

values for the Rayleigh number correspond to temperature differences of 7.8 and 11.6°C for exposed and covered upper boundary, respectively, with an average temperature of 0°C. For thicker layers, the critical temperature difference will be less, since T_k is inversely proportional to the thickness. The effect of this in the thermal resistance of rock fill is outlined in Figure 20. The material is assumed to be dry and to have the same permeability as the rock used in the experiments.

It is clear that doubling the depth, e.g. from 0.5 m to 1.0 m, may in the worst case result in the same thermal resistance, provided that the temperature difference is above the critical limit in both cases.

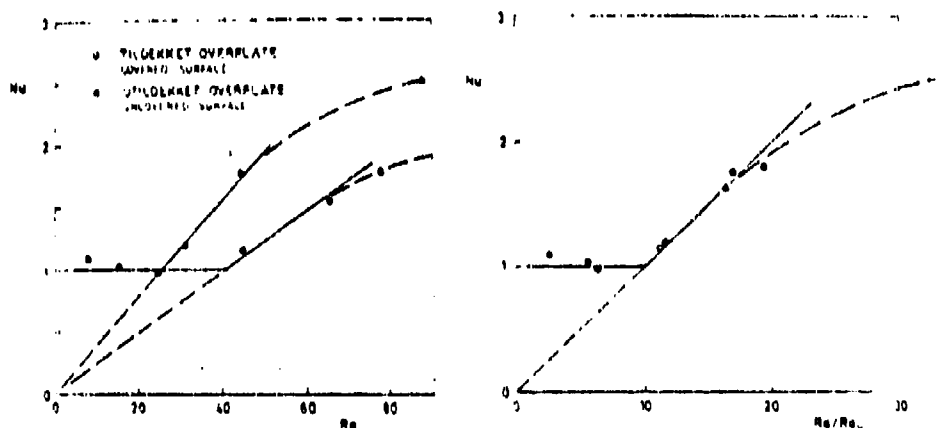


FIG. 19. Dimensionless representation of experimental results for the investigation of free convection in beds of crushed rock.

found to be $0.12 \cdot 10^{-6} \text{ m}^2$, as opposed to $0.97 \cdot 10^{-6} \text{ m}^2$ for crushed rock (32). This means an increase in the critical temperature difference from $\Delta T = 6^\circ\text{C}$ for a rock layer that is 1 m thick to $\Delta T = 48^\circ\text{C}$ for a macadam layer with the same thickness.

In materials saturated by water, convection will set in for significantly lower temperature gradients. This is primarily due to the higher density and specific heat of water, as well as its lower viscosity (c.f. Eq 37, where the Rayleigh number is defined). Table III compares actual values of the parameters which enter the Rayleigh number for air and water

Table III: Parameters included in Rayleigh's number. Temperature = 0°C

	α ($^\circ\text{C}$) $^{-1}$	λ W/mK	c_p J/kg $^\circ\text{C}$	ρ kg/m 3	a_m m 2 /s	ν m 2 /s
Dry	1/273	0.45	1000	1.251	$3.6 \cdot 10^{-4}$	$13.6 \cdot 10^{-6}$
Saturated with water	$2 \cdot 10^{-4}^*)$	1.50	4187	1000	$0.36 \cdot 10^{-6}$	$1.792 \cdot 10^{-6}$

*) $t_m = 20^\circ\text{C}$

In a material having a permeability $k = 0.12 \cdot 10^{-6} \text{ m}^2$, equal to that of the macadam mentioned before, one finds that free convection in a 0.1 m thick layer will begin already when the temperature difference is 0.6°C , if the average temperature is 20°C .

The low critical temperature differences for water saturated materials mean that free convection in connection with up-ward heat flow can occur in a saturated gravel with d_{10} as low as 1 mm. In a 1 m thick layer of such a material ($k = 10^{-9} \text{ m}^2$), the critical temperature difference is 7.3°C , for an average temperature of 20°C . However, in practice one will find that temperature differences of sufficient magnitude and duration only occur during the winter months, when the temperature is too low for convection in water to take place. In addition, materials as coarse as that referred to here will mostly have a water content well below saturation.

4. HEAT TRANSPORT IN FREEZING SOILS

The most common approximate methods for calculating frost penetration in the ground (35) are usually based on the assumption that water in the pores freezes at the normal freezing point for water. If the heat capacity of the soil is neglected and the initial temperature is assumed to be 0°C throughout the material, one arrives at the simple Stephan's equation:

$$\xi(t) = \sqrt{\frac{2\lambda F}{w \gamma_d L}} \quad 37$$

where ξ is the frost penetration (depth)
 λ is the thermal conductivity of frozen soil
 w is water content by weight
 γ_d is dry density
 L is the latent (freezing) heat of water
 F is the frost quantity (s C)

$$F = \int_0^t (T - T_0) dt$$

where T_0 is the freezing point
 t is the time at which freezing occurs

This simplified approach can be extended to stratified media and be further refined by introducing a contribution from heat flowing from (lower levels of) the ground up to the freezing zone (frost border-line).

There are strong indications that this rather simplified approach is justified when determining the approximate fill depth needed to prevent freezing in frost-heave prone sub-strata, i.e. when one can assume that the freezing zone will not extend down to the finer grain, frost-heave prone materials (36).

In more fine grain materials, the assumption that all of the pore water freezes at the normal freezing point for water will no longer be valid. As an example, Figure 21 shows the portion of un-frozen water in some silt and clay materials at temperatures below the (normal) freezing point. The finer the grain, the more water will, as a rule, remain unfrozen at a certain temperature. This subject will be discussed in more detail in Chapter III. Only the effect of this condition on heat transport will be discussed here.

In a soil material where water freezes over a range of temperatures, heat conductivity in the partially frozen material can be described by the following equation

$$\gamma_d \left[c_s + c_w \cdot w_u + c_{is} (w - w_u) + L \frac{\partial w_u}{\partial T} \right] \frac{\partial T}{\partial t} = \nabla (\lambda \nabla T)$$

c_s , specific heat of mineral particles (~ 0.8 kJ/kgK)

c_w , specific heat of water (4.2 kJ/kgK)

c_{is} , specific heat of ice (2.1 kJ/kgK)

w_u , unfrozen water ratio by weight (water/dry material)

Other symbols as in the preceding equation (Eq 37)

This (last) equation shows that release of latent heat can be included in an apparent specific heat for the freezing soil material. This specific heat will, however, be strongly dependent on temperature, which makes the equation quite non-linear.

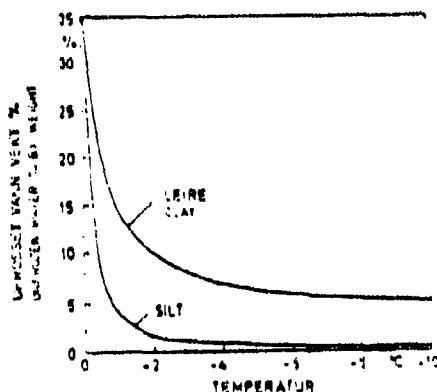


FIG. 21. Eksempler på ufroset vanninnhold i vannmettet silt og leire. Examples of unfrozen water content in saturated silt and clay.

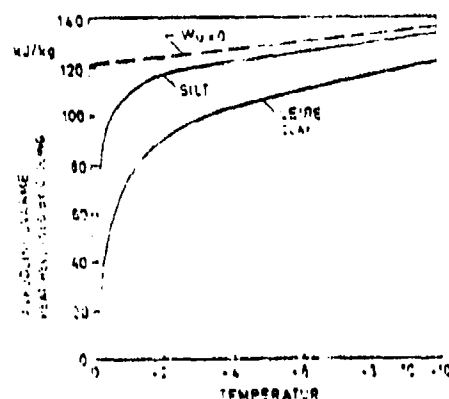


FIG. 22. Frikitt varme ved avkjøling av jordarterne fra Fig. 21 til temperaturer under frysepunktet. Varme released in the soils at Fig. 21 by cooling below freezing points.

This property is clearly important when one tries to measure the thermal conductivity of frozen soils, using transient (not stationary) methods and must use the linear equation for thermal conduction. This will be discussed in more detail in Chapter IV, in connection with experimental investigations of thermal conductivity in soil materials.

The effect of the un-frozen water content upon frost penetration can be illustrated by considering released heat during cooling down of different soil materials to temperatures below the freezing point. Figure 22 shows calculated values for the same two materials as in Figure 21. For comparison, released heat for the case where all the porewater freezes at the normal freezing point are shown in the same figure. In all cases, the dry density is assumed to be $1,400 \text{ kg/m}^3$, corresponding to a saturated water content of 36 percent by weight.

It is clear, that the amount of heat released at a certain temperature be reduced significantly for a soil material where the water freezes only partially. The greatest reduction will naturally be found in cases where the soil is cooled only to a temperature close to the freezing point. This effect will clearly result in an increased frost penetration, in comparison to the case when all the water freezes at the normal freezing point, which is assumed when deriving Stefan's equation (Eq 37).

Calculations using the simplified method derived by Skaven-Haug (36) for determining the frost resistance of roads, for which frost depths and frost quantities have been measured, point in the same direction. The discrepancy between calculated frost resistance (i.e. the calculated frost quantity required to freeze the ground down to the registered frost depths) and the measured frost quantity was largest for the cases where frost had penetrated into very clay-rich materials (37). This experience shows that knowledge of un-frozen water content at temperatures below the freezing point is an important condition for satisfactory calculations of temperature distributions in freezing ground.

When fine grain materials freeze, still another specialized condition will be important. As frost penetrates the material, suction is created at the frost border-line. Depending on the permeability of the un-frozen material, this creates water transport up towards the frost border-line, where water freezes and releases latent heat.

It would be logical to assume, that determining the velocity of the up-wards moving water would be a relatively simple matter when the rate of frost penetration is known. However, measurements of water content during spring and autumn below the sections of road where the previously mentioned experiments were made (37) indicate that frost heaves often can be due to local re-distribution of water. Such local re-distribution occurs most often in clays where the suction is strong near the frost border-line, while the permeability is low. Under such conditions, the water flow velocity will also be low. In somewhat coarser materials, where the permeability is significantly higher, one can expect that a larger portion of frost heaves can be related to up-ward flowing water.

Clarification of these matters require a comprehensive experimental investigation of soil samples which freeze under controlled conditions. Such experiments should include determination of heat

as well as (liquid) mass balance versus time, through measurements of both heat flow and water transport velocity.

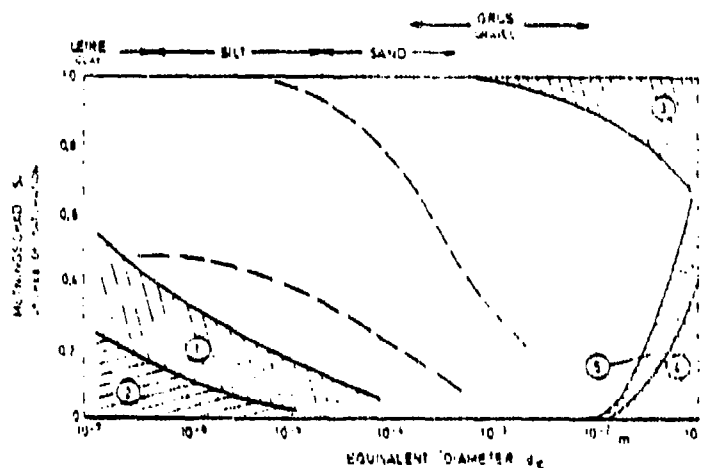
The water flow towards the freezing zone referred to above will clearly tend to reduce frost penetration and will to some degree counteract the effects of un-frozen water content.

5 THE EFFECTS OF VARIOUS HEAT TRANSPORT MECHANISMS

An evaluation of theoretical and experimental studies of heat transport in moist, porous materials shows that the effects of various mechanisms to a large extent depend on the particle size of the material, the degree of saturation and the temperature level. This will in the following be utilized in an effort to determine limits for the effects of each of the different mechanisms. As mentioned previously, the goal is to clarify limitations for mathematical models which use pure heat conduction aspects to find temperature distributions in and around structures placed on the ground.

The regions of pre-dominance (influence) of different heat transport mechanisms in un-frozen soil materials are shown in Figure 23 as function of average (equivalent) particle size (d_{10}) and degree of saturation. Types of soil corresponding to certain ranges of d_{10} are indicated in the same figure. Dotted lines show expected limits of saturation level in base materials, sands and gravels in a road structure. The basis for this presentation will be discussed in the following, with reference to previous descriptions of the different mechanisms.

For fine grain materials, such as silt and clay, there is a region at the lower saturation levels where moisture content gradients will cause vapor diffusion due to changes in relative humidity in the pore air as function of water content. From Figure 5 in this chapter one can conclude that large variations in relative humidity



- | | |
|---|--|
| 1. Temperatur avhengig fuktavdring. Temperature-dependent moisture migration. | 4. Konveksjon i vann. Convective heat transfer in water. |
| 2. Fuktavhengig dampdiffusjon. Moisture dependent vapour diffusion. | 5. Varmerestråling i hulrom. Radiation of heat in voids. |
| 3. Konveksjon i luft. Convective heat transfer in air. | |

FIG. 23. Innflytelsesområder for de aktuelle varme-transportmekanismer i forskjellige jordtyper. Regions of influence for the possible heat transfer mechanisms in different soils.

BEST AVAILABLE COPY

as function of water content only occur at low saturation rates, where the moisture potential (suction) exceeds about 10 bar. For silt this may correspond to water content of about 5 percent by weight ($S_r \approx 10$ percent), while it may correspond to a saturation level exceeding 30 percent in a clay material.

For moderate saturation levels in fine grain materials, temperature gradients will cause vapor diffusion in the pore air due to corresponding gradients in the water vapor saturation pressure in the pores. For low saturation levels, this process is slowed down by the lower relative humidity in the pore air. For higher saturation levels, the re-distribution of moisture caused by this process is counteracted by capillary water transport in the opposite direction. The latter is determined by the moisture potential gradients and the hydraulic conductivity for the saturation level at hand. The hydraulic conductivity is strongly dependent on water content for low to moderate water contents as well as the grain size in the material (c.f. Figure 7). This means that the region in which the temperature dependent vapor diffusion can cause significant moisture gradients will move towards higher saturation levels as the material becomes finer, as shown by the region labeled "2" in Figure 23.

The temperature dependent vapor diffusion will also contribute to the transport of latent heat when vaporisation or condensation occurs. However, this contribution can be treated as an added thermal conductivity in the pore air, since the vapor diffusion in the pore are governed by the temperature field in the pores in the same manner as pure heat conduction in air.

For coarse grain soil materials, two regions are indicated at comparatively low and high saturation levels, when the heat transport is influenced by convection in water and air, respectively. The effect of free convection in horizontal layers (of fill) with an up-wards heat flow is particularly limited by the permeability. For example, in a dryer or dry fill which is one metre deep, the

permeability must be about $0.5 \cdot 10^{-6} \text{ m}^2$ for convection to occur at a temperature difference of 10°C . Permeabilities of this high magnitude will only be present in very coarse gravel materials or crushed rock. By comparison, a permeability of 10^{-9} m^2 is required for free convection to take place at the same temperature difference in a material saturated with water and for an average temperature of 20°C . Such permeability values can be expected in medium sand with equal particle size. However, up-ward heat flow will primarily occur during the cold (frost) season when convection in water can not take place.

Forced convection due to ground water flow may affect heat transport in materials having permeabilities in the range just mentioned (see Figure 15). For axial liquid flow in particle filled columns having radial heat conduction (flow) it has been demonstrated that the flow rate (velocity) affects radial heat transport, which may be explained by "lateral mixing" or dispersion. Corresponding studies involving horizontal liquid flow in fills (layers) having vertical heat conduction (flow) are not known (to the author). However, such conditions will normally not occur in conventional road structures due to flow within the coarser materials in the structure itself.

Water permeability will clearly decrease when the degree of saturation falls below 1. In the same manner, the permeability in air will decrease when the degree of saturation exceeds 0. Since actual permeability values for air and water in such systems are not available, the limiting curves for convection are rather approximate¹⁾ for saturation levels between 0 and 1, but are intended to correspond to permeabilities of $0.5 \cdot 10^{-6}$ and 10^{-9} m^2 , respectively.

Heat transport in coarse materials can also be partially due to thermal radiation between particles. At an average temperature of 20°C , the contribution due to heat radiation may increase the

1) In other words "guesstimates" based on "informed ignorance"
(Translator's note)

effective heat conductivity by 5 percent in dry gravel with a uniform particle size of 10 mm (see Figure 4). This contribution increases in proportion to particle size. Reduced pore cross-section due to a certain water content and an increase in conductivity due to increased saturation levels will tend to reduce this contribution in moist materials. The boundary of the region where thermal radiation is important was derived under certain assumptions regarding the effect of saturation level on the effective pore cross-section and the increase in conductivity due to increased degree of saturation. The boundary corresponds to a contribution to the conductivity, due to heat radiation, of 5 percent.

In principle, the effect of heat radiation can be included in the effective or apparent conductivity of the porous material and thus does not present a problem in numerical determination of temperature fields, provided that one takes the temperature dependence of the parameters into account. However, this requires knowledge of the effect of radiation in such structures (systems).

If one compares the indicated boundaries with the saturation levels in sub-strata and upper layers, (Figure 23) one finds that heat transport in un-frozen materials will be affected only slightly by mechanisms other than thermal conduction, except for the coarsest materials where heat transport due to convection and radiation may become significant.

The preceding overview (discussion) has been limited to un-frozen soil materials. In frozen, fine grain materials (frost prone), water transport towards the freezing zone (boundary) will affect the heat transport due to loss of latent heat. The mechanism behind this effect, which includes coupled heat and moisture transport, has not been clarified. However, thermal design of road structures is normally performed so that frost penetration will not occur. Under these circumstances, these mechanisms can be disregarded.

REFERENCES - CHAPTER I

1. W. B. Argo, J. M. Smith: Heat Transfer in Packed Beds. Chemical Engineering Progress. 49, (8), 1953, pp. 443-451.
2. S. Yagi, D. Kunii: Studies on Effective Thermal Conductivities in Packed Beds, A.I. Ch. E. Journal, 3, (3), 1957, pp. 373-381.
3. P. Zetner, E. U. Schlunder: Einfluss der Wärmestrahlung und des Druckes auf den Wärmetransport in nicht durchgestromten Schüttungen. Chemie-Ing.-Tech, 44, (23), 1972, pp. 1303-1308.
4. N. Wakao, K. Mato: Effective Thermal Conductivity of Packed Beds, Journal of Chemical Engineering of Japan, 2 (1), 1969, pp. 24-33.
5. N. Wakao et al: View Factor between two Hemispheres in Contact and Radiation Heat-Transfer Coefficient in Packed Beds. Int. J. Heat Mass Transfer, 12, 1969, pp. 118-120.
6. N. Wakao: Effect of Radiating Gas on Effective Thermal Conductivity of Packed Beds. Chemical Engineering Science, 28, 1973, pp. 1117-1118.
7. E. Schmidt: Einführung in die Technische Thermodynamik, Springer Verlag, Berlin 1963, p. 394.
8. F. Birch, H. Clark: The Thermal Conductivity of Rocks and its Dependence upon Temperature and Composition. American Journal of Science, 238, (8), 1940, pp. 529-558.
9. O. Krischer, H. Esdorn: Wärmeleitung und Dampfdiffusion in feuchten Gütern. VDI-Forsch,-Heft 402, Berlin 1940.
10. C. W. Rose: Water Transport in Soil with a Daily Temperature Wave. I. Theory and Experiment, Aust. J. Soil Res., 6, 1968, pp. 31-44.
11. C. G. Gurr et al: Movement of Water in Soil due to a Temperature Gradient. Soil Science 74 (5) 1952, pp. 335-345.
12. D. Croney, J. D. Coleman: Pore Pressure and Suction in Soil. In "Pore Pressure and Suction in Soils". Butterworths, London 1961, pp. 31-37.
13. J. A. Currie: Gaseous Diffusion in Porous Media, Part 2 - Dry Granular Materials. British Journal of Applied Physics, 11, 1960, pp. 318-324.
14. J. A. Currie: Gaseous Diffusion in Porous Media, Part 3 - Wet granular Materials. British Journal of Applied Physics, 12, 1961, pp. 275-281.
15. J. R. Philip, D. A. de Vries: Moisture Movement in Porous Materials under Temperature Gradients. Transactions American Geophysical Union, 38, (2), 1957, pp. 222-232.

16. W. O. Smith: Thermal Conductivities in Moist Soils. Soil Sci. Soc. Am. Proc. 4, 1939, pp. 32-40.
17. O. Krischer: Die Leitfähigkeit des Erdbodens. Beiheft zum Gesundheits-Ingenieur, Reihe I Heft 33, München (Munich) 1934.
18. C. G. Gurr et al: Movement of Water in Soil due to a Temperature Gradient. Soil Science 74, (5), 1952, pp. 335-345.
19. H. L. Rollins et al: Movement of Water in Soil due to a Temperature Gradient, Highway Research Board Proc. 33 1954, pp. 492-508.
20. J. W. Cary: Water Flux in Moist Soil: Thermal Versus function Gradients. Soil Science. -CO, (3) 1965, pp. 168-175.
21. W. D. Joshua, E. De Jong: Soil Moisture Movement under Temperature Gradients, Can. J. Soil. Scie., 53, 1973, pp. 49-57.
22. R. J. Kunze et al: Factors Important in the Calculation of Hydraulic Conductivity, Soil Sci. Soc. Amer. Proc., 32, 1968, pp. 760-765.
23. D. A. de Vries: Simultaneous Transfer of Heat and Moisture in Porous Media. Transactions, American Geophysical Union, 39 (5), 1958.
24. D. A. de Vries: Het warmtegeleidingsvermogen van grond, Med. Landbouwhogeschool, Wageningen, 52, 1952.
25. P. Adivarahan et al: Heat Transfer in Porous Rocks, Society of Petroleum Engineers Journal 1962, pp. 290-296.
26. S. Yagi, D. Kunii: Studies on Effective Thermal Conductivity in Packed Beds, A.I.Ch. E. Journal, 3 (3), 1957, pp. 373-381.
27. A. E. Scheidegger: The Physics of Flow through Porous Media. Univ. of Toronto Press, 1957.
28. Bygg. Huvuddel 1B. Almänna Grunder: Avd. 17:4 pp. 306-308.
Ab Byggmästarens Förlag Stockholm 1972.
29. S. Ergun: Flüssigkeitsströmung durch Füllkörpersäulen, (Festbetten) Referat i Chemie Ing.-Techn., 25 1953, p. 262.
30. Burke & Plummer: Referat i Chemie Ing.-Techn., 25, 1953, p. 262.
31. Ø. Johansen: Undersøkelse av varmetransporten i kult og pukklag. Det store eksamensarbeid, Inst. for kjøleteknikk, NTH, Trondheim, 1970.
32. Ø. Johansen: Innflytelse av fri konveksjon i grovkornede vegbyggings-materialer. Institutt for Kjøleteknikk, NTH, Trondheim, 1970.

33. E. R. Lapwood: Convection of a Fluid in a Porous Medium. Proc. Cambr. Soc. 44, 1948, pp. 508-521.
34. J. W. Elder: Steady Free Convection in a Porous Medium Heated from Below. J. Fluid Mech., 1967, 27, pp. 29-48.
35. E. Palm et al: On steady convection in a porous medium. Preprint series, Matematisk Institutt, Universitetet i Oslo, 1971.
36. Sv. Skaven haug: The Design of Frost Foundations. Norwegian Geotechnical Institute, Publ. 90, Oslo 1971.
37. A. F. Knutson: Upubliserte resultater, 1973.
38. E. Angen: Analyse av vanninnhold i vegkonstruksjoner, Intern rapport, SINTEF, NTH, Trondheim, 1973.
39. A. K. Fleming: Applications of a Computer Program to Freezing Processes. Proceedings of the XII International Congress of Refrigeration, Washington D.C. 1971.

CHAPTER II

THEORIES FOR HEAT CONDUCTION IN COMPOSITE MATERIALS

The previous chapter described (discussed) various mechanisms for heat transport in moist and frozen soil. It was found that, in most practical cases, thermal conduction plays a dominant role in the heat transport (transfer). This prompts a more detailed study of the factors which determine thermal conductivity in composite materials.

The following sections present an overview of the most important relations that apply to derivation of theoretical models for determining thermal conductivity in such materials. Emphasis will be placed on organizing the different methods in a set of major approaches.

Many of the methods (to be) mentioned are developed for determining transport coefficients which are analogous to thermal conductivity, e.g. parameters such as electrical conductivity, dielectric constant, magnetic permeability, permeability associated with liquid flow in porous materials and diffusion coefficients. To simplify matters, all these analogue transport coefficients will in the (following) text be denoted by "conductivity", without specific mention of the nature of the transport coefficient. That will be evident from the list of references.

1. EXACT THEORY

The problem of determining conductivity in a composite material can be formulated as follows: A material is homogeneous on a macroscopic scale and isotropic. On a microscopic scale it consists of regions having different conductivities. How do these regions together form a macroscopic conductivity?

Ideally (in principle), this problem can be solved by integrating the heat flow equation for steady state (stationary) conditions over a region of the material, large enough to give a representative picture of the average microgeometrical conditions⁽¹⁾.

That is only possible in simple systems, e.g. regular configurations of spheres. Solutions for such cases will be given in section 3 of this chapter. For natural materials, where the microgeometry is very complicated, such calculations are impractical.

However, there exists a general solution, for which one treats the microgeometric conditions in a general (idealized) form.

If the material is homogenous on a macroscopic scale, one can describe the microgeometry by means of a set of random parameters (p-point correlations). The basic form for these correlations¹⁾ is a function $\phi_1(\vec{r})$, defined by

$$\phi_1(\vec{r}) = 1 \quad \text{if (the position vector) } \vec{r} \text{ is in component "1"}$$

$$\phi_1(\vec{r}) = 0 \quad \text{if } \vec{r} \text{ is outside component "1"}$$

The volume average for the function $\phi_1(\vec{r})$ will correspond to the relative volume (volume share) of the component "1" in the material, provided that the integration is carried over a sufficiently large volume in a macroscopically homogenous and isotropic material. That relative volume also gives the probability that a point selected at random will fall in component "1"²⁾.

1) "Correlations" is a literal translation. The context indicates a joint probability density function.

2) From the context it appears that "components" refers to "regions" or "cells" with certain thermal properties (Translator's notes).

In the same manner, a volume average of the type $\langle \phi_1(\vec{r}_1) \phi_1(\vec{r}_2) \dots \phi_1(\vec{r}_p) \rangle$ expresses the probability that all the points \vec{r}_1 through \vec{r}_p are located within the same component. Such a volume average is called a p-point correlation. As an example, a two-point correlation will define the probability that both end-points of a line segment fall within the same component. In a macroscopically homogenous and isotropic material, this probability will be a function of the length of the line segment. Three-point correlations will give the probability for the three corners of a triangle to fall within the same component. This probability is a function of the angle between two sides in the triangle and their lengths.

With this kind of random characterization of the microgeometry of a material as a starting point, W. F. Brown (1955) (2) derived a general expression for the conductivity of a two-component material. The expression can be written under the form:

$$\frac{1}{3\beta} = \frac{1}{3(1-n)\beta_0} - 3\Lambda_1\beta_0 - \dots - \Lambda_1(3\beta_0)^1 - \dots \quad 1$$

where $\beta = \frac{\lambda - \lambda_1}{\lambda + 2\lambda_1}$, λ is the macroscopic conductivity

$$\beta_0 = \frac{\lambda_2 - \lambda_1}{\lambda_2 + 2\lambda_1}, \quad \lambda_2 > \lambda_1 \text{ (conductivity of the components)}$$

Λ_1 are integrals containing the p-point correlations

n is the volume share (relative volume) of phase 1

W. E. A. Davies (1971)(3) has shown that Λ_1 contains the three-point correlation, while higher order correlations are included in the expressions for other Λ .

Eq 1 shows that the macroscopic conductivity depends on the random properties of the component microgeometry, as well as the conduc-

tivity of each component and their relative volumes. This may appear to be a trivial result, but has nonetheless been overlooked in many studies within this field: "The flow of papers seeking an¹⁾ universal formula (for the conductivity of composite materials) is unending". Quote from P.J. Beran (1971)(4).

For a geometry where all $\lambda_1 = 0$, Eq 1 shows that the conductivity is exactly given by

$$\frac{\lambda - \lambda_1}{\lambda + 2\lambda_1} = (1 - n) \frac{\lambda_2 - \lambda_1}{\lambda_2 + 2\lambda_1} \quad 2$$

Davies (3) has shown that such a geometry can be represented as a system consisting of concentric spheres, where a nucleus (core) of one material is surrounded by a spherical shell of the second material. These spherical units (cells) may be assumed to occur in all sizes, so that they together completely fill the given material. The diameter ratio in each one equals the macroscopic volume ratio.

A material which consists of dispersed spherical particles, together forming a small percentage of the volume, will closely approximate this geometry. Consequently, the conductivity of such a material can be calculated exactly²⁾ from Eq 2. The same is true for a system where a small portion of the total volume consists of spherical pores, dispersed in a material with higher conductivity. (In this case, the properties of the materials change places in the equation.)

For other microgeometries it will clearly be impossible to calculate the conductivity exactly, since it is difficult to see how all the p-point correlations involved could be determined.

1) Sorry about this one, but that is exactly what the original says. (Translator's note)

2) Probably some-what overstated (Translator's note).

However, in a more recent report, Brown has pointed out the possibility of determining limits for the conductivity in a certain system, based on knowledge of the p-point correlations up to a given order (5). The more information one has of the statistical properties of the microstructure in the material, the narrower these limits are.

The evaluation of such limits will be discussed in the following section.

2. EVALUATION OF LIMITS

A. Limits according to Hashin-Shtrikman

It is trivial to state that the conductivity of a composite material must fall between the highest and lowest conductivity of the components which make up the material. This is the best one can do based on knowledge of the conductivity of each component only. If, in addition, one knows the relative (share of) volume for each material component, limits for the conductivity can be found from the arithmetic and harmonic means of the conductivities for each component

$$\lambda_H \leq \lambda \leq \lambda_A$$

3

where

$$\lambda_A = \sum_{i=1}^m n_i \lambda_i \quad (\text{arithmetic mean})$$

$$\lambda_H = \left(\sum_{i=1}^m n_i / \lambda_i \right)^{-1} \quad (\text{harmonic mean})$$

The proof for this (relation) is usually based on (the work by) Wiener (1912)(6), so the limits could be called Wiener limits. These limits are general and will apply even if the material is not homogenous or isotropic.

Using calculus of variations, Z. Hashin and S. Shtrikman (1962)(7) developed limits (limiting values) for macroscopically homogenous and isotropic materials, which represent a further refinement (improvement) of limits for the conductivity of a composite material.

For a two component material these limits can be expressed by the following inequalities:

$$\frac{\lambda - \lambda_1}{\lambda + 2\lambda_1} \geq (1 - n) \frac{\lambda_2 - \lambda_1}{\lambda_2 + 2\lambda_1}, \quad \lambda_2 > \lambda_1 \quad 4$$

$$\frac{\lambda - \lambda_2}{\lambda + 2\lambda_2} \leq n \frac{\lambda_1 - \lambda_2}{\lambda_1 + 2\lambda_2}, \quad \lambda_2 > \lambda_1 \quad 5$$

These expressions are identical to those which were previously proven to hold exactly for a system of concentric spheres (Eq 2) and do thus correspond to a geometry for which the integrals $\Lambda_1, \dots, \Lambda_p$ are zero, which Davies also proved in his report (3).

For a material composed of m components, the limits can be expressed in terms of similar, dimension-less, ratios between conductivities. The conductivities of the components (involved) are arranged in order of increasing value so that:

$$\lambda_1 < \dots < \lambda_i \quad \lambda_{i+1} < \dots < \lambda_m$$

The inequalities can then be written under the following general form:

$$\frac{\lambda - \lambda_1}{\lambda + 2\lambda_1} \geq \sum_{i=2}^m n_i \frac{\lambda_i - \lambda_1}{\lambda_i + 2\lambda_1} \quad 6$$

$$\frac{\lambda - \lambda_m}{\lambda + 2\lambda_m} \leq \sum_{i=1}^{m-1} n_i \frac{\lambda_i - \lambda_m}{\lambda_i + 2\lambda_m} \quad 7$$

If lower and upper limits are denoted λ_* and λ^* , respectively, while the sums in the right hand members of Eqs 6 and 7 are denoted s_* and s^* , the following expressions for the limits can be derived:

$$\lambda^*/\lambda_1 = (1 + 2\beta^*)/(1 - \beta^*) \quad 8$$

$$\lambda^*/\lambda_m = (1 + 2\beta^*)/(1 - \beta^*) \quad 9$$

As indicated previously, the Hashin-Shtrikman limits constitute the best(possible) estimate of conductivity limits in a material when information about its microgeometry is lacking. These limiting values also correspond to extreme microgeometries. The distance between them can thus give an idea of the sensitivity to variations in the microgeometry.

Figure 1 compares the Hashin-Shtrikman limits to those given by Wiener, as function of porosity and for various ratios of conductivity (in the two material components). It is evident that the Wiener limits give the best improvement at low conductivity ratios. One also finds that the Hashin-Shtrikman limits are practically identical (coincident) for conductivity ratios less than 3 and that the spread between these limits is less than 10 percent for conductivity ratios up to 10. Thus, for most applications these limits will by themselves give an estimate of the conductivity which is sufficiently accurate.

For larger conductivity ratios, the improvement is insignificant and the limits are too far apart in order to give a (reliable) estimate of the conductivity. As indicated previously, the large spread between limits is due to a considerable sensitivity to variations in microgeometry in the case of large conductivity ratios. This condition has significant practical implications.

As mentioned at the end of the previous section, the range between these limits can only be improved by including information about the statistical properties of the microgeometry in the materials. In recent years, a number of reports have been published which seek to improve these limits on that basis. These reports will be discussed in the following section.

B. Limits based on point correlations

Using the previously mentioned statistical description of micro-geometry, M. Beran (8) and W.F. Brown (5) reported, in the same year, improved limits for the conductivity by utilizing three-point correlations. W.T. Brown found it possible to calculate his limits for a particular form of geometry where the components have the same relative (share of) volume and identical geometry (symmetrical material). The calculations show a significant improvement (narrowing) of the limits in comparison to the Hashin-Shtrikman limits, particularly for low conductivities.

However, the requirement that the three-point correlations must be known makes it difficult to find the limits for other types of materials.

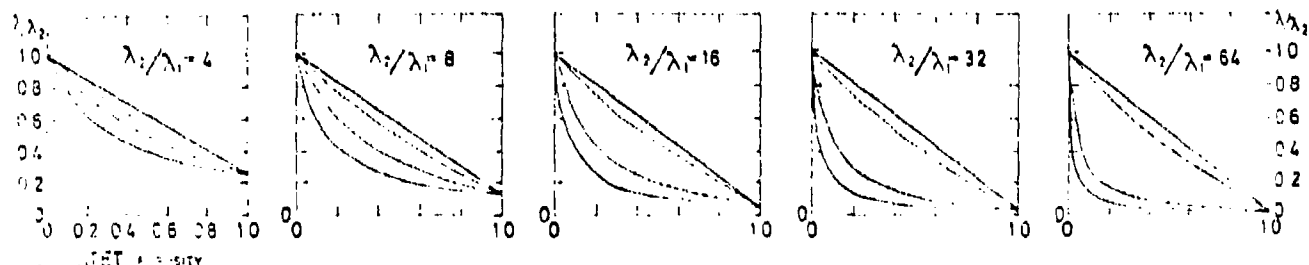


FIG. 1. Hashin-Shtrikman upper (solid line) and lower (dashed line) bounds for conductivity as a function of porosity for different conductivity ratios. The Hashin-Shtrikman bounds (solid lines) for isotropic materials are shown as the Wiener bounds at a set of conductivity ratios and porosity percentages.

BEST AVAILABLE COPY

An article from 1974 by P.B. Corson (9) gives the results of experimental determination of three-point correlations in selected alloys (lead-aluminum, iron-lead). From these experimental results, Corson derives empirical formulas which express the three-point correlations for the investigated materials as a function of the length of the three sides in the triangle and the relative volume for the components.

These empirical formulas were then used to calculate values for the limits in materials with similar microgeometry (11). The expressions given by M. Berans for limits of conductivity were used, since the three-point correlations there are included in generalized form (8).

For low conductivities, these calculations also show a significant improvement, in comparison to the Hashin-Shtrikman limits. However, the method can not be expected to have wide-spread applications. The effort required for determining three-point correlations in a given material is extensive and the calculations required for finding the limits using empirical three-point correlation expressions are complicated.

Also M.H. Miller (1969)(12) used the general expressions previously published by Beran as a starting point. He points out that these expressions have limited usefulness as long as the three-point correlations are difficult to determine. However, by defining a particular type of materials which he calls cell materials he has been able to express three-point correlations as a numerical value for each component. These values vary in magnitude from $1/9$ to $1/3$ and have a simple geometrical interpretation. The number $1/9$ represents spherical cells while $1/3$ signifies flat (plate-shaped) cells. All other geometries are characterized by values between these limits, regardless of how complicated the geometry is.

Miller makes a distinction between symmetrical and asymmetrical cell materials. In the first type, the two components have the

same average geometry, while in the other types the component geometries are different. The most important restriction for the cell materials is that the conductivity of one cell must be statistically independent of the conductivities of all other cells. In addition, the material must be homogenous and isotropic in a macroscopic sense.

For an asymmetric cellular material, the Miller limits can be expressed as

$$\lambda/\lambda_1 \geq 1 + (1-n) (\alpha-1) - \frac{n(1-n) (\alpha-1)^2}{2(n+\alpha(1-n) + (1-n)^2 [G_2 - (1-n)^2 G_1])} \quad 11$$

$$\lambda/\lambda_1 \geq \alpha \cdot \left(1+n (\alpha-1) - \frac{2n(1-n) (\alpha-1)^2}{2(1+n\alpha(1-n) + (1-n)^2 G_1 - n^2 G_2)} \right)^{-1} \quad 12$$

where $\alpha = \lambda_2 / \lambda_1$, $\lambda_2 > \lambda_1$

n is the relative volume (share) of component 1

G_1, G_2 are numerical values given by the cell geometry

For a symmetrical cellular material, $G_1 = G_2$. In general, materials are of the asymmetrical type and in addition it is usually possible to determine the cell geometry for only one of the materials.

In such cases, limits for the conductivity can be determined by using G -values for the component with un-known geometry, which result in the highest upper limit and the smallest value for the lower limit. From expressions for the limits one obtains the following numerical values:

Granular materials (G_2 known)

$G_1 = 1/3$ gives upper limit, $G_1 = 1/9$ gives lower limit

Porous materials (G_1 known)

$G_2 = 1/9$ gives upper limit, $G_2 = 1/3$ gives lower limit

(Note: Index 1 always refers to the component having the lower conductivity)

Figure 2 shows calculated values of the Miller limits, as function of volume ratio for a number of conductivity ratios. Examples are given for both granular materials containing spherical particles ($G_2 = 1/9$) and porous materials having spherical pores ($G_1 = 1/9$). The Hashin-Shtrikman limits are shown for comparison and the cross-hatched regions define the Miller limits.

One finds that the largest improvement is obtained for small concentrations of particles or pores, where both Miller limits asymptotically approach one of the Hashin-Shtrikman limits.

For low conductivity ratios, the improvement is also significant at larger concentrations. Here the Miller limits indicate that in the case of spherical particles only the lower half of the range defined by the Hashin-Shtrikman limits should be considered, while in the case of spherical pores one should consider the upper half of that range.

Miller indicates that the variations in conductivity represented by his limits for a given particle geometry is due to the many possible packing configurations which may occur for a certain geometry. To improve on (narrow) the limits one thus needs information about the packing configuration, in addition to the particle geometry. This kind of information will also be included in point correlations of an order higher than 3.

M.A. Elsayed (1974)(13) has recently presented a report where he has succeeded in including five-point correlations in expressions for the conductivity of materials with two components.

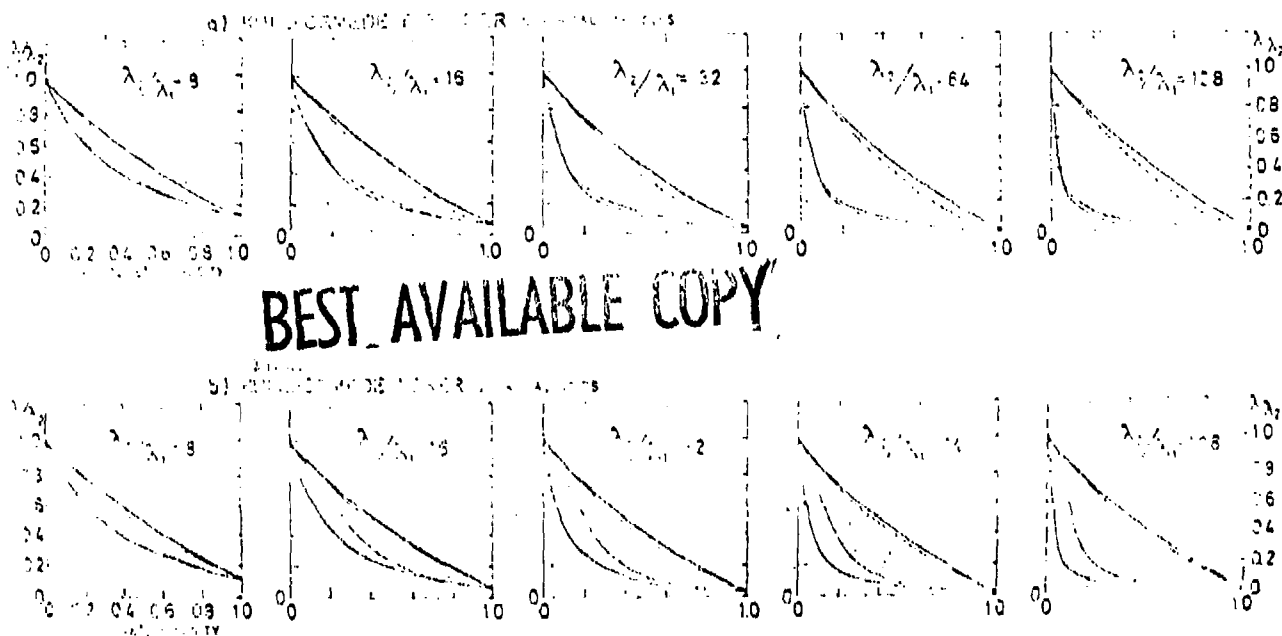


FIG. 2. Comparison of the improved expressions (a) and Miller's formulas (b) for the conductivity ratio λ_2/λ_1 as a function of the packing factor P . The curves are calculated for $\lambda_2/\lambda_1 = 3, 16, 32, 64, 128$.

These expressions also include factors which depend on the packing configuration, much like Miller's formulas.

On the other hand, Elsayed has not been able to give a geometrical interpretation of the factors which represent packing configuration in the improved expressions for (conductivity) limits. This causes practical difficulties when using his (expressions for these) limits. However, he has calculated limits for two geometries which he claims are typical for spherical and flat (plate-shaped) particles, respectively. The results show a significant improvement relative to the Miller limits, particularly for low conductivity ratios.

Further investigations along the lines developed by Elsayed may result in a geometrical interpretation of the packing factors and

thus contribute to better accuracy for estimates of conductivity in certain systems.

C. Other evaluations of limits

S.R. Corriell and J.L. Jackson (1968)(14,15) used a cubical elementary cell in a material with known microgeometry and an approach based on calculus of variations. They proved, that approximate upper and lower bounds for the conductivity can be obtained by assuming planar isotherms and parallel heat flow-lines, respectively (Figure 3).

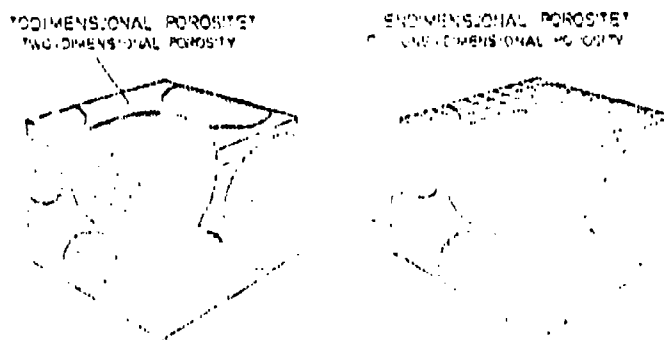


FIG. 3. Schematic representation of two types of porous media. The left diagram shows a cube with internal channels that are parallel to the faces, representing a planar isotherm assumption. The right diagram shows a cube with internal channels that are parallel to the edges, representing a parallel heat flow-lines assumption.

BEST AVAILABLE COPY

The general expressions for these limits are given by the following integrals:

$$\lambda \geq \frac{1}{\int_0^1 \int_0^1 \left(\frac{dx dy}{\int_0^1 dz / \lambda(x,y,z)} \right)} \quad 12$$

$$\lambda \geq 1 / \int_0^1 \left(\frac{dz}{\int_0^1 \int_0^1 \lambda(x,y,z) dx dy} \right) \quad 13$$

As illustrated by Figure 3, these expressions are obtained by assuming that each elementary cell is divided into an infinite number of filaments parallel to, or plates perpendicular to the direction of heat flow, respectively. The relative volume (share) of the lower conductivity component in each of these filaments or plates can be regarded as, respectively, one and two-dimensional porosity.

The way the calculation methods are structured, these "porosities" can be re-arranged according to magnitude, one obtains a cumulative distribution functions as the number of filaments or plates tends toward infinity. Examples of such cumulative distributions are shown in Figure 4, for the case of tightly packed face-centered spheres.

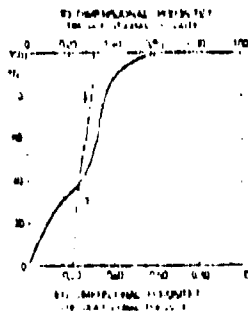


Fig. 4. Examples of cumulative distributions of the two-dimensional porosity (solid line) and one-dimensional porosity (dashed line) for tightly packed face-centered spheres.

If the statistical distribution of these two "porosities" has been determined for a given material, one can consequently determine upper and lower limits for the conductivity in the material. For cubic configurations of face-centered spheres with different particle concentrations, such calculations yield results which are insignificantly better than the previously mentioned Wiener limits, except for low particle concentrations. However, in materials with other distributions for the two porosities one finds that the limits (so derived) give a better result than the more general limits.

In principle it may be possible to improve on the limits (further), provided that one can account for the statistical distributions of one and two-dimensional porosities. However, no such efforts have been reported in the literature.

The problem of describing the microgeometry in actual materials has led to a third type of formulation for limits, based on experimental (empirical) values of conductivity in a material having a given composition by volume and certain conductivities for the components. (S. Prager (1969)(16)). Empirical values of conductivities in a porous material, in which the cavities are saturated by a certain gas, can be inserted in these formulas in order to determine the conductivity for cases where the material is saturated by a different gas or liquid. In a similar manner, measured values of the dielectric constant for a material can be used to determine limits for the thermal conductivity in the same material.

These limits are given by relatively complicated expressions which will not be reproduced here (see reference 16, Eqs 27 and 28).

As an illustration the Prager limits were computed under the (fictitious) assumption that the conductivity has been experimentally determined for two different conductivity ratios ($\lambda_2/\lambda_1 = 10$ and $\lambda_2/\lambda_1 = 125$) but for the same porosity ($n = 0.40$). Figure 5a shows the limits computed for $\lambda_2/\lambda_1 = 10$, while Figure 5b shows values computed for the other ratio.

For the case where the (net) conductivity is assumed known for $\lambda_2/\lambda_1 = 125$, the Prager limits fall outside the Hashin-Shtrikman limits over part of the range. It is also evident, that the Prager limits diverge rapidly for values of λ_2/λ_1 higher than that where the conductivity is assumed to be known.

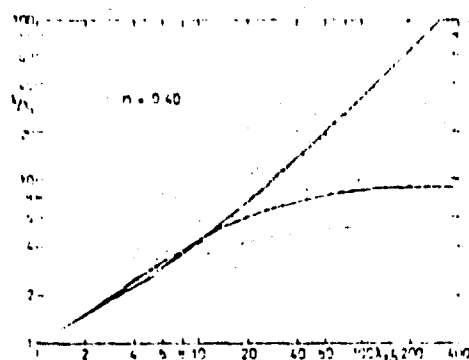
Figure 5c illustrates the case where the average conductivity has been measured at two different conductivity ratios (for the same

porosity). The limits (bounds) for the conductivity are here given as the lowest upper limit and the highest lower limit for the two cases, respectively. As shown by the Figure (5c), the resulting limits (bounds) constitute a very substantial improvement relative to the Hashin-Shtrikman limits. For conductivity ratios below 125, the conductivity is defined within a narrow band with a deviation from the average which is less than ± 10 percent.

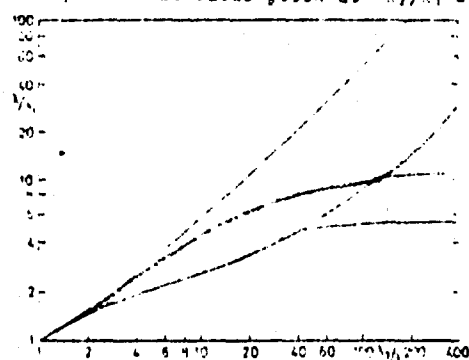
By determining the Prager limits from two experimental values, in the manner illustrated by this example, one can thus find the average conductivity ratio less than the largest value for which the conductivity has been (experimentally) determined. However, one important condition is that the microgeometry must be the same for the two cases where the conductivity is measured. This condition is most easily met by saturating the sample with different liquids, provided that the porosity stays the same.

D. Conclusion

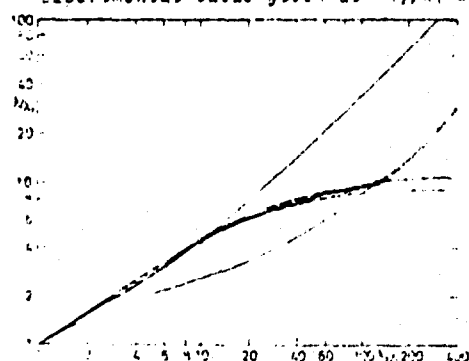
Together, the different limits (bounds) for the (average) conductivity described in this section illustrate that the conductivity can not be determined exactly unless one has complete information about the microgeometrical conditions. However, all the different formulations show that the ratio of conductivities for the two components are of primary importance in this context. For low conductivity ratios one can find the (average) conductivity with sufficient accuracy, based on volume ratios and conductivities for the components, but without information about the microgeometry. When the conductivity ratio is large, even relatively detailed information about the microgeometry, in the form of three-point correlations, will still result in widely separated limits so that the conductivity can not be determined with sufficient accuracy.



a) Eksperimentell verdi gitt ved $\lambda_2/\lambda_1 = 10$, $n = 0,40$.
Experimental value given at $\lambda_2/\lambda_1 = 10$, $n = 0,40$



b) Eksperimentell verdi gitt ved $\lambda_2/\lambda_1 = 125$, $n = 0,40$.
Experimental value given at $\lambda_2/\lambda_1 = 125$, $n = 0,40$



c) Eksperimentelle verdier gitt ved begge de nevnte ledningsevneforhold.
Experimental values given at both conductivity ratios mentioned above.

FIG. 5. Pragergrenser for to-komponentmaterialer ved konstant porøsitet beregnet ut fra eksperimentelle verdier.
Prager-bounds for two-phase materials at constant porosity calculated from experimental results.

In such cases, only experimental investigations will result in acceptable conductivity values, either directly or indirectly by means of the Prager limits.

Best Available Copy

3. MATHEMATICAL MODELS

A. Introduction

The basic theory for conductivity of composite materials, treated in the previous section, showed that the conductivity depends on three sets of parameters: conductivity of the components, their relative volumes and the microgeometry of the system. The fundamental treatment involving limits (bounds) showed that the latter parameter set plays an important role, particularly when the conductivity of components are different from each other. Even with relatively extensive information about the microgeometry (knowledge of three-point correlations) one can in principle not determine the conductivity with sufficient theoretical accuracy for these cases.

However, a number of efforts to develop mathematical models for determining the conductivity of composite materials have been reported in the literature. Such models are usually based on approximate calculations of the conductivity for idealized geometries. The choice of approximation will most often cause the calculated conductivity to deviate significantly from the conductivity in the idealized geometry. At the same time, the choice of geometry will in itself constitute an approximation relative to the microgeometry of the particular material for which the model is created. Both these factors will be of increased importance for large differences in the conductivities of the components. This means that such equations at best can be justified as semi-empirical relations, which by suitable choice of idealized geometry may be fitted to experimental values for certain groups of materials.

In the following section, different (mathematical) models will be discussed, with reference to these conditions.

B. "Exact" calculations

For simple geometries, such as regular configurations of spherical particles, one can compute the conductivity analytically or numerically with a high degree of accuracy. An analytic solution for spherical particles in a cubic (gitter) configuration was presented by Rayleigh already in 1892(17). The calculations contain certain approximations which apply to spheres which are nearly or completely in contact with each other. An improved solution was later developed by Meredith and Tobias (1960)(18). deVries (1952)(19) extended Rayleigh's methods to other configurations of spheres. A different analytical approach was used by Walther (1970)(20) to compute conductivity for spheres arranged in cubical and tetrahedral configurations (gitters). Recently, computers have been utilized for numerical determination of conductivity in regular configurations of spherical particles (21, 22, 23). Such results are available for tightly packed cubic and orthorhombic configurations of spheres with volume ratios of 0.524 and 0.605, respectively.

A comparison between numerical results for spheres arranged in a cubic configuration and the previously mentioned analytical solutions indicate that the latter give lower (conductivity) values than the numerical methods, except for very low particle concentrations where all calculated values coincide with the lower Hashin-Shtrikman limit. Among the analytical results, those calculated by Walters give the best agreement.

Figure 6 compares Walters' solutions for cubic(al) and tetrahedral configurations (packing) of spheres, for a conductivity ratio of 100. Even if the values are somewhat low for large particle concentrations, these results give a good indication of how the configuration affects conductivity for a certain porosity.

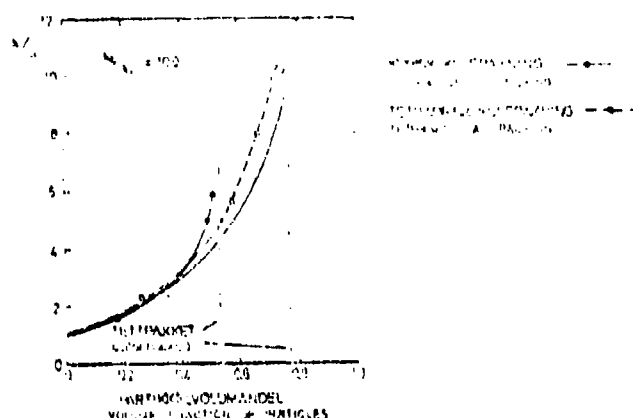


FIG. 6. Analytiske beregninger af ledningsevnen af regelmæssige kulepakninger ved varierende partikkelkoncentrationer ($\sigma_2/\sigma_1 = 300$). Analytical computations of the conductivity of regular sphere packings at variable particle concentrations ($\sigma_2/\sigma_1 = 300$). (Mittum 1972)

Figure 7 shows numerically determined values for regular configurations of spheres, drawn together with the Miller limits for similar structures. The shaded region shows the expected variations for granular materials with dispersed particles and a conductivity ratio of 300. This region is derived by interpolation of experimental data for such materials with conductivity ratios in the range between 100 and 1000. These data were taken from Chen and Vachon (1970)(24), as well as from measurements made by the author on dry soil materials (see chapter V).

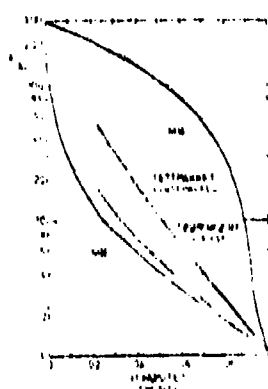


FIG. 7. Numeriske beregninger af ledningsevnen af regelmæssige kulepakninger ($\sigma_2/\sigma_1 = 300$). Det shadede feltet angiver forventede variationer i ledningsevnen af granulære materialer med dispergerede partikler ved det angivne ledningsværdierforhold. Numerical calculations of the conductivity of regular sphere packings ($\sigma_2/\sigma_1 = 300$). The shaded area represents the expected variations in the conductivity of granular materials and dispersed particles.

These results show that the expected variations in conductivity of granular materials with dispersed particles is considerably less than the theoretical limits (derived) for spherical particles. The numerically determined values all fall within the empirical limits.

Based on these studies one can state that the conductivity of materials containing spherical particles can not be expressed as a function of porosity and conductivity ratio only. In addition to these parameters, the geometrical (packing) configuration is also significant. However, the latter parameter has less importance (influence) than indicated by theoretical limits derived for spherical particles. However, these computed values are valid for a rather narrow range of porosities. This condition, as well as the relatively wide incertainties that may be expected, mean that an empirical determination of conductivity will be much superior to this (analytical) method in most cases.

C. Approximate methods based on electrical field theory.

The conductivity of a composite material is defined by the following equation:

$$\langle q \rangle = \lambda \langle \nabla T \rangle \quad 14$$

where $\langle q \rangle$ is the volume average of the heat flux

$\langle \nabla T \rangle$ is the volume average of the temperature gradient

These volume averages can be expressed in terms of volume averages for each of the material components:

$$\langle q \rangle = n \langle q \rangle_1 + (1-n) \langle q \rangle_2 \quad 15$$

$$\langle \nabla T \rangle = n \langle \nabla T \rangle_1 + (1-n) \langle \nabla T \rangle_2 \quad 16$$

Since each of the components is homogenous and isotropic, the following also holds

$$\langle q \rangle_1 = \lambda_1 \langle \nabla T \rangle_1 \quad 17$$

$$\langle q \rangle_2 = \lambda_2 \langle \nabla T \rangle_2 \quad 18$$

By combining these equations one can express the conductivity of the composite material in terms of the volume averages of temperature gradient in both components:

$$\lambda = \frac{\lambda_1 n + \lambda_2 (1-n) \langle \nabla T \rangle_2 / \langle \nabla T \rangle_1}{n + (1-n) \langle \nabla T \rangle_2 / \langle \nabla T \rangle_1} \quad 19$$

This expression gives exact values for conductivity if the ratio between volume averages of temperature gradient is known.

A common method for determining this ratio is based on an analogy with the electrostatic case. If a spherical particle is inserted into a homogenous electrostatic field, one obtains the electric field inside the sphere from

$$E_1 = \frac{3\epsilon_1}{\epsilon_2 + 2\epsilon_1} E_1 \quad 20$$

E_1 is the impressed homogenous field

ϵ_1 is the dielectric constant of the impressed homogenous field¹⁾

ϵ_2 is the dielectric constant of the sphere

At best, such a treatment of a single particle may be valid in a strongly dispersed systems, where the field in the continuous component²⁾ is not significantly affected (changed) by the (presence of) the spheres. In such cases, the impressed field can be set equal to the field in the continuous component and the (internal) field in the spheres can be found from Equation 20.

1), 2) see next page

Inserted in Equation 19, this results in the following expression for the conductivity:

$$\lambda/\lambda_1 = \frac{(\lambda_2 + 2\lambda_1)n + 3\lambda_2(1-n)}{(\lambda_2 + 2\lambda_1)n + 3\lambda_1(1-n)} \quad 21$$

This equation was originally derived by Maxwell (1881). Later, Friche (25) developed a similarly based equation valid for ellipsoid-shaped particles. In this equation, the ratio between temperature gradients is given by:

$$\langle \nabla T \rangle_2 / \langle \nabla T \rangle_1 = \frac{1}{3} \epsilon_{a,b,c} \frac{1}{1 + (\lambda_2/\lambda_1 - 1)g_1} \quad 22$$

where g_a, g_b, g_c are parameters which depend on the (geometrical) shape of the ellipsoid. ($g_a + g_b + g_c = 1$)

For spherical particles : $g_a = g_b = g_c = 1/3$

discshaped particles: $g_a = 1, g_b = g_c = 0$

needle-shaped particles: $g_a = g_b = 1/2, g_c = 0$

As mentioned previously, these equations are only valid for the case of (widely) dispersed particles. The expression for spherical particles is also identical to the lower Hashin-Shtrikman limits, while their upper limit is found by considering (widely) dispersed pores in a continuous material ($\lambda_2 < \lambda_1$). For other geometries, the equation yields results between or on these limits.

In an effort to find a more accurate approximation for cases other than that of (widely) dispersed particles, a different formulation of the exact expression for conductivity has been used:

- 1) That is, the dielectric constant of the (homogenous) medium surrounding the sphere. (Translator's note)
- 2) The material in which spheres are imbedded or "dispersed" (Translator's note)

$$\lambda = \lambda_1 + (\lambda_2 - \lambda_1) \cdot (1-n) \langle \nabla T \rangle_2 / \langle \nabla T \rangle \quad 23$$

The ratio between temperature gradients is in this case found by assuming that a single sphere is inserted in a homogenous field which is equal to the macroscopic (average) field. This gives

$$\langle \nabla T \rangle_2 / \langle \nabla T \rangle = \frac{3}{\lambda_2 + 2\lambda} \quad 24$$

When inserted in Equation 23, this results in the following equation

$$n \frac{\lambda_1 - \lambda}{\lambda_1 + 2\lambda} + (1-n) \frac{\lambda_2 - \lambda}{\lambda_2 + 2\lambda} = 0 \quad 25$$

This equation is usually ascribed to Böttcher (1945)(26). Later, Folden and van Santen (1946)(27) developed a (corresponding) expression for particles with ellipsoidal shapes.

Not even this assumption will be valid for the case of concentrated particles, since the temperature field around each particle (then) must depend on neighbouring particles.

Many different efforts have been made to solve this problem. Bruggeman (1935)(28) used Equation 23 to determine the increase in conductivity due to a small addition of particles in a material. This results in a separable differential equation, which after integration yields the following expression for the conductivity

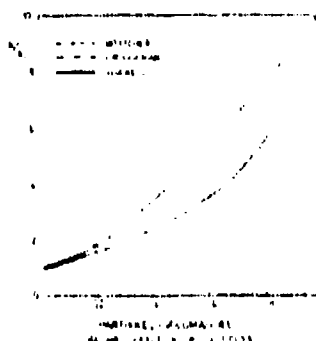
$$n = \frac{\lambda_2 - \lambda}{\lambda_2 - \lambda_1} \sqrt[3]{\frac{\lambda_1}{\lambda}} \quad 26$$

Also in this case it is in effect assumed that the field inside the few added particles does not depend on adjacent particles.

To include interaction between adjacent particles one must obviously form a description of the geometry of the system, including the packing configuration. Since the latter can take many forms for

a given article geometry it is evident that a general expression for conductivity in a material containing particles cannot be formulated. This was also shown, by means of a study of limits, in the previous main section.

Figure 8 compares (results derived from) the three previously mentioned equations, formulated for spherical particles, and the Miller limits (bounds) for spheres having a conductivity ratio of 10.



BEST AVAILABLE COPY

FIG. 8. The limiting case of spheres for conductivity ratio of 10. The solid line represents the Miller upper limit, the dashed line represents the Miller lower limit, and the solid line represents the Maxwell equation. The graph shows that the Maxwell equation gives values below the lower limit.

As shown, the equations by Böttcher and Bruggeman (give values which) fall between the (Miller) limits, while Maxwell's equation gives values below the lower limit.

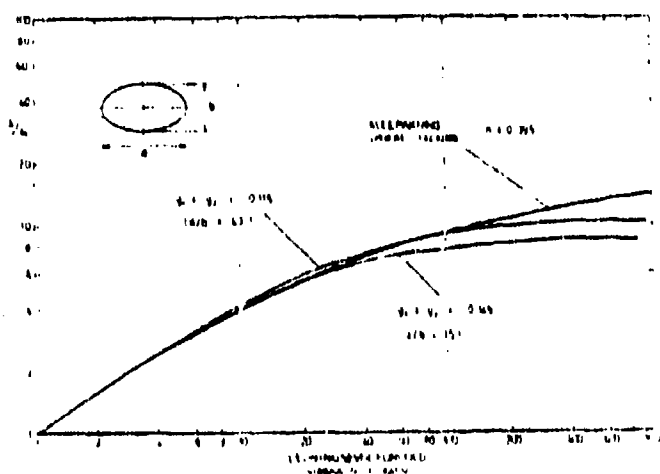
All the different equations mentioned here lend themselves to adjustments (fitting) to experimental result by choice of geometry (-related parameters) in the equations. However, one can not expect this (best fit) particle geometry to agree with the particle shapes in the material at hand.

If two g -values are equal, the shape of the ellipsoid(s) can be found from the third g -value (27). For this case, Fricke's equation can only be fitted to one point on an experimental curve

which gives the conductivity as a function of conductivity ratio for constant porosity. The result of such a fitting to a numerically computed functional dependence of the conductivity for spheres in an orthorhombic (packing) configuration is shown in Figure 9.

It can be seen, that the fitted curves fall below the curve for orthorhombic (packing) configuration at high conductivity ratios. As mentioned, the particle geometry corresponds to more elongated ellipsoids which become less like spheres as the conductivity ratio increases.

This discussion shows that equations of this type only have theoretical relevance for rather low particle concentrations, where the theoretical limits for a given particle shape coincide. In other cases, they may give acceptable results when the conductivity ratio is low and the theoretical limits for the particle shape at hand define a relatively narrow range of conductivities. For cases other than these, the equations are only relevant as semi-empirical (mathematical) models which can be fitted to experimental conductivity curves within limited ranges of conductivity ratios and porosities, as well as for a certain choice of geometrical (form) factors.



viq. 9. Eksempler som illustrerer tilnærmning av Prickses teori til et gitt ledningsoverforhold. Tilmerke den uenighetene av ledningsveien av den enkelte ledningsveien. Sammenlign illustrering av et gitt ledningsveien til et gitt ledningsveien. (The conductivity of the conductor is of the order of the conductivity of the conductor.)

D. Approximate calculations based on elements connected in series or shunt

One group of (mathematical) models is based on a conceptual subdivision of the heat transfer mechanism in a particle-filled material into (lumped) thermal resistance elements. Examples of such elements are given in Refs 29 through 32. This concept can be pictured in terms of cubical models (cells), within which the dispersed material forms a parallelepiped (see Figure 10).

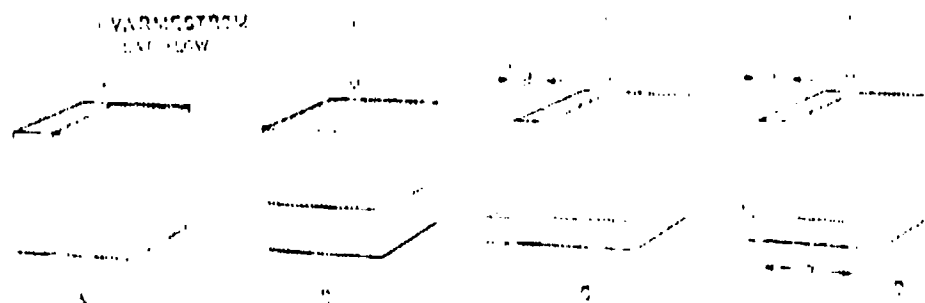


FIG. 10. Examples of cubical models for heat transfer. A) Horizontal liquid film at the bottom. B) Horizontal liquid film at the top. C) Vertical liquid layer on the left. D) Vertical liquid layer on the right.

The most commonly used model is shown in Figure 10 C. The conductivity of such a cubical elementary (unit) cell is, according to the basic assumption, usually calculated from the thermal resistance of the vertical liquid layer (thickness λ) connected in shunt across the series combination of resistances associated with the horizontal liquid film (thickness ϕ) and the particle, see Figure 10(C). This results in the following expression for the conductivity¹⁾.

$$\lambda = \lambda_1 s + (1 - s) / \left[\phi / \lambda_1 + (1 - \phi) / \lambda_2 \right] \quad 27$$

It is worth noting, that connecting (a resistance representing) the horizontal liquid film is series with a shunt combination of (resistances representing) the vertical liquid layer and the particle gives a different result¹⁾

1) See appendix to the translation

$$\lambda = 1 / \{ \phi / \lambda_1 + (1 - \phi) / [\lambda_1 \beta + \lambda_2 (1 - \beta)] \} \quad 28$$

These equations represent lower and upper bounds for the conductivity, respectively, for this particular (type of) cell. These bounds are identical to those given by Coriell and Jackson, discussed in the previous section. In this case, the difference between limits (bounds) is relatively small, but for other configurations (e.g. that of Figure 10 D), the difference may be significant.

The choice of (equivalent circuit) representation will, however, in such cases be of minor importance, as long as the geometrical conditions of the cell are selected based on a semi-empirical fitting to experimental values.

During such a semi-empirical fitting process one will in most cases find it necessary to vary the geometry along with conductivity ratio and porosity, in order to obtain a satisfactory fit to the experimentally determined conductivity dependence. This is illustrated in Figure 11, which shows an effort to fit Eq 27 to the numerically computed conductivity variation in a material consisting of spheres in an orthorhombic configuration. For geometrical conditions which result in agreement at conductivity ratios of 10, 100 and 1000, one finds that the agreement is poor for other conductivity ratios, except at the low end of the scale where the three (cell) models give practically speaking the same values.

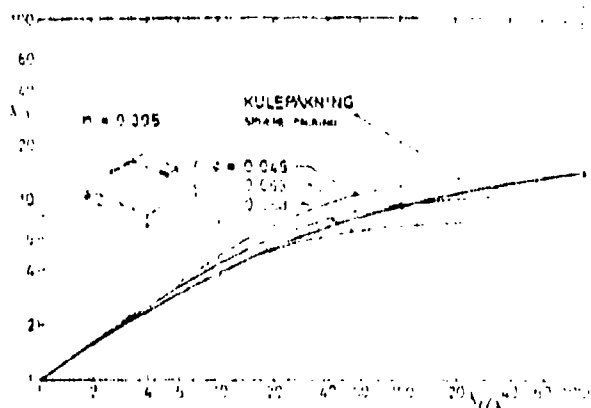


FIG. 11. Example of fitting a model of type a (Fig. 10 A) to the conductivity variation of a sphere packing as determined by numerical calculations. The curves represent the results of fitting Eq. 27 to a given porosity for different conductivity ratios of the conductivity of the solid phase to the porosity.

A variable geometry parameter, such as ϕ in Figure 10, was used by Vii et.al. (33,34,35). These reports give the geometry parameter in graphical form, as function of conductivity ratio, for two porosities. The authors recommend linear interpolation for other values of porosity. The cell geometry is selected on the basis of approximate calculations of conductivity in a (packing) configuration of spheres, using the principle of parallel heat flow lines. By considering the number of contacting points in other types of configurations, an effort was made (by the authors) to extend these results to other values of porosity.

The results of these studies are somewhat in doubt due to a number of inconsistencies. On the other hand, they present a single model which gives conductivities in good agreement with numerical calculations in regular configurations of spheres.

In other report-, efforts are made to fit the geometrical parameter to conditions in configurations of spheres by considering only the volumetric properties of the liquid layers near the contact points in various configurations. This results in constant values for the geometry parameter for given porosities, independent of the conductivity ratio (36). This gives less freedom in fitting the results computed from the (mathematical) model to conductivity variations in a given material.

As evident from the preceding discussion (mathematical) models of this kind will always be semi-empirical to a certain extent, both in terms of choice of model type and choice of approximate computation method, as well as in the choice of geometrical parameters. The usefulness of a given model depends primarily on how well it can be fitted to the functional dependence of conductivity in a given material. In cases where this (fit) is accomplished by means of geometrical parameters that depend on conductivity ratio and porosity, they (the models) offer in reality no advantage over purely em-

pirical correlations derived from experimental data for the material at hand.

A closely related class of (mathematical) models involves efforts to base the calculations on a geometry which to a greater extent is similar to the microgeometry of the actual material. The microgeometry is then characterized in terms of statistical (stochastic) distributions of the one or two-dimensional porosities, as discussed in the previous section in connection with the limits (bounds) given by Coriell and Jackson.

A model of this kind was first presented by G.T. Tsao in 1961(37). This model contains certain fundamental errors but efforts have been made to correct these in models of the same type (38). However, all these models are based on an erroneous assumption concerning the relation between distribution functions for one and two-dimensional porosities.

Tsao's model has received considerable attention in the literature. For example, S.C. Cheng and R.I. Vachon have published a series of papers based on this model (39, 24). They claim that the stochastic distribution of the dispersed medium justifies the assumption that the one-dimensional porosity is normally distributed. This normal distribution is then approximated by a parabolic distribution. However, the theoretical foundation for this model is unacceptable in several respects. In effect, the model used by Cheng and Vachon can be reduced to an idealized case where the dispersed component is represented by a parabola whose volume corresponds to the volume ratio of particles in the material at hand.

Even if the theoretical foundation for the model is questionable, comparisons between calculated and experimental values for a relatively large number of materials show a fairly good agreement (24). If one compares values computed from this model with expected conductivity variations in dispersed granular materials one finds that the model yields values within the same range.

The agreement with experimental data gives this model a certain credibility as a toll for computing conductivity in granular and dispersed materials. However, the uncertainty becomes large for relatively small to moderate porosities, as shown in the corresponding figure. In addition, the model does not allow fitting to moderate porosities, as shown in the corresponding figure. In addition, the model does not allow fitting to experimental function and is thus worthless as a semi-empirical relation.

The theoretical weaknesses inherent in models of this kind can obviously be compensated for by a correct application of theoretical methods developed by Coriell and Jackson for determining conductivity of composite materials. However, this does not imply an improved accuracy of these models, since one will only be able to determine the conductivity within rather wide limits in materials with certain (given) statistical distributions for the one and two-dimensional porosities. To even determine these statistical distributions will also be quite a complicated task. It therefore seems more realistic to attack the problem more directly by means of empirical investigations of the conductivity on materials at hand, in order to develop practical values for the range of variation in conductivity for different groups of materials. Such an approach will represent an empirical parallel to the purely theoretical derivation of limits (bounds) described in section 2 of this chapter.

E. The geometric mean model

Warren and Price (1961)(41) presented results from a series of numerical experiments which are closely related to empirical determination of limits for the conductivity in certain groups of materials. Warren used a three-dimensional model in the form of a cubic lattice where each element was given a different conductivity in relation to determined distribution functions. The location of

individual elements in the lattice was made random. For each such configuration, the effective conductivity was calculated by numerical solution of the heat flow equation in the three-dimensional lattice. The configurations were changed a sufficient number of times to give the most probable (expected) conductivity with reasonable accuracy¹⁾.

For all the different types of continuous distribution functions that were selected for the conductivities of the elements, it was demonstrated that the geometric mean of these conductivities forms a good approximation to the expected conductivity:

$$\lambda = \sqrt[p]{\prod_{i=1}^{n_i} \lambda_i} \quad 29$$

where n_i is the relative number of elements having conductivity λ_i

In a discontinuous distribution where each element is given one of two conductivity values (corresponding to a two-component system), the expected conductivity was found to nearly equal the geometric mean for low conductivity ratios ($\lambda_2/\lambda_1 < 10$). However, for higher ratios between the two conductivities, the expected conductivity deviated significantly from this.

Standard deviations of the calculated conductivities could in principle have given information about expected variations in conductivity for a given distribution of element conductivities. However, this parameter was not reported for the discontinuous distributions. In addition, the standard deviations for continuous distributions were dependent on the selected discrete approximations for these distributions.

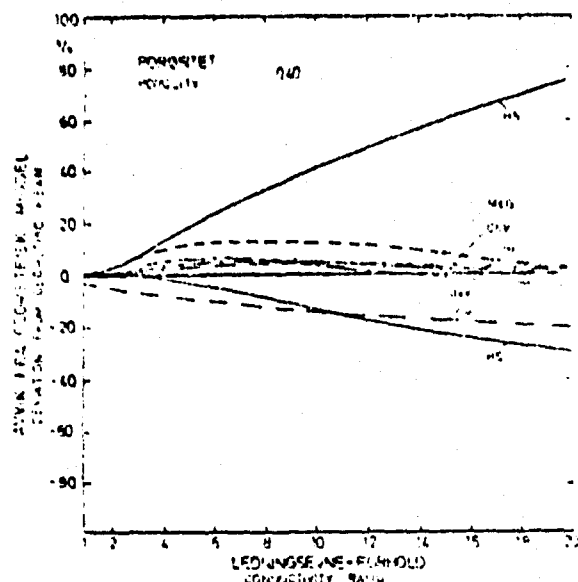
The geometric mean equation has also been suggested by other authors as a model for conductivity calculations for two component materials.

1) A Monte Carlo type simulation (Translator's note)

For example, W. Woodside and J.H. Messmer (1961)(30) found that this model gave good agreement with conductivity measurement in water-saturated sand at various porosities. Also, J.H. Sass et.al. (1971) recommended this equation for use in connection with water saturated crushed rock (41).

An important property of the geometric mean equation is that it always yields values which fall between the Hashin-Shtrikman limits. For low conductivity ratios where these limits are close together, it will thus give a good approximation for the conductivity of composite materials which can be considered macroscopically homogenous and isotropic. Since it also gives a good fit to experimental values for granular material with moderate conductivity ratios ($\lambda_2/\lambda_1 \sim 10$), there are obvious reasons for favouring this comparatively simple equation over other more complicated mathematical models described previously.

Figure 12 compares four of the previously discussed equations developed for calculating conductivity in granular materials with the geometric mean equation, for constant porosity ($n = 0.40$) and conductivity ratios up to $\lambda_2/\lambda_1 = 20$. The Hashin-Shtrikman limits are also shown in Figure 12. Evidently, the deviation from the geometric mean is less than 20 percent for these equations, while the Hashin-Shtrikman limits deviate considerably more. The three equations which most closely agree with the geometric mean (Cheng and Vachon, de Vries and Bruggeman) have been shown by many to give good agreement with experimental conductivities, for low conductivity ratios (23, 31, 42).



deV: Priole's equation with $p_1 = p_2 = 0.125$ (19).
 Kut: Kunit's equation (22, 34, 35).
 McG: McGau's equation with $n_0 = 0.04$ (20).
 CHV: Chung and Vaishn's equation (23).
 Br: Bruggeman's equation for spherical particles (28).
 HS: Upper and Lower Hashin-Shtrikman bounds (7).

FIG. 12. Sammenlikning mellom modeller for tilnærmet beregning av ledningsevnen i to-komponentmaterialer og geometrisk middelberegning ved konstant porøsitet og varierende ledningsevneforhold. Comparison between models for approximate calculation of the conductivity of two-phase materials and the geometric mean equation at constant porosity and variable conductivity ratios.

F. Conclusion

This discussion of different types of models for calculating the conductivity in composite materials shows that such models in general tend to consist of semi-empirical equations which are only applicable to the extent that they can be fitted to experimental results for a given group of materials.

For low conductivity ratios (<10), where the different models give almost identical values, it seems logical to prefer the simple geometric mean model as a basis for conductivity estimates.

For large conductivity ratios, the conductivity of a certain group of materials will always show relatively wide variations.

In this case, any given model will give large uncertainties. For this reason it seems more fruitful to work towards generating an empirical data base for estimated variations in conductivity in different groups of materials. Such investigations should result in a form of empirical parallel to the purely theoretical limit considerations.

REFERENCES - CHAPTER II

1. K. H. Walter: Zur matematischen Behandlung der stationären Wärmeleitung in stückweise homogenen Medien, Kernforschungs-anlage Jülich, JÜ1-657-NA, April 1970.
2. W. F. Brown: Solid Mixture Permittivities. The Journal of Chemical Physics, 23, (8), 1955, pp. 1514-1517.
3. W.E.A. Davies: The theory of composite dielectrics. J. Phys. D: Appl. Phys. 4, 1971, pp. 318-327.
4. M. J. Beran: Application of Statistical Theories to Heterogeneous Materials. Phys. Stat. Sol. (a), 6, 1971, p. 365.
5. W. F. Brown, Jr.: Dielectric Constants, Permeabilities, and Conductivities of Random Media, Trans. of the Soc. of Rheology 9, (1), 1965, pp. 357-380.
6. O. Wiener (1912): Referert av W.F. Brown (1965) See ref. 5.
7. Z. Hashin and S. Shtrikman: A Variational Approach to the Theory of the Effective Magnetic Permeability of Multiphase Materials, J. Appl. Phys., 33, (10), 1962, pp. 3125-3131.
8. M. Beran: Use of the Vibrational Approach to Determine Bounds for the Effective Permittivity in Random Media. Nuovo Cimento, 38, (2), 1965, pp. 771-782.
9. P. B. Corson: Correlation functions for predicting properties of heterogeneous materials. I. Experimental measurement of spatial correlation functions in multiphase solids. J. Appl. Phys., 45, (7), 1974, pp. 3159-3164.
10. P. B. Corson: Correlation functions II. Empirical construction of spatial correlation functions for two-phase solids. J. Appl. Phys. 45, (7) 1974, pp. 3165-3170.
11. P. B. Corson: Correlation functions IV. Effective thermal conductivity of two-phase solids. J. Appl. Phys., 45, (7), 1974, pp. 3180-3182.
12. M. N. Miller: Bounds for Effective Electrical, Thermal, and Magnetic Properties of Heterogeneous Materials. J. Math Physics, 10, (11), 1969, pp. 1988-2004.
13. M. A. Elsayed: Bounds for effective thermal, electrical, and magnetic properties of heterogeneous materials using higher order statistical information. J. Math. Physics, 15, (11), 1974, pp. 2001-2015.

14. J. L. Jackson, S. R. Coriell: Transport Coefficients of Composite Materials. J. Appl. Phys. 39, (5), 1968, pp. 2349-2354.
15. S. R. Coriell and J. L. Jackson: Bounds on Transport Coefficients of Two-Phase Materials. J. Appl. Phys. 39, (10), 1968, pp. 4733-4736.
16. S. Prager: Improved Variational Bounds on Some Bulk Properties of a Two-Phase Random Medium. J. Chem. Phys. 50, (10), 1969, pp. 4305-4312.
17. Lord Rayleigh (1892). Referert av Meredith (1969) (18).
18. R. E. Meredith and C.W. Tobias: Resistance to Potential Flow through a Cubical Array of Spheres. J. Appl. Phys. 31, (7), pp. 1270-1273.
19. D.A. De Vries: Het warmtegeleidingsvermogen van grond. Med. Landbouwhogeschool. Wageningen, 52, 1952.
20. G.K.H. Walther: Zur mathematischen Behandlung der Stationären Wärmeleitung in stückweise homogenen Medien. Kernforschungsanlage Jülich, 657-MA, 1970.
21. R.S. Deissler, J.S. Boegli: An Investigation of Effective Thermal Conductivities of Powders in Various Gases. Transactions of the ASME, October 1958, pp. 1417-1425.
22. N. Wakao, K. Kato: Effective Thermal Conductivities of Packed Beds. Journal of Chemical Engineering of Japan, 2, (1), 1969, pp. 24-33.
23. T.P. Fidelle, R.S. Kirk: A study of Unidirectional Versus Tridirectional Heat Flux Models. AIChE Journal, 17, (6), 1971, pp. 1427-1434.
24. S.C. Cheng, R.I. Vachon: A Technique for Predicting the Thermal Conductivity of Suspensions, Emulsions and Porous Materials. Int. J. Heat Mass Transfer, 13, 1970, pp. 537-546.
25. J.A. Reynolds, J.M. Hough: Formulae for Dielectric Constant of Mixtures. Proc. Phys. Soc. (London) B70, 1957, pp. 769-775. (Referert H. Fricke (1924))
26. C.J.F. Bottcher (1938): Referat av D. Polder (1946). See ref. (36).
27. D. Polder, J.H. van Santen: The Effective Permeability of Mixture of Solids. Physica, 12, (5), 1946, pp. 257-271.
28. D.A.G. Bruggeman: Dielektrizitätskonstanten und Leitfähigkeiten von Vielkristallen der nichtregulären Systeme, Ann. Physik 5, (25), 1936, pp. 645-664.

29. W.O. Smith: The Thermal Conductivity of Dry Soil. Soil Science, 53, 1942, pp. 435-459.
30. W. Woodside, J.H. Messmer: Thermal Conductivity of Porous Media. I. Unconsolidated Sand., J. Appl. Phys., 32, (9), 1961, pp. 1688-1699.
31. R. Mc Caw: Heat Conduction in Saturated Granular Materials. Highway Res. Board., Spec. Rep. no. 103, 1969, pp. 114-131.
32. G.S.G. Beveridge, D.P. Haughey: Axial Heat Transfer in Packed Beds. Stagnant Beds Between 20 and 750° C. Int. J. Heat Mass, 14, 1971, pp. 1093-1113.
33. S. Yagi, D. Kunii: Studies on Effective Thermal Conductivities in Packed Beds. A.I. Ch. E. Journal 3, (3), 1957, pp. 373-381.
34. D. Kunii, J.M. Smith: Heat Transfer Characteristics of Porous Rocks. A.I. Ch. E. Journal, 6, (1), 1969, pp. 71-78.
35. K. Ofuchi, D. Kunii: Heat-Transfer Characteristics of Packed Beds with Stagnant Fluids. Int. J. Heat Mass Transfer, 8, 1965, pp. 749-757.
36. S. Masamune, J.M. Smith: Thermal Conductivity of Beds of Spherical Particles. Ind. and Engl. Chem. Fundamentals, 2, 1963, pp. 136-143.
37. G.T. Tsao: Thermal Conductivity of Two-Phase Materials. Ind. Eng. Chem. 53, (5), 1961, pp. 395-397.
38. P.B. Desphande, J.R. Cooper: Thermal Conductivity of Two-Phase Systems. J. Heat Transfer. Trans. of the ASME, May 1972, pp. 249-264.
39. S.C. Cheng, R.I. Vachon: The Prediction of the Thermal Conductivity of Two and Three Phase Solid Heterogeneous Mixtures, Int. J. Heat Mass Transfer, 12, 1969, pp. 249-264.
40. J.E. Warren, H.S. Price: Flow in Heterogeneous Porous Media. Society of Petroleum Engineers Journal, Sept. 1961, pp. 153-169.
41. J. H. Sass et al: Thermal Conductivity of Rocks from Measurements on Fragments. J. Geophysical Research, 76, (14), 1971, pp. 3391-3401.
42. K. Gotoh: Thermal Conductivity of Two-Phase Heterogeneous Substances. Int. J. Heat Mass Transfer, 14, 1971, pp. 645-646.

CHAPTER III

Soil parameters

The previous analysis of heat transport mechanisms in soil materials showed that heat transfer in soils can be regarded as a pure thermal conduction process controlled by temperature gradients. During the discussion of methods for calculating thermal conductivity in composite materials it was shown that the conductivity in such a material will depend on three sets of parameters: the conductivity of each component, their relative volumes and the micro-geometry of the system. These sets of parameters are here collectively denoted thermal conductivity parameters.

In a soil material, these thermal conductivity parameters are more or less completely described (defined) by the mineralogical and mechanical composition of the material, as well as information about dry specific weight, water content and temperature level (frozen, un-frozen). The different material characteristics from which the fundamental parameters can be derived will be discussed in the following.

1. THERMAL CONDUCTIVITY OF SOIL GENERATING MATERIALS

A. Soil generating minerals

The mineralogical composition of soil materials is the result of processes such as weathering, transport, sedimentation and possibly chemical withering of solid rock. These processes contribute to giving the soil a different average composition than that of solid rock. For example, less crush-resistant minerals such as feldspar will be crushed at a more rapid rate during transport. This results in an enrichment of more resistant minerals in coarser depo-

sits (sand, coarse silt). In addition, finely crushed feldspar is particularly prone to chemical withering, which gives rise to new types of minerals. These minerals will occur in the form of rather small flakes, rich in Aluminum, while the content of the more easily soluble elements Na and Ca is reduced. Hydromica is such a residual product while different types of clay (kaolinite, montmorillonite) represent an even more complete change during which all Na or Ca has been lost (1).

These processes will thus result in differences in average mineralogical composition for loose deposits and bedrock, as well as certain differences in the mineralogical composition due to particle size in the soil materials. These conditions are illustrated in Table I and in Figure 1, respectively (2,3).

Table I Comparison between average mineralogical composition in volcanic rocks and sediments (2).

Mineral	Average, volcanic rocks	Average, sediments
Quartz	12	35
Feldspar	59.5	16
Mica	3.8	15
Miscellaneous	24.7	34

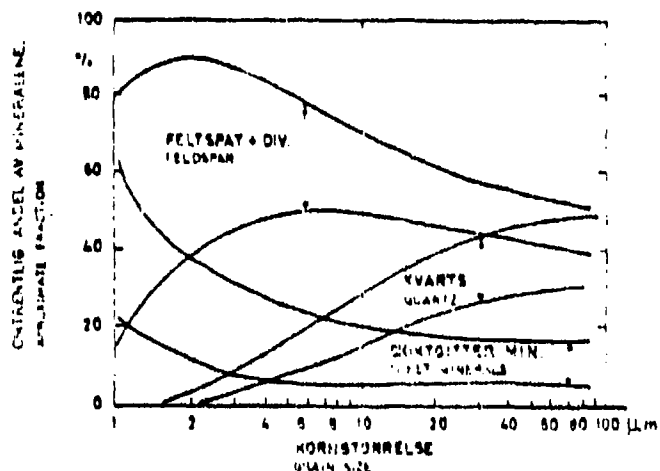


FIG. 1. Diagrammatic average composition for the average mineral components in normal igneous rocks. Sketch of variations in the three main mineral components in sedimentary rocks (1).

In Norway, most older loose deposits were removed during the ice age. Present soils were primarily deposited during the last melting period, between 8,500 and 12,000 years ago, or in later times. Thus, the previously mentioned (chemical) changes in the most fine grain materials have had a short time in which to occur and Norwegian clays in general contain small amounts of the typical clay minerals, except for hydromica.

For these reasons, Norwegian soils primarily consist of minerals normally occurring in the bedrock. Of these, three groups are in general dominant in Norway: Quarts, feldspar and mica. Together, these form more than 90 percent of common rocks such as granite and gneiss. In addition, these rock materials dominate the bedrock in large parts of Norway, except for streaks of sediments and a few streaks where quartz-free rocks such as gabbro and amphibolite are predominant. These rocks consist mostly of feldspar (plagioclase) in addition to pyroxene (gabbro) or amphibolite. Such quartz-free rocks can be found in the Cambrosilurian field stretching from Bergen over Jotunheim¹⁾ in to southern Trøndelag²⁾. (See map in Figure 2)³⁾ Large regions of predominantly gabbro can also be found in the Cambrosilurian field in Troms²⁾ and Finnmark²⁾. The Telemark²⁾ formation also contains significant amounts of the same rock type.

Depending on ice movements and transport in rivers during the ice age, these rock types may have given rise to significant contents of minerals such as pyroxene and amphibolite also in soils where such materials occur to a very limited extent in the bedrock. This in general means that the mineralogical composition of loose deposits will deviate from the mineralogical composition of the local bedrock.

1) Mountain formation (Translator's note)

2) These names refer to "Fylken", county-type districts (Translator's note).

3) Not present in the original (Translator's note)

The most common minerals occurring in the loose deposits will thus, as indicated, be quartz, feldspar, mica, amphibolite and pyroxene. The first three of these will normally dominate, while in limited areas amphibolite and pyroxene may occur in significant amounts, together with feldspar.

B. Quartz content in loose deposits

Of the minerals mentioned previously, quartz plays a particularly important role in this context (as will be evident from next section), due to its relatively high conductivity. This led to a study by H. Sveian of the quartz content in Norwegian loose deposits (5, 6). During this study, the quartz content was measured in a total of 131 samples from different types of deposits and bedrock regions, by means of differential thermal analysis (DTA). In some samples, the quartz content as function of particle size was also investigated. This study supplements in many respects the investigation made by Selmer-Olsen of the mineralogy of Norwegian clays (7), which included determination of quartz content in about 160 clay samples from the entire country by means of DTA (see Figure 1).

Table II shows the distribution of quartz content in the samples investigated by Sveian. The results are arranged according to bedrock region. As can be seen, there are rather wide variations. Together, the results indicate an average quartz content of 37.5 percent. The lowest quartz contents are found in samples for the Bergen region and areas having Caledonian intrusives, as well as in some samples from the Cambrosilurian field. This indicates, that the lowest quartz content in general occurs for high incidence of gabbro or other alkaline types of rock.

For a small number of selected samples, the quartz content was determined for several fractions (by particle size) of the samples. Based on these experiments, one can plot quartz content versus

Table II. Quartz content in Norwegian loose deposits (131 sample)(5).

Interval, percent	Gr. fjell 1)	The More field 2)	Eocam- brian	Bergen ²⁾ region	Caledonian Intrusives	Cambro- silurian	Others
0 - 5	0	0	0	0	1	2	0
5 - 10	0	0	0	3	3	1	0
11 - 15	0	0	0	2	1	0	1
16 - 20	0	0	1	0	0	3	1
21 - 25	2	1	1	0	1	4	0
26 - 30	6	4	0	0	0	3	1
31 - 35	9	1	2	0	0	9	1
36 - 40	1	0	2	0	0	4	2
41 - 45	7	1	3	0	0	8	3
46 - 50	3	0	1	0	0	7	2
51 - 55	2	0	1	0	0	4	0
56 - 60	2	0	0	0	0	3	2
61 - 65	1	0	1	0	0	1	0
66 - 70	0	0	0	0	0	1	0
71 - 75	1	0	1	0	0	0	0
76 - 80	0	0	0	0	0	0	0
81 - 85	0	0	2	0	0	0	0

Translator's notes

1) "Fjell" means "mountain" or "rock". "Gr." is either the name of a mountain or short for

"grå" = gray. "Gray rock" is a lay-man's expression for a group of minerals including granite, gneiss and other crystalline rocks.

2) These notations probably refer to regions marked on Figure 2. However, that map was not available during the translation.

grain size for these materials. These curves are shown in Figure 3. Most of these samples were sand or gravel materials with low content of silt or finer fractions. The results from these samples are drawn as bold solid lines, while results from samples of moraine and lake-shore sediments having a more even particle size distribution are shown as broken lines. The thin solid lines define the range of quartz content variations in more fine grained materials found by Selmer and Olsen (3).

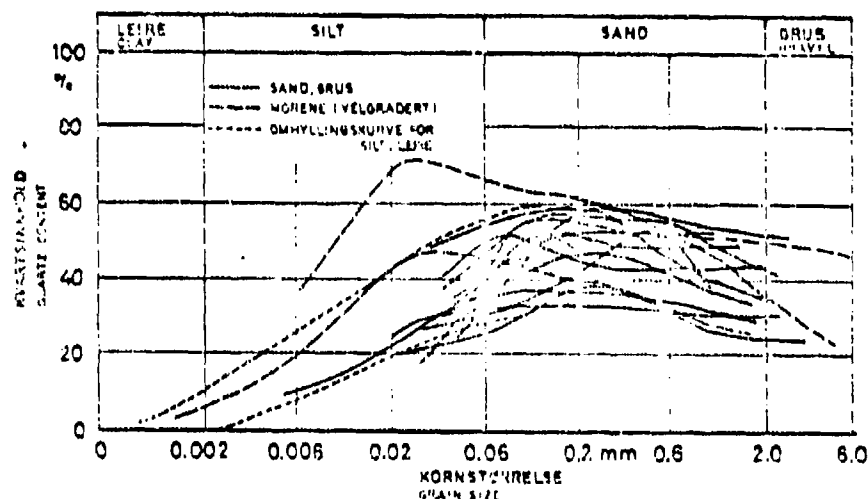


FIG. 3. Kvartsinnholdets variasjon med kornstørrelsen i prøver av norske løsmasser. Variation of quartz content with grain size in samples of Norwegian deposits. (Lundén 1973) (6)

As can be seen, all samples are characterized by a more or less pronounced maximum in the quartz content. For the different sand and gravel materials, the maximum occurs for particle sizes in the range fine to average sand, while maxima fall somewhat lower (coarse silt to fine sand) for samples having more even size distributions.

All told, this study shows that the quartz content in Norwegian loose deposits can vary between wide limits. These limits depend partially on the particle size distribution within the materials and partially on variations in mineralogical composition of the original (rock) material. The first of these "mechanisms"

will cause fine grain materials with relatively high content of materials finer than average silt ($d < 0.02$ mm) to, in general, have lower quartz contents than coarser materials where silt and finer fractions are scarce ($d > 0.06$ mm). In regions where the bed-rock contains little quartz, the second mechanism will come into play and cause low quartz content for all fractions.

Fraction mm	Average quartz content, percent	Range of vari- ation, percent
$d > 0.02$	45	20 - 60
$0.002 < d < 0.02$	15	0 - 40
$d < 0.002$	0	0 - 10

Figure 4 shows a comparison between measured and calculated quartz contents (for the samples where particle size distributions are reported), based on this "model". With a few obvious exceptions, most of the results fall within ± 30 percent of calculated values.

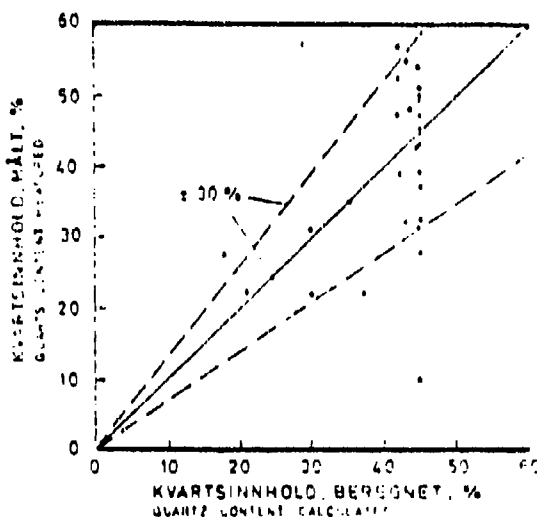


FIG. 4. Sammenlikning av målte kvartsinhold og verdier beregnet ut fra kornfordelingskurver. Sammenlikning av målte og beregnede kvartsinhold og verdier beregnet ut fra kornfordelingskurver.

If higher accuracy is desired, one may perform direct measurements of the quartz content.

C. Thermal conductivity for the components

Measurement of the thermal conductivity made by Birch and Clarkes (1940) for a number of rock materials over the temperature range 0 to 400°C show that the conductivity in most materials decreases with increasing temperature. Their results for pure quartz, certain granites and a few gabbro-type rocks are shown in Figure 5. The horizontal scale is $1/T$ and the parameter is $t = T - 273$. It is evident, that this representation results in a linear dependence for the conductivity in most rock materials (8).

Of the different materials, quartz has both the highest conductivity and the largest variation with temperature, while the gabbro minerals have the lowest conductivity and show small or no temperature dependence. One should also note the large difference in quartz for directions parallel and perpendicular to the optical axis. When quartz occurs as mineral particles in a rock or soil material, the optical axis¹ will have random directions. This results in an average conductivity for quartz of about 7.7 W/mK at 20°C (90) and the variation with temperature shown as a thin line in Figure 5¹.

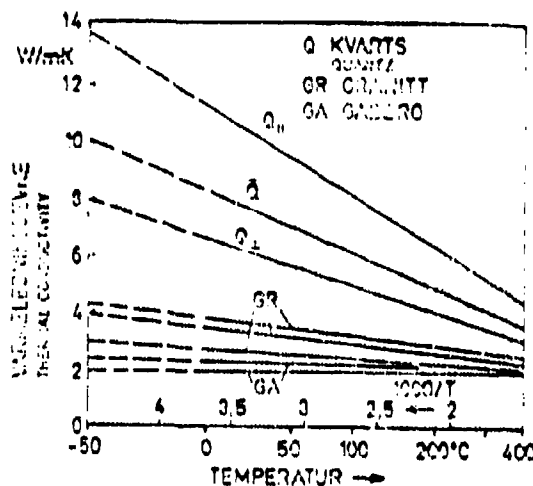


FIG. 5. Variation of thermal conductivity with temperature. Thermal conductivity of rocks in relation to temperature. (Birch and Clark 1940: 141)

1) Probably refers to the line marked \bar{Q} (Translator's note)

Figure 6 shows how the conductivity of some other soil materials vary with temperature. The contribution from the temperature dependent vapor diffusion is included (see chapter I). Little data exist about the conductivity of organic materials which may be present in the soil (plant residue, humus). However, Watzinger (10) gave a value of $0.45 \text{ W/m}^\circ\text{C}$ for the solid organic components in peat or bog. The temperature dependence is not known.

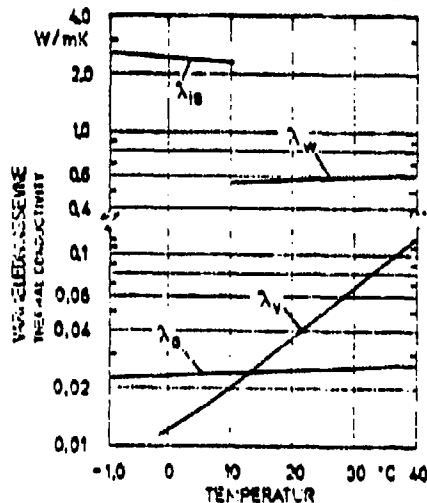


FIG. 6. Värmlektigheten av förskjutna jordbeständigheter som funktion av temperaturen. Thermal conductivity of some soil-components in relation to temperature.

The results of Figures 5 and 6 show that the temperature dependence of moist soil materials is quite small within the normal range of soil temperatures. However, one important exception is the contribution to conduction via pore air by the temperature dependent vapor diffusion, which in reality is the most important factor in temperature dependence of conductivity in moist soil materials (See Figure 11 of chapter I). The transition from frozen to unfrozen material and the effects of variations in relative unfrozen water content will be discussed in the next section.

From Figure 5 it is evident that the conductivity of rock materials can vary over relatively wide ranges for a given temperature. This variation, which depends in the mineralogical composition of the

rocks, is much more significant than the temperature dependence within the normal (actual) range of temperature for the different types of rock. A very comprehensive study of thermal conductivity of rock minerals was presented by Horai in 1971 (11). The measurements were made at 25°C, using a heat conduction probe in crushed and water saturated powders consisting of the various minerals. Horai calculated conductivity for the mineral particles from the arithmetic mean of upper and lower Hashin-Shtrikman limits. Sass (1971) has performed similar measurements of conductivity for rock fragments and compared those results with measurements in the original rocks¹⁾ under stationary conditions. He claims, that equations based on geometric means give a more accurate base for calculations than the average of the Hashin-Shtrikman limits. However, the difference is no more than about 10 percent, on the average, with the highest values given by the geometric mean equations (12).

Table III shows the distribution of results for the most important rock-generating minerals. As can be seen, the variation is relatively large for the same mineral. However, both feldspar and mica show relatively small variations around a common mean of about 2.0 W/m°C. For pyroxene-amphibolite the variations are more significant, with means of about 4.4 and 3.5 W/m°C, respectively. Quartz has a notably higher conductivity of 7.7 W/m°C. The latter result is also in agreement with measurements by Birch and Clark on pure quartz, provided that the following rule (formula) is used for computing the conductivity of randomly oriented crystals

$$\lambda = \frac{1}{3} \lambda_{11} + \frac{2}{3} \lambda_{\perp} \quad 1$$

Variations for each material can be ascribed to differences of composition within each type of mineral. Thus, a more accurate determination of conductivity than the averages indicated here will require detailed geological investigations. However, the varia-

1) That is, the rocks from which the fragments were made (Translator's note)

tions are lowest for the most common minerals. Thus, the errors in conductivity estimates for a rock material, based on these averages, should normally be relatively small.

Birch and Clark specified the mineralogical composition for most of the eruptive (volcanic) and metamort rock types they studied. Table IV summarizes these data and gives the conductivity for each type at 25°C.

Table III. Thermal conductivity of important soil generating minerals at 25°C, after Horai (11).

Conductivity W/mK	Feldspar	Mica	Pyroxene	Amphibol.	Olivine	Chlorite	Quartz
1.4 - 1.8	6	3	0	0	0	0	0
1.9 - 2.2	4	5	0	2	0	0	0
2.3 - 2.6	5	5	0	3	1	0	0
2.7 - 3.0	1	0	1	1	1	0	0
3.1 - 3.4	0	0	0	2	1	0	0
3.5 - 3.8	0	0	1	4	1	0	0
3.9 - 4.2	0	0	4	3	0	1	0
4.1 - 4.6	0	0	2	1	1	0	0
4.7 - 5.0	0	0	2	2	2	1	0
5.1 - 5.4	0	0	1	0	4	0	0
5.5 - 5.8	0	0	2	0	0	0	0
5.9 - 6.2	0	0	0	0	0	0	0
6.3 - 6.6	0	0	0	0	0	1	0
6.7 - 7.0	0	0	1	0	0	0	0
7.1 - 7.4	0	0	0	0	0	0	0
7.5 - 7.8	0	0	0	0	0	0	1

Table IV. Mineralogical composition (percent) and conductivity at 25°C for rock materials.
After Birch and Clark (8).

Rock material	Quartz	Feldspar Mica	Pyroxene Amphibol. Olivine	Others	$\lambda_{25^\circ\text{C}}$ (W/mK)
Granite Rockport 1					3.61
Rockport 2	28	64	6	2	3.44
Barre	26	71		3	2.73
Westerly	19	79		2	2.43
Gabbro French Creek		52	47	1	2.31
Mellen 1					1.93
Mellen 2		73	26	1	2.00
Diabase Maryland		49	50	1	2.31
Vinyard Haven		65	32	3	2.19
Westfield		66	32	2	2.12
Quartz monsonite	34	45	5	1	3.04
Augite-syenite		85	14	1	2.23
Tonalite	28	65	7	0	2.65
Quartz, sandstone	80	6		4	5.25

Table V. Specific weight of important soil generating minerals, Horai (11)

Interval	Feldspar	Mica	Pyroxene	Amphibolite	Clorite	Quartz
2.5 - 2.6	6				1	
2.6 - 2.7	5				1	1
2.7 - 2.8	5				1	
2.8 - 2.9	0	7	2		1	
2.9 - 3.0	0	1		3		
3.0 - 3.1	0	0		5		
3.1 - 3.2	0	0	2	2		
3.2 - 3.3	0	0	6	4		
3.3 - 3.4	0	0	4	3		
3.4 - 3.5	0	0				
3.5 - 3.6	0	0	1	1		

Among other things, it is evident that rocks containing quartz have small or no quantities of pyroxene, amphibolite or olivine. These can thus be approximately represented as a two component system consisting of quartz and feldspar - mica with conductivities 7.7 W/mK and 2.0 W/mK (feldspar, etc.), respectively. The conductivity of such two component system can be determined approximately from the geometric average equation

$$\lambda = 7.7^q 2.0^{1-q} \quad 2$$

where q is the relative quartz content.

Figure 7 shows results obtained by Birch and Clark for rock materials containing quartz, plotted versus the relative quartz content. The values obtained from Eq 2 are drawn in for comparison. The data indicate that knowledge of the quartz content will make it possible to estimate the conductivity of quartz-bearing rocks with errors not exceeding 20 percent.

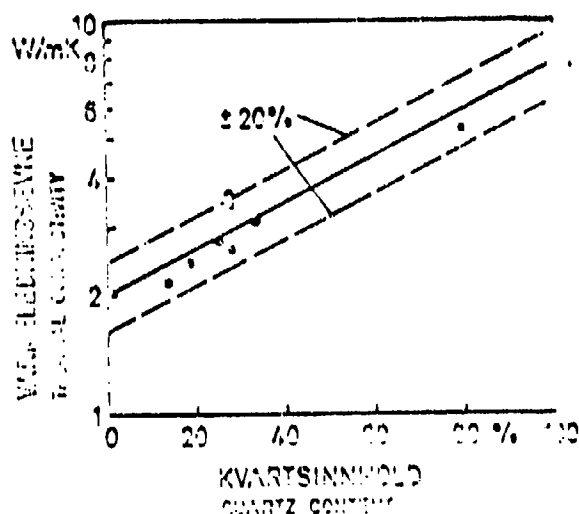


FIG. 7. Thermal conductivity of igneous rocks (after Birch and Clark, 1950) plotted against relative quartz content. Theoretical relationship from Eq. 2 is shown for comparison. (Dashed lines indicate $\pm 20\%$ error.)

A corresponding mathematical model could be used for eruptive rocks not containing quartz. One component would be feldspar-mica (conductivity 2.0 W/mK) while the other would be pyroxene, amphibolite, etc., (with a conductivity of 4.0 W/mK). However, the large variation in conductivity within the latter group will result in relatively large uncertainties.

In loose deposits for which the quartz content is known, Eq 2 can be used for estimating the particle conductivity. In case minerals such as pyroxene, amphibolite, etc. occur, some uncertainties will enter the picture.

For loose deposits where the quartz content is un-known, one may use the results obtained by Sveian to estimate quartz content based on the grain size distribution in the material. In the previous section it was suggested that the following values may be used

$d < 0.002$ mm	0 percent
$0.002 < d < 0.02$ mm	15 percent
$d > 0.02$ mm	45 percent

This forms the basis for sketching a triangular diagram of the form shown in Figure 8, which can be used to estimate quartz content when the grain size distribution is known.

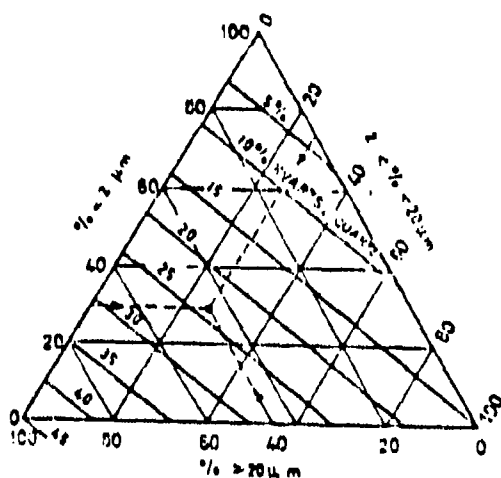


FIG. 8. Trekantdiagram for anslagsvis bestemmelse av kvartsinnhold ut fra kornfordelingskurver. Triangle diagram for estimation of quartz-content from grain size distribution.

As shown in Figure 4 of the previous chapter, this mathematical model normally gives uncertainties for the quartz content which are less than 30 percent. This means a somewhat higher uncertainty (about 40 percent) in the estimated particle conductivity, when calculated as a weighted geometric mean of conductivities for quartz and feldspar/mica. To this one must add the uncertainty due to any occurrence of minerals such as pyroxene, amphibolite, etc. Overall, this method will therefore give an uncertainty in the particle conductivity of up towards 50 percent of the estimated value, i.e. twice that which seems possible to obtain when the quartz content is known.

2. VOLUMETRIC COMPOSITION AND TEXTURE

A. Volume ratios in soil materials

The volumetric composition of a soil material is usually specified in terms of dry specific weight γ_d and the ratio between water and dry material contents, by weight, w . When using the MKSA system (of units) it is more correct to use dry density ρ_d ¹⁾ and corresponding density conditions also for the water content. However, to avoid misunderstanding, the conventional concepts will be used in the following.

These two parameters do not give a complete definition of volumetric conditions in a soil material. The specific weight γ_s (=density) of the mineral particles will also affect these conditions. For example, the relative (share of the) volume for particles in a soil material is given by

$$1 - n = \gamma_d / \gamma_s \quad 3$$

However, the specific weight of mineral particles will vary within relatively narrow limits, with a mean of about 2700 kg/m³ for

1) Except for a possible difference in units, the distinction between γ_d and ρ_d is unclear (Translator's note)

the sand fraction and about 2800 kg/m³ for the finest fractions where the content of mica and heavier minerals usually is larger (see Table V). For organic materials (plant residues, etc.), γ_s will vary between 1460 and 1500 kg/m³ (13). In soils containing both organic materials and minerals, the volume ratio between the two types of material is given by the average specific weight of solid components. Thus, the relative volume (share) of organic materials is given by

$$\sigma_v = \gamma_d \frac{\gamma_m - \gamma_s}{\gamma_m - \gamma_o}$$

4

σ_v is the relative volume of organic materials

γ_d is dry density (kg/m³)

$\gamma_s, \gamma_m, \gamma_o$ are specific weights for solid components, mineral components and organic components, respectively

Skaven Haug (1972) discussed different methods for determining γ_s and comments on the heat loss method¹⁾ (13), among others. γ_s is determined from the ash content (ash/dry material) after heating the soil material to a state of glowing.

In the following, we will primarily discuss pure mineral soil materials. However, in the next chapter, thermal conductivity measurements on peat and bark will be discussed, along with measurements on soils containing minerals only.

The degree of saturation in a soil material, S_r , can be determined from information about dry density γ_d , specific weight of the solid component, γ_s , as well as the water content by weight, w . S_r represents the ratio between ice or water volume and the total volume of the pores.

1) A literal translation which is not very specific. Hopefully, the following sentence gives a better idea of what is involved (Translator's note)

$$S_r = \frac{w \gamma_d}{(\gamma_s - \gamma_d)} \frac{\gamma_s}{\gamma_w} \quad 5$$

As mentioned previously, dry density γ_d and relative water content by weight w are the only parameters normally specified. The uncertainty about degree of saturation will in such cases depend on the uncertainty in estimating the specific weight of the mineral particles. That relation is given by

$$\frac{\Delta S_r}{S_r} = \frac{\gamma_d}{\gamma_s - \gamma_d} \frac{\Delta \gamma_s}{\gamma_s} \quad 6$$

where S_r and $\Delta \gamma_s$ are the relative errors in S_r and γ_s , respectively. Figure 9 presents this relation in graphical form.

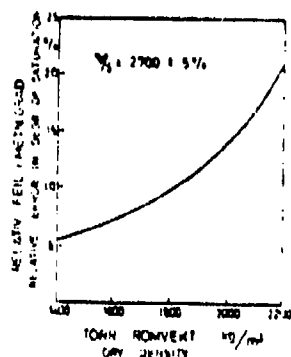


FIG. 9. Formula for relative error in determining S_r or relative error in specific weight γ_s versus nominal dry density. Ratio between packing - relative error in degree of saturation and relative error in specific gravity in relation to dry density.

For the most tightly packed materials, the relative error in determining the degree of saturation can thus be 3 to 4 times greater than the relative uncertainty in specific weight of the mineral particles. If the latter uncertainty is assumed to be about ± 5 percent (corresponding to $\gamma_s = 2700 \pm 150$) the error in S_r can thus amount to 15 - 20 percent in tightly packed gravel materials. The corresponding error in determining the relative particle volume is ± 5 percent i.e. the same as the specific weight uncertainty.

Higher accuracy in determining volume ratios in soil materials requires knowledge about the specific weight of the mineral particles. This is normally obtained by means of a pyknometer (14).

To describe the volume ratios in a frozen soil material one must also know the ratio between frozen and un-frozen water. This topic will be discussed in section C.

B. The importance of texture

The texture of soil materials is often related to the grain size distribution but will clearly also be affected by the particle shape. Together, these factors will affect the packing geometry and the soil material density. A gravel material with widely distributed particle sizes can thus be packed to a considerably higher density than, for example, a fine sand with particles of equal size. Figure 10 indicates the relation between particle size distribution and maximum packing density (15).

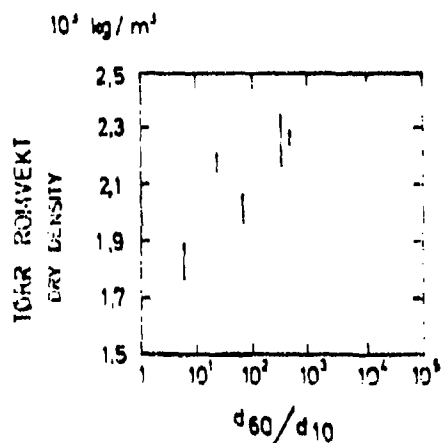


FIG. 10. Maksimal pakningsgräns som funktion av gradningskoefficienten d_{60}/d_{10} . Maximum compressibility in relation to uniformity coefficient d_{60}/d_{10} . (15)

However, in more fine grained materials there will exist a finely porous system with a very large specific surface area. Large amounts of water can be bound to this area, which gives these types of soils special properties, both in terms of packing configuration and in other respects (e.g. un-frozen water content). In addition, one can expect that a certain water content in a coarse soil material will mean different microgeometric conditions than the same water content in a more fine grain soil where larger amounts of the water is bound to the surface of the particles. Such conditions indicate that specific surface area may be at least as important a parameter as particle size distribution.

The particle size distribution is normally determined by screening of the coarser fractions ($d > 0.06$ mm) and by means of sludge analysis (hydrometer analysis) for more fine grain materials (16). Both methods give uncertainties in the particle size distribution due to variations in particle shapes. Particle size distributions are normally represented as cumulative distribution curves in diagrams having a logarithmic scale for the particle size. These particle (size) distribution curves are often used for classification of soil materials. For example, concepts such as gravel, sand, silt and clay refer to certain well defined intervals of the grain size scale in these diagrams (see Figure 11). Unfortunately, these concepts are not uniquely defined, but Figure 11 shows the definitions most common in Norway.

From curves of this type one can determine such parameters as the size distribution coefficient $C_u = d_{60}/d_{10}$ ¹⁾ or the sorting number $S_o = d_{75}/d_{25}$, which together with the median $M_d = d_{50}$ can be used to obtain a numerical approximation to the particle size distribution or to represent this distribution as one point in a diagram (17). This can also be achieved by separation into three fractions and plotting the result in a triangular diagram as indicated in Figure 8.

1) The subscripts for d indicate the percentage of particles which are smaller than the diameter in question. Thus, 60 percent of the particles have a diameter $\leq d_{60}$, etc. (Translator's note)

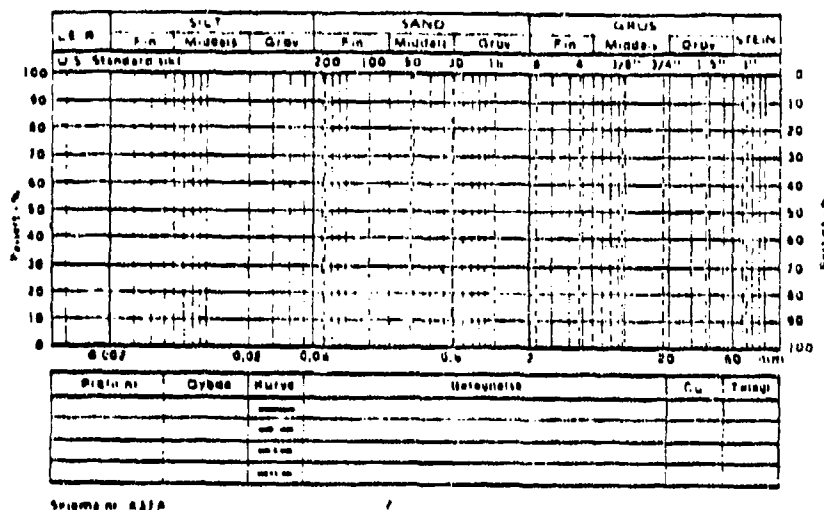


FIG. 11 Klassifikasjon av jordarter etter kornfordeling. Soil classification according to grain size distribution.

Legend for Figure 11:

Passert 1 %	Passed (through screen), percent
Leir	Clay
Fin	Fine
Middels	Medium
Grov	Coarse
Grus	Gravel
Stein	Rock
U.S. Standard sikt	US Standard screen (measure)
Rest på 1 %	Residue on (screen), percent
Profil nr.	Profile No
Dybde	Depth
Kurve	Curve
Betegnelse	Notation
Telegr.	Degree of frost susceptibility

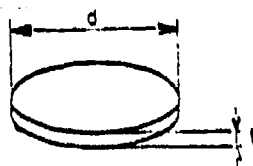
In connection with thermal properties of soil materials it may seem as if the particle size distribution curve plays a secondary role as "parameter" for the more central factor of specific surface area. For a certain particle shape (e.g. spherical), the ratio between surface area and volume (specific surface area) is inversely proportional to the particle size.

$$S = f/d$$

7

where f depends on the particle shape. For spheres, $f = 6$ and for discs or cylinders one obtains the following expressions for the ratio between surface area and volume.

Discs



$$S = \frac{1}{d} (2 \frac{d}{t} + 4)$$

Cylinders



$$S = \frac{1}{l} (2 + 4 \frac{l}{d})$$

The specific surface area is clearly strongly dependent on the particle shape. For example, if the ratio diameter/thickness is $d/t = 10$ the factor f will be 24 for a disc, but 6 for a sphere with the same diameter. If the d/t -ratio is 100, the factor f will be as high as 204!

For a continuous variation in particle size one finds that the specific surface area per unit particle volume is strongly dependent in the size distribution. As an example, if the cumulative distribution function is linear between a smallest diameter d_1 and a largest diameter d_2 , the specific surface area is given by the following expression

$$S = \frac{f}{d_2 - d_1} \ln \frac{d_2}{d_1} \quad (\text{linear distribution}) \quad 8$$

while a logarithmic distribution gives

$$S = \frac{f}{\ln d_2/d_1} \quad (1/d_1 - 1/d_2) \quad 9$$

(logarithmic distribution)

Based on these expressions one may define an equivalent diameter d_{eqv} , i.e. the particle diameter which alone will result in the same specific surface area as the given size distribution. For the two types of distributions one obtains

linear distribution $d_{eqv} = \frac{d_2 - d_1}{\ln d_2/d_1} \quad 10$

logarithmic distribution $d_{eqv} = \frac{\ln d_2/d_1}{1/d_1 - 1/d_2} \quad 11$

Figure 12 shows the ratio d_{eqv}/d_1 ²⁾ as function of d_2/d_1 for the two distributions.

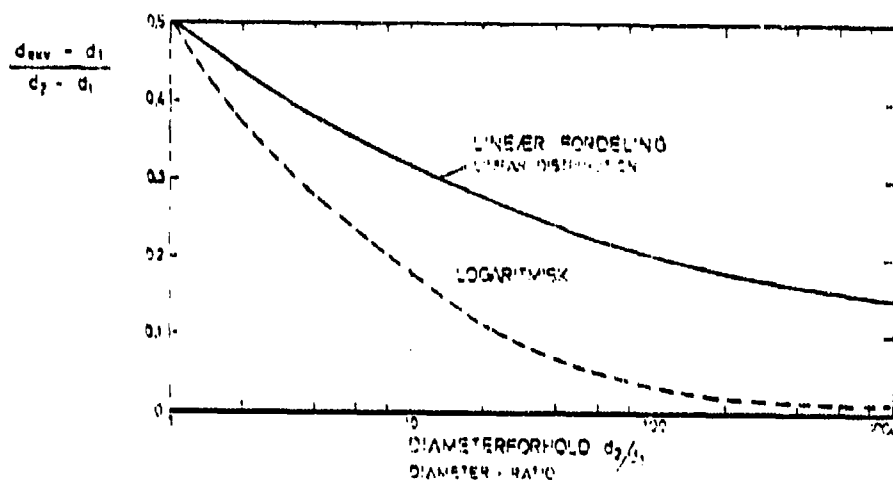


FIG. 12. Equivalent diameter vs linear or logarithmic modeling.
Equivalent diameter from linear and logarithmic distributions.

- 1) The original states $d_2 - d_2$, which must be a "typo" (Translator's note)
- 2) Note that a different function is shown in the figure (Translator's note)

The logarithmic distribution will clearly always give lower equivalent diameters than the linear distribution. For wide size variations one also finds that the equivalent diameter is close to the minimum diameter d_1 .

Selmer-Olsen (1961) used an electron microscope to study the particle shapes in six clay materials and found that between 25 and 65 percent of particles smaller than 2 μm had a width/thickness ratio larger than 5 (18). There is some evidence that also the size fraction $2 < d < 20 \mu\text{m}$ contains considerable numbers of thin particles. Selmer-Olsen (18) estimated specific surface areas for the six clay materials ($d < 2 \mu\text{m}$) from 16 m^2/g to 43 m^2/g . In terms of surface area per unit volume this corresponds to the range from $4.5 \cdot 10^7$ to $1.2 \cdot 10^8 \text{ m}^2/\text{m}^3$. The equivalent sphere diameter is 0.05 to 0.15 μm . Sludge analysis in effect also implies determination of the equivalent spherical particle diameter. How these compare to results obtained from specific surface area considerations has not been investigated.

At any rate, these results indicate that the specific surface area of a soil material is largely determined by the content of finer fractions, with the clay content being the most important parameter.

Within the past few years, a method for determining specific surface area has been developed based on adsorption of a monomolecular layer of ethylene glycol (19) or ethylene glycol and monoethyl ether (20). These methods have been used by Anderson and Tice (1972) in connection with a study of unfrozen water in soil materials (21). The results from this study will be discussed in the next section.

C. Un-frozen water

The water in a fine grain soil material with a water content below full saturation will freeze at a temperature below the normal freezing point for water. The decrease in freezing point is often related to the moisture potential in the soil material at the actual degree of saturation. For example, Williams (1973)(22) gives the following relation

$$\Delta T = \frac{v \cdot T_0}{L} \psi \quad 12$$

ΔT is the decrease in freezing point ($^{\circ}\text{C}$)

T_0 is absolute temperature at the normal freezing point (K)

L is the latent heat of water (J/kg)

v is the specific volume of water (m^3/kg)

ψ is the moisture potential (N/m^2)

Insertion of numerical values with ψ expressed in bar ($10^5 \text{ N}/\text{m}^2$) gives

$$\Delta T = 0.0815 \psi \text{ (bar)} \quad 13$$

Low, Anderson and Hoekstra (1968) point out that this equation is valid only for soil materials with relatively high degrees of saturation (23). Using thermodynamic theory they formulated a more general relation between freezing point decrease, moisture potential and latent heat. This complicated expression for ΔT was also used to generate an extensive table from which either of the parameters mentioned can be found when the other two are known.

This relation between water content and freezing point decrease in a soil material corresponds to the relation between un-frozen water content and temperature in the material, e.g. when a saturated sample freezes (24). This makes it possible to deter-

mine the content of un-frozen water as function of temperature when performing freezing experiments on samples with different water content (degree of saturation). For relatively low water contents, this method can be expected to give low accuracy. For this reason calorimetric methods are mostly used to-day.

Anderson and Tice used such a method to determine un-frozen water content in 11 different soils and mineral powders. The specific surface area (determined by means of the ethylene glycol method) varied from 6 to 800 m²/g for these materials. In general, the results could be fitted to an exponential function of the form (21)

$$w_u = \alpha (\Delta T)^\beta \quad (\text{percent by weight}) \quad 14$$

where w_u is the relative amount of un-frozen water (by weight)
 α, β are empirical parameters which depend on the specific surface area

ΔT is temperature below the normal freezing point

$$\ln \alpha = 0.552 \ln S + 0.262 \quad 15$$

$$\ln (-\beta) = 0.264 \ln S + 0.371 \quad 16$$

Since specific surface area is a parameter which is seldom known for a given soil material, the same authors made an effort to relate their measured data on un-frozen water content to the flow (liquid) limit for the soil materials. This parameter, which is a more common geotechnical concept, gives a measure of the consistence limit when water is added, i.e. a limit for the water content where the soil materials after stirring are no longer plastic but "flowing". This limit was earlier most often determined by means of Cassagrande's flow-limit test-set (25), which also was used in the study mentioned previously. However, a technique more widely used in Norway today is the cone sinking method, whereby the consistence limit is defined by the water content which allows a 60 degree cone

weighing 60 g to sink 10 mm (sometimes 5 mm) into the sample (v_{10} , v_5). Selmer Olsen (1954) show that the water content defined in this manner agrees very well with previous definitions of the flow limit (26).

Anderson, Tice and Banin found a linear correlation between the flow limit at 25 blows¹⁾ in the Cassegrande test-set (w_{25}) and the un-frozen water content at -1°C . In addition, they found a linear relation between the flow limit after 100 blows (w_{100}) and the un-frozen water content at -2°C . The latter consistence limit (w_{100}) seems to approximately equal V_5 obtained in cone sinking experiments while, as mentioned, w_{25} seems to agree well with v_{10} . The two relations are (27)

$$w_{u1} = 0.346 \quad w_{25} = 3.0 \quad 17$$

$$w_{u2} = 0.338 \quad w_{100} = 3.72 \quad 18$$

where w_{u1} and w_{u2} are the un-frozen water contents at -1 and -2°C , respectively.

The relation between un-frozen water content and temperature can be written

$$w_u = w_{u1} \left(\Delta T \exp \frac{\log w_{u2}/w_{u1}}{0.3010} \right) \quad 19$$

where w_{u1} and w_{u2} are given by the previous equations.

By plotting w_{u1} and w_{u2} in a log - log diagram for each of the two temperatures one can determine the contours for un-frozen water content by drawing straight lines between these values, due to the exponential nature of the equation. This results in a graphical method for determining the un-frozen water content at various temperatures, as shown in Figure 13.

1) Literal translation of "slag". It seems that this test involves beating on the sample in some manner. (Translator's note)

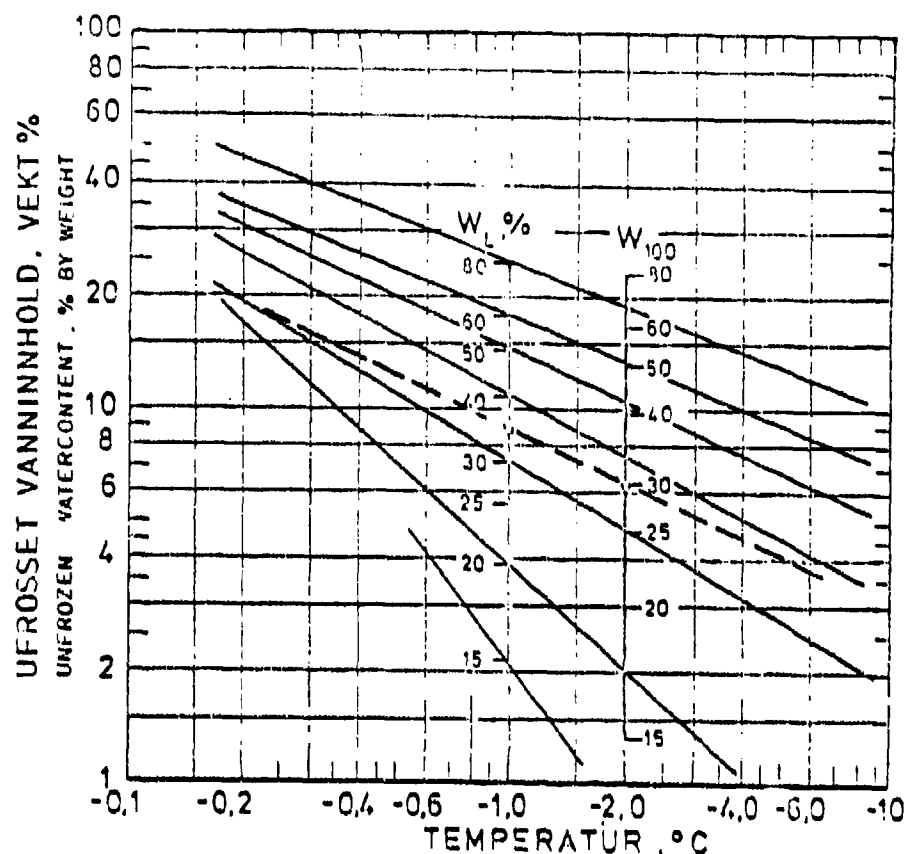


FIG. 13. Grafisk metode for bestemmelse av ufrosset vanninnhold ut fra Jordartenes flytegrenser. Basert på Anderson og Tice's empiriske relasjoner (likn. 17, 18 og 19). Graphical method for estimation of unfrozen water content from liquid limit determinations. Based on empirical equations derived by Anderson and Tice (likning 17, 18 og 19).

In many cases only the flow limit w_{25} (V_{10}) is determined. However, Selmer Olsen's consistence limit determinations for a number of Norwegian clays show an average ratio of about 1.2 between V_{10} and V_5 , as illustrated by Figure 14. The values of w_{25} for the materials studied by Anderson and Tice are also shown, as function of w_{100} . These data¹⁾ indicate that the same relation exists between these two parameters.

1) Rings in Figure 14 (Translator's note)

Consequently, if only one of the consistence limits is given, the other can be found from the relations

$$v_{10} = 1.2 v_5 \quad 20$$

or $w_{25} = 1.2 w_{100} \quad 21$

This forms the basis for the thin un-frozen water contours in Figure 13. If both consistence limits are given, the two scales may be used as described previously.

At temperatures near the normal freezing point, the calculated un-frozen water content may exceed the actual water content in the soil material. Anderson and Tice recommend that the curve for un-frozen water content in such cases is terminated at the latter value. The corresponding temperature may then be considered as a freezing point reduction. This condition indicates that water content measured in relation to dry density is not entirely relevant at temperatures near 0°C. If the soil material is nearly saturated for the actual water content, the real freezing point reduction may be considerably less than if the material were far from saturation for the same water content. The empirical equation, which is based on water content by weight, gives no basis for distinguishing between these conditions.

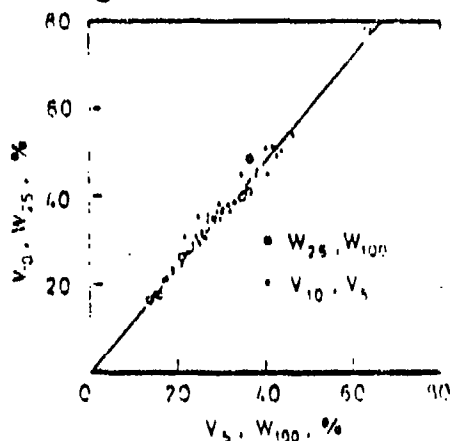


FIG. 14. Plot of V_{10} on V_5 or W_{25} on W_{100} for various soil types. The solid line represents the 1:1 relationship. The data points are labeled W_{25}, W_{100} and V_{10}, V_5 and are plotted on the same scale.

Until determinations of un-frozen water content in Norwegian soil materials become available, the approach taken by Anderson and Tice may be applied also to Norwegian conditions. Figure 14 also indicates that the normal range of flow limits for Norwegian clays is well covered by the materials studied by Anderson and Tice.

3. SOIL MATERIAL CLASSIFICATION

The previous discussion of various thermal conductivity parameters gives a certain basis for generating classification requirements for soil materials. The fundamental thermal conduction parameters were earlier shown to be of three types:

Thermal conductance of the components $\lambda_1, \lambda_2, \dots, \lambda_n$

Relative volume (shares) of the components n_1, n_2, \dots, n_n

Microgeometric properties of the material

As shown, each one of these parameter groups pose special requirements on soil material classification. In practice, one will to a large extent have to rely on geotechnical classification and sampling normally performed in connection with road construction or other types of in-ground work. It will thus be of interest to find out to what extent this kind of classification covers the parameters which are important from a thermal point of view.

A. Geotechnical analysis

In connection with major road construction, samples are normally taken of the sub-soil at every 20 or 100 metres along the road-bed and in some cases also perpendicular to its centerline. These samples are primarily taken in order to determine stability properties of the sub-soil. In fine grain materials such as silt or clay one

normally uses a sampling tube (diameter 54 mm) to extract "undisturbed" samples. The samples are taken for each metre (a metre at a time) to a depth which depends in soil conditions. From these samples one determines volumetric conditions (density, water content), consistence limits, screening curve¹⁾ and various other properties of importance to stability and compressibility.

If the sub-soil consists of coarser materials, from coarse silt through fine sand to sand and gravel, it will be difficult to obtain undisturbed samples. In such cases, so-called representative (stirred up) samples are taken, from which water content by weight and grain size distribution curves are determined.

In connection with construction of large foundations (buildings, etc.) the same procedures for sub-soil sampling as in road construction are usually followed.

Figure 15 shows a sketch of a road bank, including the normally used terminology (28).

Materials used in a road bank must meet certain requirements on wear resistance (petrographic composition), stability, degree of compression (grain size distribution) etc. To ensure that these requirements are met, the materials used are subjected to certain evaluations which also may serve for classification from a thermal point of view.

1) Particle size distribution (Translator's note)

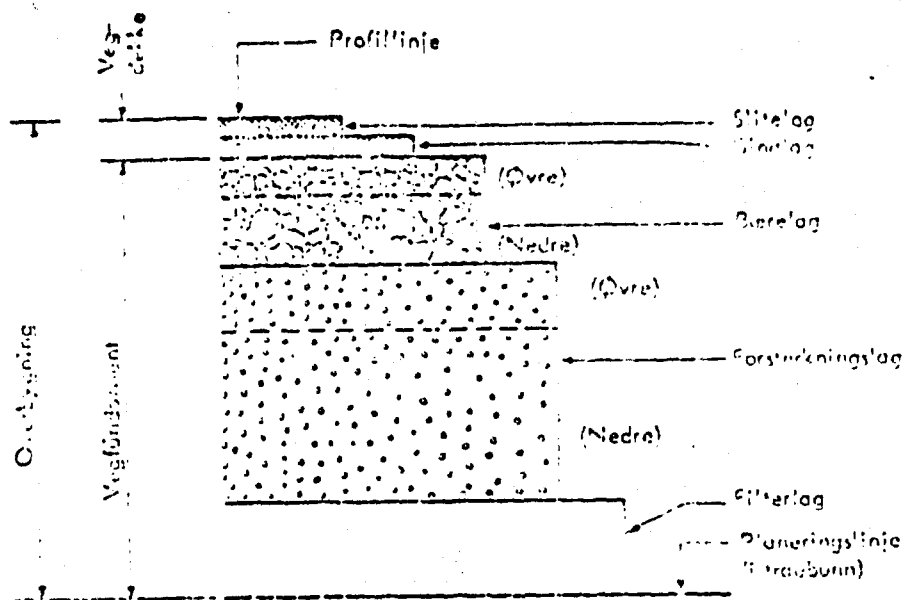


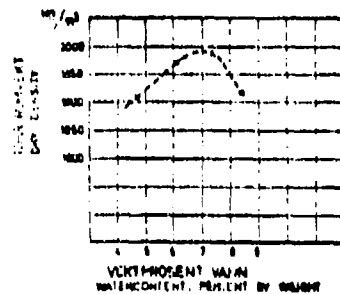
FIG. 15. Skisse av oppbygning av en vegoverbygning med angivelse av den vanlig benyttede terminologi. Sketch of the construction of a road pavement.

Legend: Overbygning	Road pavement
Vegdekke	Road finish
Vegfundament	Road foundation
Profillinje	Upper surface
Slitelag	Wear layer
Bindlag	Binder layer
Baerelag	Structural (support) layer
Øvre	Upper
Forsterkningslag	Reinforcement layer
Nedre	Lower
Filterlag	Drainage layer
Planeringslinje	Baseline

Compression properties are determined by means of packing experiments (standard proctor), using a packing force defined by water content. From these experiments one finds the maximum degree of compression (packing) for a related "optimum" water content. The results are presented in curve form, as shown in Figure 16. This leads to requirements in dry density for the materials after preparation. The requirements are 100 percent proctor¹⁾ in reinforcement layers (corresponding to maximum density in Figure 16)

1) Hopefully a standard term. (Translator's note)

103 percent proctor in structural (support) layers and about 95 percent proctor in the drainage layer. The density of materials in the road pavement are thus given within narrow limits (provided that regulations are followed) (28).



Optimalt vanninnhold: 7,5%
Maks. tørre konsentri: 1,95 kg/l.
Merknader:
Standard proctor
1 liters cylinder

FIG. 16. Tørre konsentri som funksjon av vanninnhold ved innstampningsforhold (Standard Proctor). Dry density in relation to water content from compaction test (Standard Proctor).

For the structural (support) layer (mechanically stabilized) one has comparatively strict requirement on grain size distribution, defined in terms of limiting curves such as those shown in Figure 17. In the reinforcement layer it is required that the content of fine material ($d < 2 \mu\text{m}$) does not exceed 13 percent. The normal variation in grain size is shown in Figure 17. (See Figure 11 for legend. The bottom scale is labeled "Screen with mesh size..... mm").

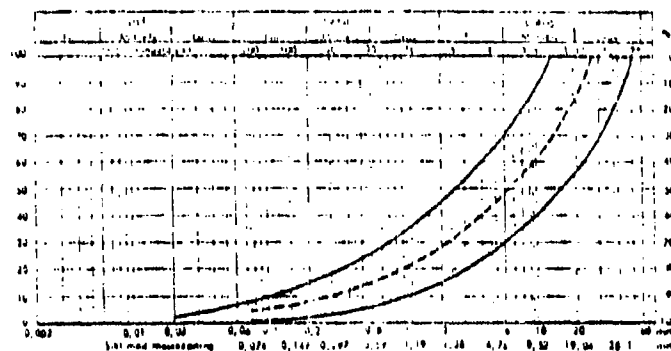


FIG. 17. Knytt til kornfordelingskurver for belagsmaterialer. Standard grain size distributions for pavement base materials.

Requirements in wear resistance for the materials are checked through fall tests (crush tests) and passing through a rod screen. A petrographic determination of the rock fraction is also included (30). However, this evaluation is primarily of a qualitative nature. Artificially crushed rock materials are subjected to a more quantitative evaluation, including the percentage of different minerals.

The results obtained from these analyses are listed in Table V, where a distinction has been made between sub-soils containing fine grain and coarser materials, as well as materials which are to be used for the road pavement.

Table V: Classification of samples taken during road construction

Type of material		Type of analysis					
		Particle size distribution	Dry density	Water content	Consistence limits	Humus content	Petrographic evaluation
Sub-soils	Clay, silt	x	x	x	x	x	
	Sandy soils	x	x				
Pavement materials		x	x ¹⁾			x	x

1) Given by proctor

B. Supplemental analysis

Based on the different thermal conduction parameters discussed in the previous section it is possible to list the most important parameters which must be determined to obtain as accurate a value as possible for the conductivity. Figure 18 summarizes these parameters in a block diagram. The diagram is arranged in terms of information levels, I, II, and III, corresponding to different uncertainties in conductivity when determined on the basis of parameters listed in each level. The first and lowest level only requires knowledge of water content, dry density and mechanical composition (screening curve). The highest level, III, requires more detailed information about physical properties of the material.

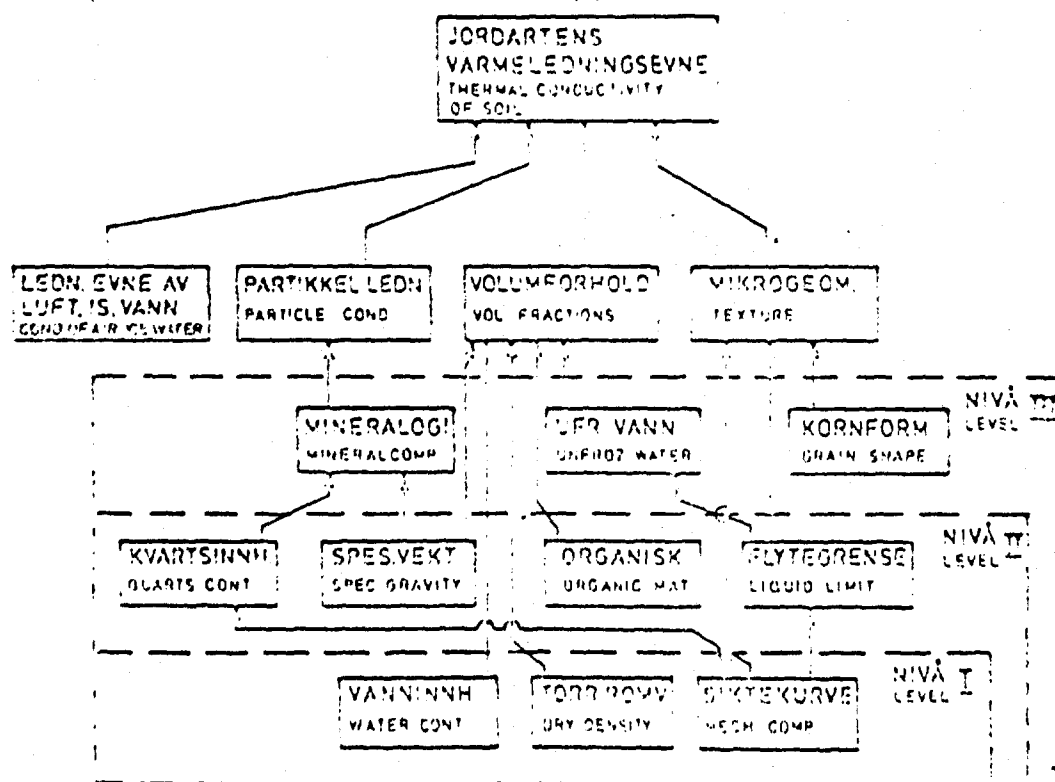


FIG. 18. Sammenheng mellom vanlige jordartparametere og de grunnleggende parametersett som er nødvendige for å beregne jordens varmeledningsevne.
Relation between soil parameters and the fundamental parameters which determine the thermal conductivity.

Best Available Copy

Together, Table V and Figure 18 give an overview of how comprehensive the tests normally performed during road construction are for the factors which determine thermal conductivity. One finds that the tests listed for fine grain sub-soils are almost equivalent to level II, except for knowledge of quartz content in the material. However, this parameter can be estimated from the particle size distribution (screening curve) with sufficient accuracy for this case. For coarser (sandy) sub-soils, information about dry density is lacking. This makes results of common analysis incomplete for all the levels shown in Figure 18. For materials used in the upper levels, information on water content will be lacking. One must therefore make an estimate based on experience from similar road bed designs and take into account expected variations. The petrographic analysis, which is limited to rock fractions and also is rather superficial, gives little information about quartz content in the material at hand. For that case, the sample analysis may thus at best give sufficient information for the lowest level of conductivity determination.

Supplemental studies required to reach level II will first of all be the following: Determination of density in coarser sub-soil materials, more accurate estimates of water content in upper layers and quartz content determination for sand and gravel materials (e.g. by means of DTA).

The uncertainty involved in determining the conductivity for the three levels defined here will be discussed in detail in the final chapter. It may be worth mentioning at this point, that the lowest level (I) will in this respect correspond to Kersten's empirical materials. Kersten claims that correct use of his method will give uncertainties below 25 percent. (Indications are that the error limits are some-what wider than that.) Transition to level II will give a significant narrowing of these error limits.

REFERENCES - CHAPTER III

1. A. Holmes: Principles of Physics-Geology, Nelson, London 1965, p. 84.
2. F.J. Pettijohn: Sedimentary rocks, Second Edition, Harper & Brothers, New York 1957, p. 115.
3. R. Selmer-Olsen: Ingeniørgeologi, Del II, Løsmasser, Kompendium, Geologisk Institutt, NTH, 1973.
4. R. Selmer-Olsen: Ingeniørgeologi, Del I, Generell geologi, Tapir forlag, Trondheim 1971, p. 175.
5. H. Sveian: Norske jordarters kvartsinnhold. Hovedoppgave i Ingeniørgeologi, Geologisk Institutt, NTH Høst 1972.
6. H. Sveian: Undersøkelser av kvartsinnhold i løsmasser ved hjelp av DTA. Utført for Institutt for kjøleteknikk, Trondheim 1973.
7. R. Selmer-Olsen: En regional undersøkelse av norske kvartars leirers finfraksjon basert på DTA. Rapport sendt til NTNF, Geologisk Institutt, NTH, Trondheim 1961.
8. F. Birch, H. Clark: The Thermal Conductivity of Rocks. American Journal of Science, 238, (8), 1940, pp. 529-558.
9. D.A. de Vries: Het warmtegeleidingsvermogen van grond. Med. Landbouwhogenschool. Wageningen, 52, 1952, pp. 1-73.
10. A. Watzinger et al: Masseutskiftningsmaterialer for teleforbygning på veg og jernbane. Norges Geotekniske Institutt, Oslo 1965, p. 106.
11. K. Horai: Thermal Conductivity of Rock-Forming Minerals. J. Geophys. Res. 76, (5), 1971, pp. 1278-1308.
12. J.H. Sass et al: Thermal Conductivity of Rocks from Measurements on Fragments. J. Geophys., Res. 76, (4), pp. 3391-3401.
13. S. Skaven-Haug: Romforhold i jordmaterialer. Meddelelser fra det norske myrselskap, 70, (4), 1972, pp. 89-102.
14. Analyseforskrifter, Statens vegvesen, Vegdirektoratet, 1966. 1. Jordarter, 111, Spesifikk vekt - vanninnhold - romvekt.
15. E. Hogberg: Vattenhaltens innverkan på densitet og kompressibilitet hos packade jordarter. Byggforskingen. Rapport R8, 1972, p. 87.

16. R. Selmer-Olsen: Ingeniørgeologi. Del I. Generell geologi. Tapir forlag. Trondheim 1971, p. 8.
17. R. Selmer-Olsen: Ingeniørgeologi. Del I. Generell geologi. Tapir forlag. Trondheim 1971, p. 12.
18. R. Selmer-Olsen: En regional undersøkelse av norske kvartære leirers finfraksjon basert på DTA. Rapport sendt til NTWF. Geologisk Institutt, NTH, Trondheim 1961, p. 29 f.f.
19. C.A. Bower, J.O. Goertzen: Surface area of soils and clays by an Equilibrium Ethylene Glycol Method. Soil Science, 87, 1959, pp. 289-292.
20. I.M. Eltantawy, P.W. Arnod: Reappraisal of Ethylene Glycol Mono-Ethyl Ether (EGME) Method for Surface area Estimation of Clays. Journal-Soil Science, 24, 1973, pp. 232-238.

CHAPTER IV

EXPERIMENTAL METHODS FOR DETERMINING THERMAL CONDUCTIVITY IN SOIL MATERIALS

In this chapter, the emphasis will be placed on discussing the most commonly used methods for measuring thermal conductivity in soil materials. However, other pertinent approaches will also be treated in the last section. The general influence of moisture transport on experimental results will be discussed in section 1 but this topic will also be dealt with in connection with the various methods of measurement.

1. THERMAL CONDUCTIVITY MEASUREMENTS IN MATERIALS CONTAINING MOISTURE

Experimental determination of thermal conductivity is usually based on the equation which defines conductivity

$$q = -\lambda \nabla T$$

q is the thermal flux (W/m^2)

∇T is the temperature gradient ($^{\circ}\text{C/m}$)

The discussion of heat transport mechanisms in moist materials (chapter I) showed that the heat transfer in a soil material containing moisture is influenced by transport mechanisms other than pure thermal conduction, for which this equation is valid. However, it was shown that these mechanisms could be included in a temperature dependent "apparent" or "effective" thermal conductivity.

Introduction of a temperature dependent thermal conductivity leads to a non-linear thermal conduction equation (Fourier's equation). For constant thermal conductivity this equation has the form:

$$\frac{\partial T}{\partial t} = \frac{\lambda}{c\rho} \nabla^2 T$$

2

c is the specific heat (J/kgK)

ρ is the density of the material (kg/m³)

From this equation one defines a diffusivity for the material

$$a = \frac{\lambda}{c\rho} \quad (\text{m}^2\text{s})$$

3

For variable conductivity:

$$\frac{\partial T}{\partial t} = \frac{1}{c\rho} \nabla (\lambda \nabla T)$$

4

Most methods for experimental determination of thermal conductivity are based on the linear equation (Eq 2). Use of the non-linear equation will require detailed information about the temperature distribution and a considerable effort for temperature data reduction. However, such methods have become feasible due to availability of modern computers (1, 2).

If one neglects the temperature range where freezing and thawing occur in the soil materials, the temperature dependence of the thermal parameters is so small that the errors due to use of the linear equation can be reduced to negligible magnitudes, provided that the temperature variations are kept within reasonable limits during the experiments.

In the temperature range where phase changes water/ice take place, the nonlinearities will be large, particularly as a result of wide variations in the apparent thermal capacity per unit volume, so that the linear equation becomes almost non-useable.

For the case where no water transport occurs during freezing, the thermal conduction equation for the partially frozen zone in a soil material can be written:

$$\left(\rho c_p + \frac{\partial w_u}{\partial T} \gamma_d L \right) \frac{\partial T}{\partial t} = \nabla \cdot (\lambda \nabla T)$$

5

w_u is relative un-frozen water content by weight
 L is latent heat of water, when freezing (J/kg)
 ρc_p is the thermal capacity per unit volume (J/m³K)

The latent heat when freezing can thus be included in the apparent thermal capacity/volume, but this parameter will vary extremely fast with temperature near the freezing point. An example is shown in Figure 1. The curves apply for a silt-clay material having a dry density of 1400 kg/m³ and a flow limit of 30 percent by weight (see Figure 13 of chapter III).

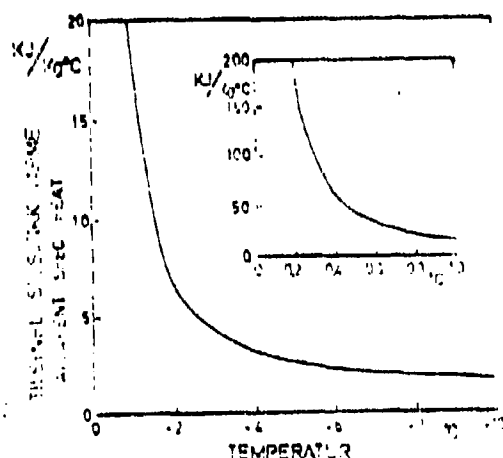


FIG. 1. Relationship between apparent specific heat and temperature under dry conditions (1) and different water contents (2) for a silt-clay material.

For such extreme nonlinearities in the thermal parameters it is obvious that the linear version of Fourier's equation can not be used in conjunction with transient methods for determining conductivity.

In stationary experiments ($\partial T / \partial t = 0$), where only non-linearities in the thermal conductivity come into play, smaller errors can be

expected. The approach will then be to determine an average thermal conductivity, based on heat flux and temperature difference. This average conductivity can then be related to the average temperature in the samples. Non-linearities in the conductivity due to varying amounts of un-frozen water can be expected to give certain errors in this relation. If the temperature coefficient for the conductivity can be assumed constant within the given temperature interval, the errors should be insignificant. However, this will be true only if relatively small temperature differences are used across the samples.

At temperatures above the freezing point, the different heat transport mechanisms will cause difficulties of a different kind. The nonlinearities in thermal parameters will, as mentioned earlier, play a minor role. However, some of the heat transport mechanisms discussed previously will cause a certain mass transport which may disturb the homogeneity of samples. These mechanisms were detailed in section 2 of chapter I.

In that section it was shown that the change in moisture distribution caused by a temperature gradient is largely dependent on the water content in the material and its moisture related properties, such as moisture potential (suction), hydraulic conductivity and moisture diffusivity. It was indicated that large changes in the moisture distribution can be expected in a "critical" region of low to moderate water content (degree of saturation), where the moisture diffusivity decreases rapidly while the thermal vapor diffusivity lies close to its maximum value. It was also shown that the location of this saturation region tends to move towards higher saturation levels for more fine grain materials.

For saturation levels above this region, the moisture diffusivity will increase sharply so that any tendency for change in moisture content due to thermal vapor diffusion will readily be counteracted by capillary water transport in the opposite direction.

One must clearly impose certain requirements on methods used for measuring thermal conductivity within the region of critical saturation. The goal must be to maintain changes in the moisture distribution within certain acceptable limits. This could be accomplished by lowering the temperature gradient or by reducing the time during which samples are subjected to this gradient, or by combining these approaches.

In addition, methods used should give an indication whether major changes in the moisture distribution occur during the experiment. The following section will describe commonly used methods and discuss these from this point of view.

2. STATIONARY METHODS

Stationary methods usually employ one-dimensional heat flow (conduction perpendicular to a plate) or radial heat flow through a cylindrical shell. Both methods have earlier been used for studying thermal conductivity of soil materials (3, 4, 5, 6).

A. Kersten's cylindrical test unit.

A cylindrical test unit (arrangement) employing radial heat flow was used during an extensive experimental investigation of thermal conductivities in soil materials, published in 1949 (6). A sketch of the equipment is shown in Figure 2.

The cylindrical shape is supposed to allow a more efficient packing of soil materials than for a traditional plate arrangement. However, the geometry also has the advantage of permitting direct measurement of the heat transfer through samples without use of special "heat screens" required for one-sided planar units. An effort is made to obtain the desired radial heat flow by separating the heating elements into one measurement section and two screening sections. The

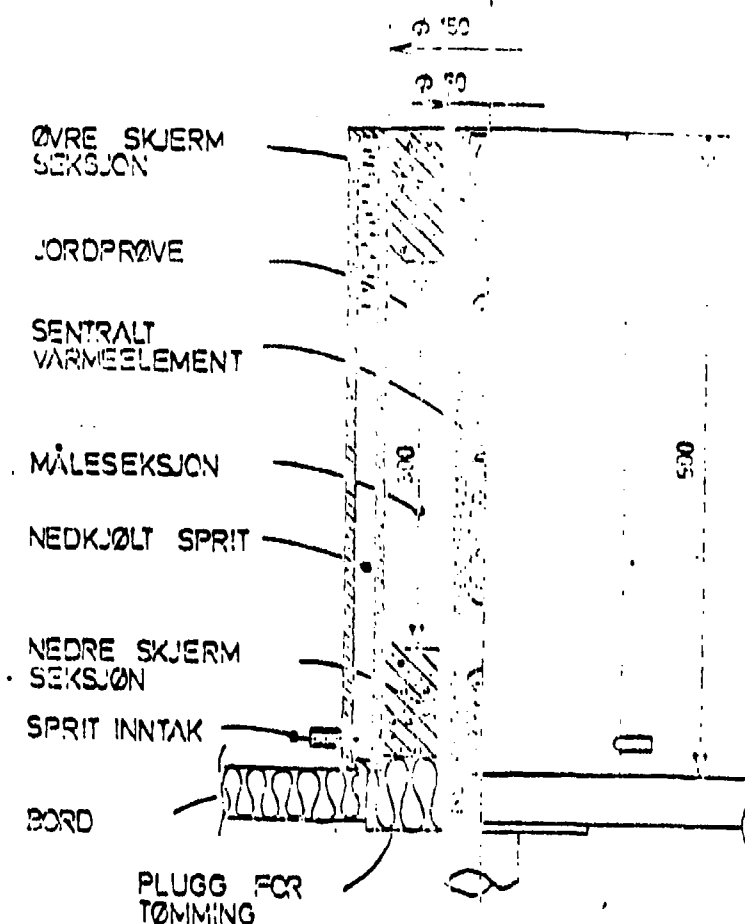


FIG. 2. Kjerfoss's apparatus for making av jordarteres varme-
ledningsevne. Kjerfoss's apparatus for thermal
conductivity measurements in soil.

Legend for Figure 2

Ø 150, Ø 50	: Diameters 150 mm, 50 mm
ØVRE SKJERM SEKSJON	: Cross-section, upper screen
JORDPRØVE	: Soil sample
SENTRALT VARMEELEMENT	: Center heating element
MALESEKSJON	: Measurement zone
NEDKJØLT SPRIT	: Cooled alcohol
NEDRE SKJERM SEKSJON	: Cross-section, lower screen
SPRIT INNTAK	: Alcohol inlet
BORD	: Board (table)
PLUGG FOR TØMMING	: Drain valve

latter correspond to the ring-shaped screens used in planar arrangements¹⁾. One tries to minimize the temperature differences across the gaps between sections by adjusting the (heating) power in the screen sections. These adjustments are made manually.

Kersten does not report typical stabilization times, but his description of the procedure used at the end of each experiment gives an indication of the conditions.

Temperatures at the inner and outer surfaces of the sample were recorded each time, as well as current and voltage for the center heating element. If the thermal conductivity calculated from these values was found to be constant within error limits of one percent during three to five hours, the final conductivity was computed as the mean of results obtained for the final hours.

The stabilization periods should have been significantly longer, at least 12 hours. For each sample placed in the test unit, conductivity was determined for from four to six different temperatures of 20, 4, -4 and -30°C, or 20, 4, -4, -18 and -30°C, in addition to a repeat test at +20°C in the latter case (6 levels). The total time that each sample remains in the test unit should thus amount to between 48 and 120 hours, for a stabilization time between 12 and 20 hours. Against this background, the completed test program is quite impressive: A total of 240 samples were tested, utilizing two test units of the type previously described.

The long time required for each experiment is perhaps the biggest drawback with the stationary methods. This is also the reason why non-stationary (transient) methods (particularly thermal conduction probes) have come into use, despite the considerably higher accuracy obtained with stationary methods. However, the long duration

1) The word "screen" is probably adopted from similar structures used to eliminate edge effects in electrostatic measurements.
(Translator's note)

of each experiment may also be a questionable factor due to the previously mentioned moisture transport.

In this context it is also worth noting that the cylindrical geometry causes some-what higher temperature gradients on the warm side than that obtained with planar geometry.

Kersten used a temperature difference between warm and cold surfaces of about 5.6°C (corresponding to 10°F). With the actual test unit dimensions this implies a temperature gradient on the warm side close to $1^{\circ}\text{C}/\text{cm}$. In a planar test unit with a sample thickness equal to the width of the ring-shaped sample gap, the same temperature difference will result in a gradient of about $0.6^{\circ}\text{C}/\text{cm}$. For larger diameter ratios, the difference will be more pronounced and for thermal conductivity probes, the cylindrical geometry will definitely be unsuitable (see the section on conductivity probes).

The thermally excited moisture transport will cause the sample to become inhomogenous. The cold side will have an increased moisture content while the warm side dries out. The measured conductivity then represents the apparent conductivity for an inhomogenous material and does not represent the real conductivity of the initially homogenous material.

One can obtain an estimate for the magnitude of resulting errors by assuming that the moisture content varies linearly with radius in the cylindrical test unit. If one also assumes that the conductivity varies linearly with moisture content, one can derive the following expression for the apparent conductivity after the moisture has been re-distributed.

$$\frac{\lambda_1}{\lambda_2} = \frac{r_2/r_1 - \lambda_2/\lambda_1}{\ln r_2/r_1 - \ln \lambda_2/\lambda_1} \frac{\ln r_2/r_1}{r_2/r_1 - 1} \quad 6$$

r_2/r_1 is the ratio between outer and inner radii

λ_2/λ_1 is the ratio between conductivities at the cold and warm surfaces

Under the assumptions made, the conductivity obtained for even moisture distribution is given by

$$\frac{\lambda_m}{\lambda_1} = \frac{1}{2} \left(\frac{\lambda_2}{\lambda_1} + 1 \right) \quad 7$$

Figure 3 shows calculated ratios of the apparent conductivity after moisture re-distribution and the conductivity with evenly distributed moisture. Curves are given for three different radius ratios as well as for the planar case ($r_2/r_1 \rightarrow 1$, broken curve).

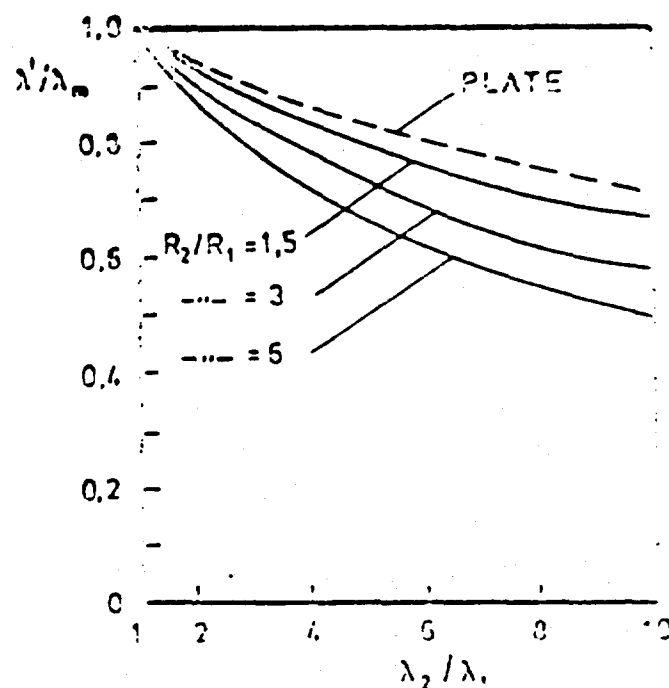


FIG. 3. *Inflytelse af linear omfordeling af fugtindholdet på den cylindriske ledningsevnen ved varmetransportmålinger i apparater med cylindriske varmerør. Influence of linear redistribution of moisture on the apparent thermal conductivity at thermal conductivity measurements with radial heat flow.*

For relatively moderate distortions of the moisture content, corresponding to $\lambda_2/\lambda_1 < 2$, the errors will not exceed 10 percent for each of the calculated cases. One also finds, that the errors increase with increasing radius ratio and that the cylindrical geometry is always less favourable than the planar (plate test unit).

Best Available Copy

As mentioned previously, Kersten performed measurements for up to six temperature levels on each sample. For a number of samples, the final measurement was made at the same temperature as the first ($+20^{\circ}\text{C}$). A comparison of the results obtained in these two measurements will illustrate the influence of moisture transport in these experiments. Figure 4 shows such a comparison.

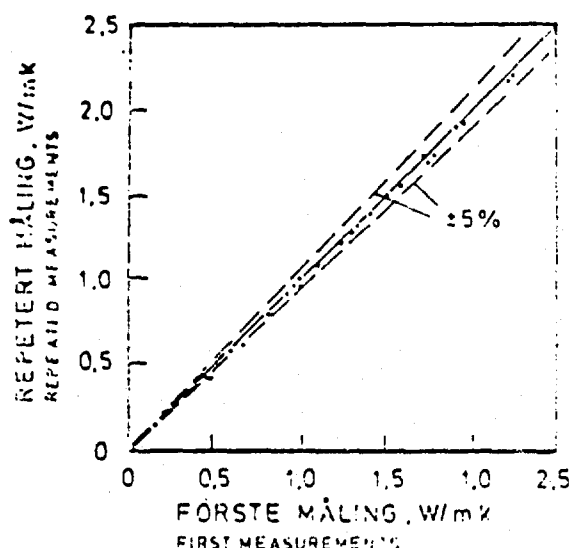


FIG. 4. Sammenlikning mellom første måling ved 20°C og repeteret måling ved samme middeltemperatur. Kerstens resultater (5). Comparison of initial measurement at 20°C and repeated measurement at same mean temperature. Kersten's results (6).

It can be seen, that the final (repeated) test with few exceptions gave a lower value for the conductivity than the first measurement at 20°C . However, the deviation is in the majority of cases less than 5 percent.

B. Planar test unit

Experiments with moist soil in a planar (plate) test unit show considerable influence by moisture transport. Thermal conductivity measurements performed on moist soil materials by Smith were discussed earlier (chapter I). A few years earlier (1934) comparable results were reported by Krischer (4). Woodside (1958) published results from stationary measurements on moist sand and clay, using a planar test unit. These results also indicate the importance

of moisture transport (7, 8). Common to all these experiments is a relatively high average temperature in the samples, 20°C or higher.

During his measurements on sand and clay, Woodside placed emphasis on obtaining stationary conditions, including a stationary moisture distribution. In the experiments with moist sand this required stabilization periods up to 200 hours, while for clay stable conditions were obtained in 163 hours. Figure 5 shows recorded heat flow into and out from the sample in an experiment with clay containing 18 percent water, by weight.

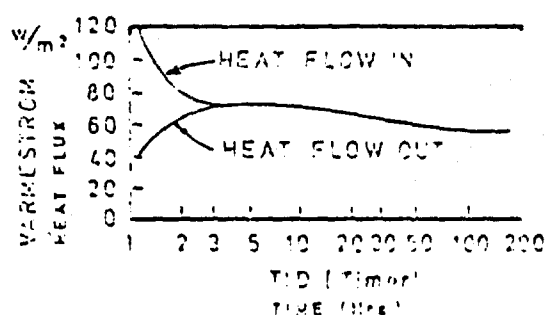


FIG. 5. Värmeström inn og ut av prøven ved varmeledningsforsøk med fuktig leire. Woodside's resultater (7). Heatflow in and out of sample at thermal conductivity experiments with moist clay. Woodside's results (8).

As can be seen, there is a period of 5 to 10 hours after the initiation of the experiment, during which conditions appear to approach a steady state. After this time there is a significant redistribution of moisture, which continually changes the balance.

One may also note the large thermal flux at the warm surface of the sample during the early phase of the experiment. This indicates that large temperature gradients occur at the warm sample surface following a step-wise increase in heater temperature at the start of the experiment. Correspondingly large gradients will also occur initially when experiments are performed in Kersten's circular (cylindrical) test unit. These large gradients will obviously accelerate the moisture transport.

Best Available Copy

One could possibly reduce these gradients by using a "softer" initial temperature transient (step). However, this would lengthen the stabilization period and allow the moisture transport more time to re-distribute the moisture content.

As indicated in the introduction to this chapter, use of the linear thermal conduction equation as a basis for thermal conduction experiments really requires that the material under test be homogenous. If realistic values of conductivity are to be derived from experiments where significant changes in moisture distribution have occurred, like in the experiments reported by Woodside, one has to perform detailed measurements of both temperature and moisture profiles (distributions) at the end of the experiment. In such cases, conductivities can be calculated for thinner layers within the material over which temperature gradients and moisture content can be expected to change by small amounts. In effect, this means utilizing the non-linear version of Fourier's equation:

$$C \frac{\partial T}{\partial t} = \nabla \cdot (\lambda \nabla T)$$

8

This will mean a very time-consuming procedure, not least due to the long stabilization times required.

Another possibility is to arrange experiments so that the redistribution of moisture is minimized, by reducing both experiment duration and temperature gradients as much as possible. (For very special cases, where the conductivity is to be measured at particularly high temperatures, this problem may have to be approached in a different manner, e.g. by transient experiments and continuous recording of both temperature and moisture profiles.)

The principle indicated above was utilized for the development of planar (plate-type) test units used for determining thermal conductivity in soil materials at the Institute for Cold Technology at NTH. This test equipment was constructed as part of a research

program named "Frost in the Ground", directed by NTNF and the Highway Authority with participation of the "Research Group for Thermal Analysis of Frost in the Ground" at the Institute for Cold Technology.

The test equipment is designed for planar, one-sided heat conduction. Considerable emphasis is placed on obtaining planar, horizontal isotherms within the field of measurements and to ensure the best possible stability of temperature and heat flux.

The construction and function of this equipment has been described in more detail by Brendeng, Frivik and de Ponte (9, 10), who have also together been responsible for its development. Only the main aspects on this equipment will be discussed here.

Figure 6 shows a sketch of one of these units, with major construction features indicated. The same figure contains details of the heating plate and the power screen.

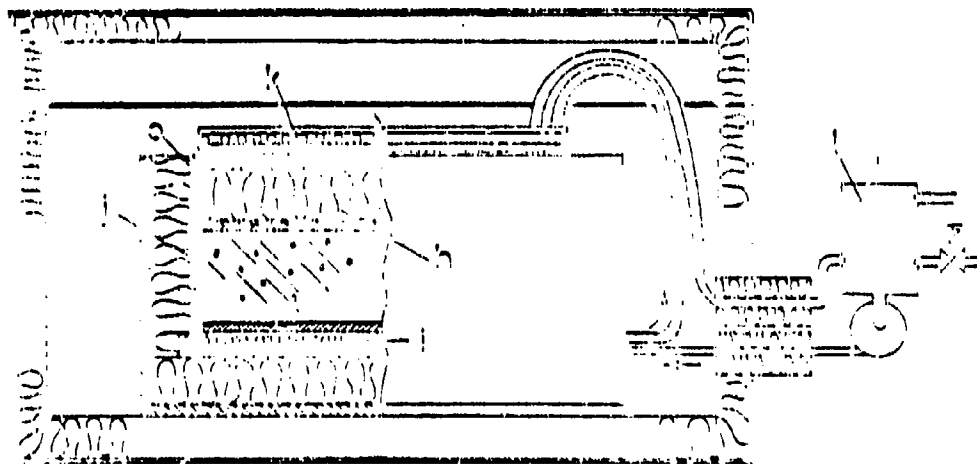
Power to the power screen is regulated automatically, by means of a signal from the central measuring plate, so that any temperature difference between power screen and measuring plate is eliminated. This ensures that the entire power applied to the measuring plate will pass through the sample. Thus, the thermal flux through the sample can be recorded by direct measurement of current and voltage applied to the measurement plate.

Figure 6 also shows that the heating plate is divided into a measurement area and a screen area. The power applied to the screen is automatically controlled by means of thermal sensors placed across the gap between measurement and screen areas so that the temperature difference across that gap is maintained at zero.

To further ensure planar isotherms, an additional heating element (coaxial cable) is placed around the outer rim of the screen area.



- A. Cross-section of the heating plate unit.
- B. Top view of heating plate unit.
 - a. Central heating plate with heating foil $0.2 \times 0.2 \text{ m}^2$
 - b. Ring-shaped screen with heating foil
 - c. Gap between measurement and screen areas
 - d. Power screen with heating foil
 - e. Heating cable
 - f. Insulation and spacers
 - g. Temperature sensors (platinum elements)



- C. Assembly sketch of plate unit.
 - h. Heating plate
 - i. Cold plate with pipes for circulating alcohol and heating foil
 - j. Gradient screen. Heating cable at top.
 - k. Upper cold plate.
 - l. Mixing tank with magnetic valve and pump.

The power applied to this element is also controlled by thermal sensors so that its temperature is maintained equal to that of the central measurement area. The stainless steel sample holder connects warm and cold plates thermally such that one obtains approximately the same temperature profile in the connecting member as in the sample material (gradient screen). This prevents heat leakage from the sides of the samples.

The design is shown in Figure 6 and Figure 7 shows the function of the automatic controls.

As indicated, the temperature of a cold plate is controlled by a regulated flow of the cooling medium (methanol) through a magnet valve into a mixing tank. To ensure stable temperatures, a heating foil is included with the cold plate and the power applied (to the foil) is automatically regulated by temperature sensors in the cold plate (feed-back). The reference temperature for the cooling medium (set point) is a few degrees lower than the desired cold plate temperature, in order to provide a nearly constant power consumption in the heating foil.

The power applied to the heating plate is controlled by means of feed-back, by means of a temperature sensor in the heating plate. A common adjustment (set-point) is used for the temperatures of warm and cold plates, along with a variable difference between these temperatures. This makes it possible to maintain a set temperature difference while changing the temperature level.

To obtain short stabilization times, the warm plate temperature is regulated towards a constant value already at the beginning of each experiment. However, this step-wise change in temperature is somewhat limited by the thermal capacity of the heating plate itself, as well as the limited power capacity of the heater. Figure 8 shows an example of how applied power and warm plate temperature may vary from the start of an experiment and until stability (steady-state condition) is reached. This also gives an indication of the degree

of temperature stability that can be obtained with this test equipment.

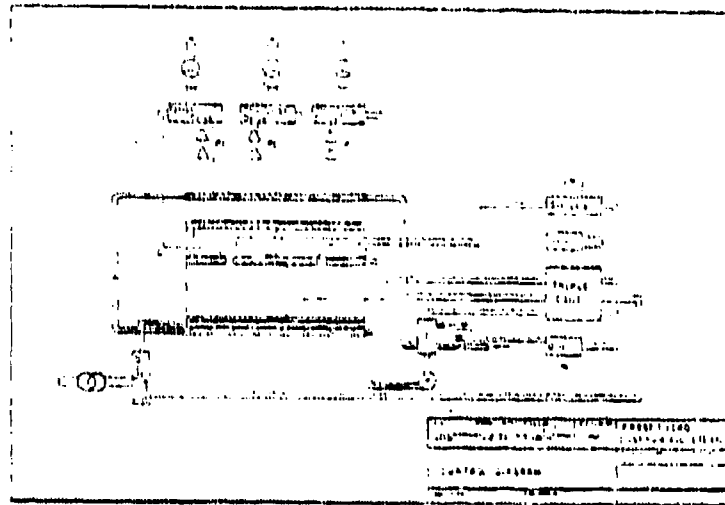


FIG. 7. Principalskisse af regulerings-system i plateapparatet som er vist på fig. 6. Schematic diagram of the guarded hot plate apparatus described in fig. 6.

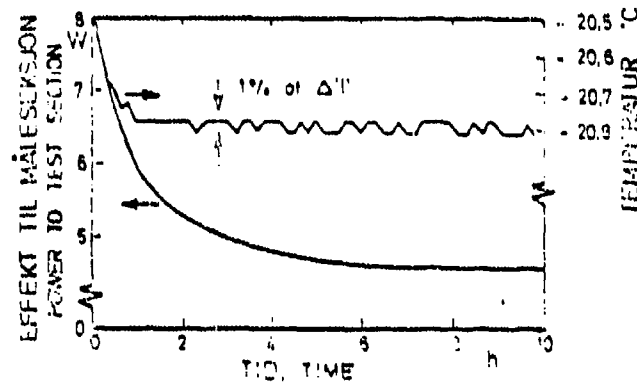


FIG. 8. Eksempel på variation i effekttilførsel og temperaturstabilitet af den kontrollede varmeplade i plateapparatet som er beskrevet ovenfor. Power input and temperature stability of the control test section in the guarded hot plate apparatus described above.

In addition to the plate units described (3 units), equipment was developed and built for transient measurements by means of thermal conduction probes. This will be described in the following section.

3. THERMAL CONDUCTION PROBES¹⁾

As mentioned in the previous section, there is today a tendency to abandon traditional stationary (steady state) methods in favour of non-stationary (transient) methods. This is due partly to a requirement for reduced experiment times, partly to a desire to minimize the influence of the previously mentioned moisture transport. Of the different methods in question, the so called thermal conduction probe approach has seen the widest use for measuring thermal conductivity in granular materials. This method will be discussed in this section while other applicable methods are treated in section 4.

A. Influence of finite size and varying thermal properties

A thermal conduction probe can ideally be considered as a filament²⁾ of infinite length, surrounded by a homogenous medium of infinite extent in all directions. It is assumed, that the temperature field in that medium initially is homogenous ($T = T_0$). Starting at a time t_0 , a constant power q (W/m) is applied to the filament. Based on the linear thermal conduction equation (Fourier's equation), the temperature field around the filament can be determined (12).

-
- 1) The original use the word "sonde", literal translation "sounding device" or "probe", which usually refers to a passive sensor. However, the device described here is active (Translator's note).
 - 2) "Linjekilde" also implies an "infinitely thin" filament (Translator's note).

$$T - T_0 = \frac{q}{4\pi\lambda} \left[-Ei \left(-\frac{r^2}{4at} \right) \right]$$

9

a is thermal diffusivity (m^2/s)

$$Ei(x) = \int_x^\infty \frac{e^{-x}}{x} dx$$

The integral function Ei can be expanded in a power series:

$$-Ei(-x) = -\gamma - \ln x + x - \frac{1}{2}x^2 + \dots$$

10

γ is Euler's constant = 0.5772

For $4at/r^2 \gg 1$ one can thus write the equation describing the temperature field in the approximate form

$$T - T_0 = \frac{q}{4\pi\lambda} (-\gamma + \ln t + \ln 4a/r^2)$$

11

If the power to the filament is disconnected at time t^1 , the temperature field can be approximated by

$$T - T_0 = \frac{q}{4\pi\lambda} \ln \frac{t}{t^1}$$

12

The increase in temperature, $T_2 - T_1$, between times t_1 and t_2 , derived from Eq 11, becomes

$$T_2 - T_1 = \frac{q}{4\pi\lambda} \ln t_2/t_1$$

13

The two latter expressions do not contain the thermal diffusivity and the radius r , while the thermal conductivity can be solved for explicitly. Eq 13 is the expression normally used for calculating the thermal conductivity in connection with experiments utilizing thermal conductivity probes. Eq 12 may be valuable as a check of the results obtained, particularly for measurements in moist materials.

1) This integral defines $-Ei(-x)$. The original is probably in error. (Translator's note)

Use of the thermal conduction probe was originally proposed in 1931 by Stålhane and Pyk (11). They developed an empirical method for computing conductivity from the temperature rise in the probe. The analytical foundation was later developed by Van der Held and Van Drunen (1949)(12). In both cases, the method was used for measuring conductivity of soil materials(13).

For measurements in liquids, the probe can be configured as a wire or thin filament. Probes for use in soil materials are usually made from thin tubes, typically filled by an insulating material into which heating wires and temperature sensors are molded. The geometry of the probe will then deviate significantly from the ideal model on which the analytical solution is based.

Several researchers have investigated the effect of this deviation from the ideal case (14, 15, 16, 17). De Vries and Peck (1958) have for example treated the case of a probe having finite thickness (diameter) but containing a filament¹⁾ (16). They find, that Eq 13 can be used for determining thermal conductivity, provided that $4 \text{ at}/r^2 \gg 1$, if the contact resistance between probe and the material under test is small and the thermal capacity is not significantly larger than that of the material under test. They also claim that this condition is met for soils made up of minerals, while conditions are less favourable for organic soil materials.

Probes of finite extent (length) were first treated by Blackwell (1953, 1956) (17, 18). He considered the case where a probe is immersed in a homogenous material of infinite extent. With the aid of various mathematical approximations he arrived at an expression for the errors caused by axial heat flow in the probe. For a particular type of probe he found that these errors are less than one percent if the length to radius ratio exceeds 30.

1) It seems implied that this (thin) filament carries the heating current (Translator's note).

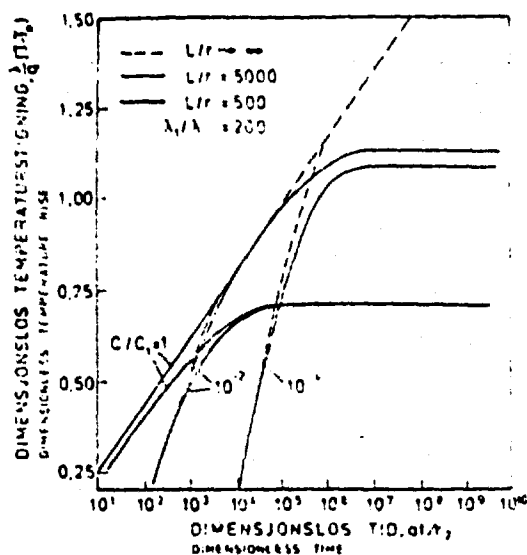
Kierkus et.al. (1973) (19) have performed an analysis for a thin filament of finite length, with some-what different boundary conditions. The study was performed in conjunction with conductivity measurements in liquids, when the probe consists of a thin metal heating wire. Since the conductors required for supplying the heating current have significantly larger cross-sections (than the heater wire itself), the temperatures at the ends of the probe are assumed constant during the entire experiment and equal to the initial temperatures. Using modern computer methods for numerical integration, the temperature rise in such heating wires of finite extent was computed for different length/radius ratios and differences in thermal properties between heating wire and the surrounding medium. The results obtained (from these computations) give a good illustration to the dependence of different parameters. Some of these results are shown in Figure 9, where temperature rise and time are given as normalized¹⁾ numbers.

Figure 9a shows the effect of finite length and different thermal (heat) capacities for the case where the probe has a much higher thermal conductivity than the surrounding medium ($\lambda_1/\lambda = 200$). As mentioned previously, this applies to conductivity measurements with the heating wire placed in liquids. The dependence on the conductivity ratio is given by Figure 9b for a given length/radius ratio of 500.

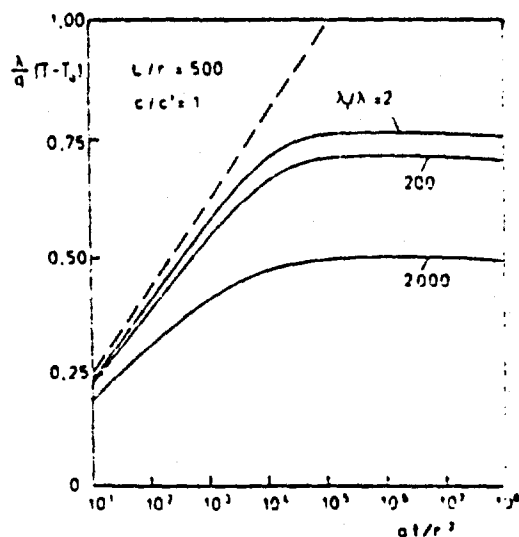
These results show that an infinite long thin²⁾ cylinder has the same response as an infinitely thin filament when the cylinder has the same heat capacity as the surrounding medium. If the infinitely long cylinder and the medium have different heat capacities, the temperature rise will initially be steeper than for a filament but after a certain time the response will flatten out and coincide with that of a filament.

1) The English text in Figure 9 uses the word "dimensionless".

2) The English text under Figure 9 uses the word "compact" (Translator's notes).



a. Gitt leiningsevneforhold $\lambda_1/\lambda = 200$ og varierende lengderadiusforhold og varmekapasitet. Conductivity ratio $\lambda_1/\lambda = 200$ and variable length-radius ratio and heat capacity.



b. Varmekapasitet og lengde-radiusforhold gitt. Varierende leiningforhold. Heat capacity and length-radius ratio given. Variable conductivity ratios.

FIG. 9. Temperatur-respons av en kompakt cylinder med konstant varmekraft på overflaten. Temperature response of a compact cylinder with constant surface heat flux. (Xierkus 1973) 419).

The finite extent (length) of the probe will, after a certain time, cause another bend in the temperature rise curve towards values below those for the infinitely long probe. This bend will occur earlier for lower values of C/C_1 . Thus, for different heat capacities and finite length one may at best expect that the probe will have the same response as a thin filament over a limited time interval,

such as that shown by the curve for $C/C_1 = 10^{-2}$ and $L/r = 5000$.

For equal thermal capacities and finite length, the conductivity ratio will determine how closely the response will follow that of a filament, see Figure 9b. In principle, high conductivity in the probe is not desirable, since a low conductivity brings the response closer to the filament response.

Traditionally, probes for use in soil materials have been fabricated from thin wall tubing, e.g. stainless steel, filled by an insulating (plastic) material in which heater wire and thermoelements are placed¹⁾. This makes it difficult to apply the results just discussed to probe measurements in soil materials. The boundary conditions at the ends of the probe will also deviate from those assumed in the analysis performed by Kierkus, which further complicates matters.

Practical considerations dictate that the length/radius ratio of probes should be limited, e.g. to about 200, which for a probe of 2 mm thickness (diameter) gives a length of 20 cm. The results described here also indicate that the thermal properties of the probe should be matched to those of the material under test as well as possible, both in terms of thermal capacity and conductivity, in order for satisfactory results to be obtained (c.f. Figure 9b). However, the limited length/radius ratio will not guarantee that the response is the same as that of a thin filament.

Another alternative would be to increase the length/radius ratio significantly, e.g. by using the heater wire itself as a probe. This would result in extreme temperature gradients near the probe, which is not desirable for measurements in moist materials (c.f. next section). However, this approach may be practical for measurements in completely dry or saturated materials.

1) The original uses the word "innbakt", literal translation "baked in" (Translator's note).

Comparative investigations initiated by the Institute for Cold Technology indicate that probes having the previously given dimensions ($d = 2$ mm, $L = 20$ cm) give up to 20 percent higher conductivity values than steady state measurements performed in a planar test unit. This applies both for dry and moist soil samples. However, experiments performed with longer probes ($d = 1$ mm, $L = 100$ cm) gave much better agreement with results obtained in the planar test unit. Experiments using "probes" consisting of a heating wire (alone) also gave results in good agreement with planar measurements in dry and saturated soils. Even if these studies are still going on, they still serve to support the analytical results discussed here, including the new requirements for length/radius ratios developed here (20).

B. The effects of moisture transport

Heat conduction probes constructed in the form of heater wires appear to be suited for measurements in dry or saturated soil materials. However, special problems arise in moist soil materials where the large temperature gradients occurring near the probe can cause moisture transport and a drying out of a "kernel" around the probe. By taking the derivative of Eq 11 with respect to r one obtains the following expression for the temperature gradient:

$$\frac{\partial T}{\partial r} = \frac{q}{2\pi r \lambda} \quad 14$$

A reduction of the temperature gradient will thus require an increase of the probe diameter and/or reduction of the applied power. However, both these parameters have practical limitations. Low power results in a small rise in temperature, which may cause uncertainties in the conductivity measurements. A large probe diameter leads to a longer probe in order to maintain a certain length/radius ratio. This would require larger sample volumes and more work for preparation of samples in the laboratory.

If one wants to use a power which causes the temperature to rise by 1°C over a 10:1 time interval (e.g. from $t_1 = 1$ min to $t_2 = 10$ min) one finds from Eq 13 that the ratio $q/(2\pi\lambda)$ should be very close to 1. During the measurement period, the temperature gradient near the probe then becomes:

$$\frac{\partial T}{\partial r} = \frac{1}{r}$$

15

A probe diameter of 2 mm would thus result in temperature gradients of 10°C/cm. Even larger gradients will occur immediately after the start of the experiment. During that period, the probe temperature will normally rise by a larger amount than during the measurement period itself.

The gradients which occur are significantly larger than those occurring during stationary experiments in a planar test unit. It is doubtful whether the much shorter measurement times (using the probe method) can compensate for this difference.

Experiments in moist materials also show effects which can be related to drying out of the material near the probe. For example, Woodside registered a steady decrease in measured thermal conductivity during experiments with moist clay (21). The probe diameter was in this case about 0.5 mm. A series of experiments conducted at the Institute for Cold Technology at NTH indicates, however, that this effect is most pronounced for degrees of saturation within a certain range. Figure 10 shows the temperature rise in experiments with a silt material at different degrees of saturation.

As shown by Figure 10, the temperature rise changes significantly beyond a certain time for the three cases having the highest degree of saturation. This significant increase in the rise can be directly related to a drying out of the material near the probe, since an increased (temperature) rise corresponds to reduced conductivity (c.f. Eq 13). For the lower degrees of saturation there

is no similar effect and the effect is also relatively small for the highest degree of saturation.

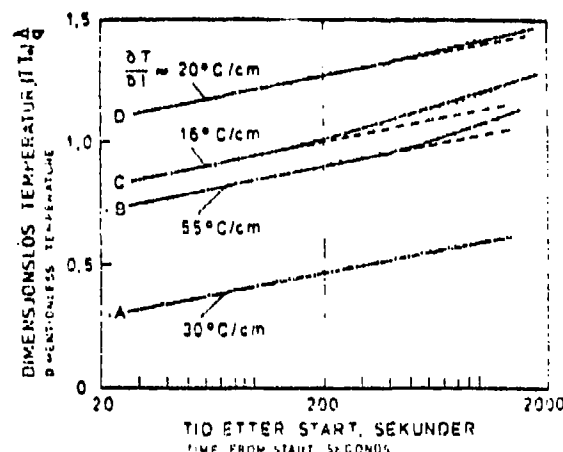


FIG. 10. Innflytelse av fuktvariering på temperaturresponsen i varmekulemåler. Resultat for et siltmateriale ved forskjellige fuktighetsgrader. Influence of moisture redistribution on the temperature response in thermal conductivity probes. Results from experiments with a silty soil at different degrees of saturation. A, $S_p = 5\%$. B, $S_p = 10\%$. C, $S_p = 15\%$. D, $S_p = 20\%$.

The quoted values of the temperature gradient near the probe were calculated from Eq 14.

A comparison of cases B and D, which pertain to nearly the same degree of saturation, illustrate the dependence on gradient. These results show that the effects of moisture transport are limited to a relatively narrow range in terms of degree of saturation in moist soil materials, for the probe design used. However, the previously mentioned comparative studies indicate that this in itself does not guarantee that measured data are correct, as long as length/radius ratio for the probes are as limited as for the probes used. For an increase in the length/radius ratio not to impair the practical usefulness of the probes, one may, as mentioned, have to resort to probes consisting of heater wires only. This would result in significantly higher gradients than in the experiments mentioned here and much more severe problems in terms of moisture transport and drying-out near the probe can be expected.

C. Experimental arrangement

Based on experience from the investigations on the effects of moisture transport, an experimental arrangement was developed at the Institute for Cold Technology, utilizing six probes that can be operated simultaneously (22). This equipment was built before results from the previously mentioned comparative investigation were available. A comprehensive series of experiments was conducted by the author on dry soil materials, using this equipment. Later, a series of experiments on six different soil materials at various degrees of saturation was performed. The results from these experiments will be discussed in the chapter on experimental investigations of conductivity in soil materials.

The material samples were packed into cylindrical steel containers which were placed in a chamber where the air temperature was recorded automatically, by means of a data logger and punched out on paper tape. Figure 11a shows a sketch of the arrangement, while Figure 11b contains a simplified circuit diagram for the electrical components.

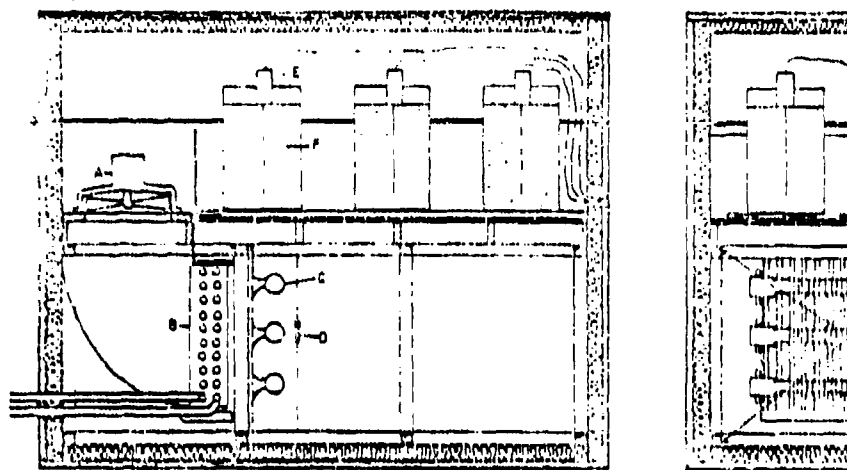
Experiments with measuring the thermal conductivity of frozen soil materials, using a heat conduction probe in the same set-up, have to date not given satisfactory results. This may be due to the previously mentioned non-linearity that occurs when water freezes, as well as to the homogeneity of the samples being disturbed near the probe during the freezing process.

The actual measurement period in this test unit is only 30 minutes. However, a stabilization period is required to obtain homogenous temperature fields in the samples before measurements. For this reason, the samples are usually prepared on the day before the experiments and placed in the chamber at 4°C (or other selected temperature) over night. As mentioned earlier, the sample containers are cylindrical and made of (sheet metal) steel. A diameter of 20 cm was chosen, while the depth is 30 cm. This gives a sample volume of about 7.5 litres, corresponding to sample weights between 12 and

15 kg. Preparation of six samples normally requires one man-day. The next day, following the thermal conductivity measurements, tests are made of the moisture content in the containers.

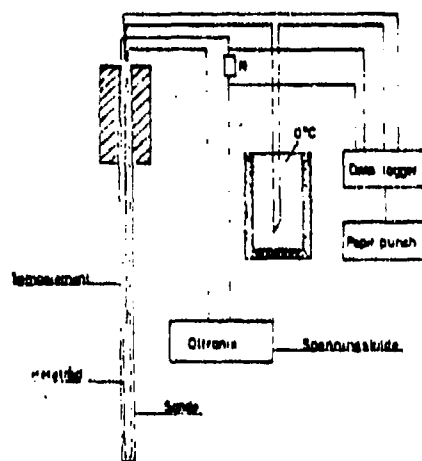
As mentioned before the results are coded on punched paper tape. They can be decoded or printed out in the form of a table showing temperature rise and currents supplied to the probes at given time intervals. As an alternative, the paper tape can be fed into a computer which calculates conductivities and plots the temperature rise. An example of such a plot is shown in Figure 12, where also part of the computer print-out is reproduced. The program was written by Mr. K. Aflekt at the Institute for Cold Technology. Data reduction by means of a computer results in considerable time savings, as compared to manual reduction which involves an extensive plotting effort following each experiment.

The equipment for probe measurement was developed by the author, in cooperation with P.E. Frivik, M.Sc., Institute for Cold Technology. Mr. Frivik carried the main responsibility for the development, including selection of components for registration and temperature control. Initial experiments were conducted by Mr. K. Witso Jonsen for his Master's Thesis in the fall of 1972. The series of experiments with dry materials was performed by the author. Mr. Sigurdson of the Institute for Cold Technology has since assumed the responsibility for sample preparation and conducting experiments using this test equipment.



- A - Vifte
B - Kjelte
C - Qm
D - Pt element
E - Sonde
F - Motorgie

a) Skisse av termo-kasse med seks prøvebeholdere med sonder..



c) Skisse av sonde med spenningskilde og registreringutstyr.

Fig. 11. Skisser av forsøksoppstilling for varmeledningmåling med sonder utviklet ved Institutt for Kjøle- og Frysingsteknikk, NTNU. Lay-out of experimental stand for thermal conductivity measurements with probes developed at Division of Refrigeration Engineering, Univ. of Trondheim.

Legend, Figure 11.

A - Fan
B - Cooling element
C - Oven
D - Pt element (Thermal sensor)
E - Probe
F - Material

a) Sketch of chamber with six sample containers and probes.

Termoelement : Thermal sensor
Hetetrad : Heater wire
Sonde : Probe
Oltronix : Power supply (trade-name)

c) Sketch of the probe with power wupply and recording equipment.

Translation of print-out, Figure 12.

THERMAL CONDUCTIVITY - PROBE MEASUREMENT

EXPERIMENT No 5

PROBE No 4

INITIAL PROBE TEMPERATURE : 4.29°C

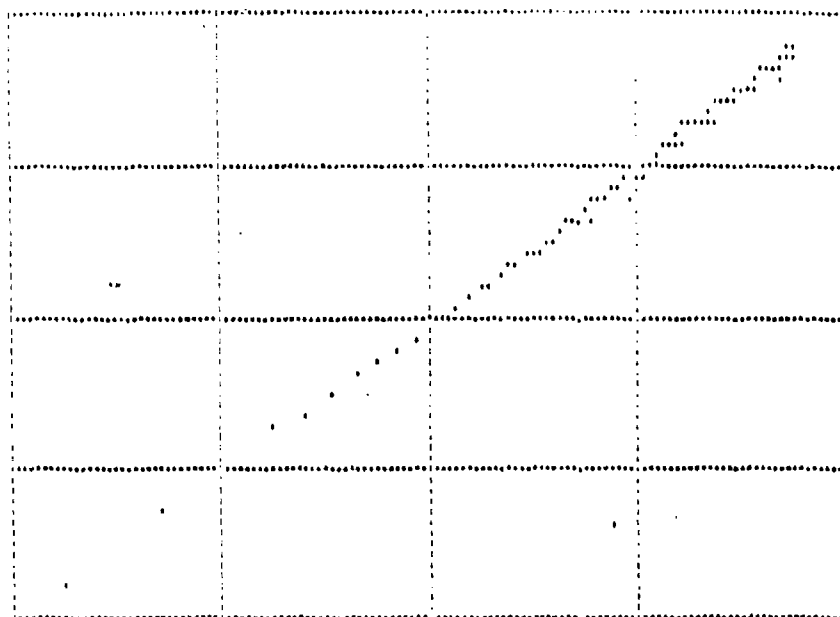
STARTING TEMPERATURE IN (TEST) PERIOD : 13.80

FINAL TEMPERATURE IN (TEST) PERIOD : 20.01

TEMPERATURE RISE IN (TEST) PERIOD : 1.21

AVERAGE CURRENT IN (TEST) PERIOD : -.6508

CALCULATED CONDUCTIVITY 2.097 W/mK



THE X AXIS RUNS FROM -1299.321001 TO .392489001
THE Y AXIS RUNS FROM .10061271002 TO .20796102002

: FERNISK KONDUKTIVITET - SONDENLINGEN :

PROBE NO: 1
SONDE NO: 1
TEMPERATURE : SONDEPROBE FOR START: 0.29 UNOC
DISTANCE FROM PROBE TO PROBE: 14.40
DISTANCE FROM PROBE TO PROBE: 20.00
TEMPERATURE FROM PROBE: 1.27
TEMPERATURE FROM PROBE: 1.27

WE RECENTLY KONDUKTIVITET 2.000 UNOC

Fig. 12. Temperaturstigning i sonden med logaritmisk tidskala plottet på datamaskin ved hjælp af datamaskinprogram for bearbejdning af registreringer ved sondeallinger. Temperatur-rise in the probe is plotted to a logarithmic time scale. The plot is done by a computer, programmed for handling data from probe-experiments.

BEST AVAILABLE COPY

4. OTHER TRANSIENT METHODS

From the previous discussion it is evident that the thermal conduction probe really does not constitute a suitable solution if one wants to reduce the effects of moisture transport. The method may give short measurement times in comparison to traditional steady state methods but the temperature gradients will be much larger. The comparatively large sample volumes required are also inconvenient. For these reasons it has become desirable to search for other methods which can meet the combined requirements of small temperature gradients, short measurement times and small sample volumes. With regard to sample preparation it may be suitable to take a cylindrical (sample) geometry as a starting point. The types of test equipment with cylindrical geometry that will be discussed here can also be realized in planar configurations (c.f. Refs. 23, 24, 25, 26). However, only test equipment utilizing cylindrical geometry will be treated in the following.

The various methods which have been utilized are based on either a programmed temperature variation on the cylindrical surfaces or constant thermal flux. The latter case is most applicable for a hollow cylinder when heat is applied from its inside. As will be evident in the following, thermal diffusivity can be derived from data on temperature only, while computation of thermal conductivity and heat capacity by volume always required knowledge about both thermal flux and temperature distribution.

A. Linear temperature rise

One of the simplest methods is based on a linear rise of temperature in the surface of the material under test, when shaped as a small (compact) cylinder. After a certain time, the temperature difference between periphery and centerline in such a sample will assume a constant value, while temperatures throughout the sample rise at the same rate as the surface temperature (Figure 13). This condition may be described as a quasi-stationary state.

If the temperature rise on the surface is given by

$$T(R, t) - T_0 = \beta t \quad 16$$

the rise of temperature at each point within the sample, under quasi-stationary conditions is given by

$$T(r, t) - T_0 = \beta t - \frac{\beta}{4a} (R^2 - r^2) \quad 17$$

T_0 is the initial temperature in the entire sample

β is the rate of temperature rise ($^{\circ}\text{C/s}$)

R is outer radius

r is arbitrary radius

a is thermal diffusivity (m^2/s)

The thermal diffusivity can be determined from measured temperatures at the periphery and centerline of the sample

$$a = \frac{\beta R^2}{4\Delta T} \quad 18$$

where ΔT is the temperature difference between periphery and centerline.

The maximum temperature gradient over the quasi-stationary period is obtained by taking the derivative of eq 17.

$$\left(\frac{\partial T}{\partial r} \right)_R = \frac{\beta R}{2a} \quad 19$$

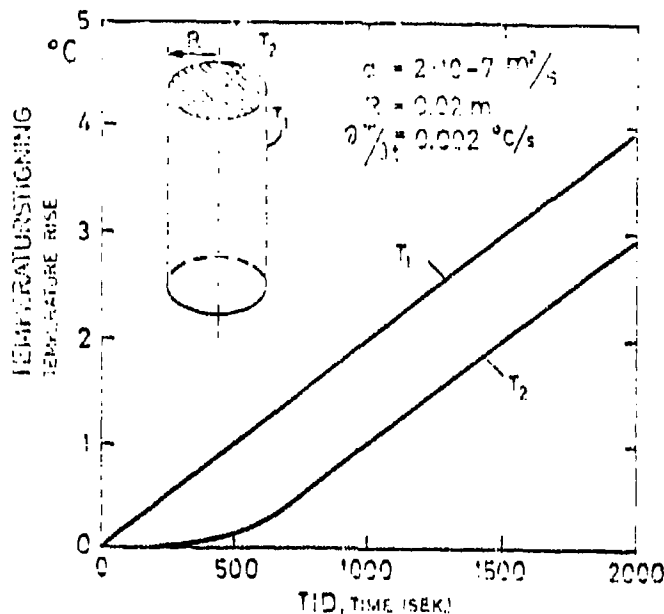


FIG. 13. Temperature response in cylinder with constant temperature rise at the surface. Temperature response in a cylinder with constant temperature rise at the surface.

The gradient can consequently be reduced by lowering the rate of temperature rise and by reducing the sample diameter. The sample diameter is also limited by the desire to reduce the time before the quasi-stationary phase is reached. A lower limit for the diameter of the sample is given by the requirement for accurate temperature measurements and problems associated with (precise) location of the centerline temperature sensor.

For example, when considering a fine grain soil material within the previously discussed critical range of saturation levels, the thermal diffusivity can be estimated to $2 \cdot 10^{-7} \text{ m}^2/\text{s}$.

If one requires a maximum temperature gradient below $1^\circ\text{C}/\text{cm}$ and a minimum temperature difference $\Delta T = 1^\circ\text{C}$, one can use Eqs 13 and 19 to find the possible range for rate of temperature rise δ with different sample diameters. According to Luikov (28) one can estimate the times for quasi-stationary conditions from

$$Fo = at/R^2 = 0.2$$

Fo is Fourier's number

The results of this example are summarized in Figure 14.

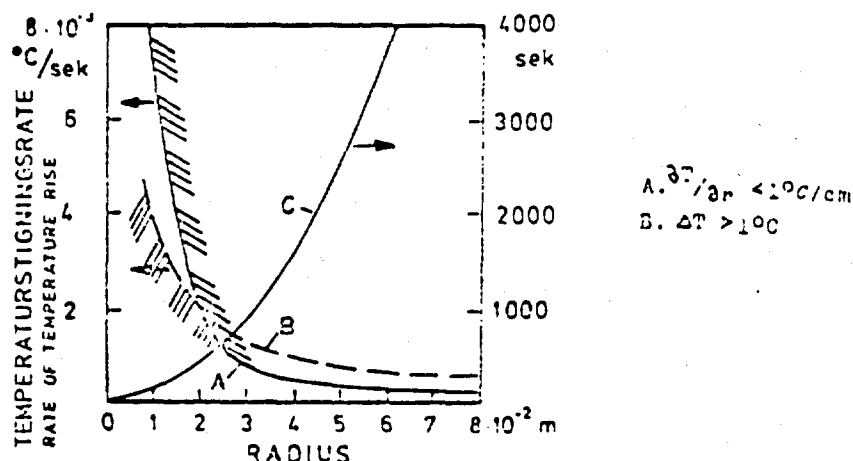


FIG. 14. Tillatte temperaturstigningshastigheder i en cylindrisk prøve med termisk diffusivitet $a = 2 \cdot 10^{-7} \text{ m}^2/\text{S}$. (Kurve A og B.) Tid for den kvasistationære fase og radius er givet ved kurve C. Acceptable temperature rise rates in cylindrical samples with thermal diffusivity $a = 2 \cdot 10^{-7} \text{ m}^2/\text{S}$. (Line A and B). Time to reach the quasi-stationary domain given by line C.

One finds that the smallest radius which satisfies both conditions is 2 cm. This leads to a quasi-stationary period of 400 seconds. The rate of temperature rise which satisfies the requirements is $2 \cdot 10^{-3} \text{ }^\circ\text{C/sec}$, corresponding to about 7°C/hour .

This effect means that this method can be used for soil samples taken with the 54 mm diameter sampler normally used for geotechnical studies. Some trimming around the periphery will probably be advantageous, but this is common practice in most normal studies of samples of this kind.

One draw-back with this method is the relatively complicated automatic temperature control circuitry required for each sample holder. However, the small sample volumes represent a large advantage over the probe method. Except for diameter, the sample volume also depends on the length of each sample, which should be rather large to

Best Available Copy

avoid edge effects. The required length/diameter ratio can be reduced by insulating the end surfaces. If a length/diameter ratio of 4 is selected, the required volume for the case mentioned previously ($d \approx 50$ mm) is less than 0.5 liter. However, the requirement for homogeneity will preclude experiments with coarser materials than sand in such a unit.

As mentioned previously, equipment of this type will only give information about thermal diffusivity. Szanto and Aguirre-Puente (23) have proposed a modified version of this method, in which also heat flux is recorded. In their test unit, the samples are surrounded by a material with known thermal properties, e.g. plexiglass. During the quasi-stationary phase, the thermal flux through the plexiglass pipe can be determined from temperature measurements at both surfaces of the pipe.

When the thermal flux is known one can determine both thermal capacity and conductivity for the sample material, as well as diffusivity. Aguirre-Puente give the following expressions for c_p and λ

$$c_p = \frac{q}{\pi R^2 \delta} \quad 21$$

$$\lambda = \frac{q}{4\pi \Delta T} \quad 22$$

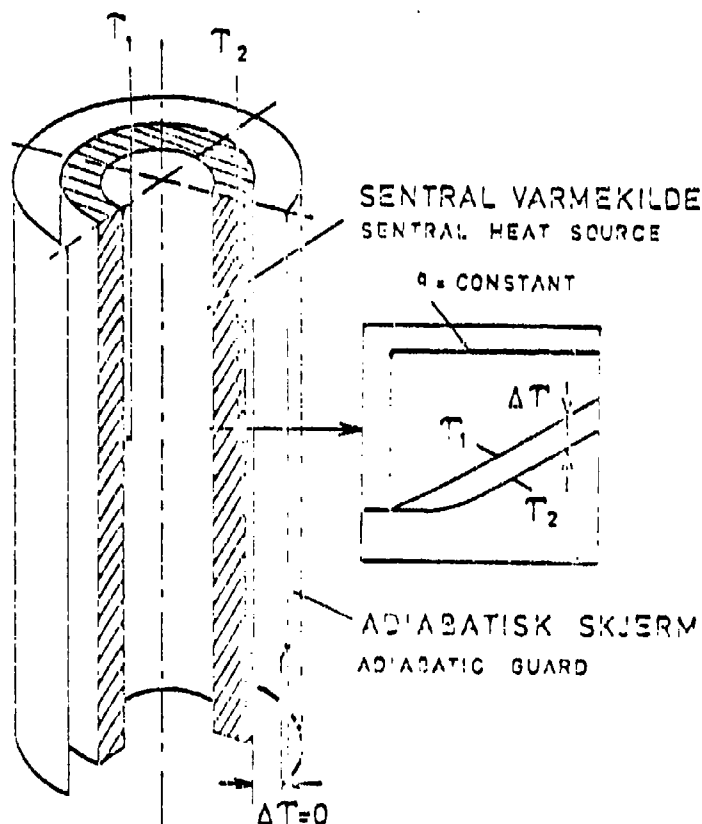
Since this method is based on indirect measurement of the thermal flux, accuracy will depend partly on the calibration of the flux-meter.

B. Constant thermal flux

(1972)

Shashkov et.al. have developed a method in which the thermal flux can be measured directly (29). The test sample is bounded by two

concentric cylinders. The heating elements are attached to the inside of the hollow cylinder. The outer cylindrical surface faces a heat screen (guard) which is controlled by a signal from a temperature sensor at the outside of the sample. In this manner, adiabatic conditions (no exchange of heat) are ensured on the surface of the samples. A sketch illustrating this method is shown in Figure 15.



BEST AVAILABLE COPY

FIG. 15. Skisse av apparat for maling av jordarters varme-
parametre basert på konstant varmekilde inne i en
hul cylindrisk prøve med adiabatisk ytre over-
flate. Sketch of an apparatus for measurement of
soil thermal properties based on constant heat flux
inside a cylindrical tube sample with adiabatic
outer surface. (29).

The method utilizes the principle of constant heat flux. However, also in this case a quasi-stationary state will be reached after some time where the temperature rises linearly (with time) and a constant temperature difference ΔT exists between inner and outer surfaces of the sample. In this phase, the temperatures are given by

$$T(r, t) - T_0 = \frac{q}{\lambda} R_1 \frac{R_1^2}{R_2^2 - R_1^2} \left[\frac{2Fo - 1}{4} \left(1 - 2 \frac{r^2}{R_2^2} \right) - \frac{R_2^2}{R_1^2} \left(\ln \frac{r}{R_2} + \frac{R_1^2}{R_1^2 - R_2^2} \ln \frac{R_2}{R_1} + \frac{3}{4} \right) \right] \quad 23$$

R_1, R_2 , inner and outer sample radii
 F_0 , Fourier's number = at/R_1^2
 t , time after flux turn-on

The thermal parameters for the sample can be computed from the rate of temperature rise β and the temperature difference ΔT :

$$\lambda = \frac{q R_2}{2 (R_1^2 - R_2^2) \Delta T} (R_2^2 - R_1^2 - 2R_1^2 \ln \frac{R_1}{R_2}) \quad 24$$

$$a = \frac{\beta}{4 \Delta T} (R_2^2 - R_1^2 - 2R_1^2 \ln \frac{R_1}{R_2}) \quad 25$$

$$cp = \frac{q R_2}{\beta (R_1^2 - R_2^2)} \quad 26$$

The temperature rise within the samples is determined by taking the derivative of Eq 23 and setting $r = R_1$.

$$\left(\frac{\partial T}{\partial r} \right)_{R_1} = \frac{q}{\lambda} \quad 27$$

where q is the thermal flux per unit area of the inner surface. If the heat flux is measured per unit length of the cylinder (like for the thermal conduction probe) one obtains

$$\left(\frac{\partial T}{\partial r} \right)_{R_1} = \frac{q'}{2\pi R_1 \lambda} \quad 28$$

where q' is the thermal flux per metre cylinder length. Figure 16 illustrates the temperature gradients that will occur for different sample dimensions, if the temperature difference also in this case is kept below 1°C .

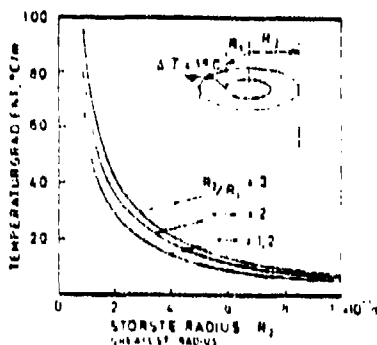


FIG. 16. Temperaturgradienter i et apparat som skissert på fig. 15 ved forskjellige radiusforhold og ytre dimensioner. Temperaturforskjellen mellom innre og ytre flate på 1°C . Temperaturgradientene i de apparatet skissert på fig. 15 med forskjellige radiusforhold og ytre dimensioner. 1°C temperaturforskjell mellom inner og outer overflate.

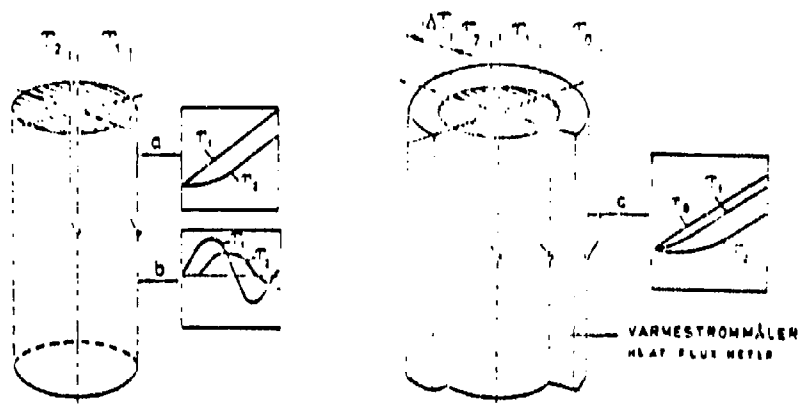
The temperature gradients will evidently be much less than 1°C/cm , except for very small sample dimensions.

As mentioned previously, this method has the advantage that the thermal flux can be measured directly as current and voltage for the heating elements. An axial heat screen similar to that used in Kersten's cylindrical test unit should contribute to increased accuracy in these measurements and ensure radial heat flow. The fact that temperature sensors can be mounted directly on the walls of the sample holder also represents an advantage in comparison to the previously described method where one of the temperature sensors had to be centered within the sample itself. However, the geometry is somewhat less favourable than the small (compact) cylinders in terms of sample preparation. In addition, undisturbed samples can not be used.

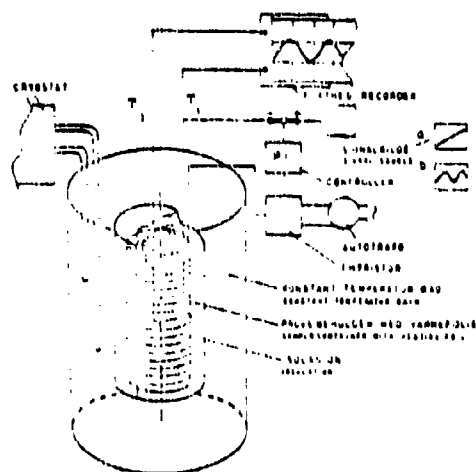
C. Periodic variation of temperature

This method is, like the preceding, based on a linear temperature rise in the samples. In some cases, it may be desirable to avoid a temperature rise with time during the experiment. This can be accomplished by controlling the surface temperature of the samples with a sinusoidal signal having a constant average value. Van Zee and Babcock (1951) proposed such a method for measuring thermal diffusivity in glass (30). The corresponding test unit can in principle be constructed in the same manner as the unit developed by Aguire-Puente, but using a different signal source. This is indicated in Figure 17, which shows a test set-up of this type.

For such a stationary, sinusoidal surface temperature variation, the temperature within the samples will also have a sinusoidal variation around a constant mean value, but with a certain phase-shift and attenuated amplitude. The thermal diffusivity can be calculated either from the phase shift (radians) between the temperatures in the center and at the periphery or from the amplitude attenuation. Appendix I summarizes the mathematical basis for this method. For this reason, only the expressions for phaseshift and attenuation are listed here.



- a. Linear temperaturstigning. Linear temperature rise.
- b. Stasjonær periodisk temperaturvariasjon. Steady harmonic temperature variation.
- c. Linear temperaturstigning. Varmestrommåler for registrering av overflatofluksen. Linear temperature rise. Fluxmeter for recording surface flux.



1. Prinsippskisse av apparatoppstillingen.
Schematic sketch of equipment.

FIG. 17. Skisse av sylindriske apparater for måling av jordarters varmeledningsevne, basert på programmert overflatetemperatur. Sketch of cylindrical apparatus for measuring soil thermal properties based on programmed surface temperatures.

$$\text{Phaseshift } \phi = \frac{\text{bei } x}{\text{ber } x} \quad 29$$

$$\text{Attenuation } A = \frac{1}{2} \left[(\text{bei } x)^2 + (\text{ber } x)^2 \right] \quad 30$$

$$x = R \sqrt{\omega/a} \quad 31$$

where ω is the angular velocity¹⁾ of the temperature (radians/sec). The relation between frequency (H_z or sec^{-1}) and angular velocity is given by $f = \omega / 2\pi$, while the cycle time (period) t_0 is given by $t_0 = 2\pi / \omega$.

bei and ber are Kelvin functions, which are tabulated in mathematical handbooks (e.g. (31), page 430).

Figure 18 shows the relation between x and phaseshift and attenuation²⁾ in graphical form.

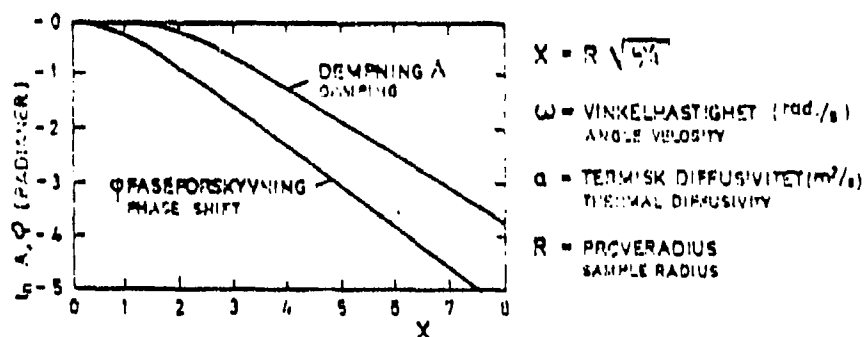


FIG. 18. Faseforskyvning og demping i en cylindrisk prøve med stationær periodisk temperaturvariation på overflaten. Phase shift and damping in a cylindrical specimen with steady periodic temperature variation at the surface.

- 1) Normally called "angular frequency" or "radian frequency"
- 2) The English text in Figure 18 uses the word "damping" and the ordinate scale for A is in Nepers. (Translator's notes)

Such a diagram can be used for determining x from measured phase-shift or amplitude attenuation. Thermal diffusivity can then be calculated from Eq 32, if period (frequency) and sample radius are known. In cases where the attenuation is strong, calculations based on phaseshift will give the best results, as evident from Figure 18.

Test unit dimensions may be selected based on requirements for short measurement times and accurate temperature readings. As an example, Figure 19 shows the relation between largest sample radius and period of oscillation for attenuation values no smaller than $A = 1/10$, for accurate temperature readings. As in the previous examples, the diffusivity is assumed to be $2 \cdot 10^{-7} \text{ m}^2/\text{s}$.

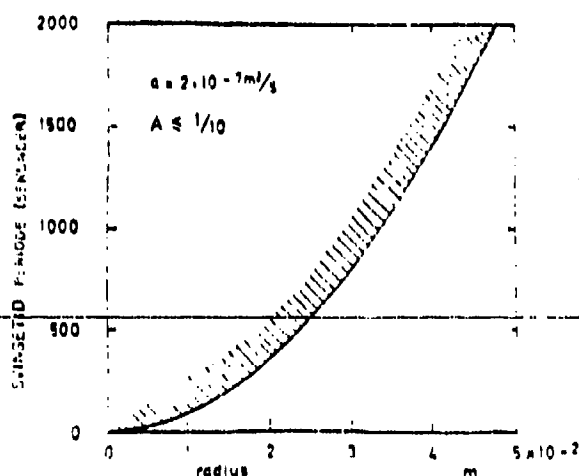


Fig. 19. Krav till cylindern i cylindriska apparater baserat på periodisk varierande temperaturer för 5 minuter mindre dämpningen $A = 1/10$. Dimensioner beräknade för cylindrisk uppvärmning baserat på värmeledningskoefficienten $a = 2 \cdot 10^{-7} \text{ m}^2/\text{s}$ för att undvika dämpning mindre än $A = 1/10$.

The sample radius can evidently not be much larger than about 2.5 cm if one wants the period to be shorter than 10 minutes.

A prototype unit of this kind was built at the Institute for Cold Technology in the spring of 1972, as part of the study reported here. Figure 20 shows a sketch of the set-up, as well as a modified ver-

sion with improved temperature control system. The sample holder was a steel tube with inner diameter 60 mm, wall thickness 2 mm and a length of 150 mm. A heating foil of type ESWA¹⁾ was wrapped around the tube. To ensure constant average temperature in the samples, a 1/4 inch copper pipe was also wrapped around the outside, separated from the sample holder by a layer of pipe insulation. In addition, the sample holder was insulated from the environment by means of pipe insulation on the outside of the cooling pipe.

The periodic temperature variation was achieved by periodically varying the power applied to the heating foil. The power was controlled by means of a function generator which permits variation of frequency, amplitude and mean level (off-set). In turn, this signal controls the power via a thyristor regulator which provides an AC power proportional to the control signal. The power level is varied by means of a variable auto-transformer (Variac). Temperatures at the periphery and center of the samples were sensed by copper-constantan thermocouples and recorded on a potentiometer recorder having a minimum full scale deflection of 100 μ V, corresponding to 2.5°C.

~~Due to the manner in which the prototype was built, manual adjustment~~ of the power level is required (via the auto-transformer) in order to obtain a stable mean temperature in the samples. This balance is reached when the power in the heating foil equals the heat loss due to the cooling pipe. A better solution has been proposed, by which the signal from the function generator is used to control the surface temperature via a feed-back loop containing a proportional integrating regulator, as well as the previously mentioned arrangement with a thyristor control and auto-transformer. This will permit automatic setting of the mean temperature by adjusting the signal source (function generator).

If the periodic signal is replaced by a linearly rising (ramp) signal, this test unit will also operate in the same manner as the unit described in the first part of this section. If the sample holder is constructed for temperature measurements this unit will

1) Probably a brand name (Translator's note)

then correspond to the equipment developed by Aguirre-Puente. As mentioned previously, such a test unit will yield information about thermal diffusivity, thermal conductivity and thermal capacity in the samples. This has also been achieved by Champoussin (1972) in a planar test unit using periodic temperature variations (27). The cylindrical configuration using sample holders made from a material with known thermal properties can also be expected to yield this (same) information.

A few preliminary experiments were conducted with the previously described prototype in a silt type soil material at a relatively low degree of saturation. The surface temperature amplitude was adjusted to about 1°C, while the frequency was varied in the range 10^{-3} Hz to 10^{-4} Hz. Three experiments within this frequency range gave approximately the same thermal diffusivity. This would indicate that the measurements were not affected by moisture transport.

Based on an evaluation of the need for new test methods, as opposed to the need for collecting more data on thermal conductivity in Norwegian soil materials, further work on this unit was postponed.

Instead, the main experimental effort was concentrated on development and construction of the previously mentioned test unit where six thermal conduction probes can be operated simultaneously. In addition to this probe unit, three planar test units for stationary measurements were built.

However, the new test method was adopted by P. Hoekstra at CRREL. He developed the method further and conducted a series of experiments with un-frozen dry and saturated sand, as well as a sandy clay material, at temperatures below the freezing point. Results from these experiments and a description of the equipment used can be found in a report from 1973 (32). In that report, the new method is recommended for replacing planar test units when measuring thermal parameter in moist soils when problems associated with moisture transport can be expected. It is also claimed that the method

is suitable for measuring thermal diffusivity of fine grain materials within the freezing zone, despite the non-linearities which occur. This is based in the possibility of using extremely small temperature variations for the tests. For example, it is stated that amplitudes as low as 0.2°C can be used without loss of accuracy. (Thermistors were used as temperature sensors).

A closer look at the fundamental differential equation for heat transport when thermal parameters are temperature dependent can to some extent clarify this:

$$\frac{\partial}{\partial x} \left(\lambda(T) \frac{\partial T}{\partial x} \right) = c_p(T) \frac{\partial T}{\partial t} \quad 33$$

By completing the derivative in the left hand member one obtains

$$\frac{\partial \lambda}{\partial x} \frac{\partial T}{\partial x} + \lambda \frac{\partial^2 T}{\partial x^2} = c_p(T) \frac{\partial T}{\partial t} \quad 34$$

If the temperature gradient is very low, one can probably neglect the term marked (1) in Eq 34. The equation is then of the same form as the linear differential equation which formed the starting point for the mathematical treatment of the method.

The fact that the thermal conductivity and capacitance are temperature dependent will cause deviations from the linear equation. However, if the variations due to temperature are sufficiently small one can possibly neglect also these effects. In this context, variations in the apparent heat capacitance will be most important. Since this parameter may vary by more than a factor of 10 for a temperature variation of only 0.5°C near the freezing point (0 to -1°C) it would seem that this condition poses unrealistic requirements on (sufficiently) small temperature variations.

A more complete mathematical analysis of the effects of these nonlinearities may give a better understanding (clarification) of these matters.

D. Conclusion

This overview of transient methods for measuring thermal parameters in soil materials shows that there are several solutions (methods) which in many ways are more useful than (provide advantages over) the conventional thermal conduction probe. The comparative studies which have been initiated at the Institute for Cold Technology indicate that (such) probes of common construction will not yield the expected accuracy, even when no moisture transport effects are present. However, for dry and saturated samples it appears as if probes configured as heating wires can give good accuracy without unreasonable requirements on sample volume, while in moist (not saturated) materials this configuration is almost out of the question due to moisture transport effects. On the other hand, extensive studies will be required to establish whether the described methods involving periodic temperature variations will emerge as a more suitable supplement to conventional steady state measurements in planar test units.

REFERENCES - CHAPTER IV

1. E. Berge, Ø. Aarvold: Some physical properties of grass silage. Meldinger fra Norges Landbrukshøgskole, 53 (1) 1974.
2. Beck: Transient Determination of Thermal Properties. Nuclear Engineering and Design, 3, 1966, pp. 373-381.
3. O. Krischer: Die Leitfähigkeit des Erdbodens. Beiheft zum Gesundheits-ingenieur. Reihe I. Heft 33, München (Munich) 1934.
4. W.O. Smith: Thermal Conductivity in Moist Soil Soil Science Soc. Am. Proc. 4, 1939, pp. 32-40.
5. A. Watzinger et al: Undersøkelse av masseutskiftningsmaterialer for veg-og jernbanebygging. Medd. fra Vegdirektøren 1938 no 6.
6. M.S. Kersten: Thermal Properties of Soils, Univ. of Minnesota, Eng. Experiment Station, Bull. 28, June 1949.
7. W. Woodside, J.B. Cliffe: Heat and Moisture Transfer on Closed Systems of Two Granular Materials. Soils Science, 87, 1959, pp. 75-82.
8. W. Woodside, C.M. A de Bruyn: Heat Transfer in a Moist Clay. Soil Science, 87, 1959, pp. 166-173.
9. F. De Ponte, P.E. Privik: Automatic Control of Guarded Hot Plate Apparatuses, Institutt for kjøleteknikk, Trondheim, NTH, 1972.
10. E. Brendeng, P.E. Privik: New Development in Design of Equipment for Measuring Thermal Conductivity and Heat Flow, Institutt for kjøleteknikk, Trondheim NTH, 1973.
11. E. Saare, C.G. Wenner: Värmeldningstal hos olika jordarter. Statens nämnd för byggnadsforskning. Handlingar no 31, 1957. (Ref. B. Stålhane and S. Pyk 1931).
12. E.M.F. van der Held, F.G. van Drunen: A Method of Measuring the Thermal Conductivity. Physica 15, (10) 1949, pp. 865-881.
13. D.A. de Vries: Het warmtegeleidingsvermogen van grond. Med. Landbouhogeschool Wageningen, 52, 1952.
14. F.C. Hooper, F.R. Lepper: Transient Heat Flow Apparatus for the Determination of Thermal Conductivities. Heating, Piping & Air Conditioning, Aug. 1950, pp. 129-134.
15. H.S. Carslaw, J.C. Jaeger: Conduction of Heat in Solids. Sec. ed. Heat Oxford Press, 1959, p. 345.

16. D.A. de Vries, A.J. Peck: On the Cylindrical Probe Method of Measuring Thermal Conductivity. Aust. J. Physics, 11, 1958, pp. 255-271.
17. J.H. Blackwell: A Transient Heat Flow Method for Determining the Thermal Constants. J. Appl. Phys. 25, (2), 1954, pp. 137-144.
18. J.H. Blackwell: The Axial-Flow Error in the Thermal Conductivity Probe. Can. J. Phys. 34, 1956, pp. 412-417.
19. W.T. Kierkus et al: Radial-Axial Transient Heat Conduction in a Region Bounded Internally by a Circular Cylinder of Finite Length.
Dept. of Mechanical Engineering University of Calgary, Calgary, Alberta (Preprint).
20. P.E. Privik: Institutt for kjøleteknikk, NTH 1974. Upubliserte resultater.
21. W. Woodside: Probe for Thermal Conductivity Measurement of Dry and Moist Materials. Heating, Piping & Air Conditioning, Sept. 1958, pp. 163-170.
22. P.E. Privik et al: Sondeapparat. Rapport fra Gruppen for termisk analyse av Frost i Jord. Institutt for kjøleteknikk, Trondheim, NTH, 1975.
23. O. Krischer, H. Esdorn: Einfaches Kurzzeitverfahren zur gleichzeitigen Bestimmung der Wärmeleitzahl, der Wärmekapazität und der Warmeindringzahl fester Stoffe. VDI-Forschungsheft. 450, 1955, pp. 28-39.
24. K. Katayama et al: Thermal Properties of Wet Porous Material Near Freezing Point. ASHRAE Journal April 1973, pp. 56-61.
25. C. Codegone et al: Desonant Thermal Waves in Insulating Slabs. IIR, Commission 2 (Trondheim) 1966. (Saertrykk)
26. J. C. Champoussin: Determination Simultane des caracteristiques termocinetiques des solides. Int. J. Heat. Mass, 15, 1972, pp. 1407-1418.
27. I. Szanto, J. Aquirre Puente: Etude des caracteristiques thermiques des milieux poreux fins humides.
Proceedings of the XIIIth International Congress of Refrigeration, Washington D.C., 1971, vol. I, pp. 751-757.
28. A.V. Luikov: Analytical Heat Diffusion Theory. Academic Press, New York 1968, p. 312.
29. A.G. Shashkov et al: Thermophysical Properties of Thermally Insulating Materials in the Cryogenic Temperature Region. Int. J. Heat Mass, 15, 1972, pp. 2385-2390.

30. L. van Zee, C.L. Babcock: A Method for the Measurement of Thermal Diffusivity of Molten Glass. J. Am. Ceram. Soc. 34 (8) 1951.
31. M. Abramowitz, I. Stegun: Ed. Handbook of Mathematical Functions. Nat. Bur. of Standards. Appl. Math. Ser., New York 1969, p. 374.
32. P. Hoekstra et al: Measuring the Thermal Properties of Cylindrical Specimens by use of Sinusoidal Temperature Waves. Cold Regions Research and Engineering Laboratory, Technical Report 244, Oct. 1973.

CHAPTER V

EXPERIMENTAL INVESTIGATIONS OF THERMAL CONDUCTIVITY IN SOIL MATERIALS

Previous chapters reviewed theoretical foundations for calculating thermal conductivity in soil materials. The theoretical investigations showed that purely analytical methods only can be expected to work for saturated materials in which conductivities of soil components differ little from each other. In such materials, variations in the microstructure are of secondary importance for the resulting thermal conductivity. On the other hand, for partially saturated materials, the presence of air with low thermal conductivity results in high sensitivity to differences in microstructure within the system. Since these properties are difficult to incorporate in a mathematical model for the thermal conductivity one must in such cases resort to an empirical approach based on thermal conductivity measurements on selected soil materials.

There is a relatively extensive amount of information on thermal conductivity measurements in soil materials available in the literature. The first major study, presented by O. Krisher in 1934 (1), was followed by a study of American soil materials by W.O. Smith (1938, 1939, 1942) (2, 3, 4) and studies of some Norwegian soil materials by Watzinger, Kindem and Michelsen (1938, 1941) (5, 6). In 1949, M.S. Kersten presented an extensive series of experiments on a number of soil materials from Alaska (7). This study is still the most valuable reference for empirical studies of thermal conductivity in soil materials. Among later contributions, the work published by M. van Rooyen and H.F. Winterkorn in 1959 constitutes the only systematic investigation that can be compared to Kersten's work in terms of extent (8).

In addition to these studies, a number of scattered single experiments have been published (9, 10, 11, 12). The lack of experi-

mental results pertaining to Norwegian soil materials is now being improved on by a series of experiments initiated at the Institute for Cold Technology, NTH. This investigation is part of the activities within the committee for frost on the ground. Some of the results will be discussed in the following section, which is devoted to measurements on dry soil materials.

1. DRY SOIL MATERIALS

A. Introduction

In a dry soil material, the ratio between thermal conductivities of particles ($\lambda = 2...5$ w/mK) and air in the pores ($\lambda = 0.024$ w/mK) is in most cases larger than 100. Based on limits (bounds) for the thermal conductivity in composite materials derived (described) previously, one find that this implies a very high sensitivity to differences in the microstructure of the material. Figure 1 illustrates this by showing the Hashin-Shtrikman limits for a two component system having a conductivity ratio of 100.

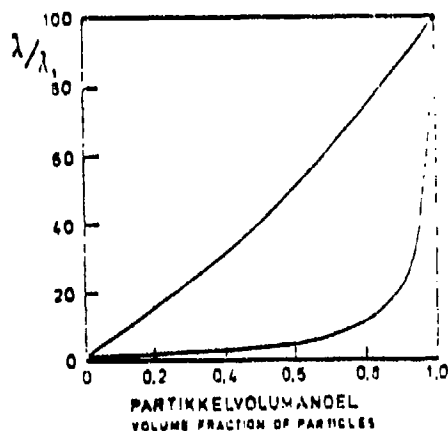


FIG. 1. Hashin-Shtrikman upper and lower bounds for the thermal conductivity ratio λ/λ_1 as a function of the volume fraction of particles for a two component material with a conductivity ratio of 100.

For a relative particle volume $1-n = 0.60$, the conductivity at the upper limit is at least 7 times that at the lower limit. For larger conductivity ratios, the distance (spread) between limits will be even larger (wider). As mentioned earlier, these limits represent extreme differences in microstructure. Even if such differences are not likely to occur in soil materials, the wide spread between these limits still indicates a high sensitivity to differences in the microstructure for dry soil materials.

The previously mentioned conductivity calculations for regular configurations of spheres can give an idea of the effect of particle conductivity on the (effective) conductivity of dry soil materials. Results obtained by Wahao and Kato for spheres arranged (packed) in an orthorhombic configuration ($n = 0.395$) are reproduced in Figure 2 (13).

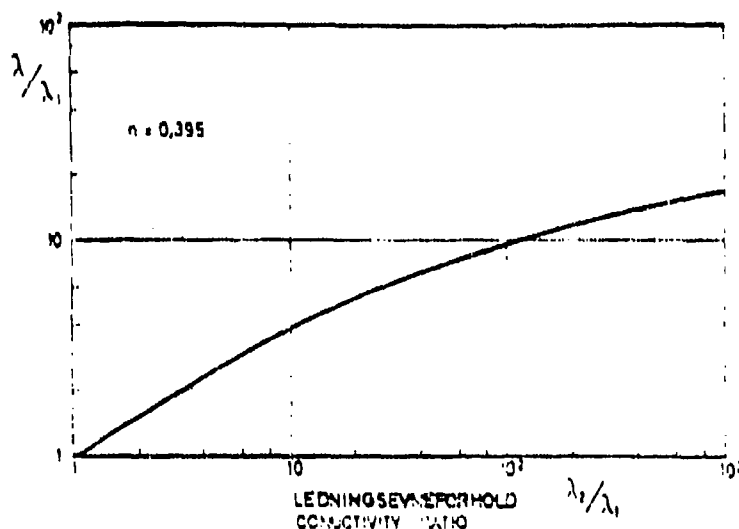


FIG. 2. Numerical calculations of the effective conductivity of spheres arranged in an orthorhombic configuration ($n = 0.395$). (Wahao and Kato, 1965 (13))

For the ratios between component conductivities normally found in dry soil materials one finds that the sensitivity due to variations in particle conductivity is relatively small. As an example, for a conductivity ratio of 100, the particle conductivity must increase by more than a factor of 10 before the (effective) conductivity in-

creases by 50 percent. By comparison, when the conductivity ratio is 10, the same relative increase in conductivity requires less than a three-fold increase in particle conductivity.

This implies that one can expect two characteristic properties of the conductivity in dry soil materials:

1. Considerable sensitivity to variations in microstructure
2. Low sensitivity to variations in particle conductivity.

B. Measurements performed by Smith

W.O. Smith has presented (results from) thermal conductivity measurements in dry soil materials, first in 1938 and later in 1942 (2, 4). Before the experiments, the soil materials were dried in an oven at 105°C for 24 hours. Results from these two series of experiments are reproduced in Figure 3, where conductivity is plotted as a function of porosity. The latter is computed on the basis of dry density and specific weight measured for the mineral particles.

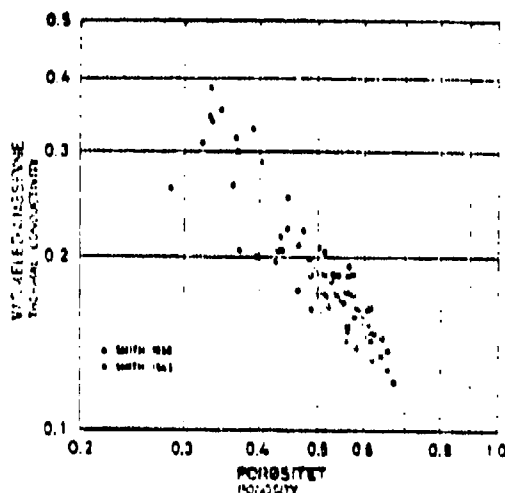


FIG. 3. Målinger av varmeledningsverdi av tørre jordarter plottet som funksjon av porositet. Målinger av varmeledningsverdi av tørre jordarter i forhold til porositet. (Smith 1938, 1942 (2,4))

As can be seen, these results show a variation of about ± 20 percent around a mean curve which can be drawn as a straight line in the log/log diagram. Variations among the results can be ascribed to differences in mineralogic composition as well as different textures (microstructure).

C. Investigation performed by the author

An investigation of thermal conductivity in dry soil materials performed by the author at the Institute for Cold Technology in the spring of 1973 can contribute to a clarification of the effects of the latter two properties. The measurements were performed in the probe test unit described in the previous chapter.

Measurements were made on 16 different materials, 11 of which were natural soil materials while the remaining 5 were crushed rock materials. For each material, experiments were performed for three or four packing densities. Specific weights were determined by (at) the Institute (Department) of Geology, NTH, for all but a couple of the materials. Quartz content was determined by (at) the same institute, using DTA equipment. In addition, particle size distribution curves were obtained for all materials.

The experimental results are given in Table I, along with calculated values for porosity, as well as specific weight and quartz content. Particle size distributions are shown in Figures 4, 5, 6 and 7. The symbols used for each material when plotting the following figures are also shown.

Figure 8 shows results for four natural soil materials, all having quartz contents in the range 48 to 53 percent. For these four materials one can expect the particle conductivities to be about the same, about 4.0 W/mK. For each material, the results follow a straight line in the log/log diagram rather closely. Variations from material to material are significantly larger than the varia-

TABLE I. VÄRMEFÖRÖRMÅNINGEN PÅ NÅRAN JORDARTER, ÅR 1900-1901. BERÄKNINGAR.

JORDART	KVADRATTMETER	AREAL I VÄRME	TEMPERATUR	BERÄKNING	BERÄKNING
Tyngt lera (slutvatten)	22	2750	1400 1510 1650	0,492 0,492 0,492	0,215 0,302 0,297
Kollo silt nu vatten	22	2800	1210 1350 1500 1620 1750	0,502 0,505 0,506 0,509 0,512	0,198 0,175 0,201 0,169 0,221
Klumpet					
Vormund silt	53	2690	1400 1480 1610 1710	0,480 0,486 0,491 0,494	0,149 0,156 0,200 0,222
Tyngt finsand	48	2600	1710 1790 1940	0,542 0,542 0,554	0,250 0,255 0,246
Jessheim finsand	49	2720	1810 1900 2020	0,495 0,492 0,505	0,174 0,198 0,246
Skander finsand	80	2670	1500 1600 1620	0,439 0,440 0,493	0,235 0,270 0,259
Heskorp finsand	58	2670	1580 1650 1740	0,408 0,481 0,490	0,214 0,238 0,259
Tiller sand	50	2700	1680 1910 1940	0,478 0,493 0,474	0,228 0,426 0,434
Tyngt fin grus	43	2650	1780 1840 1950	0,528 0,506 0,264	0,327 0,331 0,406
Östfold grus	39	2700	1920 1930 2010	0,526 0,509 0,256	0,348 0,367 0,431
Troms grus	10	2850	1870 1910 1980 2010	0,343 0,342 0,505 0,507	0,289 0,294 0,282 0,376

TABLE I.

TABLE I. THERMAL CONDUCTIVITY MEASUREMENTS ON DRY SOIL MATERIALS.
A. NATURAL SOIL MATERIALS.

Translation of terms:

JORDART	Soil material
KVARTSINN. %	Quartz content %
SPES. VEKT kg/m ³	Spec. weight kg/m ³
TORR R. VEKT	Dry density
POROSITET	Porosity
LEDN. EVNE W/mK	Conductivity W/mK
Tyholt leire	Tyholt ¹⁾ clay
(pulverisert)	(pulverized)
Follo silt	Follo ¹⁾ silt
pulverisert	pulverized
Klumpet	Lumps
Vormsun silt	Vormsund ¹⁾ silt
Tyholt finsand	Tyholt ¹⁾ fine sand
Jessheim	Jessheim ¹⁾
finsand	fine sand
Skandør	Skandør ¹⁾
finsand	fine sand
Boskorp	Boskorp ¹⁾
finsand	fine sand
Tiller sand	Tiller ¹⁾ sand
Tyholt	Tyholt ¹⁾
fin grus	fine gravel
Østfold	Østfold ¹⁾
grus	gravel
Troms grus	Troms ¹⁾ gravel

1) Locations where material samples were obtained (Translator's note)

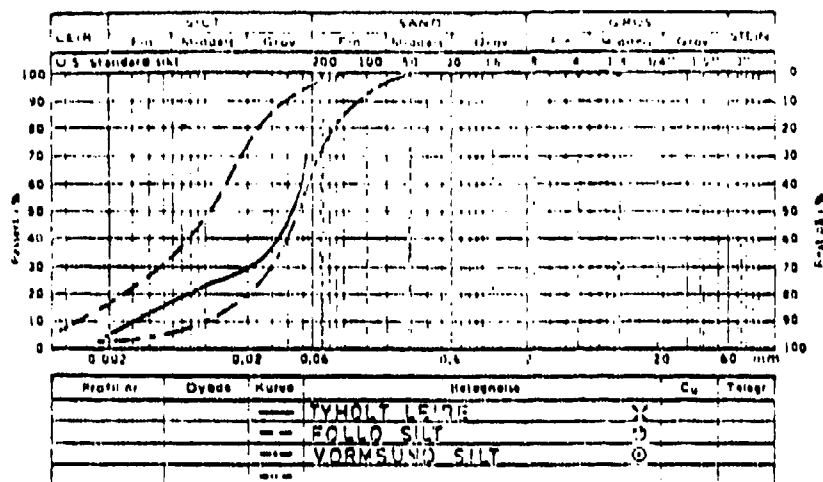
TABLE I. B. CRUSHED ROCK MATERIALS.

MATERIALE	Material
KVARTSINN. %	Quartz content %
SPEC. VEKT kg/m ³	Spec. weight %
TORR R. VEKT	Dry density
POROSITET	Porosity
LEDN. EVNE W/mK	Conductivity W/mK
Kunst kvarts	Crushed quartz
Knust glimmerskifer	Crushed mica shale
Knust grønnstein	Crushed greenstone ¹⁾
Oppland pukk	Oppland macadam ²⁾
Østfold pukk	Østfold macadam ²⁾

1) A mineral related to gabbro and diabase (Translator's note)

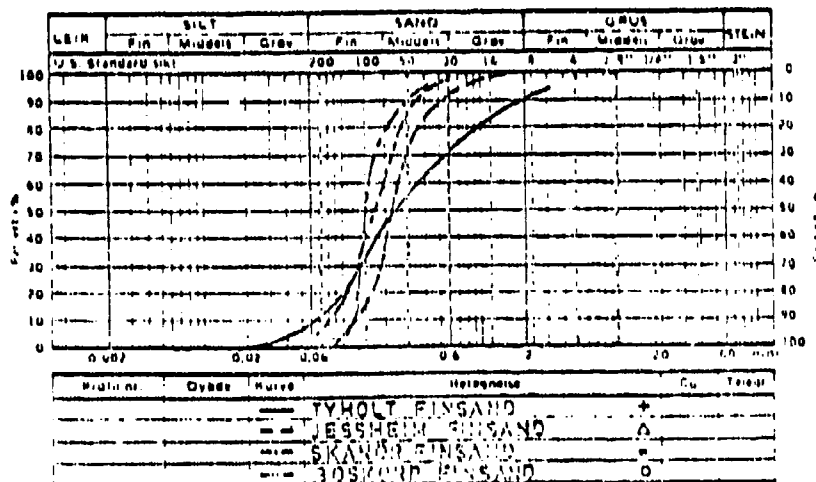
2) See note under Table I. A.

TABELL 1. B. KNUST DEGRUANTER					
MATERIALE	KVARTSINN. %	SPEC. VEKT kg/m ³	TORR R. VEKT	POROSITET	LEDN. EVNE W/mK
Kunst kvarts	100	2650	1660	0,374	0,529
			1720	0,385	0,517
			1810	0,317	0,426
			1900	0,281	0,549
Knust glimmerskifer	30	2650	1650	0,420	0,507
			1710	0,400	0,503
			1790	0,382	0,566
			1850	0,354	0,594
Knust grønnstein	3	2950	1720	0,417	0,523
			1780	0,397	0,523
			1830	0,360	0,516
			1950	0,338	0,442
Oppland pukk	2	2750	1630	0,407	0,534
			1750	0,349	0,527
			1820	0,338	0,534
Østfold pukk	31	2680	1730	0,354	0,567
			1820	0,321	0,465
			1900	0,291	0,525



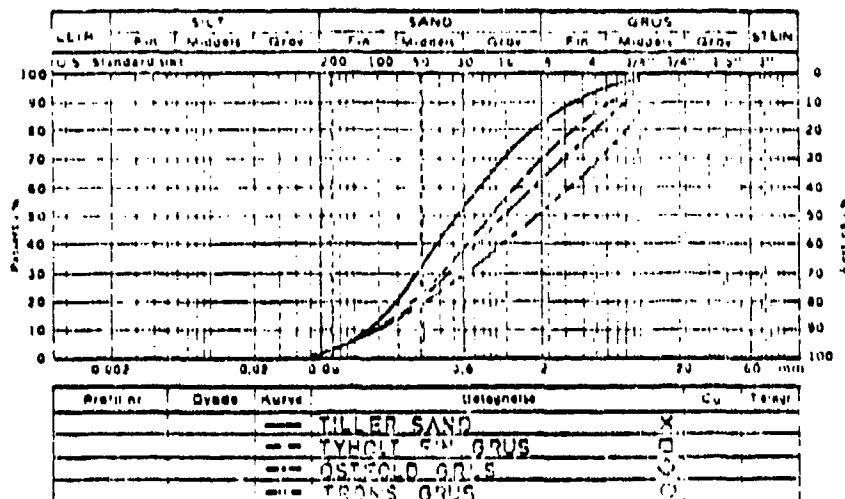
Skema nr. 427A

FIG. 4. Siktetkurver for tre finkornete jordarter fra undersøkelsen av tre materialers leiningsdybde. Grain size distributions of three fine grained soils from the investigation of conductivities of dry materials.



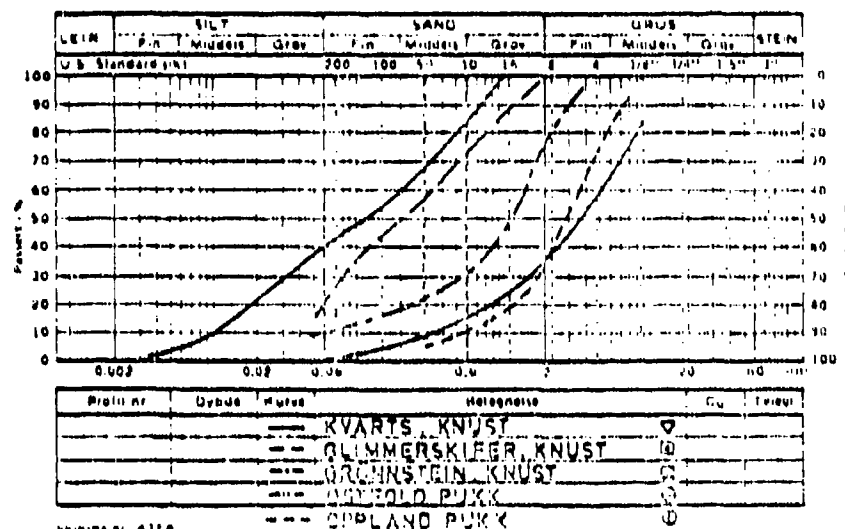
Skema nr. 427A

FIG. 5. Siktetkurver for fire finkornete fra 100 sand undersøkelsen. Grain size distributions of four fine sands from the same investigation.



Skjema nr. 437A

FIG. 6. Siktekurver for fire krusmaterialer fra samme undersøkelse. Grain size distributions of four granules from same investigation.



Skjema nr. 437A

FIG. 7. Siktekurver for fem knuste bergarter fra samme undersøkelse. Grain size distributions of five crushed rocks from same investigation.

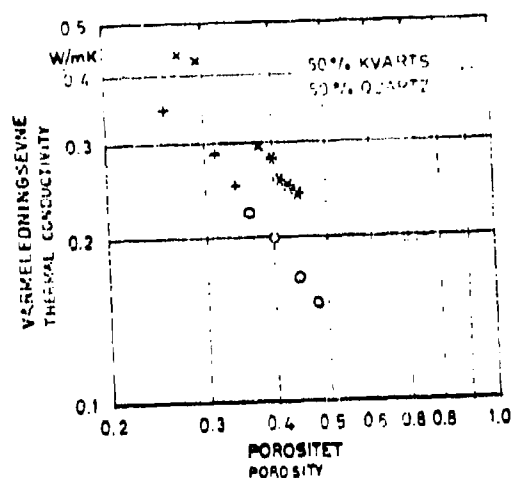


FIG. 8. Ledningsevnen av fire tørre jordarter med ca. 50% kvarts plottet som funksjon av porositeten. Conductivities of four dry soils with approximately 50% quartz in relation to porosity.

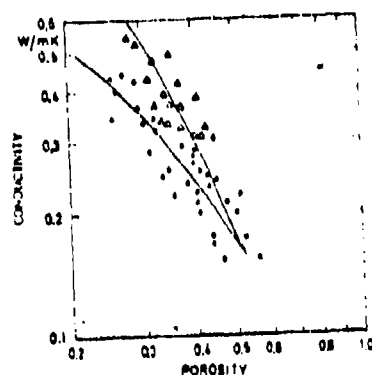


FIG. 9. Ledningsevnen av tørre jordarter og knuste bergarter plottet som funksjon av porositeten. Conductivities of dry soils and crushed rock in relation to porosity.
• Naturlige jordarter, Δ Knuste bergarter
Natural soils Crushed rock

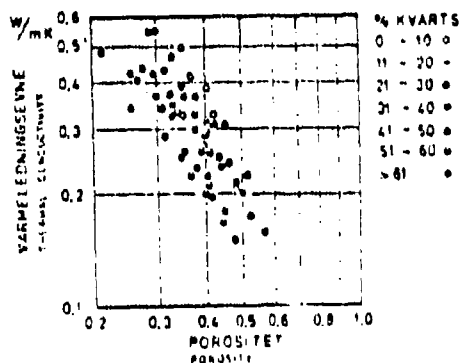


FIG. 10. Ledningsevnen av tørre materialer med kvartsinnhold antydte ved bruk av plottesymboler. Conductivities of dry materials with quartzcontent shown by use of different plotting points.

tions around these straight lines for each material.

Differences between conductivities in these materials, which here amount to about 20 percent around the mean curve, can mainly be ascribed to differences in microstructure. However, no direct relation seems to exist between particle size distribution and such differences in microstructure. The four soil materials in Figure 8 vary in mechanical composition from silt to single grain size fine sand and sand, without any traceable systematic variation in conductivity.

However, a comparison of results from natural soil materials and crushed rocks show a clear tendency towards higher conductivities for the crushed materials. This is made evident by Figure 9, where all test results are shown together, using different plotting symbols for crushed materials and natural soils.

The difference in particle form between crushed rocks and natural soil materials evidently results in systems with significantly different microstructures.

A more detailed scrutiny of individual results also show that differences in microstructure have a significantly larger effect on the (effective) conductivity than does the particle conductivity. Figure 10 shows results plotted with different symbols for different ranges of quartz content. These symbols are defined next to Figure 10. There is no obvious systematic variation of conductivity as the quartz content increases. In fact, the highest conductivity for a certain porosity is obtained for the material that has the lowest quartz content.

The low sensitivity to variations in particle conductivity makes it possible to represent the conductivity of dry materials by means of empirical relations containing only porosity as a variable. The effects of microstructure can be accounted for by distinguishing between two groups of materials, natural soils and crushed rocks.

As shown, the experiments give no basis for expecting variations within each of these groups due to differences in microstructure.

D. Empirical relations

Chapter II reviewed a number of empirical relations which could be fitted to measured results for dry soils by suitable choice of "form factors". Purely empirical correlations between conductivity and porosity could also be used. However, these empirical correlations should be consistent in the sense that they satisfy the physical bounds (limits) of conductivity for the material combination at hand:

$$\begin{array}{lll} \lambda = \lambda_1 & n = 1.0 & 1 \\ \lambda = \lambda_2 & n = 0.0 & \end{array}$$

On this basis it may be suitable to use as a starting point a semi-empirical equation which satisfies these conditions.

de Vries has used Maxwell-Fricke's equation to represent measured data for soil materials (9). This equation has the form

$$\frac{\lambda}{\lambda_1} = \frac{n}{n + (1-n) F} \cdot \frac{\lambda_1/\lambda_2}{F} \quad 2$$

The "form factor" F is given by

$$F = \frac{1}{3} \sum_{i=1}^3 \left[1 + \left(\frac{\lambda_i^2}{\lambda_1} - 1 \right) g_i \right]^{-1}, \quad i = 1, 2, 3$$

$$g_1 + g_2 + g_3 = 1.0$$

Values of the factors g_1 , g_2 and g_3 formally refer to definite geometric relations for ellipsoid-shaped particles. However, as mentioned in chapter II, the equation is based on approximations which make it impossible to derive these geometry related parameters from the particle shapes in an actual material. Thus, g_1 , g_2 and g_3 should in practice be regarded as parameters available for fitting to empirical data.

de Vries arrived at his set of these parameters by fitting (the equation) to measured values of diffusion in soil materials. This case, which corresponds to the particle conductivity being zero, results in a particularly simple form for the expressions for conductivity and form factor F .

Based on this, de Vries selected $g_1 = g_2 = 0.125$ and $g_3 = 0.750$. This gave good agreement for water saturated soils but values which are 25 percent too low for dry soil materials, according to de Vries. Also, the semiempirical nature of the equation does not give reasons to expect equally good fits over this wide range of conductivity variations.

Figure 11a shows results obtained from Maxwell-Fricke's equation, using the values for g_1 , g_2 and g_3 suggested by de Vries, together with experimental results for natural soil materials and crushed rocks. Curves are drawn for conductivity ratios of 100 and 200, respectively. Figure 11b shows curves for the same conductivity ratios but for $g_1 = g_2 = 0.10$, $g_3 = 0.80$, which results in a better fit to the experimental data.

The latter set of g -values are thus more representative for the conductivity of natural soils. If the conductivity ratio is set to 125, one obtains the following semiempirical expression for the conductivity of dry, natural soil materials.

$$\lambda / 0.024 = \frac{n + (1-n) 6.65}{n + (1-n) 0.053} \pm 20\%$$

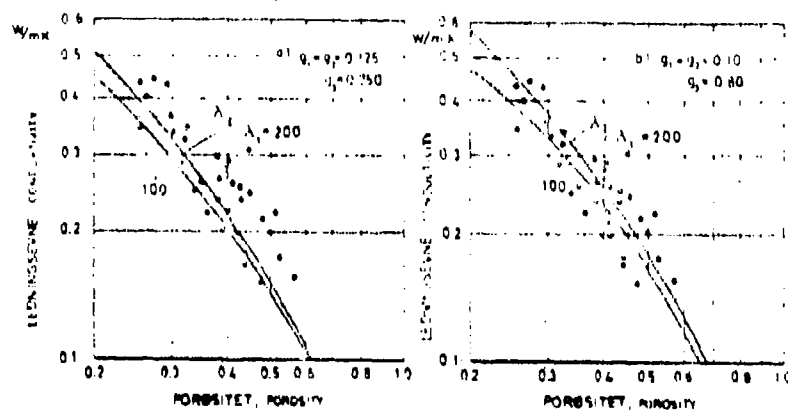


FIG. 11. Maxwell-Bridges lining sammenlikket med
liningsværdierne for tørre materialer.
Maxwell-Bridges equation compared to conductivity
measurements on dry materials.
a. $q_1 = q_2 = 0.75$; $q_3 = 0.750$. b. $q_1 = q_2 = 0.10$; $q_3 = 0.80$

As mentioned in chapter III, the specific weights of soil materials vary within relatively narrow limits (about $\pm 5\%$) around a mean of $\gamma_s = 2700 \text{ kg/m}^3$. If this mean value and dry density are used to compute porosity, this uncertainty will to some extent affect the error (confidence) limits for calculated conductivity, due to the relatively large uncertainty in the empirical relation. Eq 3 can thus be transformed to a function of dry density without significant change in the error limits. The semiempirical equation for conductivity of dry natural soil materials will then be of the form

$$\lambda = \frac{0.135}{2700} \gamma_d + \frac{64.7}{0.947 \gamma_d} \pm 20\% \quad 4$$

where γ_d is dry density expressed in kg/m^3 .

Figure 12 shows results from measurements on dry soil materials, compared with values computed from Eq 3. In addition to results obtained for Norwegian soil materials by the author, data measured by Smith on American soils are included. It is evident that most results fall within error limits of ± 20 percent.

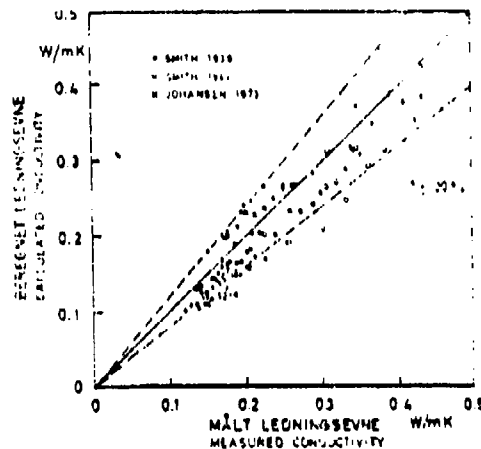


FIG. 12. Sammenlikning mellom beregnede ledningssevner etter likning 5 og målinger av varme lednings Jordartor. Comparison of conductivities calculated by equation 5 and measurements on dry natural soils.

For crushed materials it can be shown that a semiempirical equation of a different type gives a better fit to the rise in conductivity. Figure 13 shows a comparison between results obtained for crushed soil materials and Bruggeman's equation for (fill) materials having spherical particles. Data from this equation are shown for two conductivity ratios, $\lambda_2/\lambda_1 = 100$ and 200 . The conductivity is given by the following relation

$$n \left(\frac{\lambda}{\lambda_1} \right)^{\frac{1}{3}} = \frac{\lambda_2 - \lambda}{\lambda_2 - \lambda_1} \quad 5$$

One finds that this equation gives a relatively good fit to the experimental conductivity data for crushed dry materials, if a conductivity ratio of 125 is selected. However, due to the complicated structure of the equation it is more convenient to use a purely empirical relation for the mean curve. The following exponential function is found to give a good approximation to the conductivity in dry crushed rocks, within the porosity range considered

$$\lambda = 0.039 \cdot n^{-2.2} \pm 25\% \quad 6$$

However, this equation is not consistent (with all parameter values).. Thus, it should be regarded as an approximation to Bruggeman's equation (Eq 5) which meets the physical boundary conditions mentioned.

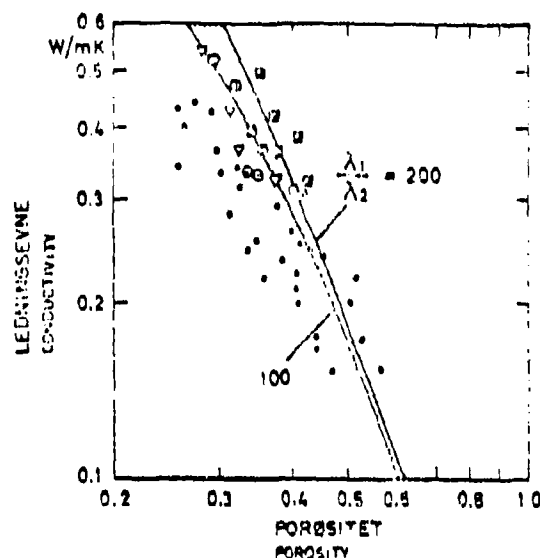


FIG. 15. Bruggemans' equation for calculating thermal conductivity of porous materials. Bruggemans' equation for porous materials compared to measurements on dry crushed rock.

E. Stabilized materials

van Rooyen and Winterkorn (1959) (8) and later Farouki (1966) (11) have published (results from) conductivity measurements on dried soil materials. For some materials, these results show much higher conductivities than even the highest values obtained at the Institute for Cold Technology. These measurements were performed with thermal conduction probes having significantly smaller diameters (about 1 mm) than those used in the previously described experiments (about 2 mm). The experiments were performed at various degrees of saturation and for different dry densities. Only the measurements performed in dry materials will be discussed here. For such materials, the small probe diameters used should not affect the results.

van Rooyen found exceptionally high (conductivity) values for materials with some-what special properties, where a certain amount of clay was mixed into otherwise sandy materials rich in quartz. These materials were used as fill around high voltage cables and high thermal conductivity was specified in order to prevent overheating even when high powers were transmitted. The materials were called "thermal sand". Figure 14 shows results obtained for these materials, along with (results from) van Rooyen's measurements on one type of quartz sand and crushed quartz, as well as measurements on crushed quartz performed at the Institute for Cold Technology.

As can be seen, van Rooyen's results for quartz sand and crushed quartz are close to the results for crushed quartz described earlier, while his results for the two special materials show significantly higher conductivities. Of these materials, "thermal sand I" had the largest clay content (6.0 percent particles $< 5 \mu\text{m}$), while "thermal sand II" contained 3.2 percent clay. Particle size distributions for these two materials are shown in Figure 15.

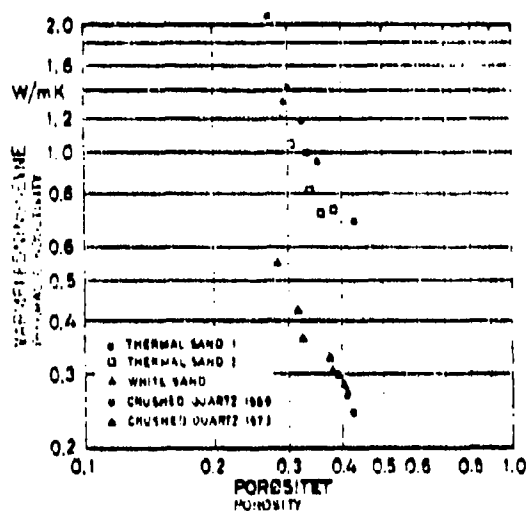


FIG. 14. Ledningsverdi for "thermal sand" sammenliknet med målinger på kvartssand og knust kvart. Conductivities of thermal sand compared to measurements on quartz-sand and crushed quartz.

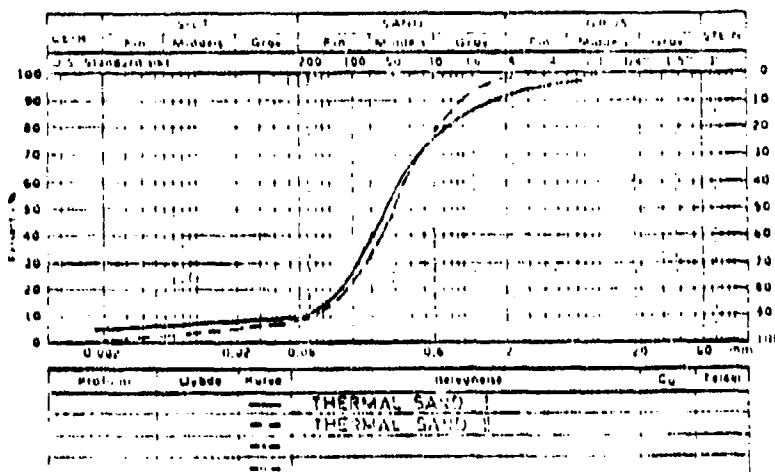


FIG. 15. Kornfordelingskurver for to "thermal sands".
Grain size distribution for two thermal sands.
(van Rooyen 1959 (11))

van Rooyen also investigated the effect of adding kaoline clay to sand containing 94 percent quartz and having one single particle size. For this mixture, the conductivity of dry material increased significantly when the clay content increased. The conductivity increased from 0.54 W/mK for 1 percent kaolinite to 0.82 W/mK for 3 percent kaolinite, while for 10 percent kaolinite added the measured conductivity was as high as 1.15 W/mK. Dry density is not given.

Farouki (1966) has also investigated the effect of various additions of kaolinite clay to sands with high quartz content (11). Also in his case, the thermal conductivity was measured by means of thermal conduction probes, for various densities and water content. The results for dry materials with a density of 2100 kg/m^3 showed a maximum conductivity for a kaolinite content of about 3 percent, while the conductivity decreased for further increase of the kaolinite content. This maximum value was measured to be as high as 2.5 W/mK for a dry density of 2100 kg/m^3 , while the conductivity was found to be 1.0 W/mK for the same density but with no kaolinite added.

In all these cases, the conductivity was determined for materials which were dried after kaolinite was added. Farouki also reports one test performed on a dry material into which dry kaolinite was mixed. This mixture showed a significantly lower conductivity than the corresponding materials which were mixed under wet conditions and subsequently dried. Measured values for a dry density of 2100 kg/m^3 were 1.25 and 2.5 W/mK, respectively.

These results indicate that the extreme (unusually high) values of conductivity found in dried samples containing kaolinite are due to microstructural conditions.

If one assumes that the clay particles initially are in suspension within the pore water in saturated samples, it is possible that these particles concentrate near the points of contact between sand particles during the gradual drying process. The plate-shaped clay particles would then form efficient "thermal bridges" between the larger (coarser) particles, as indicated by Figure 16.

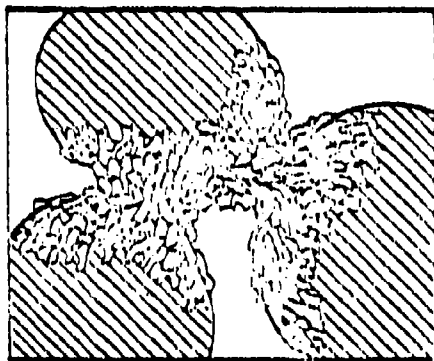


FIG. 16. Skisse av mikrostrukturen i tørket sand med tilsetning av noe leire. Sketch of microstructure in dried sand mixed with small amounts of clay.

Barden(1973) has recently showed, by means of electron microscopy, that such clay bridges exist in dried samples of soil materials having relatively low clay contents (14). When dry components are mixed, the microstructure would obviously be different, with a more

random distribution of clay particles. The occurrence of an optimum¹⁾ clay content can possibly be explained by assuming that increase of the clay content above a certain limit will result in the sand particles becoming separated by "cushions" of clay particles. This hypothesis is supported by "packing" experiments performed by van Rooyen on samples with different clay contents. When the latter increased beyond 8 percent, the densities decreased continuously for the entire sample (mixture) and thus also for the entire "sand skeleton"²⁾. Up to that limit, the density of the entire mixture increased, while dry density based on the sand alone was nearly constant. In this range one can thus assume that the sand skeleton is independent of the added clay, since the clay particles are deposited in the pores. When the clay content exceeds 8 percent, the clay disturbs the sand skeleton and separates the sand particles from each other.

In natural loose deposits with a more even particle distribution, no similar concentration of clay particles can be expected, at least no to the same degree. However, different additives used to stabilize road building materials, etc (lime, cement) can possibly cause effects on the thermal conductivity for low levels of saturation similar to those shown to occur when kaolinite is added (to sand).

F. Conclusion

To summarize, this investigation of measured conductivity data for clay soil materials shows that differences in microstructure indeed gives large variations in conductivity for such soils, as was indicated already in the introductory discussion. This is particularly evident in Figure 17, where the results given in Figure 14 are plotted in normalized form between the Hashin-Shtrikman limits for materials having particle conductivities corresponding

1) One that gives maximum conductivity.

2) The sand particles are separated further from each other by the clay "cushions" (Translator's notes).

to the minerals with high quartz content for which the measurements were made.

Based on these results and previously described measurements, a range of expected values is also indicated (in Figure 17) for the conductivity of dry soil materials. Even if this range is a small portion of the (region between the) Hashin-Shtrikman limits, this still implies a considerable variation in conductivity for a given porosity. However, if one neglects rather specialized materials of the type "thermal sand", the expected variations will be much smaller. The "center of gravity" falls some-where between the lower boundary of the bounded region and the points representing measured data for crushed quartz and quartz sand. It was shown earlier that the "center of gravity" for natural soil materials can be represented by an empirical relation between porosity and conductivity, within error (confidence) limits of about ± 20 percent (see Eq 3). A similar equation was found to represent results for dry, crushed rocks, with about the same error limits (see Eq 6). In keeping with the introductory discussion, particle conductivity variations can be neglected in both relations.

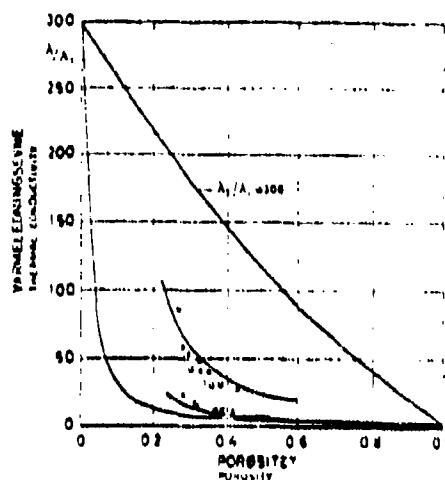


FIG. 17. Leiningseviene av tette jordarter med forskjellig tekstur sammenliknet med Hashin-Shtrikman grensene. Conductivities of dry soils with different textures compared to the Hashin-Shtrikman bounds.

2. SATURATED MINERAL SOIL MATERIALS

A. Introduction

A saturated soil material can be assumed to consist of two or three components, represented by mineral particles, water and/or ice. However, the mineralogic composition can vary considerably from particle to particle and is often related to particle size. This distribution of minerals among particles can be accounted for by an apparent particle conductivity which mainly depends on the average mineral composition in the soil material. In addition, a possible interdependence between mineral content (composition) and particle form/size may affect the apparent particle conductivity between soil generating minerals indicates that such microstructural conditions will be of minor importance.

The previously described Hashin-Shtrikman limits for a system of mineral particles, ice and water will give a rather narrow range of variations for the conductivity. Figure 18 shows these limits for a hypothetical, saturated clay material with varying relative content of frozen water. This example is valid for a porosity of 50 percent and a particle conductivity of 3 W/mK.

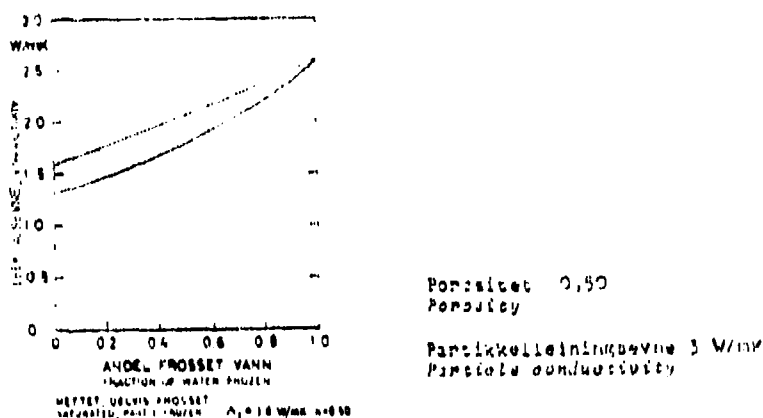


FIG. 18. Hashin-Shtrikman grenser for en vannmettet jordart ved varierende andeler froset vann. Hashin-Shtrikman limits for a water saturated soil with different ratios of water frozen.

Evidently, the limits are particularly narrow when the material is completely saturated by ice, but also for water saturated materials the limits form a basis for relatively accurate estimates of the conductivity, without regard for differences in microstructure.

In chapter II, results were also presented which indicate that the geometric mean of component conductivities, calculated on the basis of the relative volume for each component, will give a good approximation to the conductivity in such materials. As shown in the figure¹⁾ values calculated from this model fall within the Hashin-Shtrikman limits over the entire range considered. The validity of this model will be discussed in the following, based on results from experimental investigations of conductivities in saturated soil materials.

B. Measurements performed by Kersten

Kersten did not perform measurements on completely saturated samples. However, based on three or four measurements for a given density he extrapolated data for full saturation. (Pages 185 to 193 in Kersten's report from 1949 (7).) These extrapolated results are used in the following study of conductivity in saturated soil materials.

Figure 19 shows these extrapolated values for saturated materials, plotted as function of relative particle volume. In this semilogarithmic diagram, the previously mentioned geometric mean equation gives a straight line between the conductivity of water for zero relative particle volume and the particle conductivity when the relative particle volume is unity, as indicated by the thin lines in the figure.

1) The original does not specify which figure is referred to here. It could be one on chapter II. (Translator's note)

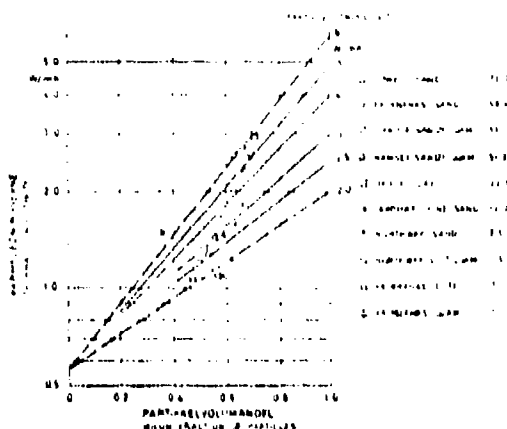


FIG. 19. Løsningsveier av partikkel-ufroset jordarter plottet som funksjon av partikkelvolumandel. Conductivities of saturated unfrozen soils in relation to volume fraction of particles. (Kersten 1949 (7))

Next to Figure 19, the soil materials concerned are listed according to decreasing quartz content, with the symbols used in the figure. By comparing the plotted data and the table one finds that, with few exceptions, the conductivities are grouped according to increasing quartz content.

In chapter IV it was proposed to use a geometric mean equation of the following form to estimate particle conductivity on the basis of quartz content in a soil material.

$$\lambda_2 = 2.0^{1-q} 7.7^q \text{ W/mK} \quad 7$$

where q is the quartz content.

When the particle conductivity is known, one may also expect that the conductivity of a saturated soil material can be estimated from the geometric mean:

$$\lambda = \lambda_1^n \cdot \lambda_2^{1-n} \text{ (W/mK)} \quad 8$$

where n is porosity

$1-n$ is relative particle volume

λ_1 is conductivity of water (ice) (W/mK)

λ_2 is particle conductivity (W/mK)

Figure 20 shows a comparison between the conductivities extrapolated by Kersten for saturated soil materials at 4°C and values calculated from Eqs 7 and 8, for the values of relative particle volume and quartz content given by Kersten.

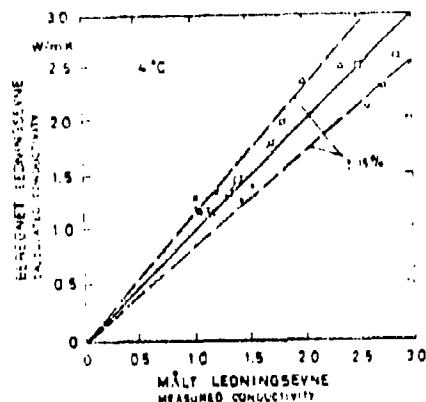


FIG. 20. Sammenlikning mellom beregnet leiningsevner etter geometrisk middel metode (likn. 7 og 8) og Kerstens målinger av ufrosne jordarter. Conductivities calculated by the geometric mean model (equation 7 and 8) compared to Kerstens measurements on unfrozen soils.

As can be seen, the calculated values fall largely inside error limits of between 15 and 20 percent of measured values. These error limits contain both the measurement uncertainties and the uncertainty of the mathematical model used.

Corresponding comparisons between measured and calculated values for saturated, frozen soil materials will be distorted due to the uncertainty in regards to the content of un-frozen water. However, for coarse soil materials containing no finer fractions than sand, one can assume that all the water is frozen. For the four soil materials studied by Kersten, which meet this requirement, one obtains a difference of less than 10 percent between calculated values and these extrapolated to full saturation by Kersten.

C. Ocean sediments

The effects of different quartz contents on the conductivity of saturated materials was also pointed out by Kasameyer et.al. (1972), in connection with studies of thermal conductivity of ocean sediments in the North Atlantic (15). Samples were taken from the ocean floor by a research ship when crossing the North Atlantic. All these experiments were performed with a thermal conduction probe, partly on board the ship and partly in a laboratory.

Earlier investigations of thermal conductivity in ocean sediments have resulted in rather stable values which mainly vary with water content in the samples (Ratcliffe 1960 (16)). Similar values were found during this investigation in the eastern and central parts of the region covered, while measurements from the western part showed significantly wider variations. A few samples gave thermal conductivities more than twice as high as for normal ocean sediments. The authors refer to geological surveys in the West Atlantic which revealed thick deposits of quartz sand and silt with high quartz content also in particles smaller than 2 μ m.

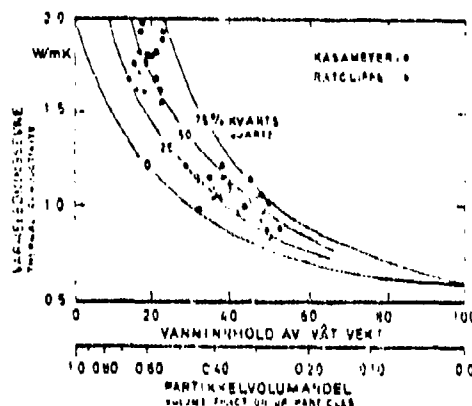


FIG. 21. Leiningenevnen av havsollimenter plottet som funksjon av våt prosent. Teoretiske kurver for forskjellige kvantinnhold er tegnet inn til sammenligning. Conductivities of ocean sediments in relation to wet density. Theoretical curves for different quartz-contents given for comparison. (16, 18)

Figure 21 shows results obtained by Kasameyer with samples from the region mentioned, plotted versus water content relative to wet weight. Since these samples were saturated, the results also give an indication of how tightly packed the sediments were. If specific weights for the mineral particles are known, dry density can be derived from this parameter by means of the relation

$$\frac{\gamma_d}{\gamma_s} = \frac{\gamma_w (1 - w_w)}{\gamma_w (1 - w_w) + \gamma_s w_w}$$

9

where w_w is relative water content by wet weight
 γ_s, γ_w are specific weights for mineral particles
 and water, respectively
 γ_d is dry density

For comparison, results from "normal" ocean sediments in the Atlantic are included in Figure 21 (Ratcliffe 1960). Theoretical curves for the conductivities in materials with quartz contents from 0 to 75 percent are also shown. The latter were derived from the previously used mathematical model for particle conductivity and conductivity in saturated materials (geometric mean equation). The volume ratios¹⁾ are based on the relation between dry density and relative water content by wet weight, given above (Eq 9), with specific weight for the mineral particles assumed to be 2700 kg/m³.

As can be seen (from Figure 21), points representing "normal" sediments fall close to the curve for 25 percent quartz, while the data obtained from the western region are grouped between the curves for 25 and 75 percent quartz and show a much wider spread. The authors give no quantitative values for the quartz content in these sediments, but in view of the qualitative descriptions of the materials as being sand or silt rich in quartz, the indicated values are not improbable.

D. Conclusion

The analysis performed of thermal conductivity measurements on saturated soil materials show that differences in mineral composition have significant effects on the conductivity. Comparisons between experimental values and calculations based on known quartz content, as well as volumetric composition, show that the proposed mathematical model for determining conductivity on saturated soil materials give satisfactory agreement.

1) "Forhol" could here also mean "conditions" (Translator's note).

However, this mathematical model should also be compared against experimental data from a representative selection of Norwegian soil materials. To this end, measurements have been initiated by the Institute for Cold Technology, which will cover a wide variety of soil materials. This research program includes measurements for varying degrees of saturation (as well as dry materials) as will be described in the next section.

3. MOIST MINERAL SOILS

A. Introduction

A partially saturated material can be assumed to consist of three or four components, particles, ice and/or water and air. For such a system, the Hashin-Shtrikman limits will enclose a relatively large region within which the conductivity may vary. This is illustrated by Figure 22, where the limits are calculated versus degree of saturation in a hypothetical sand material with a porosity of 0.30 and a particle conductivity of 4 W/mK.

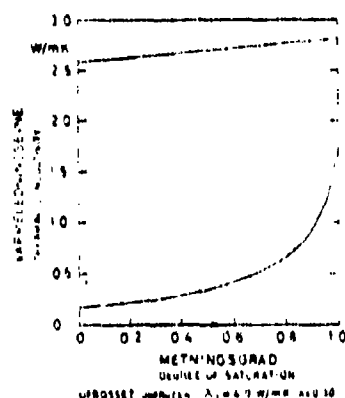


FIG. 22. Hashin-Shtrikman bounds for unproven sand in relation to degree of saturation.

Porositet 0,30
Porosity

Partikkelledningsdygtighet 4 W/mK
Particle conductivity

As mentioned previously, the wide separation between the limits is due to high sensitivity of the conductivity to variations in microstructure. Since this effect can not be incorporated into analytical models for conductivity calculation, due to the complicated geometry within natural soil materials, one must here resort to purely empirical methods for describing the conductivity dependence on the degree of saturation.

The mathematical models proposed in the previous section make it possible to determine the conductivity for two extremes in the degree of saturation, corresponding to values for completely dry and completely saturated materials. For partially saturated materials the conductivity will fall between these extreme values.

This condition forms a basis for defining a normalized conductivity, which permits results from different materials to be presented in a uniform manner. This normalized conductivity is here given the notation "Kersten's number, K_e ":

$$K_e = \frac{\lambda - \lambda^0}{\lambda^1 - \lambda^2} \quad 10$$

λ is measured conductivity for a given combination of density and degree of saturation

λ^0 and λ^1 are conductivities for dry and saturated material, respectively, for the same density

With this representation, the conductivity of dry material will give $K_e = 0$, while the conductivity of saturated materials gives $K_e = 1$. For other degrees of saturation one obtains values for K_e between these limits. This representation is particularly suitable for experimental results which pertain to a wide range of saturation levels for the same degree of packing. Values for dry or saturated materials can then possibly be determined by extrapolation.

B. Study by Kersten

As mentioned earlier, the thermal conductivity experiments performed by Kersten on soil materials from the permafrost region in Alaska remain the most extensive study of its kind. Measurements were performed on a total of 19 different materials. Measured results for the ten natural soil materials which were studied in most detail, with respect to variations in degree of saturation and density, will be treated in the following. The mechanical and mineralogical compositions of these materials are listed in Table II of this chapter. Plotting symbols used are shown in the same table.

Each of these soil materials was subjected to thermal conductivity measurements at three or four different water contents for two or three different densities. Conductivities were measured for at least four different temperature levels, two above and two below the freezing point.

Results obtained at $+4^{\circ}\text{C}$ and -4°C will primarily be discussed in the following.

Figure 23 shows results obtained by Kersten at $+4^{\circ}\text{C}$ for two soil materials, plotted on the previously mentioned normalized form (Eq 10). Different densities are indicated by means of marks on the plotting symbols. As can be seen, the results for each soil material show nearly the same functional dependence, independent of dry density, while the difference between the two soils is significant.

One of these soil materials has relatively coarse particles while the other is a fine grain material containing a total of 90 percent of silt and clay fractions. This would indicate that this kind of representation also may be used for studying the effects of different textures on the conductivity of moist soils.

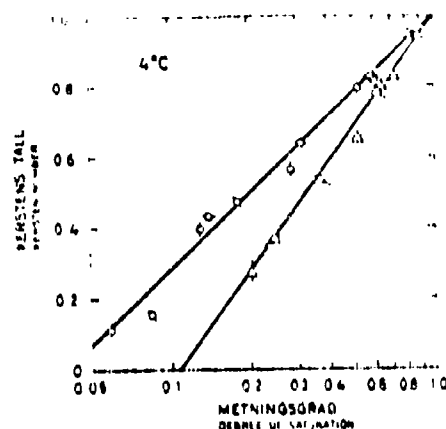
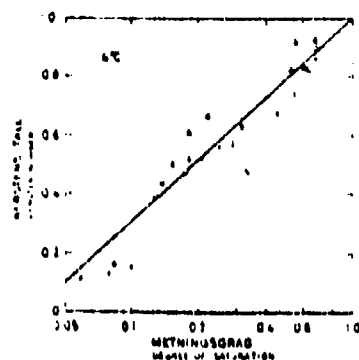
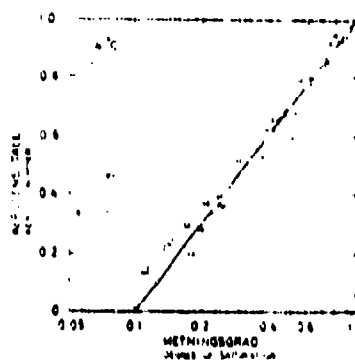


FIG. 23. Kerstens målinger på to ufrosne jordarter plottet på normalisert form som funksjon av metningsgraden. Kersten's measurement on two unfrozen soils plotted in dimensionless representation in relation to degree of saturation.

Figure 24 shows results from Kersten's measurements on ten natural soil materials at $+4^{\circ}\text{C}$, plotted in the same normalized form as before. Results obtained for the coarser materials (no silt or clay fractions) are shown in Figure 24a, while results for the fine grain soils are given in Figure 24b. One finds that soils having a certain content of silt and clay give data points which fall lower in the diagram than points representing soil materials lacking these fraction.



a. Grovkornete jordarter.
Coarse grained soils



b. Finkornete jordarter.
Fine grained soils

FIG. 24. Kerstens målinger på ufrosne jordarter plottet på normalisert form. Kerstens measurements on unfrozen soils plotted in dimensionless representation.

For the first group - fine grain materials - the spread is relatively small around a mean curve given by

$$K_e \approx \log S_r + 1.0 \quad 11$$

$$S_r > 0.1$$

For the coarse materials, the spread is somewhat larger around a mean curve given by

$$K_e \approx 0.7 \log S_r + 1.0 \quad 12$$

$$S_r > 0.05$$

Kersten's results for frozen materials at -4°C are shown in Figure 25, using the same normalization as before but with a linear scale for the degree of saturation.

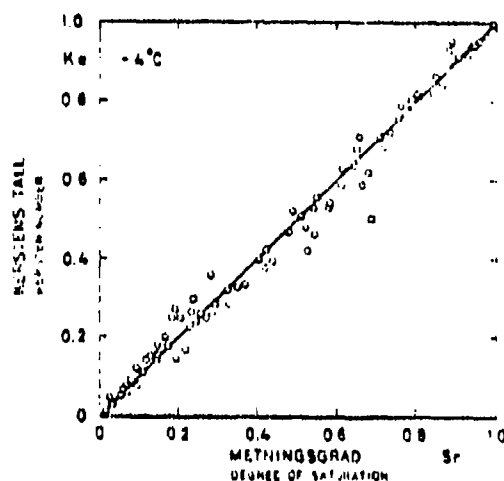


FIG. 25. Kersten's findings of frozen materials plotted in normalized form. Kersten's measurements on frozen soils plotted in dimensional representation.

As evident from Figure 25, all the results fall near a common mean curve (line), regardless of the previously used separation according to texture. The mean can be represented by the simple relation

$$K_e = S_r$$

13

with a variation somewhat less than $\pm K_e = 0.1$. This simple relation follows directly from the nearly linear relation between conductivity and degree of saturation shown by Kersten's data from measurements on frozen soils.

The previous analysis of Kersten's experimental results was limited to data obtained at two temperature levels, $+4^\circ\text{C}$ and -4°C . The conductivities of soil components are to some extent dependent on temperature. While the conductivities of water and air increase for increasing temperature, the conductivities of mineral particles and ice will decrease. As discussed in chapter I and II, the effect of water vapor diffusion on the apparent conductivity in the pore air will contribute to an increasing thermal conductivity with increasing temperature for moderate (mid-range) degrees of saturation.

Figure 26 compares results obtained by Kersten at two temperature levels above the freezing point and for varying degrees of saturation. Data for coarse and fine grain materials are shown with different plotting symbols.

A clear tendency can be seen for the largest increase in conductivity to occur for moderate degrees of saturation. This region appears to fall at some-what higher degrees of saturation for fine grain than for coarse materials. For very low or very high saturation levels, the differences between conductivities at the two temperatures are insignificant. Even at mid-range, the difference seldom exceeds 10 percent of the value obtained at $+4^\circ\text{C}$.

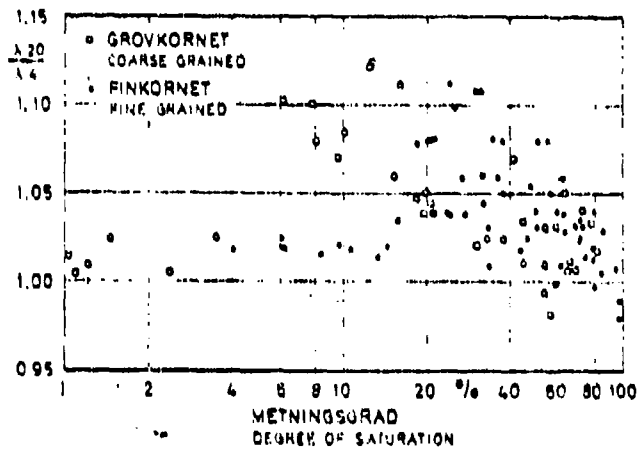


FIG. 26. Innflytelse av temperaturen på ledningssevnen av
 utvorne jordarter, Kjerfoss prøvestation.
 Influence of temperature on conductivity of uniform
 soils. Kjerfoss results.

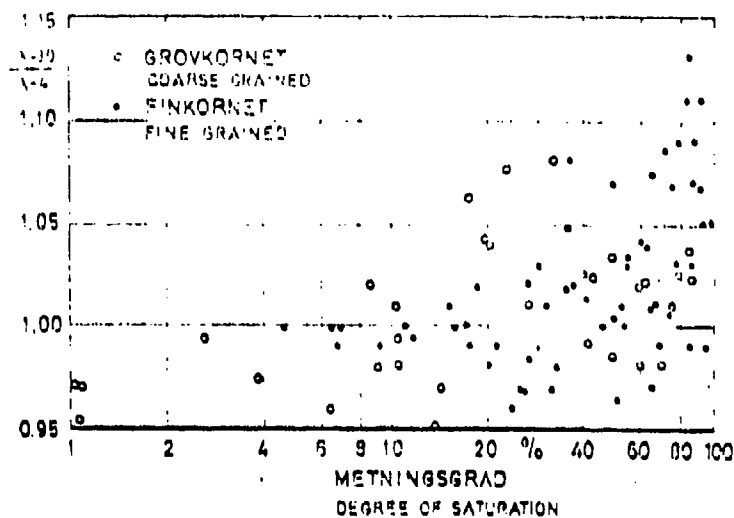


FIG. 27. Influence of temperature of thawing on the conductivity of frozen soils. Results of Korsten's experiments. Influence of temperature on conductivity of frozen soils. Korsten's results.

Figure 27 shows a similar comparison of results obtained at two temperature levels below the normal freezing point. Also here, data for coarse and fine grain materials are shown separately.

Also in this case there seems to be different trends for the two groups of materials. However, the decreasing conductivity of air with decreasing temperature seems to be the dominant factor at low and moderate degrees of saturation. For higher degrees of saturation, the increasing conductivities of mineral particles and ice with decreasing temperatures become more and more important. In the fine grain materials, the latter effect is amplified by the fact that the relative content of un-frozen water decreases both with decreasing temperature and increasing degree of saturation. For the lowest degrees of saturation, all the water may be frozen at both temperature levels at hand. For higher degrees of saturation, a significantly larger portion of the water will be frozen at the lower temperature (-30°C) than at the higher (-4°C), which contributes to an increase in conductivity with falling temperatures. Also in this case one finds that the increase in conductivity seldom exceeds 10 percent of the value at -4°C .

Tabell II. Kerkens forsøksmateriale

Table II. Description of soils tested by M.S. Kerkens (1939)

Sym. Betegnelse bølge	Kornfordeling (vekt%)					Mineralogisk sammensetning (vekt%)				
	Grus ≥2.0 mm	Sand 0.05-2.0	Silt 0.005-0.05	Leir ≤0.005	Spes. vekt γ_{sp}^*	Kvarts	Felt- spat	Glim- mer	Pyroxen, amfibol og olivin	Leir- mineraler
○ Fairbanks sand	27.5	70.0	2.5	—	2.72	50.4	9.9	0.1	8.0	—
△ Lowell sand	9.0	100.0	0.0	0.0	2.67	72.2	20.5	1.3	3.0	—
× Northway sand	3.0	97.0	0.0	0.0	2.74	7.5	9.0	—	7.5	—
• Northway fin sand	0.0	97.0	3.0	0.0	2.70	12.0	18.0	—	12.0	—
□ Dakota sandholding mo	10.9	87.9	21.2	10.0	2.71	60.1	13.0	—	12.1	12.4
◻ Harney sandholding mo	0.4	93.6	27.5	18.5	2.68	61.3	17.4	—	11.6	15.9
○ Northway siltholding mo	1.0	21.0	64.4	13.0	2.70	1.5	31.5	—	10.5	27.5
△ Fairbanks siltholding mo	0.0	7.0	90.9	11.5	2.70	53.6	—	18.1	—	28.3
☆ Fairbanks siltholding leirig mo	0.0	9.2	43.8	27.0	2.71	64.1	—	3.2	2.2	28.9
○ Heavy leir	0.0	1.0	20.1	79.0	2.69	22.5	—	—	—	65.0

Legend for Table II

Symboler

Plotting symbols

Betegnelser

Notation

Kornfordeling

Particle size distribution

vekt%

Percent by weight

Spec. vikt. t/m^3

Specific weight, metric tons
(1000 kg)/ m^3

Sammansetning

Composition

Sandholding, siltholding

Contains sand, silt

mo

Common name for fine grain soils

leirig

Contains clay

Grus

Gravel

Leir

Clay

Kvarts

Quartz

Feltspat

Feldspar

Glimmer

Mica

Pyroxen

Pyroxene

amfibol

Amphibolite

Olivin

Olivine

Leir mineraler

Clay minerals

C. Investigation of Norwegian soil materials.

A. Watzinger and E. Kindem (5) performed a series of thermal conductivity measurements on a limited selection of Norwegian soil materials in 1936/37. These measurements were made in a planar horizontal test unit with the cold plate above and the warm plate below the samples. Temperature differences across samples were measured by means of thermocouples attached to both plates. The mineral composition of the materials was not determined but screening curves are available for all mineral soil materials. Lack of information about mineral composition and variations in degree of packing from one experiment to another makes it difficult to analyze the results.

Efforts to extrapolate these results to fully saturated conditions indicate that all the investigated soils have particle conductivities in the 2.0 to 3.0 W/mK range (largest value for a sand material lowest for clay and kvabbj^{ord}). According to the proposed method for estimating particle conductivity, this corresponds to quartz contents from 0 to 30 percent. The selected materials are thus not very representative for the variations in quartz content that are found in Norwegian loose deposits.

Against this background, the need for an extensive investigation of thermal conductivities in Norwegian soils is quite obvious. As mentioned earlier, such an investigation has begun at the Institute for Cold Technology. The plan for this study calls for investigating a total of 45 Norwegian soil materials, as well as a small number of foreign soils (all together 4). The material library is described in Table III (quartz content) and Figure 8 (mechanical composition).

*kvabbj^{ord} = translation unknown.

Table III. Summary of quartz content in the mineral library at the Institute for Cold Technology

SOIL MATERIAL	NUMBER OF SAMPLES	RANGE OF QUARTZ CONTENT, PERCENT	AVERAGE QUARTZ CONTENT, PERCENT
CLAY	7	10 - 28	18.8
SILT	6	21 - 53	33.5
SAND	13	10 - 100	44.9
GRAVEL	13	2 - 57	38.8
MACADAM	10	2 - 53	12.7
TOTALS	49	2 - 100	

The mechanical compositions of all samples, except macadam, are shown in Figure 28 in the form of an Md - So diagram¹⁾, where each material²⁾ is indicated by a different plotting symbol. The numbers correspond to those used in the material library.

As shown by Figure 28, the selected soil samples cover marine sediments and glacial flow materials rather well, while moraine clays and moraine gravels (not separated into layers) are poorly represented. In terms of quartz content, the range of interest seems to be well covered for all types of soil, perhaps with the exception of quartz-poor loose deposits from regions characterized by special petrographical conditions. However, the macadams include a relatively large selection of materials with low quartz content.

According to the plan, thermal conductivity measurements on these materials will be performed in a parallel fashion in several types of test units (planar, probe and sinusoidal variation) at degrees of saturation ranging from completely dry to fully saturated. However, for the coarsest materials it is planned to measure conductivity only for water contents occurring after run-off, in addition

1) Refers to particle size distributions, see Figure 28.

2) Grus = gravel, Leire = clay (Translator's notes).

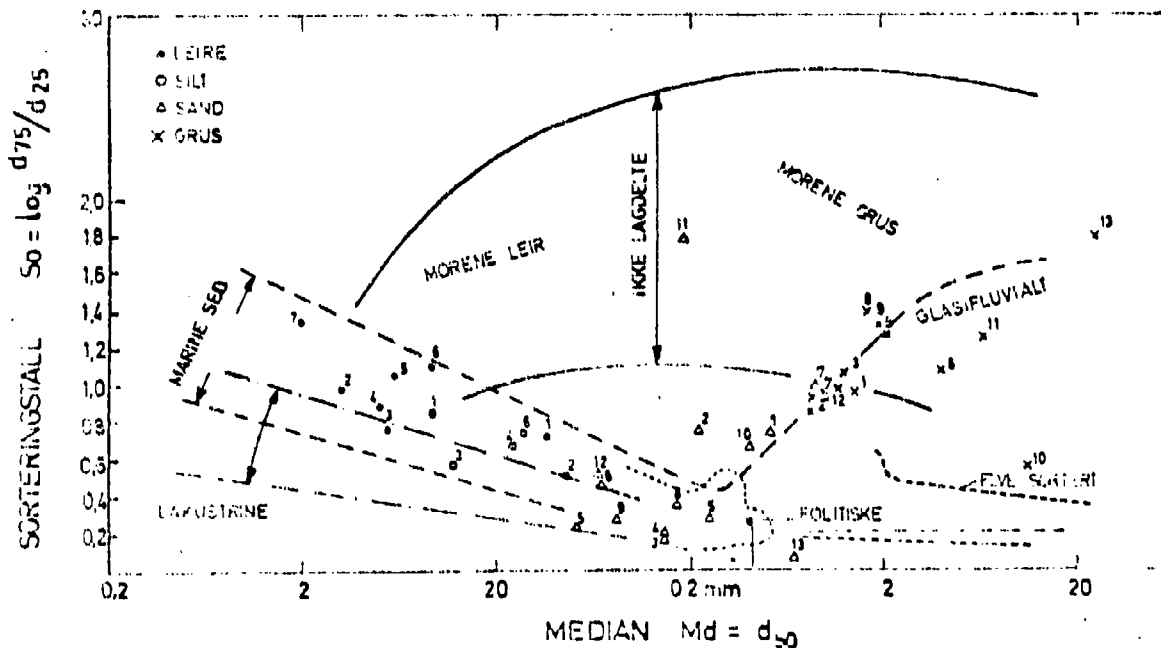


FIG. 28. Mekanisk sammensetning av jordmaterialer fra materialbiblioteket ved Institutt for Kjøleteknikk, NTH. Materialene er nummerert i henhold til materialbiblioteket.
 Mechanical composition of soils from the soil-library at Dept. of Refrigeration Engineering, Univ. of Trondheim. Medians according to the soil-library.

to experiments with dry and saturated samples.

These experiments, which according to plan will be completed at the end of 1975, will give a very valuable data base for evaluating the mathematical models described in this report.

D. Conclusion

The empirical relations derived for dry materials, the proposed mathematical model for saturated materials and the empirical relation developed here between the normalized conductivity (Kersten's number) and the degree of saturation together form a new base for calculating the conductivity of moist and frozen mineral soil materials. From the definition of Kersten's number one can compute the conductivity for a given combination of density and degree of saturation from

$$\lambda = \lambda^0 + K_e (S_r) (\lambda^1 - \lambda^0)$$

14

Conductivities for completely dry and fully saturated materials having certain densities can be computed from the empirical relations for dry materials and the mathematical model for saturated materials, respectively. The functional dependence $K_e (S_r)$ is given by one of the three empirical equations derived previously. The uncertainty inherent in this method depends, among other things, on how accurately the properties of the material at hand are known. These aspects will be treated in more detail in next chapter (VI), where also other available methods for calculating conductivity of soil materials will be discussed.

4. SOIL MATERIALS CONTAINING HUMUS

A. Introduction

Previous discussions have been limited to purely mineral-based soil materials. This section will discuss soils containing humus. The humus content is in geotechnical literature given in terms of glow loss. It is then assumed that organic materials are completely burned when heated to a state of glowing, while mineral-based materials have no glow loss. On this basis, the glow loss is a measure of the relative mineral and organic content in a soil material. These matters were discussed in more detail in the section on volumetric conditions in chapter III.

Materials having glow losses between 1 and 6 percent are usually classified as humus carrying, while materials with glow losses in the 6 to 30 percent range are described with terms such as clay-bound peat. Glow losses larger than 30 percent warrant the notation "peat". However, in the latter class of materials the mineral content may constitute up to 50 percent of the dry volume.

Few systematic measurements have been made on such mixed materials. Smith (1939) presented results from different typical ground profiles, where samples containing considerable amounts of organic material are included (3). However, the information concerning these materials is incomplete and the measurements were not reliable due to considerable re-distribution of moisture during the experiments.

On the other hand, certain reliable results are available for purely organic materials such as pure peat and bog. These will be discussed in the following.

Watzinger claims that the thermal conductivity of organic components is 0.46 W/mK (5). The same value was used by Missenard for

the conductivity of hardwood (18)¹⁾. Since the conductivity for water is 0.57 W/mK (at about +4°C), the previously mentioned Hashin-Shtrikman limits will be much narrower for water-saturated peat and the geometric mean equation can be used without major errors. The same will be true for ice-filled materials, since the conductivity of ice is 2.2 W/mK (at about 0°C), so that the conductivity ratio for the components will not exceed 5.

For dry materials, conditions are some-what complicated by the strongly porous nature of the materials, which will give heat transport by means of radiation an opportunity to come into play. The very porous structure may also cause a relatively high, temperature dependent water vapor diffusion resulting in re-distribution of the moisture content in materials with low to moderate degrees of saturation. This may be of importance for heat transport through peat layers, e.g. in permafrost regions, as pointed out by Nakano and Brown (1972) (17) and others.

B. Measurements on peat and bog

As mentioned earlier, Kersten performed measurements on one peat material from Alaska (7). Watzinger performed measurements on one bog material and one type of peat moss (3). The results of these measurements are shown together in Figures 29 and 30, for frozen and un-frozen samples, respectively.

The materials are grouped according to dry density by means of different plotting symbols. There is evidently little variation in these measured results as function of density. However, closer scrutiny reveals a tendency for the lowest densities to give the lowest conductivities at low degrees of saturation, while the opposite tendency occurs for high saturation levels, particularly for frozen materials.

1) Literal translation "compact wood", probably referring to dense varieties of wood, i.e. "hard wood" (Translator's note).

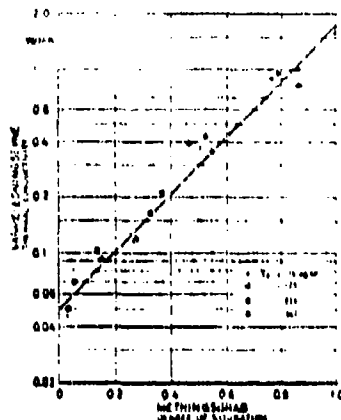


FIG. 29. Målinger på froset torv og myr plottet som funksjon av metningsgraden. Measurements on frozen peat plotted in relation to degree of saturation.

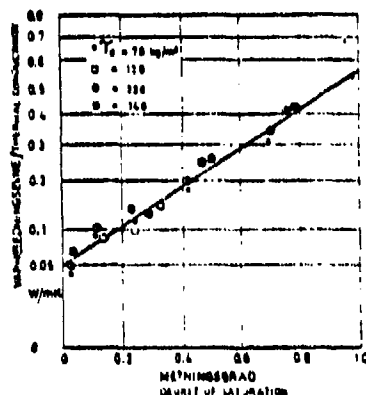


FIG. 30. Målinger på ufroset torv og myr plottet som funksjon av metningsgraden. Measurements on unfrozen peat in relation to degree of saturation. The ordinate represents the square root of the conductivity.

The explanation to this can be found in the functional dependence of the conductivity for dry and saturated materials, respectively. Figure 31 shows theoretical conductivities for dry and saturated materials, computed from the geometric mean equation. As expected, this results in values which are some-what low for dry materials, since the effects of thermal radiation are neglected. However, the trend as function of porosity will be the same.

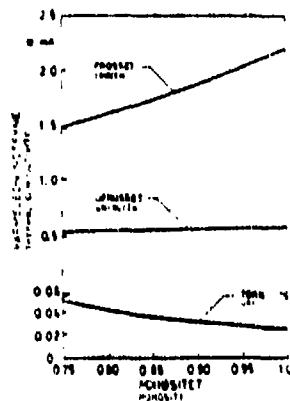


FIG. 31. Relationship between conductivity of porosity as a function of porosity for different soil states after geometric model. Conductivity-porosity relation of dry and saturated soil calculated by the geometric mean model.

One finds, that within the normal range of porosities, the conductivity of water saturated materials will vary less than 3 percent around the mean. For frozen and saturated materials, the corresponding variation is less than ± 10 percent. In both cases, the conductivity tends to increase with increasing porosity since the organic component has lower conductivity. The variations for dry materials are larger percentage-wise and the trend is the opposite.

The resulting conductivity variation as a function of dry density is on the other hand so small that one can use a common mean curve for all materials to obtain a good approximation for the conductivity at a given degree of saturation.

The curves shown in Figures 29 and 30 can be expressed by the formulas

$$\sqrt{\lambda - \lambda^0} = \sqrt{(\lambda^1 - \lambda^0)} S_r \quad (\text{un-frozen soils}) \quad 15$$

$$\lambda / \lambda^0 = (\lambda^1 / \lambda^0) S_r \quad (\text{frozen soils}) \quad 16$$

The following average values are proposed for conductivities of dry and saturated materials

$$\begin{aligned}\lambda^0 &= 0.05 \text{ W/mK} \\ \lambda^1 &= 0.55 \text{ W/mK} \quad (\text{un-frozen}) \\ \lambda^1 &= 1.30 \text{ W/mK} \quad (\text{frozen})\end{aligned}$$

REFERENCES, CHAPTER V

1. C. Krischer: Die Leitfähigkeit des Erdbodena. Beineft zum Gesundheits-Ingenieur. Reihe, Heft 33, Munchen (Munich) 1934.
2. W. O. Smith, H. G. Byers: The Thermal Conductivity of Dry Soils of Certain of the Great Soil Group. Am. Soc. Soil Sci. Proc. 3, 1938, pp. 13-19.
3. W.O. Smith: Thermal Conductivity in Moist Soils. Soil Sci. Soc. Am. Proc., 4, 1939, pp. 32-40.
4. W.O. Smith: The Thermal Conductivity of Dry Soil. Soil Science, 53, 1942, pp. 435-459.
5. A. Watzinger et al: Undersøkelse av masseutskiftningsmaterialer for vegog jernbanchbygging. Medd. fra Veglirektøren 1938, no. 6.
6. A. Watzinger et al: Unjersøkelse av masseutskiftningsmaterialer for vegog jernbanebygging. Medd. fra Vegdirektøren 1941, no. 6, 7 and 8.
7. M.S. Kersten: Thermal Properties of Soils. Univ. of Minnesota, Inst. of Technology, Bull. no. 28, June 1949.
8. M. van Rooyen, H.F. Winterkorn: Structural and Textural Influences on Thermal Conductivity of Soils. Highway Research Board Proceedings, Washington D.C. 1959, pp. 576-621.
9. D.A. de Vries: Het wärmtgeledingsvermogen van grond, Medd. Landbouwhogeschool, Wageningen, 52, 1952.
10. E. Saare, C. G. Wenner: Varmeleiningstal hos olika jordarter. Statens nämnd för byggnadsforskning, Handlingar ar. 31, 1957.
11. O.T. Farouki: Physical Properties of Granular Materials with Reference to Thermal Resistivity. Highway Res. Rec. 128, 1966, pp. 25-43.
12. R. Mc Gaw: Thermal Conductivity of Compacted Sand/Ice Mixtures. Highway Res. Rec. 215, 1968, pp. 35-47.

13. N. Wakao, K. Kato: Effective Thermal Conductivity of Packed Beds. J. Chemical Engineering of Japan, 2, (1) 1969, pp. 24-33.
14. L. Barden et al: The Collapse Mechanism in Partly Saturated Soil. Engineering Geology, 7 (1), 1973, pp. 49-60.
15. P.W. Kasameyer et al: Layers of High Thermal Conductivity in the North Atlantic. J. Geophys. Res. 77 (17), 1972, pp. 3162-3167.
16. E.H. Ratcliffe: The Thermal Conductivities of Ocean Sediments. J. Geophys. Res. 65, (5) 1960, pp. 1535-1541.
17. Y. Nakano, J. Brown: Mathematical Modeling and Validation of the Thermal Regimes in Tundra Soils. Arctic and Alpine Research (1) 1972, pp. 19-38.
18. A. Missenari: Conductivité Thermique. Editions Eyrolles, Paris 1965, p. 356.

CHAPTER VI

METHODS FOR COMPUTING THERMAL CONDUCTIVITY OF SOIL MATERIALS

The previous analysis of experimental studies of thermal conductivity in mineral-based soil materials forms the basis for a new mathematical model for computing thermal conductivity in moist and frozen soil materials. The first section reviews existing mathematical methods in the light of this analysis. The next section presents the new mathematical model in more detail.

1. EXISTING METHODS

A. Analytical methods

The important effects of the microstructure on the thermal conductivity in non-saturated soil materials was pointed out in the previous section. Such microstructural parameters are difficult to incorporate in a purely analytical mathematical model without significant simplifications, both in terms of geometry and computational methods. Still, efforts in this direction have been made.

A. Gemant (1950) (1) used a very simplified model of a moist soil material, where the soil particles were assumed to be uniform (equal size) spheres, tightly packed in a cubical lattice. Moisture was assumed to collect in meniscus-shaped bodies around the contact points between spheres. (See Figure 1)

The thermal conductivity was in this model computed by assuming planar isotherms. As shown in chapter II, this method yields an upper bound for the conductivity, while assuming parallel heat flow results in a lower bound. The calculations are further simplified by neglecting the conductivity of air, as well as the contribution from a meniscus around the "equator". In this manner, Gemant arrived at

an analytical expression for conductivity, with distance y_0 as parameter. This parameter defines the distance from the center of each sphere to the plane intersecting the lower "meridian" boundary of the meniscus, normalized to the radius. The relation between relative water volume and y_0 can be derived from geometrical considerations and is

$$1.33 w_v = \pi(0.33 - y_0^2 + 0.67 y_0^3) \quad 1$$

This equation is only valid when adjacent menisci are not in contact with each other. The expression for conductivity has the form

$$\frac{1}{\lambda} = \frac{2}{\pi f g} \log \frac{(f+g)(f-g y_0)}{(f-g)(f+g y_0)} + \frac{2}{\pi h^2} \log \frac{h + h y_0}{h - h y_0} \quad 2$$

where $f^2 = \lambda_2 - y_0^2 \lambda_1$, $g^2 = \lambda_2 - \lambda_1$, $h^2 = \lambda_2$
 λ_1 is conductivity of water
 λ_2 is particle conductivity

This method has one obvious weakness as a general way of determining conductivities in soil materials: The model does not allow for changes in the degree of packing (packing configuration). The cubic lattice gives a porosity of 0.476, which for dry sand corresponds to a density of only 1400 kg/m³.

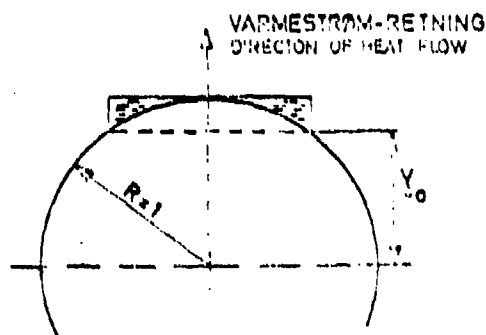


FIG. 1. Idealized model for watermen between adjacent indentations. Idealized model for approximate calculation of thermal conductivity of soil. (Gerritsen 1972)

Gemant carried out a numerical example for which the particle conductivity was assumed to be 4.2 W/mK. Figure 2 compares the functional dependence of these results with Kersten's experimental values for a silt/sand mixture (Ramsey sandy loam), which has about the same particle conductivity. The lowest density in this test run was about 1600 kg/m^3 and thus somewhat higher than that given by the mathematical model.

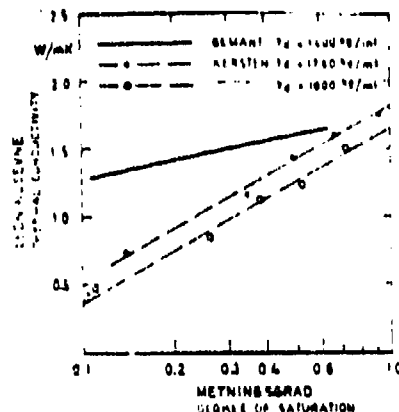


FIG. 2. Interpolating between the two curves for the degree of saturation, the calculated values are in poor agreement with the experimental values. The calculated values are from Gemant's model, which is based on the assumption that water accumulates in isolated menisci not being valid for the lowest degrees of saturation.

The calculated curve is obviously in poor agreement with the experimental results, both in terms of functional dependence and absolute values. Particularly for low degrees of saturation, the calculated values are significantly larger than corresponding experimental data. This can partly be caused by the assumption that water accumulates in isolated menisci not being valid for the lowest degrees of saturation. For this case one may speculate that a significant part of the water forms a film on the particle surfaces. This water will probably contribute little to the thermal conductivity but will "rob" the meniscus of part of the total water content.

Makowski and Mochlinsky (2) refer to a modified model, which Gemant developed later, where this condition is taken into account. Their description of the modified model is incomplete. However, it is evidently possible to fit this model also to different degrees of packing, although the method for fitting seems to be un-

pirical. Makowski and Mochlinsky have developed a relatively simple equation, based on curves fitted to data obtained from Gemant's modified model. This equation will be treated in next section.

Alberts (1966) has proposed a similar model, where the soil particles are represented by tightly packed spheres in a cubic lattice, while the water is partly spread out as a film on the surface of each particle and partly contained in a meniscus around each contact point (3). Part of the calculations were carried out numerically but the results are of little value due to the very low conductivity assumed for the particles ($\lambda = 1.0 \text{ W/mK}$), as well as some approximations which are introduced based on this assumption about the particle conductivity.

de Vries (1952) presented a method for calculating thermal conductivity in soil materials, based on the previously mentioned Maxwell-Fricke's equation (4). The foundation for this equation is discussed in chapter III. It should be pointed out here that this equation is derived under assumptions which are valid in a composite material where ellipsoid-shaped particles occur in rather small quantities (dispersed) in an otherwise continuous medium. For soil deposits in which the particles are in mutual contact, these assumptions are not valid.

The equation can be written in the form:

$$\lambda = \frac{\sum_{i=0}^N n_i \lambda_i F_i}{\sum_{i=0}^N n_i F_i} \quad 3$$

where n_i is relative volume of component "i"

λ_i is conductivity for component "i"

$$F_i = \frac{1}{3} \sum_j \left[1 + (\lambda_i / \lambda_0 - 1) g_j \right]^{-1}, \quad j = a, b, c \quad 4$$

$$\epsilon_a + \epsilon_b + \epsilon_c = 1.0$$

The factor ϵ_1 gives the ratio between the average temperature gradient in the dispersed component "i" and the continuous medium "o", provided that the indicated assumptions are valid. For more tightly packed materials, this factor can be considered as a "form factor", where values for ϵ_a , ϵ_b and ϵ_c are obtained by fitting to empirical data.

These matters were discussed in section 1 of chapter V, where it was shown that the equation can be fitted to conductivity data for dry natural soil materials by the following choice of g-values.

$$\epsilon_1 = \epsilon_2 = 0.10 \quad , \quad \epsilon_3 = 0.80 \quad (\text{Dry soils}) \quad 5$$

For water saturated soil materials, de Vries found a different set of values

$$\epsilon_1 = \epsilon_2 = 0.125 \quad , \quad \epsilon_3 = 0.75 \quad (\text{Saturated soils}) \quad 6$$

This set of g-values corresponds to a long ellipsoid with a ratio of about 5:1 between largest and smallest diameters. Such a particle geometry can hardly be considered typical for a sand material. The set of g-values for dry materials imply a further trend towards rod-shaped particles.

Figures 3a and b compare results obtained from de Vries' equation for saturated soils to values calculated from the geometric mean equation. Figure 3a shows conditions for a constant conductivity ratio ($\lambda_2/\lambda_1 = 8$) with relative particle volume as the variable. Figure 3b shows conditions with constant porosity ($n = 0.35$) and varying particle conductivity (conductivity ratio).

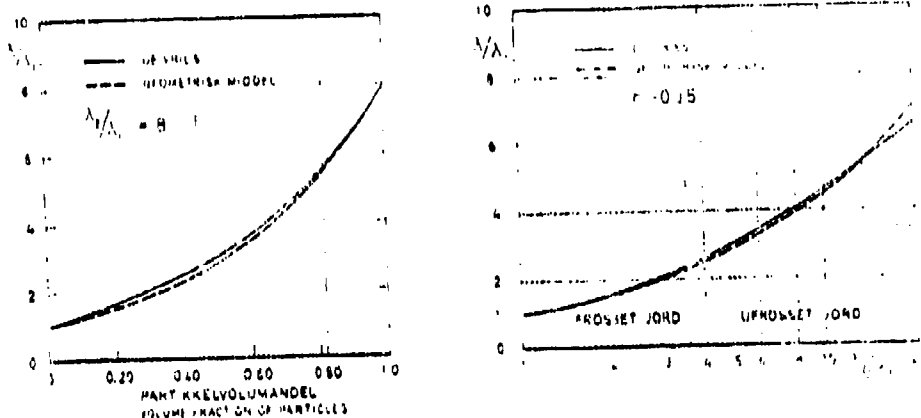


FIG. 1. Comparison of the De Vries equation and the geometric mean equation for saturated soil conductivity. Conductivities of saturated soils calculated by the De Vries equation compared to the geometric mean equation.

These graphs show that the two equations deviate from each other by less than 5 percent within the ranges of particle conductivities and porosities that are typical (may occur) in saturated soil materials.

Thus, the two equations can for practical purposes be considered equivalent. Since the geometric mean equation is the simpler of the two, it is most convenient to use for determining (calculating) conductivity in saturated soils, as proposed earlier.

De Vries suggested that the equation also could be used for calculating conductivity in moist soil materials. He separated out several degrees of saturation ranges in which the three components, particles, water and air, were treated differently with respect to geometrical conditions. For low degrees of saturation, the particles were considered to be enclosed in water, while the air was considered to be the continuous medium. For high degrees of satu-

ration, the water was considered as the continuous medium, in which either the grains of sand or air bubbles are contained in the form of particles¹⁾.

The effect of water vapor diffusion on the thermal conduction in the air-filled pores was assumed to be zero in dry materials and gradually increase to a maximum value at a given (low to moderate) degree of saturation. The different regions were selected partly by comparison with experimental data for moist sand, partly after evaluating the natural ranges in which the different mechanisms are effective. In reality, this amounts to fitting analytical results to experimental values. The applicability to other soil materials has not been investigated. In addition, the method is very cumbersome and does not offer any advantages over the purely empirical method proposed in the previous chapter for degrees of saturation ranging between dry and fully saturated conditions.

This discussion has shown that analytical methods are useful only if they can be fitted to experimental data. As will be evident from the following section, empirical methods also have their limitations, due to the large number of variables which occur.

B. Empirical methods

Kersten (1949) developed his method for calculating thermal conductivity in soil materials by fitting mathematical expressions to the extensive experimental data base described in chapter V (5). His model consists of two sets of equations for computing conductivity of frozen and un-frozen soil materials; one for coarse grain materials having less than 10 percent silt and clay content and one for fine grain soils containing more than 50 percent of

1) That is, either sand or air is considered as the "particles" distributed in water, to conform with the previously defined two-component model (Translator's note).

these fractions. When these equations were developed, results obtained for two of the coarser materials (Northway sand and fine sand) were not included due to the special mineral composition of these materials (Kersten, page 84), i.e. due to their low quartz content. This gives an indication that the chosen separation (classification) according to texture in reality means a grouping according to particle conductivity.

The equation for un-frozen materials was given the form

$$\lambda = [\alpha \log (W\%) + \beta] 10^{0.62Yd} \quad W/mK \quad 7$$

where α and β are empirical factors which are different for coarse and fine soil materials:

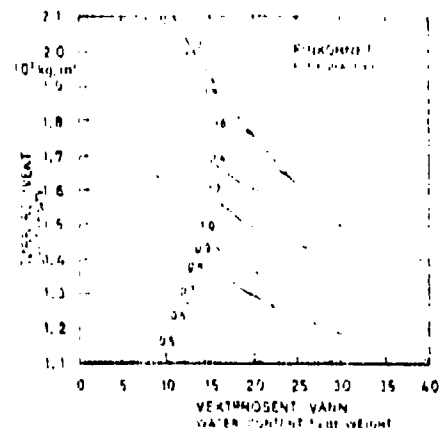
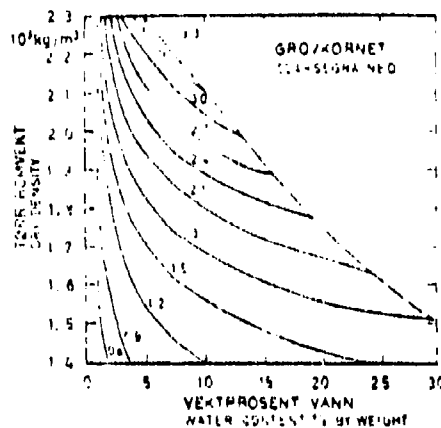
	α	β
Fine grain soils	0.13	-0.029
Coarse grain soils	0.10	0.058

For frozen materials, the equation has a different form:

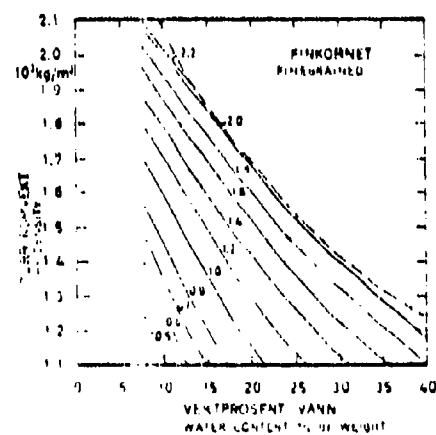
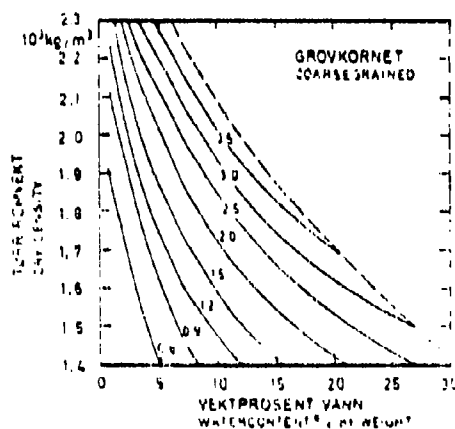
$$\lambda = a 10^{byd} + c 10^{dyd} \cdot (W\%) \quad W/mK \quad 8$$

	a	b	c	d
Fine grain soils	0.0014	1.4	0.012	0.05
Coarse grain soils	0.011	0.81	0.0046	0.91

Kersten presented these equations in a series of diagrams, as shown in Figure 4.



a) Ledningsevne av ufrosne jordarter. Conductivities of unfrozen soils.



b) Ledningsevne av frosne jordarter. Conductivities of frozen soils.

FIG. 4. Kerstens empiriske diagrammer for beregning av jordarters varmeledningsevne. Kersten's empirical nomograms for calculating thermal conductivities of soils.

Grovkornet. Coarsegrained: < 10% silt ($d < 0,05 \text{ mm.}$)

Finkornet. Finegrained: > 50% silt " " "

The previous analysis of Kersten's experimental results showed that the thermal conductivity of saturated soil materials can be determined from the geometric mean equation, when quartz content and volumetric compositions are known. Figure 5 shows values for saturated materials calculated from Kersten's equations, compared with data obtained from the geometric mean equation.

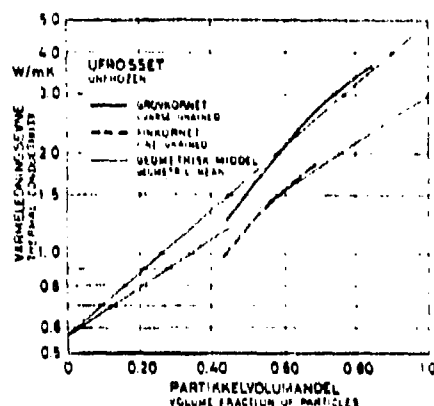


FIG. 5. Beregnede ledningsevner for vannmettede jordarter etter Kerstens likninger sammenliknet med geometrisk middel-likningen. Calculated conductivities for water-saturated soils by Kersten's equations compared to the geometric mean equation.

This comparison clearly shows that the two selected soil material groups represent differences in particle conductivity. The equation for coarse materials gives an average particle conductivity of about 5 W/mK, while the equation for fine grain soils gives about 3 W/mK. From the previously proposed mathematical model for particle conductivity one finds that these values correspond to quartz contents of 60 and 30 percent, respectively. An evaluation of reported values for the quartz content gives a mean of 57 percent for the five coarse grain soils considered. The corresponding average for the four fine grain soil materials at hand is uncertain due to incomplete information about quartz content for two of these soils.

Sveian's study of quartz content in Norwegian loose deposits, which was discussed in chapter III (6), indicates that the mean

value for quartz content in coarse grain soils that is obtained here from Kersten's equations is not representative for Norwegian conditions. Figure 6a shows a cumulative distribution curve based on quartz contents in coarser materials determined by Sveian.

As can be seen, only 6 percent of the samples have a quartz content larger than 90 percent. The median corresponds to a quartz content of 50 percent, which also is the arithmetic mean. This figure also shows that variations in quartz content are so large within this group of soil materials that use of a "representative" average value will mean large uncertainties in estimates of the conductivity.

Selmer-Olsen's studies of quartz contents for the fractions $d < 2 \mu m$ and $2 < d < 20 \mu m$ in Norwegian clays show a definite difference in distribution between these two fractions (7). Results for approximately 160 samples are summarized as cumulative distribution curves in Figure 6b. The distribution curve for coarse soil materials shown in Figure 6a can be considered representative for fractions larger than $20 \mu m$.

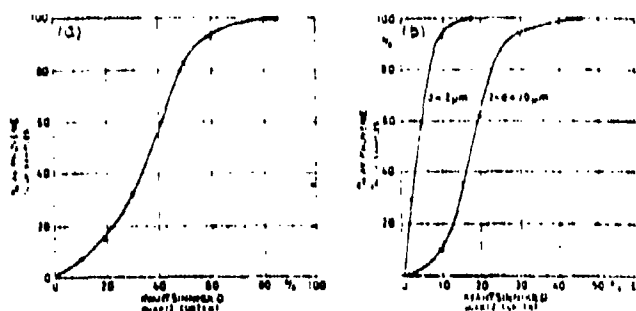


FIG. 6. Kumulative fordelinger av kvartsinnhold fra prøver av norske grovkornede jordarter (a) og fraksjoner av norske leirer (b). Cumulative distributions of quartz contents from samples of Norwegian coarse-grained soils (a) and fractions of Norwegian clays (b).

Kersten defined fine grain soils as those containing at least 50 percent silt and sand fractions. Within the frame-work of

this definition, the relative contents of the fractions $d < 2 \mu\text{m}$, $2 < d < 20 \mu\text{m}$ and $d > 20 \mu\text{m}$ can vary within wide limits. Since these three fractions show such considerable differences in their distribution curves for quartz content, the definition for coarse grain soils implies no definite classification according to quartz content.

In chapter III, a method was proposed for estimating quartz content on the basis of grain size distribution curves. This method is based in the average quartz content given by distribution curves for the three fractions. This resulted in the triangular diagram shown in Figure 7.

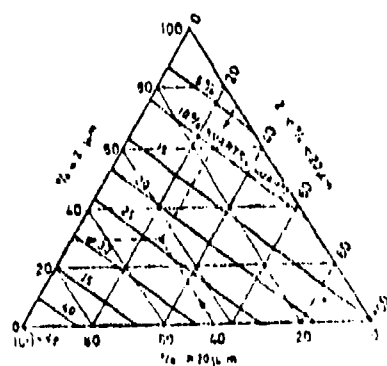


FIG. 7. Ternarydiagram for analog over konstantenhet af størrelse af kornfordelingskurver. Ternary diagram for average of three determination of quartz content from grain size distribution.

If one, some-what arbitrarily, replaces Kersten's border-line for fine grain materials with a requirement that more than 30 percent of the material shall be smaller than $20 \mu\text{m}$, one obtains a region in this diagram which represents fine grain materials. Within this region, the quartz content varies from 0 to about 30 percent. Since these numbers are based on mean values for each fraction, the possible variation is some-what larger and can be estimated to range from 0 to 45 percent.

This corresponds to a possible variation in particle conductivity from 2 to about 3.2 W/mK for fine grain soil materials. The dis-

tribution function obtained for coarse materials gave a possible variation in particle conductivity from about 2.2 to 5 W/mK, if one neglects the most extreme 10 percent of the results.

Based on these circumstances one can expect thermal conductivity variations in water saturated Norwegian soils as shown in Figure 8. Expected variations in dry density for the two groups of soil materials are also indicated. For coarse grain materials this range is from 1500 to 2200 kg/m³ while fine grain materials may vary from 1200 to 1800 kg/m³. For comparison, results obtained from Kersten's equation are included.

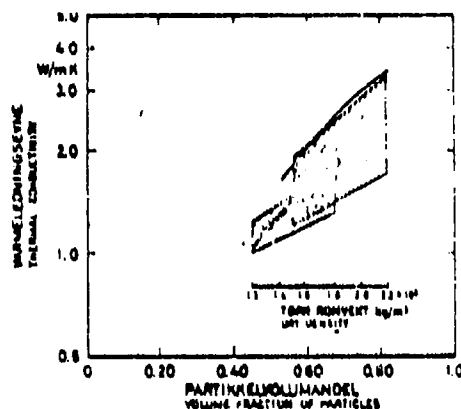


FIG. 8. Beregnede ledningsevner for vannmettede jordarter etter Kerstens likninger sammenliknet med det tilsvarende forventede variasjonsområdet for norske jordarter. Calculated conductivities of water-saturated soils by Kersten's equations compared to the corresponding expected area of variations for Norwegian soils.

As shown by Figure 8, Kersten's curves for coarse grain soils fall close to the upper limit of the region representing Norwegian coarse grain soil materials. Kersten's curve for fine grain materials cuts diagonally across the region representing fine grain soils.

One also finds variations around mean curves for the two regions of between 20 and 30 percent for coarse grain soils and from 10 to 15 percent for fine grain soil materials. The mean curves represent particle conductivities of 3.5 and 2.6 W/mK for coarse

and fine grain soils, respectively. This corresponds to quartz contents of 40 and 20 percent, respectively.

Figure 9 presents corresponding regions of variation for the conductivity in frozen, saturated soil materials, as well as results obtained from Kersten's equations for such soils. Also in this case, the latter curve falls in the upper portion of the variation region for coarse grain materials. However, for fine grain soils Kersten's curve passes through the cross-sectioned region at a significantly lower level than for the case of un-frozen materials (Figure 8).

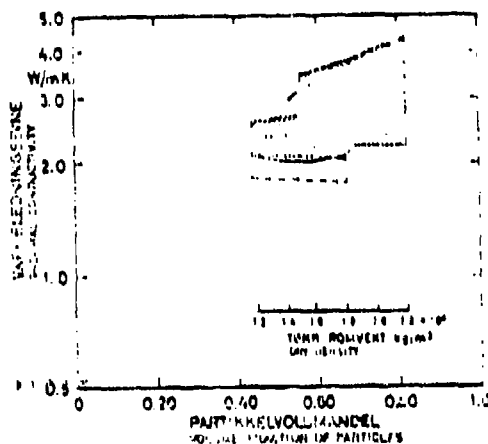


FIG. 9. Tilsvarende framstilling som på fig. 8 for metode frosne jordarter. Stiplet strek angir området for metode frosne jordarter ved 10 volt uløstet vann. (Se også fig. 8 for saturerte frosne soils, broken lines used here for saturated frozen soils with 10 to 15 volt. un-frozen water).

This lower position (of the Kersten curve) can be assumed to be caused by a certain average portion of un-frozen water in the fine grain samples, due to the temperatures used during the experiments (mean temperature -4°C , temperature difference 5.5°C). The variations around mean curves through the two regions are, as in Figure 8, between 20 and 30 percent for coarse grain materials and from 10 to 15 percent for fine grain soils. However, expected variations in relative un-frozen water content will cause significant widening of the range for fine grain soils. This is indicated in Figure 9 by extending the actual region of variations in

particle¹⁾ conductivity with a broken line, representing an unfrozen water content of 10 percent. ($W_u = 0.10$)

Variations in unfrozen water content in fine grain soil materials was discussed in chapter III. There, a diagram was presented for determining the variations in unfrozen water content at temperatures below the normal freezing point when the flow-limit for the material is known. This variation in unfrozen water content at temperatures below the freezing point will, as mentioned earlier, also affect the apparent thermal capacitance in soil materials during freezing. This effect can be expected to be more important for the temperature field distribution in freezing soil than the related effect in thermal conductivity.

The previous discussion of Kersten's equations was limited to conditions in saturated soils. As indicated earlier, this condition represents an extreme value for the conductivity variation for varying degrees of saturation. The other extreme, i.e. conductivity for dry soil materials, can not be derived from these equations since they are only valid to limits of 3 and 7 percent water content by weight, for coarse and fine grain soils, respectively. However, the empirically derived equation for variations in conductivity of dry materials can be used to estimate the lower extreme value. This permits extension of Kersten's equation, using the same normalized representation as when his experimental results were discussed. The results of such a treatment of Kersten's empirical equations are shown in Figure 10 for different densities.

1) This looks like a mistake. The variation discussed here occurs in the over-all conductivity, not in the particle conductivity.
(Translator's note)

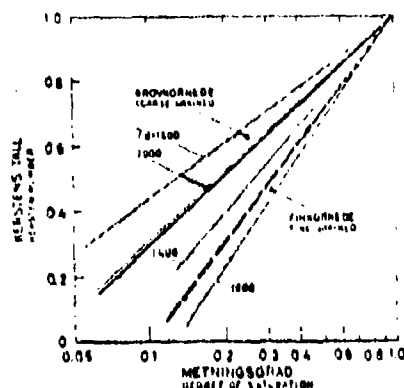


FIG. 10. Kerstens likninger framstilt på normalisert form, sammenliknet med de empiriske likninger for grovkornede og finkornede jordarter. Kersten's equations in dimensionless representation, compared to the empirical equations for coarsegrained and finegrained soils.

When presented in this form, Kersten's equations show certain variations due to dry density, while no such variations were found in the results from his study (see Figure 27 of chapter V). On the other hand, the agreement with previously derived empirical relations between degree of saturation and normalized conductivity is satisfactory, particularly for fine grain materials.

This discussion of Kersten's equations has thus shown that these equations can be regarded as a satisfactory empiric presentation of the experimental data they were derived from. However, these data are not completely representative for Norwegian soils. Particularly for the group coarse grain soils the data show a significantly higher average quartz content than one can expect to find in Norwegian soils. This will in most cases result in too high estimates for conductivity in Norwegian coarse grain soil materials. The large variation in quartz content which can be expected for such materials will also give large uncertainty in conductivity estimates, even if one manages to correct for the high average quartz content.

For fine grain materials, the expected variation in unfrozen water content is a particularly "heavy load" on the accuracy of the equations, while variations in quartz content in general will be less important than for coarse materials. An improved method

should thus include possibilities to account for varying quartz content in coarse grain materials, while the effects of un-frozen water should be included for fine grain soils. As mentioned before, it may also be desirable to change the method for classification of the two groups of soil.

As mentioned previously, Makowski and Mochlinsky (1956) developed an equation for thermal conductivity in soils, based on a semi-empirical mathematical model generated by Gemant (1951) (1, 2). This equation was put in the same form as Kersten's empirical equations for un-frozen soil materials.

$$\lambda = (\alpha \log(W\gamma_d) + \beta) 10^{0.62\gamma_d} \text{ (W/mK)} \quad 9$$

where γ_d is dry density expressed in metric tons/m³

α and β are factors depending on clay content c (percent)

$$\alpha = (1.4241 - 0.00465 \ c) 10^{-1}$$

$$\beta = (0.4192 - 0.00313 \ c) 10^{-1}$$

The clay content was said to affect the conductivity of soil particles. In clay-free materials, the particle conductivity was assumed to be 5.84 W/mK while a certain clay content c (percent) was assumed to reduce this value according to the following formula.

$$\lambda_2 = 5.84 - 0.033c \quad 10$$

According to this expression, pure clay would have a particle conductivity of 2.51 W/mK. This corresponds to a quartz content as high as 80 percent for clay-free materials and 15 percent for pure clay, according to the previously proposed model for determining particle conductivity.

Figure 11 shows the conductivity for water saturated clay-free

sand, and for pure clay determined from the equation given by Makowski & Mochlinsky. Both these curves are close to that derived from the geometric mean equation on the basis of assumed particle conductivities.

The curve for clay-free materials will consequently give significantly higher values than those which can be expected for Norwegian coarse grain materials, while the curve for pure clay is representative for fine grain materials.

Figure 12 shows data for varying degrees of saturation, obtained from the same equation and presented in normalized form for different densities. The derived relations between Kersten's number and the degree of saturation are included for comparison.

One finds that the curves for clay-free materials on the average follow the empirical relation for coarse grain materials, while for pure clay the curve falls above the empirical relation for fine grain materials.

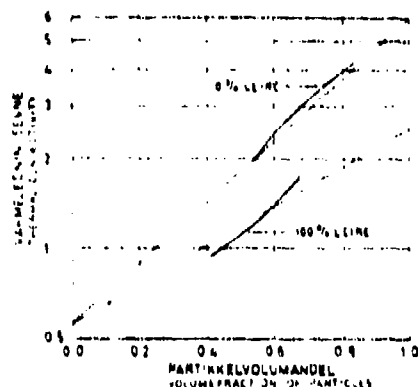


FIG. 11. Beregnede ledningsevner etter Makowski og Mochlinskis likninger for vannmettede jordarter sammenliknet med geometrisk middel-likningen. Calculated conductivities by Makowski and Mochlinsky's equations for water-saturated soils compared to the geometric mean equation.

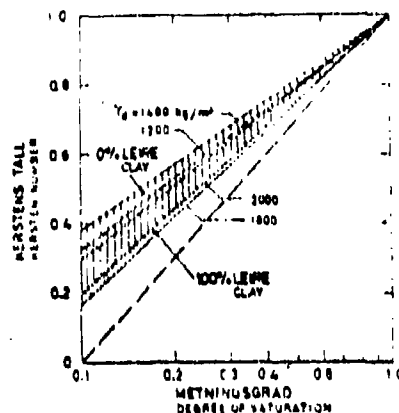


FIG. 12. Makowski og Mochlinsky's likninger framstilt på normalisert form, sammenliknet med de empiriske likninger for grovkornede og finkornede jordarter. Makowski and Mochlinsky's equations in dimensionless representation compared to the empirical equations for coarse-grained and fine-grained soils.

The method developed by Makowski and Mochlinsky is proposed as an improvement to Kersten's method, since the former offers a possibility for continuous transition between the two groups of soil materials defined by Kersten. This "transition" is tied to an expected variation of the particle conductivity for varying clay content. As shown earlier in this chapter and by others, variations in particle conductivity will primarily be due to differences in mineral composition, particularly the quartz content. In more fine grain materials it has indeed been shown that a certain correlation exists between quartz content and texture. However, this correlation can not be satisfactorily represented by a two component model (clay, "no clay"). A three component model is needed, in which the non-clay fraction is separated into two components, $d > 20 \mu\text{m}$ and $2 < d < 20 \mu\text{m}$.

The normalized presentation of Kersten's experimental results showed different functional dependence between Kersten's number and the degree of saturation for coarse and fine grain materials. This difference is not present when Makowski and Mochlinsky's method is used, see Figure 12.

The work by Makowski and Mochlinsky was directed towards conditions when high voltage cables are buried in the ground. In that case, there is a danger for overheating in the cable insulation where the surrounding ground has unusually low thermal conductivity.

For this reason, they only treated un-frozen soils.

Van Rooyen and Winterkorn (1959) later presented a report from work having the same purpose (8). They performed thermal conductivity, using thermal conduction probes, for a series of soils and modified¹⁾ materials (crushed quartz, fractions of sand with high quartz content), all with relatively high quartz content. Based on measurements performed for different combinations of densities and water content, they derived an empirical method for determining thermal resistivity of un-frozen soil materials, i.e. the inverse of thermal conductivity. Their equation has the form

$$r = A \cdot 10^{-BS} r + s \quad (\text{cm}/\text{o}_{CW}) \quad 11$$

where A, B and s are empirical functions of dry density, mineral composition and particle size distribution.

For completely water saturated materials, the thermal resistance was set equal to s, which was expressed as a linear function of dry density

$$s = s_1 - s_2 \gamma_d \quad 12$$

where s_1 and s_2 are linear functions of the quartz content, while γ_d is dry density in metric tons/m³.

This in principle agrees with what has been pointed out earlier: The thermal conductivity of water saturated soil material depends primarily on relative particle volume and particle conductivity, while the sensitivity to differences in microstructure is small. However, calculations using this equation to determine conductivity of saturated materials with different quartz contents show that

1) "Kunstig" means "artificial" or "man-made". In this context the term means "modified", e.g. by crushing or screening (Translator's note).

van Rooyen's equation tend to overemphasize the effect of increasing dry density, particularly for low quartz contents. This is illustrated by Figure 13, which shows calculated conductivity for three values of quartz content and data obtained from the geometric mean equation for comparison.

Figure 14 shows how the conductivity varies with varying degree of saturation and different densities, according to van Rooyen's equation. The data are presented in the normalized form used previously. For comparison, van Rooyen's measured results for sand with high quartz content are also shown in Figure 14.

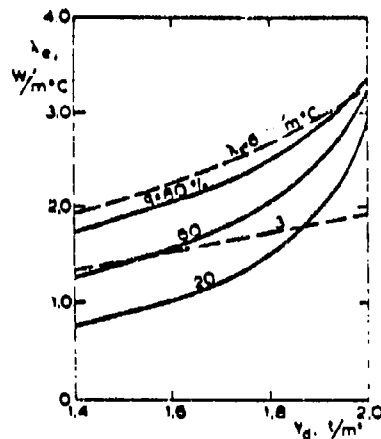


FIG. 13. Beregnede ledningsevner for mettet sand med forskjellig kvartsinhold etter van Rooyens likninger, sammenliknet med geometrisk middel-likningen (stiplet strek). Calculated conductivities for saturated sand with different quartz content by van Rooyen's equations compared to the geometric mean equations (broken lines).

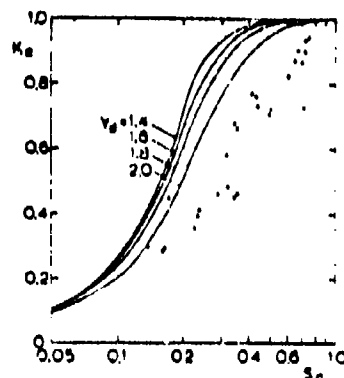


FIG. 14. van Rooyens likninger for sand med 100% kvarts framstilt på normalisert form, sammenliknet med hans målinger på kvartssand. van Rooyens equations for sand with 100% quartz in dimensionless representation, compared to his measurements on quartz-sand.

The calculated curves evidently give poor agreement with measured values for degrees of saturation above 20 percent.

For dry materials, the expression for thermal resistivity is

$$r = A + S$$

13

The term A is given as an exponential function of dry density, clay content and specific surface area for the parts of the material which have particles larger than those within the clay fraction. Due to the structure of the exponent in A, the values for dry materials are very sensitive to variations in clay content, as shown in Table I.

Table I. Effect of clay content on conductivity of dry soil, calculated from van Rooyen's equation. Dry density 1400 kg/m^3 . Specific surface area for fractions larger than clay: $2,000 \text{ cm}^2/\text{cm}^3$. 40 percent quartz.

Clay content, percent	0	5	10	20	50
Dry conductivity, W/mK	0.22	0.30	0.52	0.74	0.94

A corresponding variation is found for soils not containing clay when the specific surface area for fractions larger than clay is varied, see Table II.

Table II. Effect of specific surface area on the conductivity for dry soil calculated from van Rooyen's equation. Dry density: 1800 kg/m^3 . No clay content. 80 percent quartz.

Specific surface area cm^2/cm^3	50	100	200	500	2000
Dry conductivity W/mK	0.31	0.48	0.59	0.67	0.72

In both these cases, the conductivity variations are larger than those found for dry materials during the study discussed earlier in the last chapter. In addition, that study gave no basis for grouping conductivities in soil materials according to differences in texture, except for the proposed separation between natural soil materials and crushed rocks.

The previous analysis shows that van Rooyen's equation gives uncertain values for conductivity in soils, despite the large number of parameters involved and the complicated form of the equation. Part of the explanation for this can be found in the specialized choice of soil materials that were used for the experiments. Two of the soil samples were so called "thermal sands" which have abnormally high conductivities both when dry and moist, as was shown in the sections of the previous chapter discussing conductivity of mineral soil materials.

C. Conclusion

The previous discussion of methods for computing conductivity of soil materials has shown that analytical methods only can be used to obtain reliable results if they are supplemented by empirical relations.

Out of the purely empirical approaches, Kersten's method is shown to give the best agreement with conductivities of natural soil materials one can expect to find in Norway. The agreement is best for fine grain soils, while Kersten's values for more sandy materials will be somewhat high in comparison with the expected range of variation for Norwegian soil materials. This is mainly due to the selection of soil samples on which Kersten's empirical equations were based. In particular, the coarse grain materials showed considerably higher quartz contents than those to be expected on corresponding Norwegian materials.

Another draw-back inherent in the Kersten method is the mixture of factors related to texture and mineral content implicit in his equations. An improved method should treat the effects of these factors separately, e.g. so that both coarse grain soils having low quartz content and fine grain soil materials with high quartz content can be correctly related.

The discussion of van Rooyen and Winterkorn's empirical method showed that it is difficult to improve on the methods for calculating (determining) thermal conductivity of soil materials by means of empirical methods. The number of variables is so great, that the effect of each individual parameter on the conductivity best can be separated out by a more fundamental analysis of physical relations. However, as mentioned previously, such an analysis can not be successful without support by experimental investigations.

In the following, a new method for determining thermal conductivity will be developed on the basis of theoretical and empirical studies described in this and previous chapters. These studies also form a basis for estimating the error limits inherent in the method, depending on how much information one has about the soil material at hand. The latter is important in different applications of the method, which pose different requirements on accuracy of the results. The mathematical model will be designed accordingly and with respect to requirements for studies of materials at hand.

A discussion of the effects of variations in thermal conductivity on the development of temperature fields, e.g. in road banks and subsoils, will also be included.

2. NEW METHODS FOR DETERMINING THERMAL CONDUCTIVITY IN SOIL MATERIALS

A. Introduction

The previous evaluation of methods for determining thermal conductivity in soil materials showed that existing methods result in relatively wide error limits which can only be improved upon by introducing mineral as well as texture dependent factors as parameters in the mathematical models. The foundation for such an improved model was laid in the previous discussion of empirical methods (chapter V). In this section, the emphasis will be placed on a presentation of this mathematical model, by means of graphical methods for determining the conductivity of soil materials. Relations between information level (in the sense of knowledge about soil parameters at hand) and resulting error (confidence) limits will be discussed in the next section. The effects of variations in different soil parameters in the development of temperature fields in freezing ground will also be treated.

B. Mathematical model for mineral soils

The foundation for this model was developed in chapter V, where thermal conductivity measurements on dry, moist and saturated soil materials were discussed. In the following, the main aspects of the model will be summarized, with references to Table III, where the different parts of the model are listed.

The mathematical model can be formulated in terms of a main equation (Eq(a) in Table III) which gives the soil material conductivity for certain degrees of packing and saturation as a function of conductivities for the soil material in dry and saturated states for the degree of packing at hand, as well as values of the normalized conductivity (Kersten's number) at the actual degree of saturation.

These variables can be determined from information about the texture of the soil material (screening curve and particle shape), degrees of packing and saturation, as well as the mineral composition (quartz content) which determines the particle conductivity.

The conductivity of dry soils was found to be rather insensitive to variations in particle conductivity. On the other hand, textural conditions tied to particle shape, etc. turned out to be of major importance. However, the material studied gave no means for differentiating between soil materials having different particle size distributions, except for a special group of materials where a limited amount of clay was mixed into an otherwise typical sand material ("thermal sand"). Artificially crushed rocks were also found to have conductivities which are significantly different from those of natural soil materials. On this basis, two empirical relations were developed between dry conductivity and porosity, one for natural soils and one for crushed rock (Eqs (b) and (c) in Table III). Due to the limited variation in specific weights of soil materials, these relations can also be expressed as functions of dry density.

For saturated soil materials it was found that the conductivity is not very sensitive to variations in texture. Thus, the conductivity can in that case be determined if volume ratios and particle conductivity are known, without consideration for differences in texture. The geometric mean equation was found to yield a good approximation to the theoretical results obtained from the Hashin-Shtrikman limits (Eqs (g) and (h) in Table III). A mathematical model for the particle conductivity was developed on the basis of certain trends for mineral composition in various soils, where quartz, feldspar and mica are the dominant minerals. Of these, quartz has the highest conductivity (7.7 W/mK) while feldspar and mica have approximately equal conductivities (2.0 W/mK). Based on this, particle conductivity could be determined from a two component model, with quartz content as the main factor (Eq (i) in Table III). This model is valid for soil materials that are generated

BEST AVAILABLE COPY

Tabell III. Beregningsmodell for varmeledningsevne av mineralske jordarter.
Method for calculating thermal conductivity of mineral soils.

$\lambda = (\lambda^1 - \lambda^0) K_e + \lambda^0$		(a)	Hovedlikning. Main equation.
	NATURLIG	$0,137 \text{ yd} + 64,7$	(b)
	NATURAL	$2700 - 0,947 \text{ yd}$	Tørr ledningsevne. Dry conductivity.
	ENNST	$0,039 \cdot n^{-2,2}$	(c)
	CRUCHED		
UFROSSET UNFROZEN	GROV	$0,7 \log S_r + 1,0$	(d)
	COARSE		
	FIN	$\log S_r + 1,0$	(e)
	FINE		Kerstens tall. Porosity number.
FROSSET FROZEN		S_r	(f)
UFROSSET UNFROZEN		$0,57^n \cdot \lambda_s (1-n)$	(g)
FROSSET FROZEN		$2,2^n \cdot \lambda_s (1-n) \cdot 0,269^{W_u}$	(h)
		$7,7^q \cdot 2,0^{1-q}$	(i)
q < 0,20 GROV		$7,7^q \cdot 3,0^{1-q}$	(j)
		COARSE	Partikkelledningsevne. Particle conductivity.

mainly from rocks containing quartz, such as granite and gneiss. Soils originating from alkaline rocks, such as gabbro, will contain small quantities of quartz, as well as considerable amounts of other minerals whose conductivities fall between the two important groups mentioned. Coarse grain materials with low quartz contents should consequently be treated separately (Eq (j) in Table III). For fine grain materials it is proposed that Eq (i) be used also for low quartz contents, since minerals in the intermediate groups seem to occur in small quantities in the finest fractions.

Empirical relations between the normalized conductivity (Kersten's number) and degree of saturation were derived for the range from dry to fully saturated. These relations were found to have low sensitivity to variations in packing degree (density). However, for un-frozen materials, a systematic difference was found between materials containing no clay fractions and those having a certain clay content (Eqs (d) and (e) in Table III). No similar difference could be demonstrated for frozen materials (Eq (f)).

This mathematical model was used to generate diagrams for graphical determination of conductivity in mineral-based soils. These diagrams are shown in Figure 15, which also contains examples of their use. The input parameters are also described in more detail. This model can also be used to generate computer programs. Such programs are currently being prepared at the Institute for Cold Technology, NTH.

THERMAL CONDUCTIVITY OF UNFROZEN SOILS

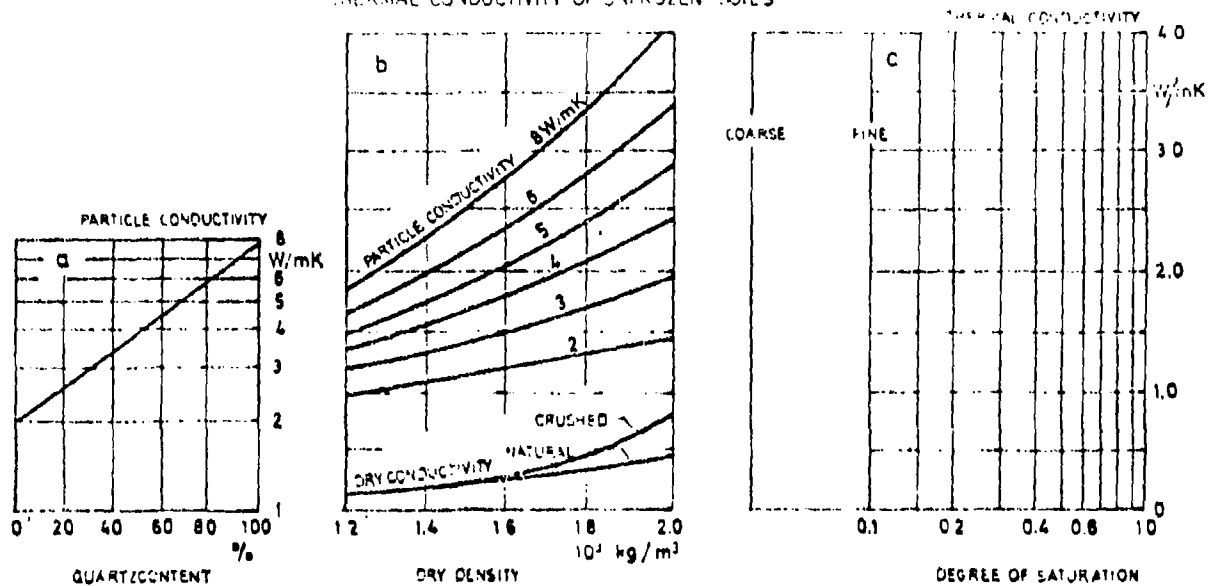


Fig. 15a. Varmednningsevne av ufrosne mineralske jordarter. Thermal conductivity of unfrozen mineral soils.

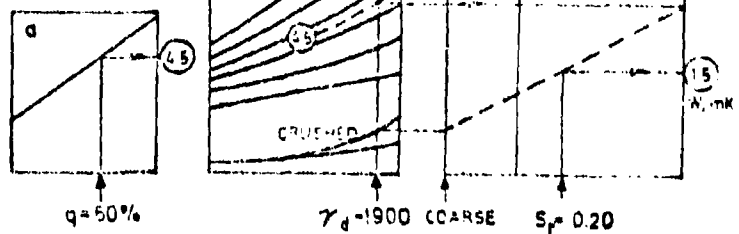
Inngangsstørrelser:

Input variables:

- | | |
|-------------------|-------------------------|
| 1. Kvartsinnhold | 1. Quartzcontent |
| 2. Knust/naturlig | 2. Crushed/natural |
| 3. Grov/fin | 3. Coarse/fine |
| 4. Torr romvekt | 4. Dry density |
| 5. Metningsgrad | 5. Degree of saturation |

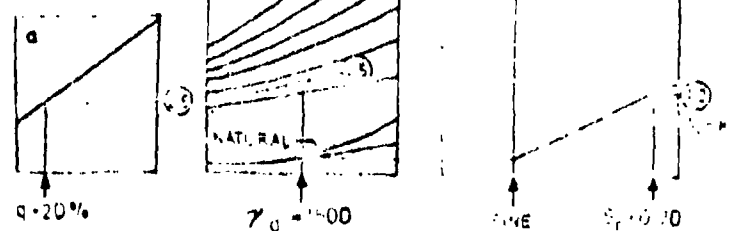
Ex. 1

CRUSHED GRAVEL



Ex. 2

SILTY CLAY



THERMAL CONDUCTIVITY OF FROZEN SOILS

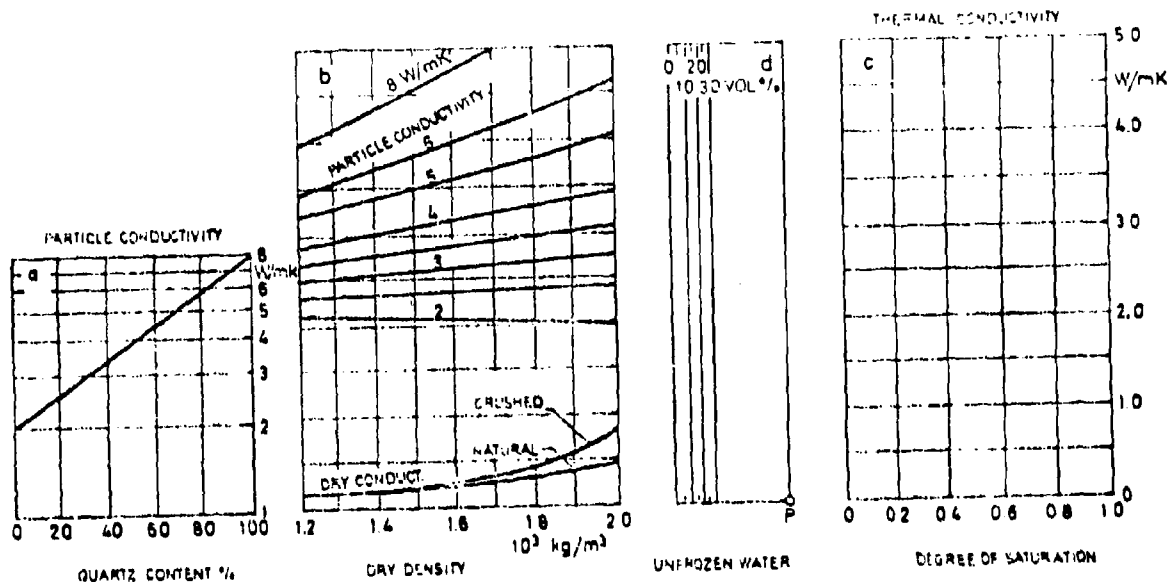


Fig. 15b. Varveledningssveve av frosne minerale jordarter. Thermal conductivity of frozen mineral soils.

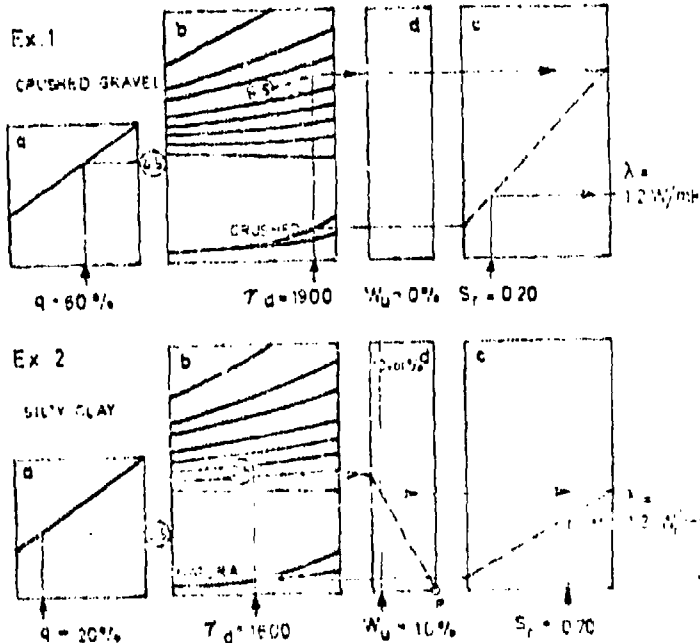
BEST AVAILABLE COPY

Inngangsstørrelser:

1. Kvartsinnhold
2. Knust/naturlig
3. Torr romvekt
4. Ufrosset vanninnhold
5. Metningsgrad

Input variables:

1. Quarts content
2. Crushed/natural
3. Dry density
4. Unfrozen water content
5. Degree of saturation

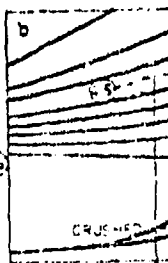


Ex.1

CRUSHED GRAVEL



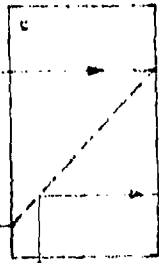
$q = 60\%$



$T_d = 1900$



$W_u = 0\%$

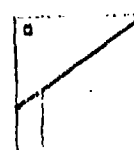


$S_r = 0.20$

$\lambda = 1.2 \text{ W/mK}$

Ex.2

SILTY CLAY



$q = 20\%$



$T_d = 1600$



$W_u = 10\%$



$S_r = 0.70$

$\lambda = 1.2 \text{ W/mK}$

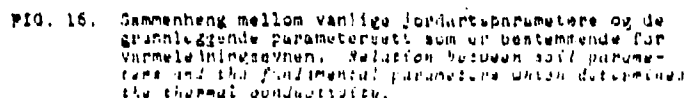
3. EFFECTS OF VARIATIONS IN SOIL PARAMETERS

A. Effects on conductivity calculations

The mathematical models developed in preceding sections make it possible to determine thermal conductivity of mineral-based soils with normally required accuracy, provided that relevant soil parameters are given (known). However, one usually has to utilize data from more or less complete geotechnical investigations. the parameters which are lacking will in such cases cause uncertainties in the estimated conductivity, which can be predicted only if one knows the statistical distribution of the parameter(s) at hand, within the soil material studied. As an example, if a soil material is classified in general terms, such as sand/gravel or silt/clay, the uncertainty of the conductivity estimate will depend on the statistical distribution of all relevant soil parameters in these material groups. If only information about quartz content is lacking, the statistical variation of quartz content in the soil type at hand will determine the error (confidence) limits for the calculated conductivity.

The two cases just mentioned can be said to represent two information levels, each having characteristic error limits for the conductivity estimate. In chapter III, such levels of information were given in a block diagram containing the different parameters which affect conductivity in a soil material. This block diagram is reproduced in Figure 16.

In addition to the three levels shown in Figure 16 one could introduce a lowest level of information where one, as mentioned, only has access to a broad classification of the soil materials, without any of the relevant soil parameters being given. For example, in connection with development of insulation designs for shallow foundations (houses without basements) this may be the situation (Thue 1973)(10).



The graph plots Thermal Conductivity (W/mK) on the y-axis (0 to 100) against Temperature (°C) on the x-axis (0 to 300). Two curves are shown: 'COMPOSITE' and 'MATRIX'. The 'MATRIX' curve starts at approximately 10 W/mK at 0°C and rises to about 95 W/mK at 300°C. The 'COMPOSITE' curve starts at 0 W/mK at 0°C, remains at zero until about 100°C, then rises sharply to meet the 'MATRIX' curve at approximately 95 W/mK at 300°C.

255

For sand materials, these results show a near normal distribution, with a mean value of about 1.90 W/mK and a standard deviation of 0.60 W/mK. 90 percent of the results fall between the limits 0.90 and 2.9 W/mK. The results for clay materials deviate significantly from a normal distribution. The mean value was determined to be 1.80 W/mK and 50 percent of the results fell within the limits 1.60 and 2.0 W/mK. However, the rest of the data showed a wider variation, with the 90 percent limits at 1.20 and 3.20 W/mK.

These results can not without reservations be assumed relevant for Norwegian conditions but they give a notion of error limits which must be accepted if conductivity estimates are based on broad classifications of soil materials.

Since no results are available from field measurements on Norwegian soils, the error limits for conductivity estimated on the lowest level (of information) must be determined from information about mean values and variations in relevant soil parameters. There are few studies on which a determination of such distributions can be based. Thus, one must resort to more arbitrary estimates.

Angen (1973) has published a table showing dry densities for 19 different Norwegian clays (12). These values are used to estimate a distribution having a mean of 1400 kg/m^3 and a standard deviation of 90 kg/m^3 . He also includes a table over typical dry densities in sand materials. The values vary from 1430 kg/m^3 for loosely packed, single grain size sand, to 2120 kg/m^3 for a morain material with large variations in particle size. If the extreme values are assumed to represent 95 percent of the cases, the standard deviation will be 170 kg/m^3 , around a mean value of 1770 kg/m^3 . These estimates of dry density distributions are shown graphically in Figure 18.

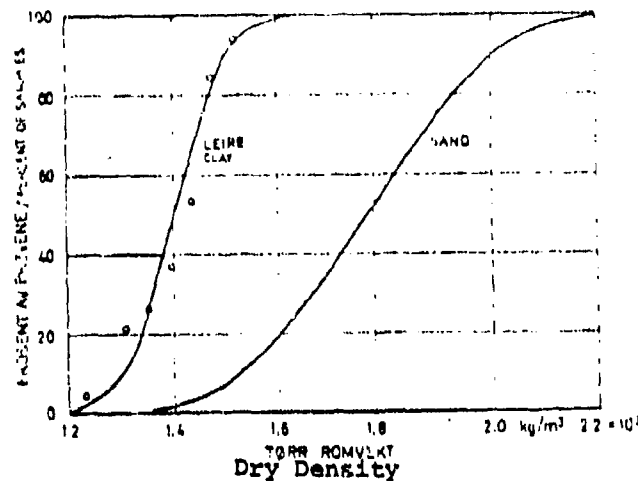


FIG. 18. Kumulative fordelinger av tørr romvekt for leire og sand basert på data vjengitt av Angen (1973) (12).
Cumulative distributions of dry density for clay and sand based on data given by Angen (1973) (12).

Angen also performed an analysis of water content in sub-soils consisting of silt and clay, based on geotechnical investigations. The variations in degree of saturation were small for these materials, with a mean of 90 percent and a standard deviation of 5 percent. For sandy materials, few measurements of water content in free ground have been reported. The distribution must for this case be a pure estimate (guess). It is proposed here to use a mean value of 50 percent and a standard deviation of 20 percent. This distribution corresponds to 95 percent of the cases having degrees of saturation between 10 and 90 percent.

In connection with frost registrations performed by the National Road Laboratory, moisture contents were measured when a total of 15 road beds were excavated in the Østland region (13). The cumulative distribution for moisture contents in road beds (pavements) shown in Figure 19 are based on these measurements. The arithmetic mean is 5.5 percent by weight. For a dry density of 1900 kg/m^3 , the median corresponds to a degree of saturation of 30 percent. In the following, this will be considered as a representative average value, while the standard deviation for the degree of saturation is estimated to be 10 percent. This distribution thus implies that 95 percent of the cases will show degrees of saturation between 10 and 50 percent, corresponding to from about 1.5 to 8 percent by weight for a dry density of 1900 kg/m^3 .

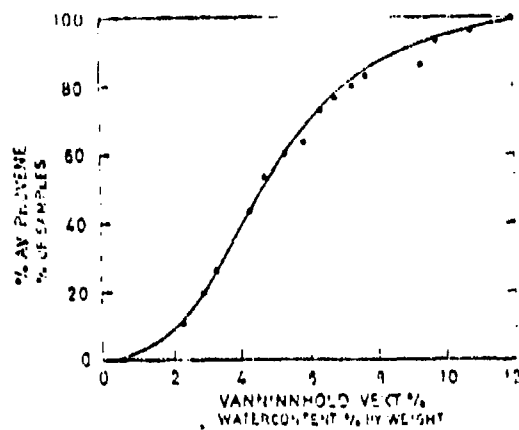


FIG. 19. Cumulative distribution, av. vanadium content in veg-overgrown near desert pl. data fr. tallgrass, steppe, etc. (11). Cumulative distribution of vanadium content in road pavements (base and subbase) (12).

Little data exist about the distribution of dry density in road beds (pavements). It is proposed here to assume a distribution having a mean of 1900 kg/m^3 and a standard deviation of 75 kg/m^3 , which implies that 95 percent of the cases fall between 1750 and 2050 kg/m^3 .

Sveian's study of quartz content in Norwegian loose deposits can form a basis for similar estimates of quartz content distributions in coarse grain materials (6). These results were given in the form of a cumulative distribution curve in Figure 5 in this chapter. This curve can be approximated by a normal distribution with a mean of 37 percent and a standard deviation of 15 percent.

In the case of fine grain materials, results from quartz content measurements are available for fractions of Norwegian clays (7). These results are also shown as cumulative distribution curves in Figure 5 in section 1 of this chapter. Based on these results, the quartz content in fine grain materials was assumed to fall between 0 and 45 percent. This may be construed to imply a distribution with a mean of 20 percent and a standard deviation 7.5 percent for clay and clay/silt, while for silt the mean is assumed to be 30 ± 7.5 percent. For the first group, 95 percent of the cases will then occur between 5 and 35 percent, while corresponding numbers for silt are 15 and 45 percent.

The distributions just described are summarized in Table IV. Even if most of these should be regarded as approximate estimates, they serve to illustrate the principle behind conductivity error limit evaluations, until more conclusive results become available.

Table IV. Assumed (estimated) distributions for key soil parameters, to be used when calculating thermal conductivity. Mean values and standard deviations.

	Dry density kg/m ³	Saturation percent	Quartz content percent
Clay/silt	1400 ± 90	90 ± 5	20 ± 7.5
Silt	1600 ± 100	90 ± 5	30 ± 7.5
Sand, free ground	1770 ± 170	50 ± 20	37 ± 15
Gravel, pavement	1900 ± 75	30 ± 10	40 ± 10

Based on these distributions, error limits for the conductivity can be determined by means of an error analysis using the proposed mathematical model as a starting point. This error analysis is performed in the normal manner, using partial derivatives and sums of squares.

Table V shows the results of such an error analysis, performed for three levels of information for both sand and clay. At the middle level, all parameters are given except quartz content, while at the third level dry density, degree of saturation and quartz content are all known.

The values in row six illustrate the effects of uncertainties in each individual parameter. For example, one finds that the uncertainty in dry conductivity is an insignificant part of the total error. When passing to the level where dry density and degree of saturation are known, one finds that the effect of uncertainties in Kersten's number is about halved. At the same time, the effect of uncertainties in saturated conductivity is reduced by about 50 percent. If also the quartz content is known, this effect is further reduced. In all cases, there is a significant reduction of relative errors in the conductivity estimates, from about ±40 percent at the "lowest" level to only 12-14 percent at the "highest"

Table V. Error (confidence) limits in calculated conductivity of soil materials. Un-frozen sand and clay.

Level	1		2		3	
	Sand	clay	Sand	clay	Sand	clay
1. Texture						
2. Dry density	1770	1400	1770	1400	1770	1400
$\Delta \gamma_d$	340	180	-0	-0	-0	-0
3. Quartz content	0.37	0.20	0.37	0.20	0.37	0.20
Δq	0.30	0.16	0.30	0.16	-0	-0
4. Deg. of saturation	0.50	0.90	0.50	0.90	0.50	0.90
ΔS_r	0.40	0.10	-0	-0	-0	-0
5. Conductivity	1.50	1.15	1.50	1.15	1.50	1.15
$(\partial \lambda / \partial \lambda^0) \Delta \lambda^0$	0.056	0.005	0.03	0.004	0.03	0.004
6. $(\partial \lambda / \partial \lambda^1) \Delta \lambda^1$	0.498	0.387	0.292	0.271	0.097	0.127
$(\partial \lambda / \partial K_e) \Delta K_e$	0.393	0.187	0.150	0.103	0.150	0.105
7. $\Delta \lambda$	0.63	0.43	0.33	0.29	0.18	0.17
8. Relative error percent	42.0	37.5	22.0	25.2	12.0	14.3

One also notes that the errors are about 25 percent in cases where the quartz content is not known, while dry density and degree of saturation are given. This level corresponds approximately to the level of Kersten's empirical equations, for which the uncertainty also was found to be ± 25 percent.

In this summary, the calculations are based on average values for dry density and degree of saturation. Table VI also shows how the error limits vary with degree of saturation for the two highest levels.

Table VI. Error (confidence) limits for different degrees of saturation. Un-frozen sand.

Degree of saturation	0.15		0.25		0.50		0.75	
Dry density	1770		1770		1770		1770	
Quartz content	0.37	*	0.37	*	0.37	*	0.37	*
Error limits, percent	18	20	13.6	18	12	20	12.1	26.5

*) Not known

Figure 20 shows calculated values plotted versus degree of saturation.

From Table VI and Figure 20 one can see that the improvement in error limits due to knowledge of the quartz content is largest for the highest degrees of saturation.

As mentioned previously, the degree of saturation is relatively low in road pavement materials, about 30 percent, while the dry density is significantly higher than in the previous example, about 1900 kg/m^3 .

Error limits for the conductivity were calculated for the variations in dry density and degree of saturation estimated previously (see Table IV) and four different cases, see Table VI. For the two first cases, dry density and degree of saturation are assumed to deviate from their means by one σ , while in the other two cases these parameters are assumed to be known. For cases 1 and 3, the quartz content deviates from the mean value by one σ while it is assumed known in cases 2 and 4.

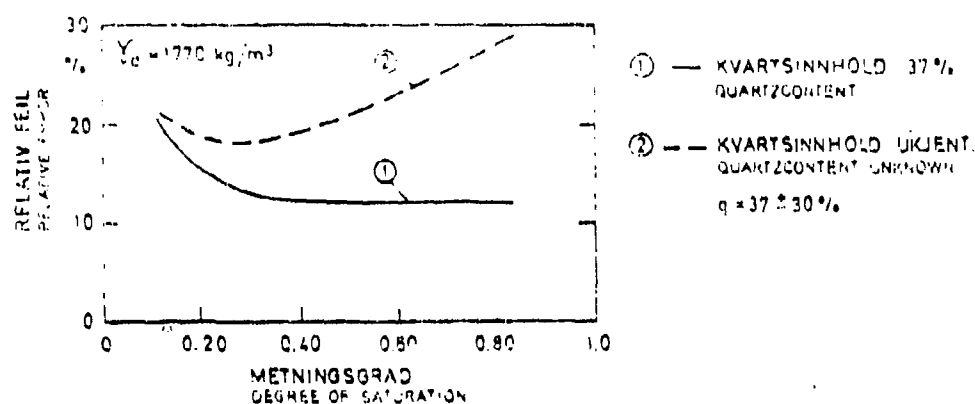


FIG. 20. Innflytelsen av usikkerhet i kvartsinhold på feilgransene ved beregning av ledningsevnen av sand.
Influence of uncertainty in quartz content on relative error in calculations of conductivity of sand.

Table VII. Error (confidence) limits for estimated conductivities in frozen gravel road bed¹⁾.

Case	1	2	3	4
Dry density	1900	1900	1900	1900
$\Delta \gamma_d$	150	150	0	0
Deg. of saturation	0.30	0.30	0.20	0.20
ΔS_r	0.20	0.20	0	0
Quartz content	0.40	0.40	0.40	0.40
Δq	0.20	0	0.20	0
Conductivity, frozen, W/mK	1.15	1.15	1.15	1.15
Relative error percent	52.7	47.3	21.2	15.2

This example illustrates that knowing the quartz content contributes little towards reducing the error limits of conductivity estimates for road surface layers, particularly when dry density and degree of saturation are not accurately known. By contrast, one finds that the error limits are reduced to about one third

1) "overbygning" refers to the upper layers in a road, e.g. "pavement" for concrete or asphalt covered roads and "bed" or "surface layer" for gravel roads (Translator's note).

when data for degree of saturation and density can be given exactly. Thus, it is more important to obtain reliable data on density and moisture content in road surface layers than to accurately determine the quartz content.

For these relatively low degrees of saturation, uncertainties in the estimate of dry conductivity are rather important. As mentioned previously, investigations of conductivity in dry soil materials gave cause for distinction between two types of texture - natural soil materials and crushed rocks. The empirical relations derived from these two groups are illustrated by Figure 21, where the range of variation also is indicated.

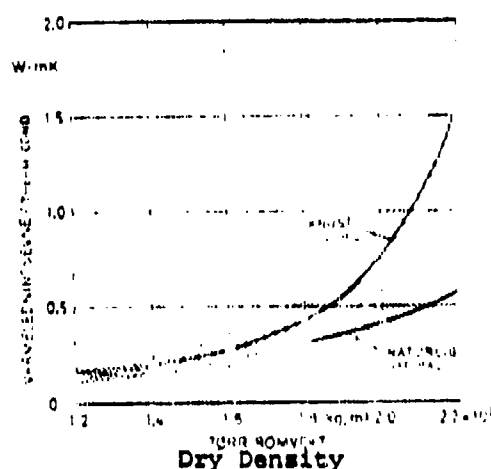


FIG. 21. Ledningssevne av tørre jordarter og knuste bergarter. Tilknyttet de empiriske relasjoner av våt og tørr ledning. Conductivities of dry soils and crushed rocks. Uncertainties in the empirical relations are indicated.

If one considers the case where no information about particle shape is available, the uncertainty in the estimate of dry density may increase significantly, particularly for high densities. For example, at a density of 2000 kg/m^3 the error limits will increase from the ± 20 - 25 percent given previously to nearly 50 percent. This increase in uncertainty will be most pronounced for low degrees of saturation, where errors in computed conductivity are

dominated by the uncertainty in dry conductivity. This is also shown in Figure 22, where error limits for the case of lacking particle shape information is compared to those obtained when all relevant information about the gravel material at hand is available.

For high packing densities, an uncertainty in the specific weight estimate will also affect the error limits for conductivity estimates. This is particularly evident for crushed gravel, where dry conductivity is most dependent on packing density. This is illustrated by Figure 23, which shows error limits when calculating conductivity of crushed gravel with and without knowledge of specific weight. For natural gravel the effect of uncertainty in specific weight is important only for lower degrees of saturation.

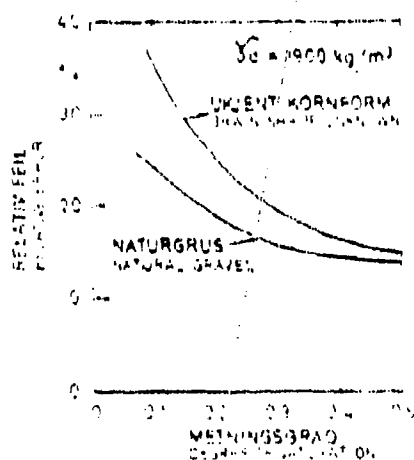


FIG. 22. Innflytelse av kornform på beregning av ledningsfærdighet av frosne grusmateriale. Influence of information on grain shape on calculation of the conductivity of frozen gravel.

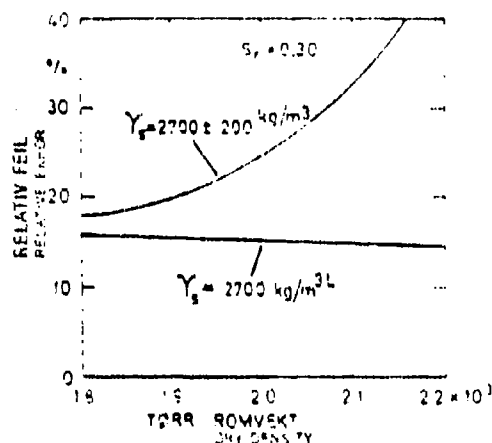


FIG. 23. Innflytelse av kjennskap til spesifikk vekt ved be-
 regning av ledningsevnen av fuktet jordstus.
 Influence of information on specific gravity on cal-
 culation of conductivities of moist soil samples.

B. Conclusions

The error analysis performed in the previous examples show that uncertainties in various soil parameters are important to a varying degree, depending on degrees of saturation, density and type of material. Without knowledge of any of the relevant soil parameters one can estimate the conductivity of different types of materials within error limits that vary from 40 to 50 percent. If dry density and degree of saturation are known, these error limits can just about be cut in half for most types of materials. Another reduction of the error limits by a factor of two can be obtained for materials near saturation, provided that the quartz content is known. For road surface materials, where the degree of saturation normally is low, information about the quartz content normally gives a small improvement of the error limits, while information concerning particle shape and specific weight can reduce the error limits to about ± 15 percent at normal degrees of saturation.

In cases where one lacks relevant soil data one must resort to using average values for the conductivity, with inherent uncertainties.

Such values are listed in Table IX. Average values and variations for the soil parameters on which these conductivity calculations are based are also included. In all cases, the variations represent one σ -limit in a normal distribution and will thus correspond to 95 percent of possible cases (occurrences). This will then also hold for the calculated ranges of conductivity variations. The results are represented in terms of histograms in Figure 24.

At this point it is prudent to again remind the reader that the data used for estimating variations in various soil parameters are approximations. Thus, mean values and ranges of variation given must be considered as highly uncertain and in some cases speculative estimates. It is obviously highly desirable to obtain more complete data in these areas. However, the average values and variations for the conductivity of different types of materials presented here may serve as guide-lines when estimating average values and variances (spreads). In the next section, these approximate results will also be utilized in an investigation of the importance of variations in actual soil parameters for thermal calculations related to road designs subjected to frost.

Table IX. Average values for variations in thermal conductivity in road materials.

Materials	$\gamma_d \pm \Delta \gamma_d$	$q \pm \Delta q$	$S_r \pm \Delta S_r$	$\gamma_s \pm \Delta \gamma_s$	Un-frozen $\lambda \pm \Delta \lambda$	Frozen $\lambda \pm \Delta \lambda$	
Crushed rock	1.60 ± 0.20	40 ± 20	20 ± 12		0.90 ± 0.34	0.80 ± 0.38	
Crushed gravel	1.90 ± 0.15	40 ± 20	30 ± 20	2.7 ± 0.20	1.46 ± 0.47	1.29 ± 0.65	
Natural gravel	1.90 ± 0.15	40 ± 20	30 ± 20	2.7 ± 0.20	1.38 ± 0.48	1.15 ± 0.64	
Sand, filter layer ¹⁾	1.7 ± 0.15	40 ± 20	75 ± 25		1.60 ± 0.42	2.24 ± 0.82	
Free ground sub-soil							
	Sand	1.77 ± 0.34	37 ± 30	50 ± 40	**)	1.50 ± 0.65	1.57 ± 1.14
	Silt	1.60 ± 0.20	30 ± 15	90 ± 10		1.44 ± 0.33	2.37 ± 0.53
Clay/silt *)	1.40 ± 0.18	20 ± 15	90 ± 10		1.20 ± 0.43	1.91 ± 0.46	

*) $W_u = 10 \pm 8$, percent by volume

**) Assumed to be of minor importance

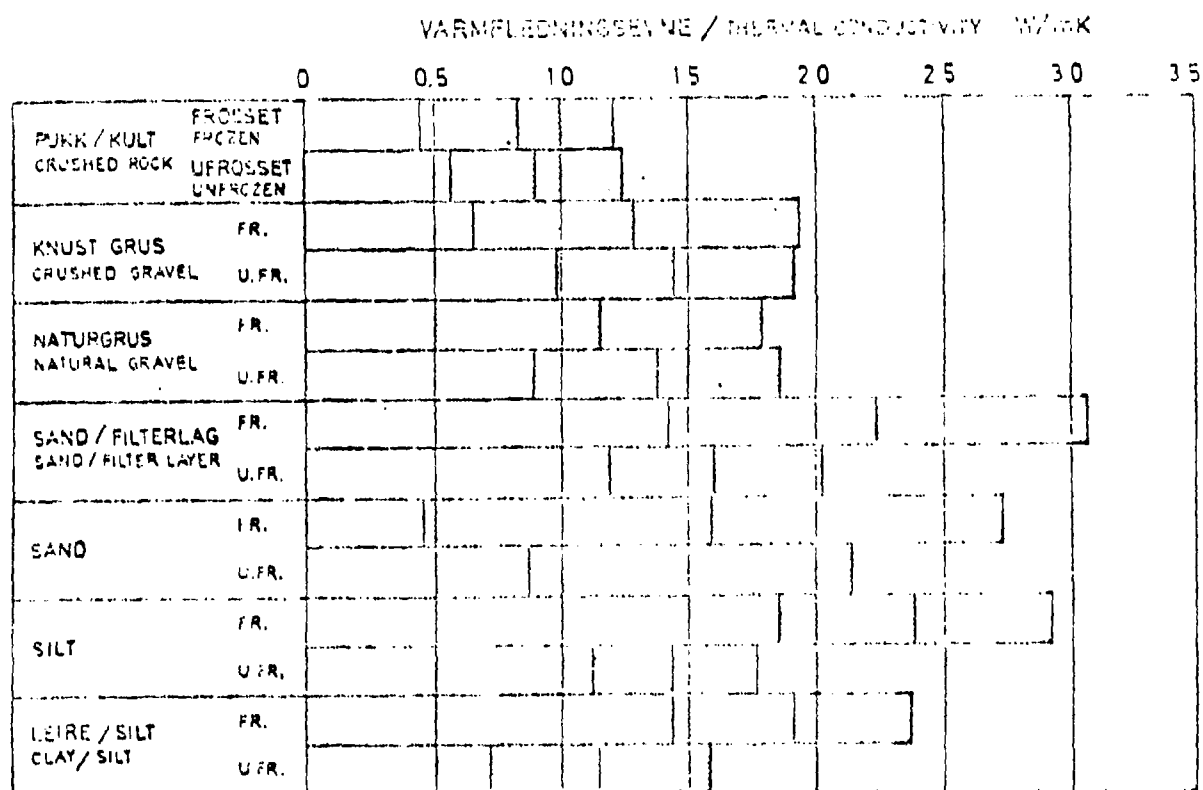


FIG. 24. Gjennomsnittlige og variasjonsintervall i ledningsevnen av sand- og grusmaterier og i leirgrunn. Beregningene er basert på feltmålinger ved utgravingspunkt i 1 m horisontale beregningsmodell og de angitte variasjonsintervall i jordarteregisteret for de forskjellige materialtypene. (Jfr. tabell IV og V). Variasjonene angis kun for de 6 grusartene, tilsvarende 95% av tilfellene.

Range and average values of thermal conductivity and resistivity of sand, gravel and clay. Calculations are based on field measurements of the material in the horizontal calculation model and the indicated variation intervals in the soil register for the different material types. (See table IV and V). Variations are indicated only for the 6 gravel types, corresponding to 95% of the cases.

BEST AVAILABLE COPY

4. EFFECTS OF CONDUCTIVITY VARIATIONS ON THERMAL CALCULATIONS

A. Introduction

Determining temperature distributions (fields) in freezing ground has many applications. These include thermal analysis of road and building foundations to ensure against frost damage, calculating frost depth for buried water or sewage lines and determining thawing depths for road or building foundations in permafrost regions. Knowledge of thermal parameters of the soil is necessary in all these cases, regardless of the calculation method (mathematical model) being used.

In principle, requirements on the accuracy with which thermal soil parameters are given will be different, depending on the accuracy of the computational method (model). First of all, the thermal soil parameters should be given with high enough accuracy to prevent that the uncertainties in these parameters become the limiting factors for the accuracy of the end result. On the other hand, it does not make sense to require high accuracy for the thermal parameters unless the computational method (model) can provide results with a correspondingly high accuracy.

No quantitative basis for such a judgement exists today, but there is reason to believe that uncertainties in the thermal parameters do not constitute the limiting factor when using available approximate procedures for determining frost penetration in and under road structures (Watzinger/Skave-Haug's method, (14, 15)), while this often may be the case with modern numerical methods based on the use of computers (16). In such cases it will thus be important to try to reduce the uncertainties due to estimates of thermal parameters as much as possible, e.g. by performing the best possible analysis of the soil materials which form the actual structure.

Effects of variations in the soil parameters at hand or uncertainties in estimated conductivities will in the following be treated for some selected cases, limited to road foundations where freezing of the ground is to be prevented.

B. Effects of conductivity variations

The error analysis performed in the previous sections showed that the conductivity of materials in various layers of a road structure can vary within relatively wide limits, due to variations in density, degree of saturation and mineral composition. To determine the effects of such conductivity variations on thermal calculations, the upper layer (pavement) thickness required for prevention of freezing in the subsoil was determined (calculated) for different types of insulation (frost preventing) layers. In these calculations, the conductivities of each layer were varied within the limits established by the previous error analysis. Variations in calculated thicknesses for the insulating layers will thus form a basis for evaluating the effects of conductivity uncertainties. The calculations were performed according to the method given by Skaven-Haug, described in detail in references (14) and (15).

The results of these calculations are shown in histogram form by Figure 25. The average values and variations assumed for the calculations are shown in the same figure. The calculations were performed for a frost quantity of $30,000 \text{ h}^\circ\text{C}^{1)}$ and three types of frost preventing (frost resistant) layers.

For frost preventing layers consisting of gravel and bark, which utilizes their cold accumulating²⁾ properties, one finds that the results are very sensitive to the conductivity of upper layers,

1) The unit for frost quantity is "Celsius degree-hours".

2) A strange expression, faithfully translated. (Translator's notes)

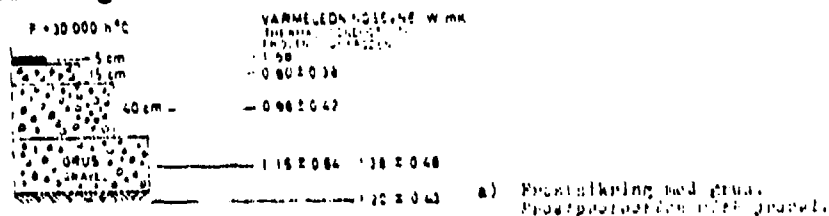
while conductivities of sub-soil and the frost preventing layers themselves have relatively small effect. The latter is particularly true for bark layers. The large variations due to upper layer conductivities indicates the importance of obtaining accurate data for dry density and water content of materials used in these layers when cold accumulating materials (layers) are used for frost protection.

For structures utilizing insulation layers for frost protection one finds that variations in sub-soil conductivity is the most important parameter for determining insulation layer thickness. However, the approximations made may be responsible for this result. In the method used, a given temperature gradient in the ground immediately below the insulation layers is used when determining the ground heat contribution to freezing resistance. The heat loss from the sub-soil is obtained by multiplying this gradient by the conductivity of the ground and the duration of the frost period. Such a simplified approach can not be expected to give reliable results when the heat loss from the ground is as high as in this case. Only a computation based on integration of the thermal conduction equation, using a digital computer, can give the required accuracy.

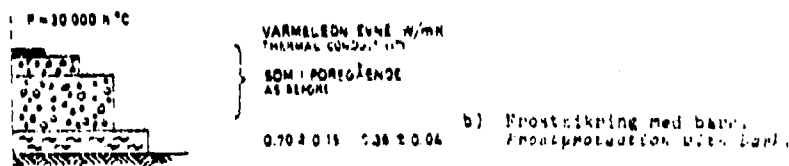
Thermal parameters for the sub-soil, except for quartz content, are normally determined by geotechnical investigations in connection with stability calculations, etc. As mentioned previously, the quartz content in fine grain soils can be estimated on the basis of particle size distribution curves. The results obtained show the importance of utilizing such data also for the thermal design.

For the calculation examples discussed here it was always assumed that frost does not penetrate into the sub-soil. In cases where this condition is not met, variations in un-frozen water content will have a much larger effect on the calculations than the expected conductivity variation in the un-frozen sub-soil. To in-

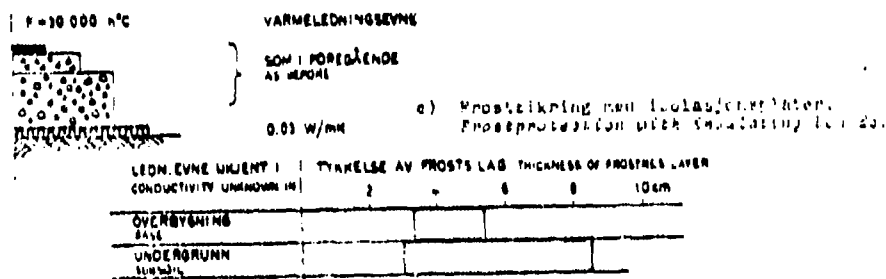
investigate this case, calculations were performed for a structure consisting of a 5 cm layer of insulation material (plates) and a pavement (upper structure) identical to that assumed for earlier calculations. According to those calculations, this kind of structure can withstand a frost quantity of about 30,000 h°C with no frost penetrating the sub-soil.



LEGN EYNEUKJENT I CONDUCTIVITY UNKNOWN IN	TYKKELSE AV FROSTLAG THICKNESS OF FROST LAYER
OVERBYGNING BASE	0 2 4 6 8 10 12 14 16 m
OVERBYGN OG FROSTLAG BASE AND FROST LAYER	
FROSTLAG FROST LAYER	
UNDERGRUNN SUBSOIL	



LEGN EYNEUKJENT I CONDUCTIVITY UNKNOWN IN	TYKKELSE AV FROSTLAG THICKNESS OF FROST LAYER
OVERBYGNING BASE	0 20 30 40 50 60 cm
OVERBYGN OG FROSTLAG BASE AND FROST LAYER	
FROSTLAG FROST LAYER	
UNDERGRUNN SUBSOIL	



LEGN EYNEUKJENT I CONDUCTIVITY UNKNOWN IN	TYKKELSE AV FROSTLAG THICKNESS OF FROST LAYER
OVERBYGNING BASE	2 4 6 8 10 m
UNDERGRUNN SUBSOIL	

Fig. 15. Innflytelse av variasjoner i varmeledningsevnen av forskjellige lag i vegkonstruksjonen på nødvendig tykkelse av frostsikringslag. Beregningene som gir nødvendig tykkelse for å hindre frostnedsivning i undergrunnen ved en frostvolum på 30 000 h°C er utført med skavensangs metode. Influence of variations in thermal conductivity of various layers in a road construction on thickness of frostprotective layers. The calculations which gives the thickness necessary to avoid freezing of the subsoil at a frostindex of 30 000 h°C are based on Skavensangs method (1).

For example, the effect of the temperature distribution in the sub-soil on the un-frozen water content is uncertain. As mentioned before, estimates of the contribution from (stored) soil heat is another uncertain quantity. However, calculations of the type indicated here should be performed as soon as experimental data are reduced and the computer program being developed by the Institute for Cold Technology becomes operable, in order to clarify the effects of under-designed frost prevention layers.

C. Conclusion

The previous analysis of effects of variations in pertinent parameters for road construction materials and sub-soil has demonstrated that the accuracy of thermal analysis largely depends on how accurately one can determine relevant material parameters for the different layers. For the upper layers (pavement), determination of water content is particularly important for the calculation accuracy.

It is also apparent that the ratio of un-frozen water is an important parameter in cases where the frost can penetrate into the sub-soil. Such cases can be adequately treated only by means of advanced programs and modern digital computers. In general, this also seems to be true for thermal analysis of structures in which the frost prevention layers consists of insulation materials. The normal method for finding the contribution from heat (stored) in the ground can not be considered satisfactory for this case.

REFERENCES, CHAPTER VI.

1. A. Gemant: The Thermal Conductivity of Soils. Journal of Applied Physics. 21, 1950, pp. 750-752.
2. M.W. Makowski and K. Mochlinski: An Evaluation of Two Rapid Methods of Assessing the Thermal Resistivity of Soil. Proceedings. Institution of Electrical Engineers. 103, A, (11), 1956, pp. 543 - 470.
3. L. Alberts et al: The Influence of Low Moisture Content on the Conductivities of a Granular Substance. Brit. J. Appl. Phys. 17, 1966, pp. 951-955.
4. D.A. de Vries: Het warmtegeleidingsvermogen van grond. Med. Landbouwhogeschool. Wageningen, 52, 1952.
5. M.S. Kersten: Thermal Properties of Soils. Univ. of Minnesota, Eng. Experiment-station, Bull 28, June 1949.
6. H. Sveian: Undersøkelse av kvartsinnhold i løsmasser ved hjelp av DTA. Institutt for Kjølleteknikk. NTH, Trondheim 1973.
7. R. Selmer-Olsen: En regional undersøkelse av norske kvartaere leirers finfraksjon basert på DTA. Rapport sendt til NTNF. Geologisk Institutt, NTH Trondheim 1961.
8. M. van Rooyen and H.F. Winterkorn: Structural and Textural Influences on Thermal Conductivity of Soils. Highway Res. Board Proceedings, Washington D.C. 1959, pp. 576-621.
9. S. Skaven-haug: Romforhold i jordmaterialer. Meddelelser fra det norske myrselskap, 70, (4), 1972, pp. 89-102.
10. J.V. Thue: Redusert fundamentdybde, - termiske problemer. Del I. Institutt for husbyggingsteknikk. Trondheim, NTH, p. 82.
11. W.A. Sinclair et al: Soil Thermal Resistivity. Typical Field Values and Calculating Formulas, part IV. In: Soil Thermal Characteristics in Relation to Underground Power Cables. AIEE Transaction paper no. 60 - 785, pp. 71-94.
12. E. Angen: Analyse av vanninnhold i vegkonstruksjoner. SINTEF arbeidsnotat. Trondheim 1973, p. 11.
13. A. Knutson and R. Saetersdal: Teleregistering 1967/68. Veg-laboratoriet. Intern rapport. Oslo 1969, p. 8.

14. S. Skaven-Haug: Frostfundamenters dimensjonering. Frysevarme og jordvarme. Frost i jord, (3) 1971, pp. 9-27.
15. A.F. Knutson: Theory and Experience Regarding Frost Penetration and Frost Heaving, Symp. on Frost Action on Roads, I, Paris 1973, pp. 223-233.
16. A.K. Fleming: Applications of a Computer Program to Freezing Processes. Proceedings of the XII International Congress of Refrigeration, Washington, D.C. 1971.

THERMAL CONDUCTIVITY OF SOILS

SUMMARY *

The aim of this investigation has been to create a mathematical model for calculating thermal conductivity of soils with ordinary soil parameters as input data. One part of this work has been devoted to literature studies on heat-transfer mechanisms in moist materials. These studies have made it possible to give bounds for the different domains where the various mechanisms have an appreciable influence on the total heat transfer.

Fig. 23, I

With important exceptions such as freezing in frost susceptible soils and convective heat transfer in coarse-grained crushed rock, the heat transfer in road-building -- and subgrade materials can be treated as a heat conduction problem.

Under these conditions, the thermal conductivity is determined by three sets of parameters -- the volume fraction of the components, their conductivities and the microgeometry of the system.

Various theories are suggested where these sets of parameters are combined in models for calculating thermal conductivity of composite materials. However, only methods where the thermal conductivity is given between upper and lower bounds, referring to extreme microstructures, can

*As already translated in the Swedish text.

Fig. 1, II

be said to give exact results because of the problem of incorporating the microgeometry of natural materials in an analytical solution of the heat conduction problem. Such bounds as those developed by Hashin and Shtrikman (1962) shows that the conductivity is very sensitive for variations in microgeometry when the component-conductivities are widely different, while the sensitivity is small when the component-conductivities are of the same order of magnitude. It follows that the conductivity may be calculated analytically if the component-conductivities are of the same order, while only empirical methods can be used under other circumstances.

Results from thermal conductivity measurements on soils are analysed on the basis of such fundamental theories with the aim of deriving empirical relations to be used in a model for calculating thermal conductivity of soils. The analysis is centered around the extensive measurements published by Kersten (1949), in addition to measurements made at the Division of Refrigeration Engineering (University of Trondheim).

From this analysis the problem of deriving a mathematical model consists of three parts. The conductivities of dry soils and saturated soils are handled as two extremes between which the conductivity must be found at a given degree of saturation. The relation between conductivity and degree of saturation is reduced to a normalized or dimensionless form.

EQ. 10, V

EQ. 5, V On the basis of the experimental results, two empirical
EQ. 6, V relations between conductivity of dry soils and porosity
were derived, with different relations for crushed rocks
and natural soils.

For saturated soils, the influence of differences in
Fig. 18, V microgeometry is found to have negligible influence, and
the thermal conductivity can be calculated with acceptable
accuracy, from volumetric composition and component-
conductivities. The problem of determining the conductivity
of soil particles was solved from an examination of certain
Tab.III,III elementary aspects of rock mineralogy and recently published
data on thermal conductivity of rock forming minerals.

EQ. 2, III This resulted in a model where the particle conductivity
is derived from the quartz content of the soil.

The dimensionless representation of the conductivity in
relation to the degree of saturation is calculated as a
ratio of the difference between the given conductivity and
the conductivity of dry soil, to the difference between
EQ. 10, V conductivities of saturated and dry soil. This ratio is
named the Kersten number. From Kersten's experimental
results empirical relations were derived between this
Kersten number and the degree of saturation, two relations
Fig. 24, V for unfrozen soils; one for finegrained soils and one for
Fig. 25, V coarsegrained soils, and one relation for frozen soils.
In the latter case no basis for discriminating between
soils of different texture was found. However, the
unfrozen water content, which is related to texture and

temperature below freezing, was found to have an appreciable influence on the thermal conductivity. This influence is incorporated by a correction in the saturated conductivity, on the basis of volume fractions of unfrozen water.

Combined with computed values for dry and saturated soils, these normalized relations make it possible to calculate the conductivities at various degrees of saturation of a soil where quartz content and dry density is given. This complete mathematical model is represented as nomograms where quartz content, dry density and degree of saturation are input values in addition to informations of grain shape (crushed v.s. naturals), grainsize distribution (finegrained v.s. coarsegrained), and volume fraction of unfrozen water.

Tab. III, VI
Fig. 15a, VI
Fig. 15b, VI

As informations of all relevant soil parameters are available only occasionally, an analysis is performed of the relationship between ordinary available geotechnical data and the fundamental parameters determining thermal conductivity. From this analysis relations are derived for indirect determination of the fundamental parameters. Such indirect relations will lead to a reduction in the accuracy of the calculation of the thermal conductivity, which however has to be accepted when incomplete soil data are to be used.

An extreme situation is present when no relevant soil data is available. Under such circumstances average thermal conductivities for the given soil group must be used. Principally, such averages may be derived on the basis of statistics on the distribution of the relevant soil parameters for different soil groups. Such data are scarce. However, in conjunction with an analysis of expected variations in thermal conductivity of different soil groups, such distributions are sketched partly on the basis of available data.

From these approximate distributions and an error analysis of the suggested mathematical model, averages and expected variations in the thermal conductivity of a set of soils and pavement materials are calculated. These averages represent a method for estimating conductivities at the lowest level of information. The estimations can only be improved by making use of more relevant information of the soil parameters.

The improvement in the accuracy in the calculation of thermal conductivity at different levels of information is discussed for some cases. It is concluded that information on grainshape (crushed v.s. natural) in addition to dry density and degree of saturation will result in an appreciable improvement in the estimation of the thermal conductivity of pavement materials with relatively small degrees of saturation. Information on quartz content will

Tab. IX, VI
Fig. 24, VI

give similar improvements when dry density and degree of saturation is given in subgrade materials with high degrees of saturation.

The influence of variations in thermal conductivities on thermal analysis is examined for some road constructions with different types of frost-resistant layers. Variations in conductivities of materials in the pavement are found to have much influence when frost accumulating layers, such as bark or moist sand are used in the construction, while variations in the conductivity in the subgrade are of greatest importance when insulating materials are used.

The results which are published in this report will be followed up with an extensive experimental investigation on thermal conductivity of Norwegian soils at the Division of Refrigeration Engineering (University of Trondheim). This investigation will make it possible to verify the suggested mathematical model, and may eventually result in some improvements. These investigations will also give valuable information on the accuracy and validity of various experimental methods for determining thermal conductivity of soils.

POST-SCRIPT

This report presents a new mathematical model for determining thermal conductivity of mineral-based soil materials. Conventional soil data and quartz content are used as input parameters. The model is developed on the basis of a literature study of thermal transport mechanisms in moist, porous materials and theories for thermal conductivity in composite materials as well as extensive experimental results obtained by M.S. Kersten. An error analysis is performed, which shows that conductivity values within error limits of from ± 10 to 20 percent can be obtained from this model if all relevant soil data are given.

The model is primarily developed for thermal analysis of structures placed on the ground and subject to frost effects. A computer program for determining temperature distributions (fields) in such structures is under development at the Institute for Cold Technology, NTH as a part of the NTNF project "Frost in the Ground". This computer program will include the model as a sub-routine with soil data as input parameters.

A major experimental study of thermal conductivities in Norwegian soil materials, which has been initiated at the same Institute, may contribute material for improvements in the model. However, initial results from this study indicated that the model is largely acceptable for Norwegian soils. Certain changes and improvements may still be required.

This report is primarily devoted to studies of conductivity in mineral-based soils. In addition, certain experimental values for peat and bog are included. Lack of results from systematic measurements on other important materials, such as soils containing humus, concrete and asphalt has prevented treatment of such materials. However, the experimental study at the Institute for Cold Technology will hopefully correct for this deficiency.

In order for the model to be used also in cases where one lacks information about materials used in the structure, it is necessary to have relevant data on expected mean values and variations of soil parameters for various types of materials. In this report, such values have been used to determine expected variations in conductivity for different types of soils. However, in some cases these values had to be estimated, due to lack of information about water content and density in sub-soils and upper layers of road structures. A study initiated by the Institute for Cold Technology, NTH, may supply the required corrections for these data. When such results become available, a new error analysis should be performed for the model, using revised mean values and variations for the soil parameters.

This analysis should include a sensitivity analysis, using the computer program mentioned previously, for a selection of typical road structures utilizing different types of insulating layers. During this analysis, thermal properties of the different materials within the structure should be systematically varied within the limits given by the previously mentioned error analysis, in order to clarify the effects of uncertainties in soil material data.

This study is primarily concerned with thermal conductivities in soil materials. To generate a computer program for determining temperature distributions in the ground one must also know specific heat, as well as latent heat exchanged during freezing and thawing. A calorimeter for determining these parameters is being built at the Institute for Cold Technology. The studies to be conducted with this unit will form an important supplement to the investigations reported on here.

These concluding remarks show that the work reported here is part of an extensive project, which is by no means finished by completion of this report. As indicated, several on-going investigations may form the basis for necessary improvements in the result given

here. These results will be reported in detail when the project "Frost in the Ground" is concluded at the end of this year (1975), e.g. in reports issued by the "Group for Analysis of Frost in the Ground", Institute for Cold Technology, NTH.

APPENDIX. PERIODIC TEMPERATURE VARIATION IN A HOMOGENOUS CYLINDER

In a homogenous cylinder of infinite length the thermal conduction equation can be expressed in the form

$$\frac{\partial \theta}{\partial t} = a \left(\frac{\partial^2 \theta}{\partial r^2} + \frac{1}{r} \frac{\partial \theta}{\partial r} \right) \quad .1$$

where θ is the temperature
 a is thermal diffusivity¹⁾
 r is the radius
 t is time

For the case at hand, $\theta(r, t)$ is to be determined when the outer surface temperature varies as a sinusoid:

$$\theta(R, t) = \theta_0 \sin(\omega t) \quad 2$$

where R is the radius of the cylinder
 θ_0 is the amplitude
 ω is the angular velocity (frequency)

To solve this problem one can use results from text-books such as Carslaw and Jaeger (1) and mathematical handbooks (2), as well as general control theory (3).

1) The original uses both α (alpha) and a for this parameter (Translator's note).

From control theory it is known that a system subjected to an applied, stationary and periodic forced input will give a stationary response which is periodic and damped (attenuated). For the problem at hand this implies that the temperature variation on the axis of the cylinder ($r = 0$) can be written (4):

$$\theta(0,t) = A \cdot \theta_0 \sin(\omega t + \phi) \quad 3$$

where A is the damping (attenuation) ratio
 ϕ is the phaseshift

Attenuation and phaseshift can be determined from the transfer function of the system. This function expresses the relation between the applied force function and the response in the Laplace transform sense. In the case at hand, the transfer function between outer surface temperature and on-axis temperature is to be determined. This is done by taking the Laplace transform of the heat conduction equation and solving the resulting ordinary differential equation for the proper boundary conditions.

Carslaw and Jaeger (5) present a solution to this problem. They give the following expression for the desired transfer function

$$G(s) = \frac{\zeta(0,s)}{\zeta(R,s)} = \frac{1}{I_0(R\sqrt{s/a})} \quad 4$$

where ζ is the Laplace transformed temperature
 s is the Laplace variable
 a is thermal diffusivity
 I_0 () represents the modified Bessel function of zero order

In the theory for frequency response, the attenuation ratio is given by the magnitude of the transfer function for $s = i\omega$ ($i = \sqrt{-1}$), while the phaseshift is given by the argument (phase angle) of the transfer function for the same value of the variable s (3).

$$A = |G(i\omega)|$$

$$\phi = \arg|G(i\omega)|$$

5

For $s = i\omega$, the transfer function becomes a complex quantity with real and imaginary parts

$$G(i\omega) = x + iy$$

6

The absolute value (magnitude) is given by $\sqrt{x^2 + y^2}$ the argument is $\arctan(y/x)$

For $s = i\omega$, the variable of the modified Bessel function takes the form

$$R\sqrt{i\omega/a} = R(1+i)\sqrt{\frac{\omega}{2a}}$$

7

$$\text{since } (1 + i)^2 = 2i$$

This complex number can also be expressed as

$$X \cdot e^{i\pi/4} = R\sqrt{\omega/a}$$

8

where X is the magnitude (absolute value) of the number.

In mathematical handbooks (6) one finds that a modified Bessel function of order zero with a variable of this form can be expressed as a complex number where real and imaginary parts are represented by the Kelvin functions $\text{ber}X$ and $\text{bei}X$:

$$\text{ber}X + i \text{bei}X = I_0(Xe^{i\pi/4})$$

9

Magnitude¹⁾ and argument for the transfer function can thus be

1) The original says "real part", which is wrong (Translator's note).

expressed in terms of these two Kelvin functions

$$A = |G(i\omega)| = 1 / \sqrt{(\text{ber}X)^2 + (\text{ber}X)^2} \quad 10$$

$$\phi = \angle G(i\omega) = -\arctan \frac{\text{bei}X}{\text{ber}X} \quad 11$$

This follows from the rule that the absolute value (magnitude) of a complex number $1/z$, $z = X e^{i\phi}$, equals $1/X$, while its argument is $-\phi$.

The functions $\text{ber}X$ and $\text{bei}X$ are tabulated in mathematical handbooks (7). Figure 1 shows phaseshift and attenuation as function of $X = R \sqrt{\omega/a}$, calculated from these tables.

This representation (ϕ and A as functions of X) makes it possible to calculate thermal diffusivity in a homogenous material formed as a cylinder, by determining attenuation or phaseshift for the periodic temperature variation from the outer surface to the center line of the sample.

The same method can be used for finding attenuation and phaseshift between two arbitrary radii within such a sample. For this case the transfer function can be expressed

$$\frac{G_{1,2}(s)}{(s)} = \frac{\zeta_1(s)}{\zeta_2(s)} = \frac{I_0(r_1 \sqrt{\omega/a})}{I_0(r_2 \sqrt{\omega/a})} \quad 12$$

This results in the following expressions for phaseshift and attenuation:

$$\phi_{1,2} = \arctan \frac{\text{beix}_1}{\text{berx}_1} - \arctan \frac{\text{beix}_2}{\text{berx}_2} \quad 13$$

$$A_{1,2} = \sqrt{\frac{(\text{beix}_1^2) + (\text{berx}_1^2)}{(\text{beix}_2^2) + (\text{berx}_2^2)}} \quad 14$$

where $x_1 = r_1 \sqrt{\omega/a}$, $x_2 = r_2 \sqrt{\omega/a}$

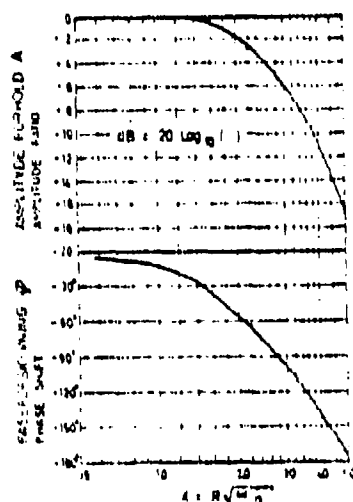


FIG. 1. Frequency response of resonant cylindrical probe and reference probe for temperature variation at overtones. Phase shift and frequency in a cylindrical specimen with steady periodic temperature variation at the surface.

BEST AVAILABLE COPY

REFERENCES

1. H.S. Carslaw and J.C. Jaeger: Conduction of Heat in Solids. Oxford at the Clarendon Press, 1959, 2, ed.
2. M. Abramowitz and I. Stegun. Ed: Handbook of Mathematical Functions, Nat. Bur. of Standards, Appl. Math. Ser. New York 1969.
3. J.G. Balchen: REGuleringsteknikk. Bind 1. Tapirs forlag 1971, 5, oppl.
4. J.G. Balchen, op. cit: pp. 71-72.
5. H.S. Carslaw, op. cit: pp. 326-327.
6. M. Abramowitz, op. cit: p. 379.
7. M. Abramowitz, op. cit.: p. 430.